Spectral aspects of a wideband frequency modulation mobile radio system employing time-compression multiplexing

Skuse, Barry

Award date:
1987

Awarding institution:
University of Bath

SPECTRAL ASPECTS OF A WIDEBAND FREQUENCY MODULATION MOBILE RADIO SYSTEM EMPLOYING TIME-COMPRESSION MULTIPLEXING

Submitted by

BARRY SKUSE

for the Degree of Ph.D.

of the University of Bath

1987

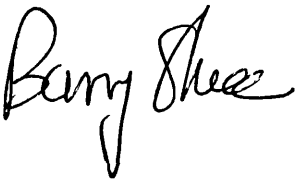

ProQuest LLC
789 East Eisenhower Parkway
P.O. Box 1346
Ann Arbor, MI 48106-1346

SUMMARY

Conventional mobile radio systems invariably utilise the available frequency spectrum by sub-division into a large number of narrow-band channels. This single message channel per carrier approach suffers from the intermodulation problems normally associated with frequency-division multiplexing systems. In addition, inefficient use is made of resources, since a separate receiver/transmitter unit is necessary for each message channel.

There has recently been a great deal of attention focussed on a radically different approach to spectrum utilisation for the next generation of cellular radio systems which, by their very nature, are particularly prone to the problems cited above. Currently, time-multiplexing systems employing wide-band channels are receiving considerable favour. However, the pre-occupation is with all digital systems, which still have technical difficulties in the areas of speech encoding and equalisation. A potentially more attractive analogue technique is to partition the signals from several message sources into segments which are then interleaved on to a common wide-band FM bearer using a time-compression multiplexing (TCM) process. This TCM-FM system retains the advantages of wide-band systems but does not attract the problems associated with an all digital technique.

The aim of this thesis is to investigate the feasibility of such a TCM-FM system from a spectral viewpoint, and to compare its predicted performance with a conventional narrow-band FM system. Classical analysis techniques are shown to be unsuitable unless severe oversimplifications are made, instead extensive use is made of numerical techniques employing the discrete Fourier transform. The use of Monte Carlo techniques with pseudo-random modulation also allows the performance to be investigated with more realistic noise like signals. Extensive analysis confirms the validity of the chosen technique and shows that the important co-channel rejection properties of conventional FM are maintained in the TCM-FM system over a wide range of parameters.

An enhanced system employing time-domain windowing techniques to remove the inter-segment discontinuities which occur in the basic system is also analysed. This enhanced windowed TCM-FM system offers a viable and attractive alternative to existing modulation systems, especially for large (national) cellular radio schemes. The most significant advantages of this system include a dramatic reduction in equipment complexity and a considerable improvement in overall spectral efficiency.

ACKNOWLEGDEMENTS

The author would like to express thanks to Dr. R. J. Holbeche for his supervision of this project.

The author would also like to thank the Science and Engineering Research Council and Racal-Vodafone Ltd. for their interest and financial support which made this work possible.

Thanks are also expressed to Mr. I. W. J. Sparry for his invaluable help with the computing facilities without which many of the results could not have been obtained.

CONTENTS

CHAPTER ONE

INTRODUCTION

1.1 HISTORY OF LAND MOBILE RADIO

1.1.1 EVOLUTION IN THE USA

Interest in land mobile radio first arose in the early 1920's out of the need of the Detroit police department to communicate with their motor vehicles. Between 1920 and 1927 there were several attempts to establish one-way communication between headquarters and patrol cars using various frequencies from below 1MHz to 2MHz [1]. These failed due primarily to the instability and insensitivity of the receivers in the moving vehicles. In 1928 the availability of improved valves and high power 135v batteries made possible the introduction of the first reliable mobile radio scheme, again for the Detroit police. This was followed in 1930 by the granting of a licence for a state police system.

The requirement for message acknowledgement soon became apparent and the first two-way mobile communication equipment was demonstrated in 1933. Base station and mobile transmitters of 200W and 20W respectively were employed along with superheterodyne receivers. Although test results were good, the lack of crystal control and

the high power consumption discouraged further expansion. Until 1935, practically all the equipment was of the 'do-it-yourself' variety, that is, developed and installed by individuals working for the various police departments. It was not until after the introduction of the vibrator power supply in place of the more expensive and unreliable rotary converter that larger companies began production of mobile radio equipment. General Electric and RCA entered the field in 1936, followed by F.M.Link, and then Motorola in 1937. An important milestone in two-way communications was the allocation of 29 channels in the 30.58 to 39.9MHz band for police communications in 1937. Subsequently crystal controlled transceivers became common and the Federal Communications Committee (FCC) introduced a frequency tolerance standard of 0.05% for equipment working above 30MHz.

Up until 1940, the several thousand systems in use all employed amplitude modulation with the base station equipment normally located at police headquarters. Although such installations were operationally convenient, the often high level of ambient noise in the receiver and poor antenna elevation gave restricted range. A radically new approach was adopted in the Connecticut system which employed angle modulation for the first time in mobile radio [2]. The location of each base station was also

optimised to obtain best aerial elevation and lowest noise, with the mobile antenna located in the centre of the vehicle roof. It was these latter factors which contributed as much as anything to the success of the scheme which led to the almost universal change to FM during the following six years.

1.1.2 EARLY DEVELOPMENTS IN GREAT BRITAIN

In Great Britain progress in mobile communications was at a slower pace. It was not until the 1930's that simple AM systems operating in the lf and mf bands were installed for the police services. Performance was limited predominantly by natural interference (static) and by man-made electrical noise (ignition interference). It was not until the late 1930's that improvements in technology allowed VHF mobile systems to be introduced operating first at 30MHz and later at higher frequencies.

The number of schemes remained small until after the second World War. During this time developments in military communications were rapid, and there was a requirement from the police (and to a lesser extent, the fire services) for more reliable systems. Before the end of the war, several of the larger districts had mobile radio systems, developed along the lines of military equipment. These employed amplitude modulation in the 80 or 130MHz

bands that had been allocated for mobile radio at the 1938 International Radio Conference. In contrast to the USA, were its use predominated, angle modulation was used in only a few experimental and some permanent schemes in the UK. By 1945 it was estimated that fewer than 1000 mobile radios were in use in Great Britain [3] compared to over 20,000 in the USA [2].

1.2 EXPANSION OF MOBILE RADIO SERVICES

1.2.1 THE SITUATION IN THE POST-WAR YEARS

The relatively low density of mobile equipment per unit area in 1945, both in the USA and UK, meant that there was little chance of interference from other users. As such, practically no attention was paid to equipment spurious responses or emissions. In the USA, a receiver IF bandwidth of 50kHz (-6dB) was normal with a rejection of only 60dB at 200kHz. Image performance was some 10-20dB worse than this. In the transmitter, there was no deviation limit, with often some 15 to 45kHz resulting for the same input signal level. There was no control whatsoever of spurious emissions and no adjacent channel specification.

In the ten years following the second World War, a considerable quantity of VHF equipment was installed in the UK, operating in the bands 71.5-88.0MHz (low band) and 156-184MHz (high band). The low band employing 50kHz channel spacings was used where coverage over as wide an area as possible was required. The high band, utilising a 100kHz channel spacing, was used for more local schemes due to its shorter range propagation characteristics. The bulk of equipment in both bands was operated on a two frequency simplex basis (chapter 2.2.2) with a spacing of

10MHz. During this period licences were granted for the first time to users other than the police and fire services, including taxi firms, ambulances and public utilities. By 1949 there were some 220 base stations and 1000 mobiles [3] being used by these new services. The total number of all mobile radio users also continued to increase rapidly with about 2000 base stations and 20,000 mobiles in operation by 1959. In the USA, growth was at an even faster rate with around 85,000 transmitters in use by 1948 and 700,000 by 1958! [2].

1.2.2 IMPROVEMENTS IN EQUIPMENT PERFORMANCE

Early equipment utilised valves with low overall electrical efficiency which placed heavy demands upon power supplies. The introduction of the transistor, at first in low level audio stages and subsequently throughout all the equipment, was a dramatic step forward in this respect. A typical 1945 mobile unit consumed 200W for 10W RF output power, weighed 50kg and had a mean time between failures of around 2 months. In the early 1960's, the corresponding fully transistorised equipment consumed only 60W for increased output power, weighed 5kg and operated for periods of two years between services.

Equally impressive improvements also occurred in the interference and stability specification of equipment,

however, which formed the essential first step towards channel splitting. The introduction of the double conversion receiver with a second IF at 455kHz employing a block LC filter provided over 80dB rejection at the channel edges. Output filters were added to transmitters and the output spectrum of FM units restricted by the inclusion of deviation limiters. The development of crystal technology made possible a frequency stability of ±15ppm to be maintained over a temperature range of 80^{o}. This was further improved to better than ±5ppm by the advent of the crystal oven, first used in the USA and Canada. Steps were also taken to reduce the susceptibility of the receiver to desensitisation and intermodulation, mainly by concentrating on the front end linearity.

1.2.3 SPECTRAL CONGESTION AND CHANNEL SPLITTING

The rapid growth in both number and type of user of mobile radio following World War II produced a considerable demand for more channels. At the 1947 International Radio Conference a modest 4.7% of the available spectrum was allocated to mobile radio. This was later reduced following the decision to curtail the upper limit of the high VHF band to 174MHz from 184MHz. Hence, the extra channels demanded had to provided by more efficient use of the existing spectrum. The only feasible way of providing a large number of extra frequencies was by a process of

channel splitting, which had only now become possible through improvements in equipment performance.

In the UK following the report of the Mobile Radio Committee in 1955, channel spacings were reduced to 25kHz in the low band and to 50kHz and subsequently 25kHz in the high band. This was accomplished by the insertion of new channels centred at the edges the old ones, thus retaining compatibility with older equipment during the changeover period. Each changeover of equipment was carried out over a five year period, although in the high band, the conversion to 25kHz spacing was started before that to 50kHz was completed. Some infrequently used equipment was not however changed until obsolescence forced the purchasing of new units.

In the USA the FCC originally established a 40kHz channel spacing for the 20-50MHz band and a 60kHz channel spacing for the 148-162MHz band. These were split to 20kHz and 30kHz respectively along the lines of the UK system to permit compatibility with older equipment during the changeover periods. It was also necessary to half the FM deviation to permit these narrower channels to be introduced. This had the effect of reducing the signal-to-noise advantage over AM systems, and also more importantly, reducing the capture effect and hence increasing the susceptibility to co-channel interference.

1.3 ADVANCED MOBILE RADIO SYSTEMS

1.3.1 PAGING

Several advanced mobile radio schemes have been proposed which seek to improve upon the spectral efficiency and/or the quality and services provided by the simple conventional systems. Radio paging is an important example of a system in the former category. There are countless situations in which there is a need to call a person who is away from the office etc. but where immediate acknowledgement is not required. By employing selective calling, paging permits the alertion of one or a number of personnel from a group utilising a single radio channel. Hence a low cost, highly spectrally efficient one-way communication capability can be envisaged, that can vary in size from the small office set-up to the country-wide fireman's call-out system.

The interest in paging systems first arose in the mid 1950's out of the need to communicate reliably with important personnel out of range of the telephone. The first systems employed inductive loop principles operating on carrier frequencies in the range 30kHz to 50kHz. Separate receiver addressing was achieved by tuning each to a different frequency. As the need for more users arose, a change took place to a 40kHz carrier with FM modulation.

Paging systems rapidly expanded in the 1960's and 70's using frequencies in the 27-42MHz band with 25kHz and subsequently 10kHz channel spacings. The former channel spacing was also employed for the UHF fireman's paging system operating in the 470MHz band. By 1973 it was estimated [3] that 15,000 units were in use nationwide for this purpose.

1.3.2 RADIO TELEPHONES

The vast majority of mobile radio systems in the world evolved as private systems consisting of one or more base stations with a larger number of mobiles operating in a relatively small area. Whilst these satisfied the needs of users requiring fleet co-ordination etc., such schemes did not provide access to the public land telephone network nor permit communication over a wide area as required by business users etc. The original aim of the Post Office radio-telephone scheme was to provide full duplex communication between any telephone connected to the PSTN and a mobile located anywhere in the country. The technical, operational and planning requirements of such a scheme are obviously immense and the actual systems installed provided only a restricted service.

The first trial system to be installed in the UK was in Manchester in 1959. Following this, a slow but steady

improvement was made leading to the first system for main population centres, known as System 1, to be installed in London in 1965. The service was operator connected however, hence it was expensive and attracted only prestige users. The next development was the introduction of System 3 in 1972 (System 2 was never practically operational). This was again a manual system and also simplex, although it catered for more users. Eventually this was extended to cover 40-45% of UK population in distinct urban areas. Further expansion was made difficult by the lack of suitable frequencies.

In 1981, the number of frequencies available was increased to 110 by the reduction in channel spacing to 12.5kHz. In the same year the first fully automatic direct dial system was introduced in London, known as System 4. System 3 was not withdrawn at this time, and since no additional spectrum was available, channels had to be shared between the two systems. Although the growth in radio telephones in the UK was well below that in Scandanavia, for example, due primarily to lack of marketing by British Telecom (formerly the GPO), it was still not possible to meet the demands in the capital. This produced a waiting list extending into thousands, although in the provinces the capacity exceeded the demand.

1.3.3 CELLULAR SYSTEMS

The cellular concept is designed to provide better quality, serve far more subscribers and offer much improved overall spectral efficiency compared to traditional mobile radio systems. By employing a large number of base stations each serving an area (cell) as little as half a km in diameter the cellular approach permits a much smaller frequency re-use distance than conventional systems. Cells are grouped together in clusters with the entire allocation of channels then being available for each cluster (chapter 2.4).

Although the advantages of the cellular concept were realised as early as the 1940's, the technology to implement low-cost multi-channel equipment did not become available until the early 1970's. It was also recognised that a large block of spectrum would be required however none was available in the conventional mobile radio bands. In 1971, the American Telephone and Telegraph company (AT&T) proposed the development of a cellular system in the USA. The FCC responded to this by allocating 40MHz of spectrum in the 800MHz band in 1974. The first trial system was installed in Chicago in 1978 for 2000 subscribers using the Automatic Mobile Phone System (AMPS) system developed by AT&T.

The introduction of cellular radio in the UK was made possible by the allocation of spectrum in the 900MHz band for mobile radio by WARC 1979. This was followed by the DTI granting licences to two operators, British Telecom-Securicor (TSCR) and Racal-Vodafone for operation to begin early in 1985. A modified form of the AMPS system, known as the Total Access Communication System (TACS) was chosen with the peak voice deviation limited to 9.5kHz for compatibility with the UK 25kHz channel spacing.

Various other cellular systems are in operation or are planned in other parts of the world. The Nordic Mobile Telephone (NMT) became operational in Denmark, Sweden, Finland and Norway in October 1981 and had reached 40,000 subscribers by March 1983 [4]. West Germany began operation of a low capacity system in 1984 also at 450MHz, called Netz-C and based upon the Siemens C-450 standard. Japan, Australia and Saudi Arabia are also among the countries currently operating cellular systems.

1.4 THE FUTURE OF MOBILE RADIO

1.4.1 CELLULAR AND RELATED SYSTEMS

The majority of European countries are at present operating or planning to operate cellular systems. In the UK, TACS has already started to take over from the established System 3 and 4 radio telephones in densely populated areas, but this latter service is likely to continue for some time. In order to cope with the ever increasing number of users and to satisfy their requirements, the cellular systems will continue to grow, aided by new technology which will provide more cost effective solutions and offer greater choice to the user. However, the four European cellular systems, TACS, NMT, MATS-E and C-450 or 900, are non-compatible especially in their control procedures, thus preventing inter-country operation.

Shortly after WARC 1979, the CEPT began consideration of a Pan-European system for operation in the 1990's which would also provide additional features compared to present systems. The new system is almost certainly to be wideband, with its many advantages, particularly the simplification of base station design. Currently there are several systems under investigation, including those from Tekade, Bosch, Ericsson and CD-900 (Autotel) [5]. In common with the present trend towards all digital telephone networks,

all of the proposed systems use digitised speech. However, in order to obtain at least as good spectral efficiency as conventional systems, a maximum speech data bit rate of some 16kb/s is available after channel coding and signalling have been included. This precludes the use of PCM and delta-modulation as used for land line systems. Instead considerably more complex (and poorer speech quality) techniques such as linear predictive coding (LPC) or sub-band coding (SBC) are necessary which still have outstanding technical problems. In view of this it seems unlikely that suitably compact equipment can be produced for operation by the early 1990's.

Analogue wideband schemes have received little or no attention. However, a technique known as time-compression multiplexing (TCM) exists [6], which in conjunction with an amplitude or frequency modulated bearer can form the basis of a system suitable for both conventional as well as cellular mobile radio systems. Unlike the proposed digital systems, the technology required to implement the necessary time-companding processes is already well-developed. However, some considerable work on the characteristics of a wideband bearer with a time-compression multiplexed modulating signal is necessary before a system can be specified.

1.4.2 USE OF ADDITIONAL SPECTRUM

In addition to the 800-900MHz band, WARC 1979 also allocated the 41-68MHz (Band I) and 174-203MHZ (Band III) to mobile radio. These have become vacant in the UK, although not in certain European countries, following the recent termination of 405-line TV transmissions,. Hence, considerable care in the choice of frequencies will be required in the immediate future, especially in SE England. Since these bands are likely to be the last significant blocks of spectrum given to mobile radio in the foreseeable future, there has been much debate over the best way to utilise the additional spectrum. In the UK, the basic proposals is to treat Band III as a high quality band due to its excellent propagation characteristics. Trunking techniques will be encouraged and the use of 12.5kHz FM channels adopted to improve efficiency. There is also the possibility of adopting SSB modulation when the remaining technical problems are solved, which can more than double the number of available channels with little degradation in quality [7]. Other recommendations [8] are that mobiles should also be synthesised with at least 5MHz switching range to permit operation in different parts of the country, and that a 1200 bit/s FSK data signalling standard should be adopted. Although not yet considered, there is no reason why wideband time-

multiplexed systems could not also be used. In addition, the various public utilities currently operating in the 104-108MHz band must be accommodated by 1995 at the latest.

1.5 REFERENCES

(1) Noble,D.E.: 'The history of land-mobile radio communications', Proc. IRE, vol.50, May 1962, pp.1405-14

(2) McCormick,J.A.: 'The radio spectrum-polluted pond or flowing river', Proc. Int. Conf. on Comms., June 1974, pp. 19B/1-6, IEEE 1974.

(3) Drybrough,D.A.S.: 'Mobile V.H.F and U.H.F radio systems in the U.K.', Proc. IEE, vol.122, no.10R, Oct.1975, IEE Reviews, pp.953-76.

(4) Billstrom,O.: 'The Nordic Mobile Telephone system', Proc. Conf. on Int. Developments in Cellular Radio', Oyez Scientific and Technical Services, Feb.1984, pp.1/11-11/11.

(5) Langewellpott,U.: 'Autotel: a novel wideband mobile telephone and data system at 900MHz', Proc. 2nd Int. Conf. on Radio Spectrum Conservation Techniques', Sept.1983, pp.85-88.

(6) Skuse,B.:'An alternative time-compression multiplexed VHF single sideband system', MSc thesis, University of Bath, 1984.

(7) Durkin,J., and Barnes,D.M.: 'An evaluation of single sideband radio for use in VHF private land mobile radio services', Proc. 32nd IEEE Conf. on Vehicular Technology, May 1982, pp.202-7.

(8) Fisher,K.P.: 'The new land mobile radio service in Band III', Proc IEE Conf. on Mobile Radio Systems and Techniques, no.238, Sept.1984, pp.100-104.

CHAPTER TWO

SPECTRUM UTILISATION IN MOBILE RADIO

2.1 INTRODUCTION

A basic land mobile radio scheme consists of a suitably located base (fixed) station and a number of independent mobile units. The vast majority of systems provide two-way communication between a mobile and base on a push-to-talk (simplex) basis. If there are no other users operating within a few MHz in range of a particular system then the service may be provided by a single frequency channel (section 2.2.1). However, in most practical cases when several channels are required in an area, the most efficient and interference free use of the spectrum is obtained by reverting to two frequency operation (section 2.2.2). The increasing use of telephone type (duplex) operation also obvious requires a two frequency channel allocation (section 2.2.3).

Originally all mobile radio equipment was single channel with a coverage area limited to that which could be provided by a single (high power) base station. When extra range was required, various area coverage schemes were introduced, some requiring manual channel change depending upon location. These systems have poor spectral efficiency since frequencies may only be re-used at vast

distances (section 2.3). As such system growth is severely limited by the lack of further channels. In addition there is a high possibility of an appreciable call waiting time, since only one channel is normally provided for 30-40 mobiles in a given area. Trunked systems, in which a channel may be selected from a group available for use have a much reduced probability of blocking (section 2.4). Both manual and automatic channel selection systems are in use, with various cellular systems combining the advantages of the latter with the efficiency of frequency re-use at short distances.

2.2 MODES OF OPERATION

2.2.1 SINGLE FREQUENCY SIMPLEX

This is the simplest mode of operation, utilising the same channel for both receive and transmit. At first sight this appears to be the most economical in the use of spectrum, and has the added advantage of allowing mobiles to communicate directly with each other. However, a number of disadvantages exist, particularly in areas of high traffic.

If a transmitter is physically located close to a receiver on the same frequency, the high incident power at the receiver will cause intermodulation to occur due to the limited dynamic range of the front end (chapter 3.3.3). The same occurs even if the frequencies are separated by several channel spacings due to the relatively wide receiver RF bandwidth. Thus, co-sited systems need to be separated from each other by at least some 4-5MHz before acceptable performance can be achieved. This situation is further complicated by the need to ensure that no two frequency separations are equal which would otherwise lead to on-channel intermodulation (chapter 3.4.3). An alternative arrangement is to gain isolation by physical separation of base station transmitters and receivers. Unfortunately adequate performance is only

achievable by locating the equipment at separate sites located some 1-2km apart. This arrangement is adopted for airborne communications but the expense is not justifiable for mobile systems. Thus for mobile systems, single frequency simplex, far from being spectrally efficient, is in fact extremely wasteful of spectrum.

2.2.2 TWO FREQUENCY SIMPLEX

The necessary frequency separation to avoid receiver desensitisation can be achieved in an alternative manner by allocating separate blocks of frequencies to transmitters and receivers as shown in fig.2.1(a). The frequency spacing between the blocks should not be some sub-multiple of the intermediate frequency (ie. not 10.7 or 5.35MHz etc.) and is typically 4-5MHz. Although twice as many frequencies are required compared to single frequency working, the overall spectral efficiency is far greater especially when many channels are needed. This mode of operation does have the disadvantage that mobiles may no longer communicate directly with other mobiles. However, it is possible for the base station to operate in a repeater mode by arranging for the receiver audio output to be connected to the transmitter. This system, commonly known as talk-through, has the added advantage that communication is possible between two mobiles that would otherwise be out of range of each other.

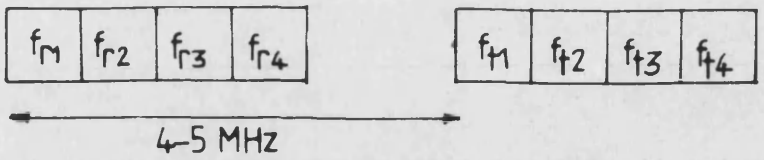

Fig. 2.1(a) Two frequency simplex channel assignment.

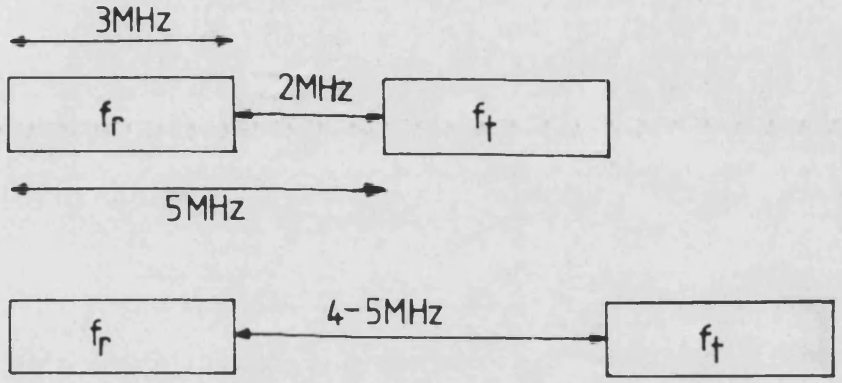

Fig. 2.1(b) Revised assignment for large blocks.

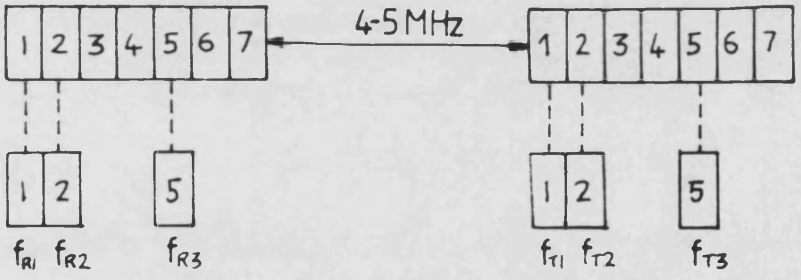

Fig. 2.1(c) Typical arrangement to avoid on-channel intermodulation.

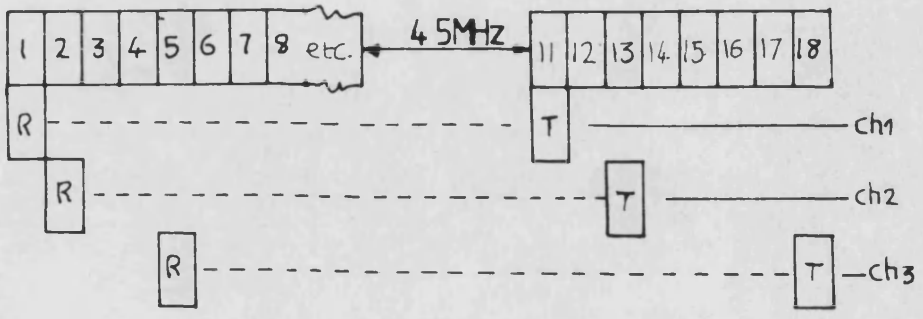

Fig. 2.1(d) Typical dual frequency duplex intermodulation free assignment.

When several frequencies in the same block are required in the same area, two additional important factors arise;

(1) The frequency separation between any receiver and transmitter in use must be some 4-5MHz, this leads to the modified arrangement shown in fig.2.1(b), where the actual separation between a receiver and its corresponding transmitter is 4-5MHz+N times channel spacing. N is the number of frequencies in the block.

(2) To avoid the otherwise strong possibility of on-channel intermodulation, the frequencies in a block should be allocated on at least a third-order compatible basis (chapter 3.4.3). A typical arrangement for four channels is shown in fig.2.1(c), it may be seen that three frequencies in the block are unusable in this location. However, the overall spectral efficiency is still better than single frequency simplex.

2.2.3 DUAL FREQUENCY DUPLEX

In many respects, this mode of operation is similar to two-frequency simplex and two suitably spaced blocks with compatible frequency allocations may be utilised. However, there is the additional possibility of a+b+c

intermodulation products arising due to interaction between frequencies from both blocks. If two base station transmitters on frequencies f_1 and f_2 are operational, and a strong mobile signal on $f_1+\Delta f$ is received, where Δf is the (common) receive-to-transmit spacing, a possible intermodulation product is $(f_2) + (f_1 + \Delta) - (f_1) = f_2 + \Delta f$ ie. the second receive frequency. Hence a mobile close to the base station can swamp a weak signal on another receive frequency. In common with the formation of other on-channel intermodulation signals, this situation arises due to the uniform receiver to transmitter frequency spacing.

Alleviation of this problem involves the extension of the compatible frequency assignment over the two blocks. This is difficult to achieve when there are a large number of channels, but a relatively simple arrangement is possible with, for example, three duplex channels [1] (fig.2.1(d)). Interference is avoided when any two duplex channels operate, but with three operational there exists the possibility of 5^{th} order products which are not catered for. Fortunately, this is statistically less likely.

An additional consideration with duplex systems is the provision of an antenna system which permits simultaneous transmission and reception. High level transmitter

outputs must be prevented from entering the receiver, and whilst a 4-5MHz frequency separation is adequate for simplex operation, some additional isolation is required when the transmitter and receiver operate simultaneously. Isolation may be achieved by physical separation of transmit and receive antennae but on a crowded mast etc. this may not be possible. An alternative is to combine the transmitter and receiver in a device known as a duplexer before connection to a common antenna. This has the advantage of improved isolation and allows the single aerial to be positioned for optimal coverage.

The duplexer consists of ferrite isolators and cavity filters and is not unlike the transmitter combiner (chapter 3.4.1). Either band-pass or band-stop filters or a combination of both may be employed. The former has the advantage of rejecting all signals outside the passband which may be beneficial when there are other unwanted signals present, whereas the latter can provide greater rejection of a particularly troublesome frequency. As the receive to transmit frequency is decreased, higher Q and hence bulkier filters which require frequent re-alignment are needed. As the frequency of operation increases, the filter size may be reduced but for a given Q, the separation must be higher. Hence for cellular systems at 900MHz, a separation of 45MHz has been adopted [6].

2.3 CONVENTIONAL SYSTEMS

2.3.1 SINGLE BASE STATION SYSTEMS

The early use of mobile radio was for local communication between a central office and a small number of police (or other service) vehicles. This was provided by a high power base station transmitting several hundred watts on a single radio channel. The relatively small total number of users allowed wide channel spacings of up to 200kHz to be used and permitted similar schemes to operate in the same locality without interference. The good co-channel rejection of high deviation angle modulation systems was also an important contributory factor. As the number of users increased, more frequencies were allocated by channel splitting and use of adjacent channels in adjacent geographical areas became necessary. There was also a move towards the sharing of base station facilities by several users. All of these factors contributed to the increased likelyhood of interference.

As the number of mobiles sharing a radio channel increased, the probability of excessive waiting time due to the channel being in in use also increased. The problem could only be solved by the provision of extra frequencies and the introduction of multi-channel equipment. However, since a new set of crystals were required for each addi-

tional frequency and manual channel selection had to be employed, this was generally limited to less than six channels in total. The spectral efficiency of the systems was low since frequencies could only be used at vast distances, especially in the low VHF band. In this respect, the introduction of 12.5kHz channels virtually removed any advantage of angle modulation since the capture effect had practically vanished.

2.3.2 MULTIPLE BASE STATION SYSTEMS

There are countless instances where users of mobile radio need to operate over an area greatly exceeding the coverage area of the typical single transmitter system above. Increasing transmitter power beyond a certain level provides little or no benefit especially when range is limited by geographical factors. One solution is to use additional base stations, and many schemes have evolved utilising this principle. The simplest system to implement is to employ extra base stations carrying the same modulation but on different frequencies. The mobile user then has to manually switch channels depending upon location. However, with untrained radio operators and coverage areas which are not clearly defined, this results in many lost calls. The spectral efficiency of the system is also poor. Another system is to use co-channel base stations but with only one operational at any one time. This places the

responsibility upon the fixed operator as when to select a particular base station. However, this system is also far from ideal since a lack of knowledge of the mobile's position often results in the wrong base station being selected. With the addition of selective calling of mobiles and a voting arrangement to access the best base station, several workable systems have evolved on this principle. Again spectral efficiency is poor, and blocking of calls becomes a problem since only one mobile in an area may be active at a time.

More recently, systems have been proposed which do not require manual selection of channel for their operation. Of these, spaced carrier and quasi-synchronous systems are the most well known. In spaced carrier AM systems [2] the same message is broadcast from, say, three base stations, whose carrier frequencies are offset by, say, -9,-3 and +9 kHz from the channel centre, such that the beat frequency is well outside the audio passband. A receiver tuned to the centre frequency can then receive an acceptable signal without adjustment for varying location. The disadvantages are that a wider than normal channel bandwidth is required and intermodulation distortion occurs in overlap areas.

The quasi-synchronous approach [3,4] is similar except that the offset, and hence beat frequency, is

arranged to be below the audio passband. Such a system with offsets of a few ten's of Hz in the VHF and UHF bands became possible with the advent of higher stability oscillators. FM quasi-sync systems do not perform well unless particular care is paid to modulation matching and tailoring of coverage areas. AM schemes are workable with the modulation less well matched but performance is improved if the offset is reduced to only a few Hz rather than ten's of Hz.

Like the single base station systems, the high transmit powers employed force co-channel systems to be widely spaced. Typically then, a frequency may only be re-used a few times in a country the size of the UK. The limited amount of mobile radio spectrum only allows a very modest number of channels to be allocated to each user. In even moderate traffic areas the channel occupancy is high and there exists a high possibility that there will be no channels available when a user wishes to place a call. In such systems there comes a time when no growth is possible unless further channels become available. This can only occur if further spectrum is allocated to mobile radio or a further reduction in channel spacing is carried out. Further VHF or UHF spectrum is unlikely due to competition from other users, although there have been proposals to use spectrum in the 60GHz band [7]. A split to 12.5kHz

channels at UHF is possible if the corresponding equipment frequency stability can be economically achieved, but the introduction of 6.25 or 5kHz channels would entail the use of radically different modulation methods (eg. SSB or low bit rate digital speech) which still have outstanding practical difficulties.

2.4 TRUNKED SYSTEMS

2.4.1 PRINCIPLES

The absolute maximum number of simultaneous calls that can be handled by any mobile radio system in any area without frequency re-use is equal to the total number of allocated channels. Conventional systems employ high transmit powers making re-use distances enormous, hence the traffic per unit area must be kept low. Much higher capacity may be achieved if the power and hence the re-use distance is substantially decreased. Greater spectral efficiency results since the increased capacity is obtained without additional channels.

This principle forms the basis of the cellular radio concept [5]. Each base station provides coverage of relatively small area (cell) which may be as little as half a km across. Additional base stations on different frequencies provide coverage of adjacent cells as shown in fig.2.2. At a suitable distance away, a frequency may be re-used, eg. A1 and A2 in fig.2.2. If there are n cells using different frequencies and a total of N channels available , then nominally N/n channels are available per cell. Mobiles are able to transceive on any of the N channels, made possible by the advent of low cost frequency synthesis. Hence communication with a mobile can be main-

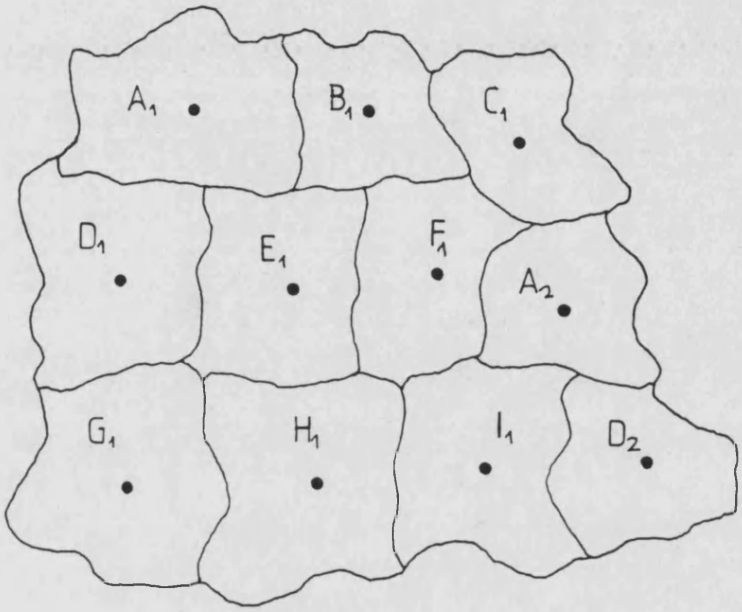

Q_i : ith cell using channel group Q

• Transmitter location

Fig.2.2 Cellular layout showing principle of frequency re-use.

tained over the entire cellular network, rather than just in the area served by the local base station(s) as with conventional systems. This facility involves automatic channel changeover as a mobile traverses a cell boundary, a process known as 'hand-off'. Thus the cellular concept has the features of high traffic density and broad coverage, made possible at the expense of an increased number of base stations and the provision of a small number of highly complex system management and switching stations.

As the traffic demand in a cell increases the capacity of the cell's (N/n) channels will eventually be reached. Further growth in traffic within the cell will require a revision of cell boundaries so that the area previously regarded as a single cell can utilise additional channel sets. A process called 'cell-splitting' satisfies these requirements. Fig.2.3(a) shows the arrangement after one cell (previously F1) has been split into four smaller cells (B6,C6,H6 and I6). As the traffic demand grows further cells may be split until eventually the entire area will have been converted into smaller cells (fig.2.3(b)). In practice, the modifications to the cell structure may not be quite as dramatic as above. Obviously, further splitting of these smaller cells may take place when the traffic demand again exceeds the capacity. The overall benefit is that decreasing the cell area

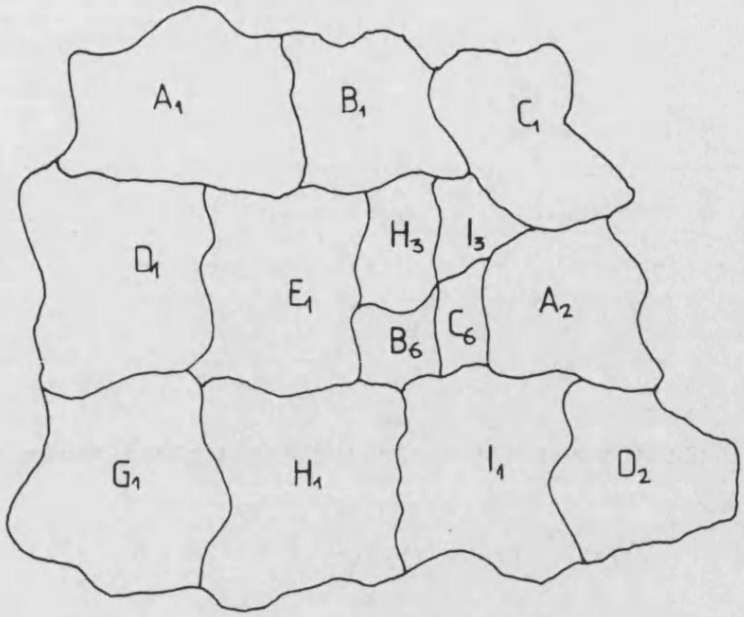

Fig.2.3(a) Cellular layout illustrating early stage of cell splitting.

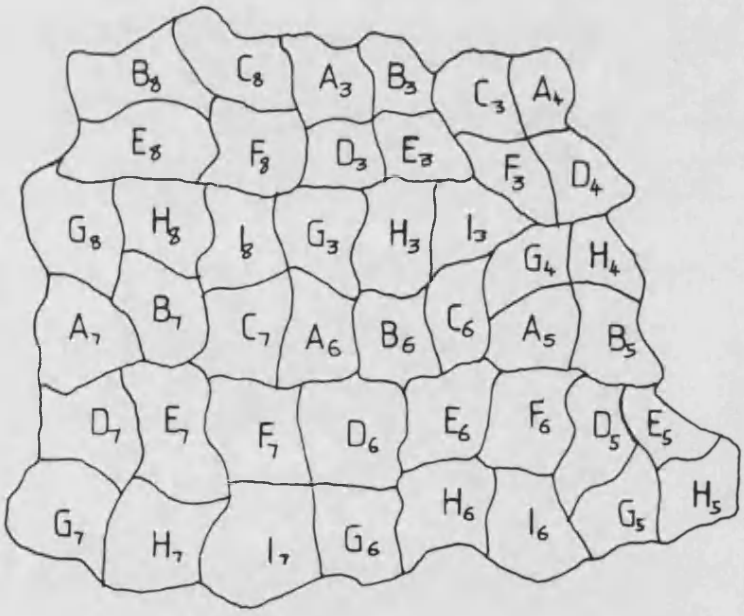

Q_i : i^{th} cell using channel set Q

Fig.2.3(b) Cellular layout illustrating advanced stage of cell splitting.

allows the system to adjust to a growing traffic demand density (ie. simultaneous calls per unit area) without further spectral requirements. In addition, the variation of traffic density over, say, urban and rural areas, may be accommodated be providing small and large cells respectively.

2.4.2 PRACTICAL SYSTEMS

There are several cellular systems in operation throughout the world operating in the 450 and 900MHz bands. Frequency modulation is adopted for its capture effect which provides some co-channel interference protection. Each cellular system has originated from a different source and as such differs in many areas from all the others. One particular area of difference is in the hand-off and other system management protocols and structures.

A modified form of the Automatic Mobile Telephone System (AMPS) has been adopted as the first generation cellular system in the UK and is known as Total Access Communication System (TACS) [6]. This system allows for 1000 full-duplex 25kHz channels in the 900MHz band to be shared between the two operators, Racal-Vodafone and British Telecom-Securicor. The former has adopted a cluster size of 7, which is a compromise between the co-channel and trunking efficiency requirements. A peak frequency

deviation of $\pm$9.5kHz for voice signals, with a frequency arrangement which does not permit adjacent channels in the same cell, serves to equalise the median levels of adjacent- and co-channel interference.

2.5 REFERENCES

(1) Panell,W.M.: 'Frequency engineering in mobile radio bands', Granta Technical Edition, 1979, Appendix 6, Annexe C.

(2) Brinkley,J.R.:'A method of increasing the range of VHF communication systems by multi-carrier amplitude modulation', IEE Journal, vol.93, pt.III, pp.159-166, April 1946.

(3) Carter,D.:'Quasi-synchronous operation of AM transmitters', IEE Int. Conf. on Communications Equipment and Systems, pp.90-93, June 1976.

(4) Gray,G.D.:'The simulcasting technique: an approach to total area radio coverage', IEEE Trans. on Vehicular Technology, vol.VT-28, no.2, pp.117-125, May 1979.

(5) Mac Donald,V.H.:'The cellular concept', Bell System Technical Journal, vol.58, no.1, pp.15-39, Jan.1979.

(6) United Kingdom Total Access Communications System, Mobile Station-Land Station Compatibility Specification, Issue 3, Oct.1984.

(7) Steele.R.:'Towards a high capacity digital cellular mobile radio system', IEE Proc. F (GB), vol.132, no.5, pp.405-15, Aug.1985.

CHAPTER THREE

INTERMODULATION IN MOBILE RADIO SYSTEMS

3.1 INTRODUCTION

Intermodulation products (IMP's) are formed when one or more input signals interact in a non-linear network to produce signals of frequencies other than those present in the original waveform (section 3.2). Whilst, for example, this process is fundamental to the operation of frequency mixers and modulators, it is extremely undesirable in the vast majority of other systems. Since all practical devices exhibit non-linearity to a greater or lesser extent, it is of foremost concern in system design to be able to predict the interference resulting in the expected operating conditions.

Intermodulation interference is frequently troublesome in mobile radio systems, which invariably utilise the available spectrum by the traditional approach of subdivision into a number of narrow-band channels. The problem is especially acute when geographical or other factors force many users to share facilities at a common base station site (section 3.3). In such circumstances, certain channels may be completely swamped, although often only intermittently, by interference thus severely impairing their intended use.

Although measures may be taken (section 3.4.1) to reduce the level of IMP's generated in transmitter outputs, there is little which may be economically achieved to alleviate receiver generated interference (section 3.4.2). In certain cases, the only solution is to avoid operation on channels particularly prone to interference. To this end, various intermodulation 'free' frequency lists have been derived but there is an immediate spectral efficiency penalty which rises sharply as the number of channels required in a given area increases (section 3.4.3). Even with the use of such groups, high order non-linearities or freak conditions may still impair operation.

An alternative approach is to allocate a much smaller number of wideband channels, typically many 100's of kHz wide. Each channel is then shared amongst a number of users by a process other than FDM, eg. a time multiplexing system. In this way the total number of possible intermodulation products may be greatly reduced (section 3.5).

3.2 FORMATION OF INTERMODULATION PRODUCTS

The response, y(t), of a typical non-linearity to an input signal, x(t), can be expressed by the polynomial expansion

$$y(t) = A_0 + A_1x(t) + A_2x^2(t) + \ldots\ldots \qquad (3.1)$$

providing $|x(t)| \leq 1$

This may be rewritten in compact form as

$$y(t) = \sum_{n=0}^{\infty} A_n x^n(t) \qquad (3.2)$$

In a perfect linear system, all coefficients except A_1 are zero. However, a practical 'linear' system will have other non-zero components, although it is possible to introduce a finite limit, N, such that all coefficients of order greater than N are negligible. N is then known as the degree of the polynomial. Thus

$$y(t) = \sum_{n=0}^{N} A_n x^n(t) \qquad (3.3)$$

The output of the non-linearity when the input consists of a single sinusoid, $a\cos[\omega_m t + \phi]$, is

$$y(t) = A_0 + aA_1\cos\left[\omega_m t + \phi\right] + \frac{aA_2}{2}\left[1 + \cos\left[2\omega_m t + 2\phi\right]\right]$$

$$+ \frac{aA_3}{2}\cos\left[\omega_m t + \phi\right]$$

$$+ \frac{aA_3}{4}\left[\cos\left[3\omega_m t + 3\phi\right] + \cos\left[\omega_m t + \phi\right]\right] + \ldots\ldots \qquad (3.4)$$

For a two tone input, $a\cos\left[\omega_1 t + \phi 1\right] + b\cos\left[\omega_2 t + \phi 2\right]$, the n^{th} order output, $y_n(t)$ is given by

$$y_n(t) = A_n\left[a\cos\left[\omega_1 t + \phi 1\right] + b\cos\left[\omega_2 t + \phi 2\right]\right]^n \qquad (3.5)$$

The expansion of this expression is tedious and is further complicated in practice by AM-PM conversion etc. which involves the use of complex coefficients, $A_n = R_n + jX_n$. The evaluation of component magnitudes involves complex analysis [1] but considerable insight may be gained from a knowledge of just the frequencies of the intermodulation products. If the amplitudes and phases of the components in eqn.3.5 are ignored then

$$y_n(t) = \left[\cos\omega_1 t + \cos\omega_2 t\right]^n \qquad (3.6)$$

which can be expressed as the summation

$$y_n(t) = \sum_{i=1}^{\lceil n \rceil} \cos i\omega_1 t \cdot \cos(n-i)\omega_2 t \qquad (3.7)$$

Expansion of this equation is still complicated for large n but the intermodulation frequencies may be evaluated by the following piece-meal process [2]. Any particular n^{th} order component has a frequency, F_n, given by

$$F_n = \sum_{j=1}^{n} \pm f_k \qquad (3.8)$$

where f_k is any of the input frequencies.

Hence any n^{th} order product has a frequency composed of the combination of n input frequencies. For n=3 and $f_2 > f_1$, the resulting positive frequency combinations are f_1, f_2, $2f_1-f_2$, $2f_2-f_1$, $3f_1$, $3f_2$, $2f_1+f_2$ and $2f_2+f_1$ as shown in fig.3.1(a).

Both the number and range of intermodulation frequencies increases dramatically as n increases. In addition, if the input signals are modulated then the intermodulation products are bands of interference rather than discrete frequencies. If all the input signals have equal bandwidth, B, then the width of each intermodulation band is nB as shown in fig.3.1(b).

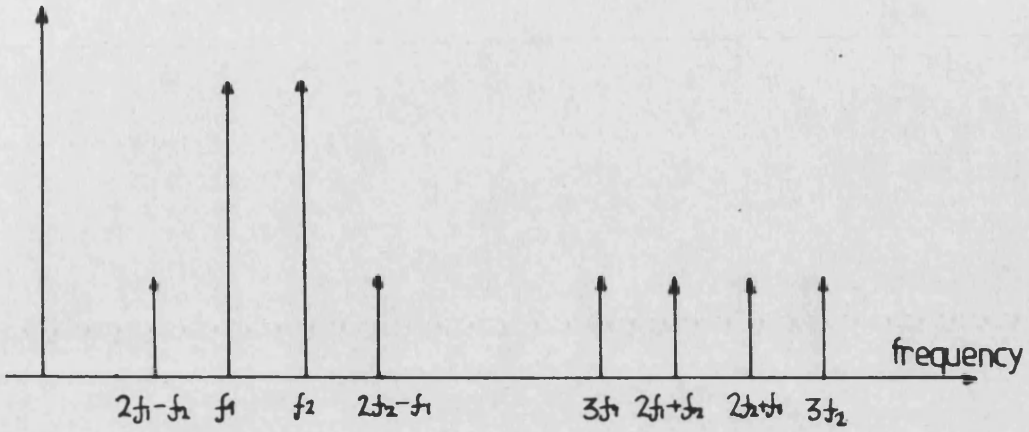

Fig. 3.1(a) Positive third order intermodulation products of two component frequencies.

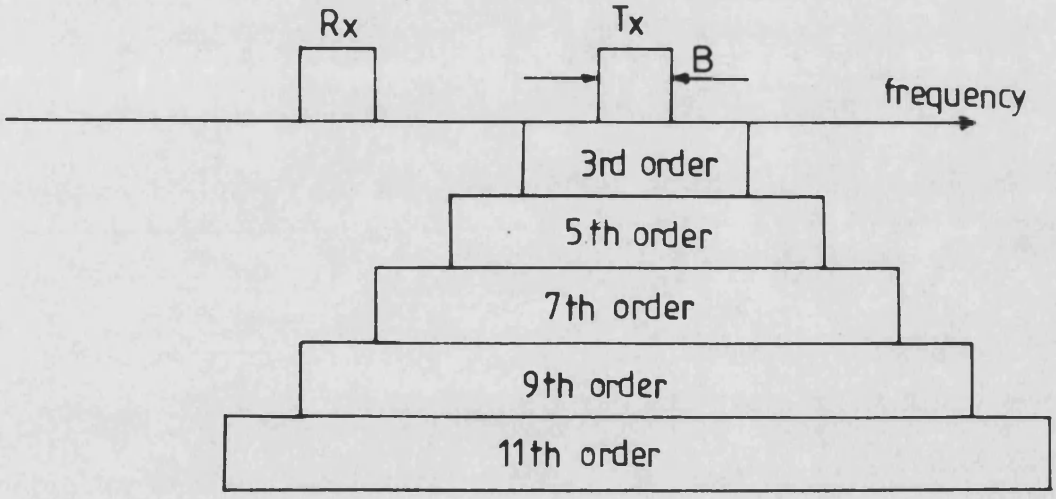

Fig. 3.1(b) Illustrating broadening of interference band when component signals have modulation bandwidth of B.

3.3 INTERMODULATION GENERATION MECHANISMS IN CONVENTIONAL MOBILE RADIO SYSTEMS

3.3.1 BACKGROUND

Historically, the various users of mobile radio have been accommodated within the available spectrum by subdivision of the allocated frequency bands into distinct channels by frequency-division multiplexing. As the channel spacings have been progressively reduced in an attempt to meet the needs of an ever increasing number of users, so the number of channels per given unit of spectrum has increased. Coupled with the limited number of base stations, this has inevitably resulted in many sets of equipment on closely spaced frequencies operating in close proximity to one another. Such an arrangement provides ideal conditions for the generation of large numbers of intermodulation products (via the process detailed in 3.2) whenever a non-linearity occurs.

Since the frequency bands allocated to mobile radio are relatively narrow, only odd-ordered IMP's will generally fall within the same band as the original signals. However, even-ordered components may well fall on frequencies in other mobile radio bands in use in the same locality. Suppose four frequencies, f_1 ,f_2 ,f_3 ,f_4 in use in the low VHF band are 77.0, 77.1, 77.2 and 77.3 MHz respec-

tively. Second order intermodulation products, eg. $2f_1$ etc., fall in the high VHF band, whilst sixth order products, eg. $3f_1 + 3f_3 = 462.6MHz$ fall in the UHF band. There are many third order combinations of the form, $f=2a-b$ and $f=a+b-c$, which fall on channel, for example $2f_2-f_1=f_3$ and $f_1+f_4-f_3=f_2$. Of these, the former type, involving only two components is statistically more likely. In addition there are an infinite number of other higher odd ordered combinations which also fall on channel, fortunately, most are normally of negligible magnitude.

There are three principle non-linearity mechanisms in a mobile radio system which are responsible for the production of IMP's. These are;

(1) In the transmitter output stages.

(2) In the receiver front end.

(3) In the surrounding metalwork of the antenna mast structure.

3.3.2 TRANSMITTER OUTPUT STAGE

Transmitter power amplifiers, particularly those of FM equipment, are highly non-linear and act as effective high power mixers when multiple signals are present. This situation is common with close spaced equipment due to

coupling via power supplies, antenna feeders, radiation etc.. The problem is even more acute when insufficient mast space forces a number of transmitters, often closely spaced in frequency, to share the same antenna/feeder combination. An unwanted signal may appear at a transmitter output port at a level only a few dB's down on the original transmit power. Coupled with a typical figure for the transmitter mixing loss of only 10dB, this can cause a multitude of intermodulation signals of appreciable magnitude to be radiated from the antenna. Consequently, the performance of any local receivers operating on these frequencies will be severely impaired. Unfortunately, due to the normal policy of allocating channels on a simple equal frequency spacing basis, there is a very high probability that this will occur.

3.3.3 RECEIVER FRONT END

Intermodulation in the front end of a receiver is extremely common and affects both mobile as well as base station equipment. It arises due to the lack of selectivity in the early stages of the majority of receivers and the limited dynamic range of the RF amplifier. The bandwidth of the RF stage, particularly if the equipment is multichannel, will be of the order of MHz and that of the first IF stage (in double conversion sets) will be several times greater than the channel spacing. A typical

dynamic range figure would be 65dB under conditions of maximum sensitivity, ie. when receiving a wanted signal of around 0.5μV (-113dBm). Hence extraneous signals within the passband of the RF amplifier and at a level of -48dBm could produce discernible intermodulation interference in the final output of the receiver. Since the magnitude of third order components increases by 9dB for each 3dB rise in all the constituent components, their is a high probability of the wanted signal being swamped completely by interference.

3.3.4 BASE STATION METALWORK STRUCTURE

The third source of intermodulation is associated with imperfect joints in the metalwork of the mast structure. Signals induced from nearby antennae are rectified by these junctions and the resulting intermodulation products re-radiated. Corrosion inevitably occurs in any steel structure and the best that can be done is to throughly clean troublesome joints and bond with copper to minimise the problem.

3.4 IMPLEMENTATION AND DEFICIENCIES OF INTERMODULATION REDUCTION TECHNIQUES

3.4.1 ISOLATION OF BASE STATION TRANSMITTER OUTPUTS

3.4.1.1 SEPARATE ANTENNA WORKING

The severity of the intermodulation produced at transmitter outputs can be lessened if the number or level of extraneous signals can be reduced. If these unwanted signals appear due to coupling between the aerial and feeder networks, then benefit may be obtained by greater antenna spacing and/or by placing isolator components at the transmitter outputs. If, however, coupling principally occurs by other means, eg. poor screening or common power supplies, then these measures will have little or no effect.

Isolation between true omni-directional antennae depends purely on separation by the normal inverse square law. Frequently, however, directional aerials are employed and greater isolation may be achieved if antennae can be placed in the nulls of others. If this were possible around 50dB could be achieved at 6m spacing [3]. However, this method can only be used for a very limited number of antennae and is frequency dependent. Typically, the best isolation that can be achieved is some 28dB at 6m and 48dB at 60m antenna spacing [3].

Two types of component may be placed at a transmitter output to increase isolation, the choice depending upon the frequency separation of the wanted and offending signals. The first component is the ferrite circulator, which is basically a three port device which ideally circulates power from one port to another in one direction but not the other. It is arranged that transmitter power is transferred to the antenna whilst reverse power (including both mis-match and incident power at the antenna) is circulated to the dummy load connected to the third port. There is typically a forward loss of 0.5dB and a reverse isolation of 25db in a single device, although two or more may be cascaded to obtain better rejection. The isolation drops to around 10db and the insertion loss also rises at $\pm$2% from the centre frequency therefore limiting the use of the device to closely spaced transmitter frequencies. Power handling is also limited by the need to keep the dummy load well matched to prevent excess power being recirculated to the transmitter output port.

The second component is the high Q cavity resonator. This consists of a $\lambda/4$ (or $3\lambda/4$ etc.) rod inside a resonant cavity with power transfer by means of coupling loops. The dimensions of the cavity and the degree of coupling may be varied to optimise the unloaded Q or insertion loss for a particular application. Generally

some 20-30dB of rejection is available at ±1% from the centre frequency with a 1dB insertion loss for Q's of a few thousand. As with the circulator, greater isolation may be obtained by cascading devices. The resonator is suitable only for widely spaced transmitter frequencies due to the limited Q which can be obtained. High Q resonators can be very bulky especially at VHF. They also require careful tuning and are prone to drift. A combination of isolators and cavities is commonly employed to provide rejection of a range of transmitter frequencies.

3.4.1.2 COMMON ANTENNA WORKING

This situation is frequently encountered due to a lack of mast space on communal sites. Isolation of transmitter outputs is a more challenging engineering task than with individual antennae. Of special significance is the cellular base station in which there are many transmitters on very closely spaced frequencies.

Unlike the case for separate antennae, combining by means of isolators alone leads to considerable power being wasted in the isolator dummy loads. For example, if two transmitter outputs are combined in this way, fig.3.2(a), one half of each transmitter's power is circulated to the aerial whilst the remainder is dissipated in the other dummy load. Widely spaced transmitter frequencies may be

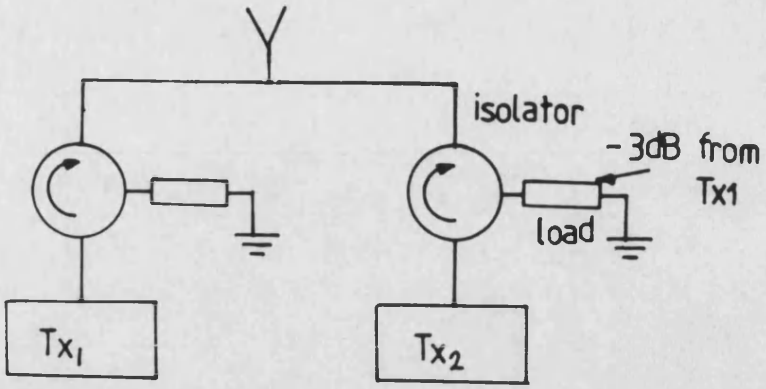

Fig. 3.2(a) Inefficient combining of two transmitters using isolators.

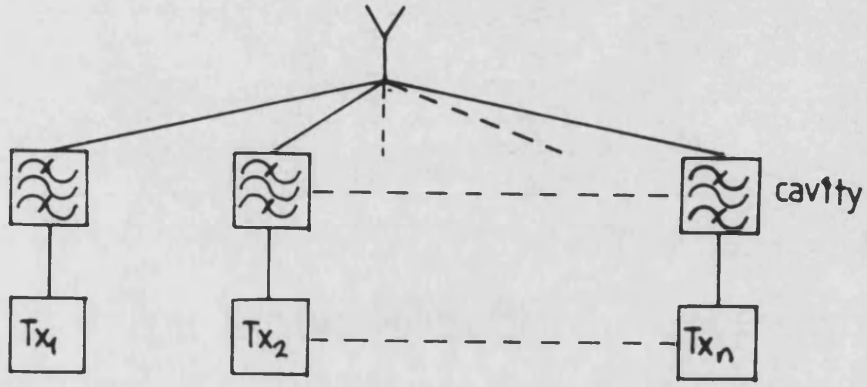

Fig. 3.2(b) Combining of widely spaced transmitters using cavity filters.

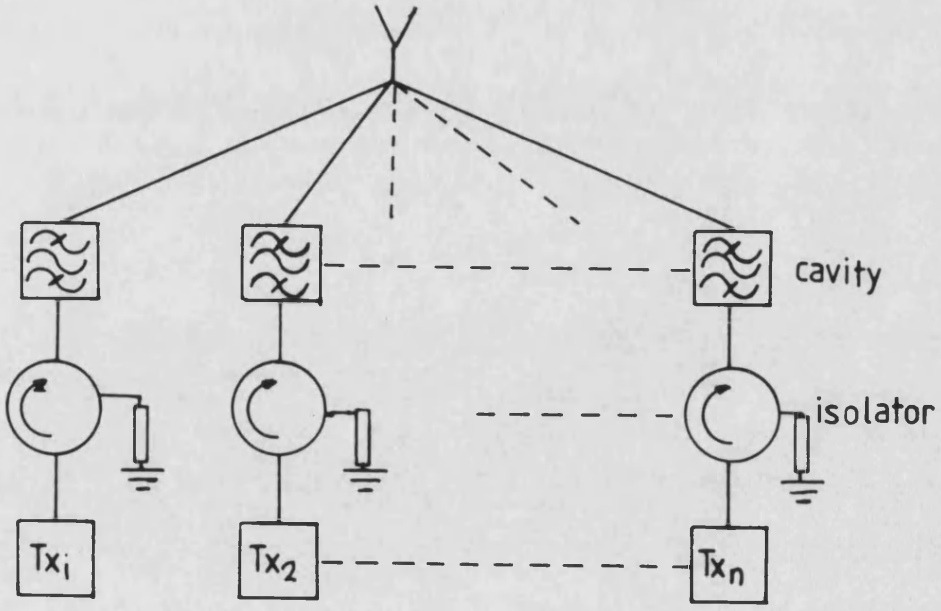

Fig. 3.2(c) Increasing isolation of (b) using additional isolators.

combined using single or cascaded cavity resonators without loss of power (fig.3.2(b)) as with separate antennae. Isolators may be added to this arrangement (fig.3.2(c)) to give additional isolation when the spacings are greater than a few percent of the transmission frequencies.

Where it is necessary to combine closely spaced frequencies as in cellular systems, a more complex arrangement involving a hybrid combiner is necessary. The hybrid can combine two closely spaced frequencies with around 25-30dB of isolation. There is, however, an inherent 3dB loss of power in the dummy load. A typical arrangement which might be used at cellular base stations is shown in fig.3.3. Signals are combined in two groups using cavities and isolators in each group. Alternate frequencies are combined in each group such that the effective frequency spacing is doubled. However the loss in such an arrangement may be around 7-8dB. This principle can be extended to more levels of combining which relieves the requirements of the cavities but at the expense of an extra 3dB hybrid loss for each additional level. For a given frequency spacing there may be an optimum arrangement [5] which minimises the insertion loss.

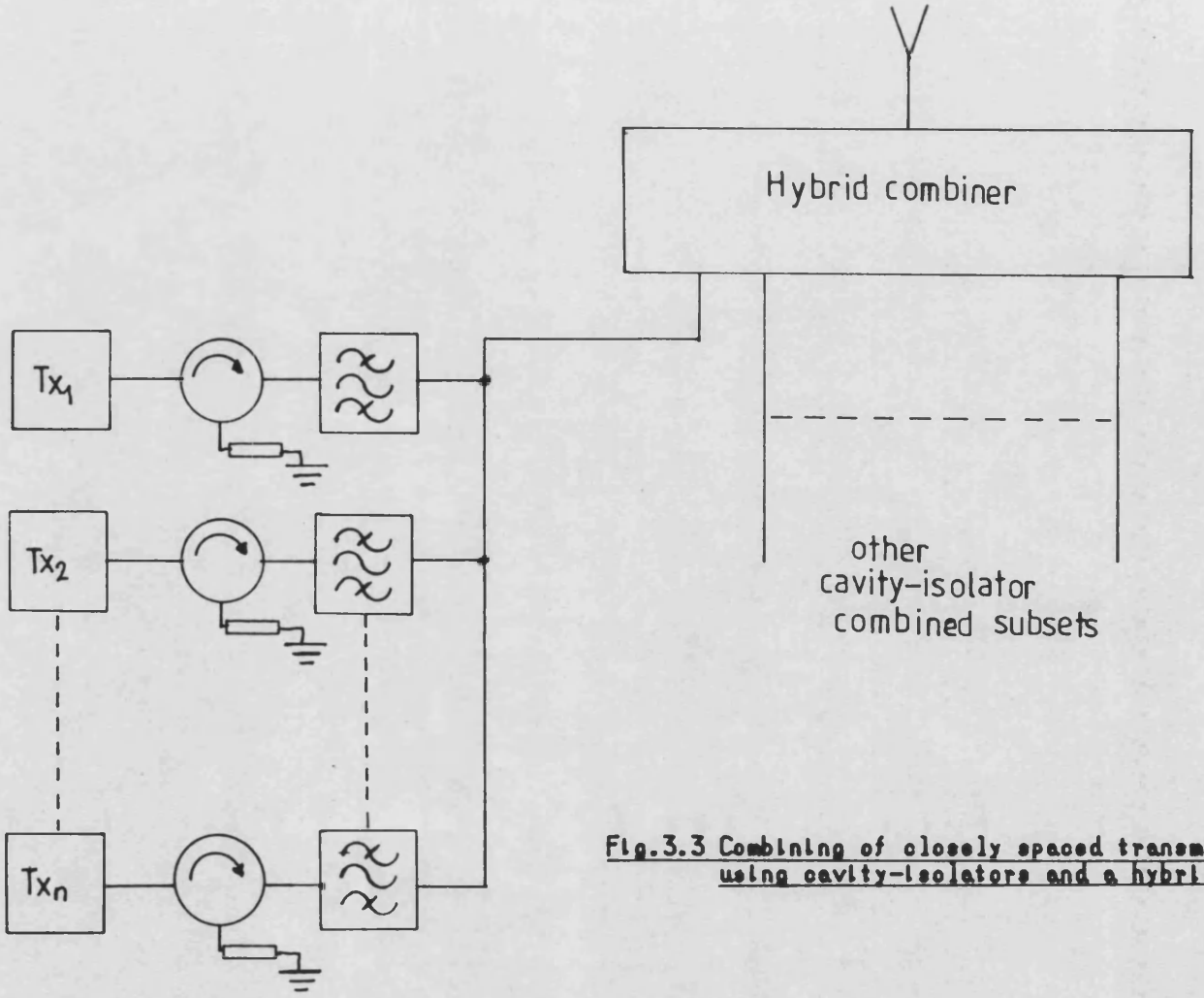

Fig.3.3 Combining of closely spaced transmitter frequencies using cavity-isolators and a hybrid network.

3.4.2 REDUCTION OF RECEIVER INTERMODULATION

Although the isolation of transmitter outputs discussed above generally reduces the number of intermodulation products, interference can still occur in the receiver due to insufficient front end selectivity and dynamic range. The RF selectivity of single channel equipment may be increased by the use of a suitable cavity filter, but this is of little use in multi-channel equipment. In the latter case a high Q filter which is adjusted according to the receive frequency is required, but the tracking of such a device especially with temperature would be extremely difficult to maintain. It is also impractical to increase the dynamic range of the receiver much above the 70dB currently obtainable.

Where the intermodulation is less severe such as to cause occasional unwanted outputs from the receiver, the use of selective calling facilities may help to alleviate the problem. The receiver audio output is then muted until it receives the correct calling sequence, hopefully only from the wanted signal not due to the interference.

3.4.3 INTERFERENCE FREE FREQUENCY GROUPS

3.4.3.1 CONVENTIONAL SYSTEMS

The most common policy of frequencing planning is based on the simple approach of allocation of channels on an equal spacing basis, which leads to a great number of odd-ordered IMP's falling upon used channels. If the spacing is varied such that all products fall upon unused frequencies, [4,6,7] then any intermodulation is no longer a problem. However, there are two main restrictions in the practical application of this technique;

(1) only 3^{rd} and occasionally 5^{th} order non-linearities can realistically be catered for, and

(2) the assumption is made that only a limited number of frequencies are present in the particular area of interest.

Various algorithms have been proposed for the calculation of lists of intermodulation 'free' frequencies of various sizes. These are normally limited to third order (ie. freedom from 2a-b, a+b-c products) to reduce computational effort. Table 3.1 shows the size of the block of frequencies, N, required to produce n third order compatible frequencies for minimum spacings between any two channels of one (adjacent channels allowed) [4] and two (no

adjacent channels) [6].

It can be seen that the total number of channels required rises sharply as the number of interference free channels increases. The spectral efficiency worsens still further when freedom from 5th order products is required. The minimum total is then 13 for 4 channels and 26 for 5 channels.

3.4.3.2 CELLULAR SYSTEMS

In cellular systems (chapter 2.3) the arrangement of channels in cells allows somewhat more efficient spectral utilisation to be achieved at the expense of tight base station transmitter combiner requirements. The feasibility of third order compatibility with 200 available channels has been considered by Gardiner [7]. Cluster sizes of 4,7 and 12 and various minimum intra-cell channel spacings were considered, this latter parameter determining the transmitter combiner requirement. With a cluster size of 7 and minimum spacing of 12, only 46.5% of the available channels can be utilised. This figure increases to 56% when the spacing is reduced to 8. A more efficient arrangement is possible for 12 cell clusters. With a spacing of 8, approximately 95% of the channels can be used, and there is little advantage in going to smaller spacings. There are two drawbacks involved with this later

Channels Required	Size of block of channels	
n	N	
	with adjacent channels	without adjacent channels
3	4	6
4	7	10
5	12	15
6	18	21
7	26	29
8	35	40
9	46	50
10	62	64

Table 3.1: Size of block of continuous channels required to give n third order intermodulation free channels both with and without adjacent channels allowed.

system;

(1) The inter channel spacing of only 200kHz places severe requirements on the multi-coupler at 900MHz. With existing technology losses in the region of 8-10dB can be expected in each transmit path [5]. Alternatively the isolation between outputs must be reduced, leading to greater intermodulation thus negating any other benefits.

(2) Channels may not be transferred from one cell to another. This is a considerable disadvantage, since it is frequently desirable to be able to adjust the number of channels per cell in sympathy with the non-uniform user distribution.

Hence although providing third order compatible frequency allocations for cellular systems is more spectrally efficient than non-trunked systems, the price to be paid in other areas (particularly in the transmitter combiners) is high. Suppression of intermodulation interference therefore depends upon the degree of isolation obtainable between transmitter outputs and the inherent muting of receivers between periods of use.

3.5 WIDEBAND SYSTEMS

If the frequency spectrum available to a particular group of users is sub-divided into a relatively small number of wideband channels as opposed to the conventional approach, the problem of intermodulation is lessened considerably. The message signals from a number of users are then combined onto a single wideband bearer using some form of time multiplexing. The system then has superior spectral efficiency and/or simplified base station design compared with an equivalent fdm system, providing the time multiplexing process itself is spectrally efficient.

Considering a cellular arrangement, the original TACS system uses a maximum of 297 channels (for urban areas) arranged into 21 groups with a constant spacing of 525kHz (21x25kHz) between channels of the same group (cell). Hence, although all the available spectrum is used, the conditions are ideal for troublesome intra-cell intermodulation (section 3.3). The complex base station combining procedures used serve to reduce the degree of transmitter generated intermodulation, but receiver generated products are still a problem.

An alternative wideband system could still have 21 'groups' (and hence would retain the cell assignment properties of the current system) but each 'group' would now

be a single channel approximately 250kHz wide. Since there would be only one frequency bearer per cell, intermodulation would not be a problem. Several proposed pan-European cellular systems (chapter 1.4.1) utilise this principle, with channel spacings ranging from 250kHz to 6MHz using TDMA as the multiplexing technique. The latter 6MHz channel system is an example of the single 'super' channel cellular system, which has the additional advantage of also avoiding inter-cell intermodulation. The principal problem with these TDMA systems is the high data rate required for the digital speech. Hence freedom from intermodulation is obtained at the expense of inferior spectral efficiency compared to the TACS 25kHz channel non-intermodulation free frequency assignment. However, a bandwidth efficient analogue technique such as time-compression multiplexing with a wideband FM bearer offers a potentially more attractive solution to the problem.

3.6 REFERENCES

(1) Al Hafid,H.T., Atek,K., Abbas,M.A.H., and Gardiner,J.G.: 'Computer modelling of nonlinear interactions between co-sited transmitters', Proc. IERE Conf. on Civil Land Mobile Radio, no.33, Nov.1975, pp.123-32.

(2) Gardiner, J.G., and Fudge,R.E.: 'Aerials and base station design', Land Mobile Radio Systems, chap.4, p.54, IEE Telecomms. Series no.14, 1985.

(3) Panell,W.M.: 'Frequency Engineering in Mobile Radio Bands', Appendix 6.

(4) ibid. Appendix 8

(5) Gardiner,J.G., Hammond,D., and Heathman,A.C.: 'Intermodulation control requirements at cellular base station sites', Proc. Int. Conf. on Radio Systems and Techniques, no.238, Sept.1984, pp.118-21.

(6) Edwards,R., Durkin,J., and Green,D.H.: 'Selection of intermodulation-free frequencies for multiple-channel mobile radio systems', Proc. IEE, vol.116, no.8, Aug.1969, pp.1311-18.

(7) Gardiner,J.G., and Kotsopoulos,S.A.: 'Relationship between base station multicoupling requirements and frequency planning for cellular mobile radio', Proc. IEE, vol.132, Pt.F, no.5, Aug.1985, pp.384-7.

CHAPTER FOUR

TIME-COMPRESSION MULTIPLEXING

4.1 INTRODUCTION

Time-compression multiplexing (TCM) is a technique of combining several baseband signals by contracting their waveforms in time such that they may be transmitted over a common communications channel. If R incoming message signals are first partioned into segments of duration T, then time compression by a factor of R allows all the signal segments to be interleaved upon a single bearer. Subsequent time expansion after transmission, by the same factor, recreates the original continuous signals. Since both time compression and expansion processes are necessarily involved, a more appropriate title would be time-companding multiplexing, but the former title will be retained for compatibility with other work.

TCM is by no means a new technique. Its uses date back over 100 years [1] although the first application for telephony was patented by Veaux in 1943 [2]. This was followed by several other proposals, but it was not until 1964 that the results of any significant practical work were published (Flood and Urquhart-Pullen [3]). However, this early work received little attention due largely to practical difficulties. It was not until the mid-

seventies, with the development of the charge-coupled-device (CCD) allowing simple companding circuits to be produced (section 4.2.1), that interest in TCM was rekindled. Morgen and Protonatarios [4] (1974) and Aniebona [5] (1976) published work on the basic properties of time-compressed waveforms, and more recently there has been considerable interest in its use for systems that traditionally have employed FDM (Holbeche and Mannings [6] and Eng, Haskell and Schmidt [15]). With the availability of low cost digital integrated circuits (section 4.2.2) and the surface-acoustic-wave filter for wider bandwidth companding operations applications (section 4.2.3), time-compression multiplexing has become a serious challenger to the more well established TDM and FDM systems.

4.2 CHARACTERISTICS OF TIME COMPANDING TECHNIQUES

4.2.1 SAMPLING SYSTEMS

4.2.1.1 PRINCIPLE

It is well-known that any real signal in which the high frequency energy is small or can be reduced by filtering can be described to a sufficient degree of accuracy by a set of suitably time spaced weighted impulses. Hence, within this restriction, it is possible to represent each of the segments of the input signals to a TCM system (fig.4.1) by a finite number, N, of equally spaced samples. Now, linear time companding can be viewed as a process which uniformly varies the time spacing of these samples. Hence, for example, time compression may be conveniently achieved by temporarily storing the N samples comprising one segment and subsequently re-transmitting at a higher rate. If the original sampling rate is f_s and the new rate is f_r, then the companding factor obtained is $\frac{f_r}{f_s}$. The complementary expansion process is simply achieved by interchanging the two sampling frequencies.

In practice, a sample-and-hold device must be used to facilitate sampling and subsequent storage. This produces stepped approximations to the continuous time functions and hence introduces aperture distortion of the form

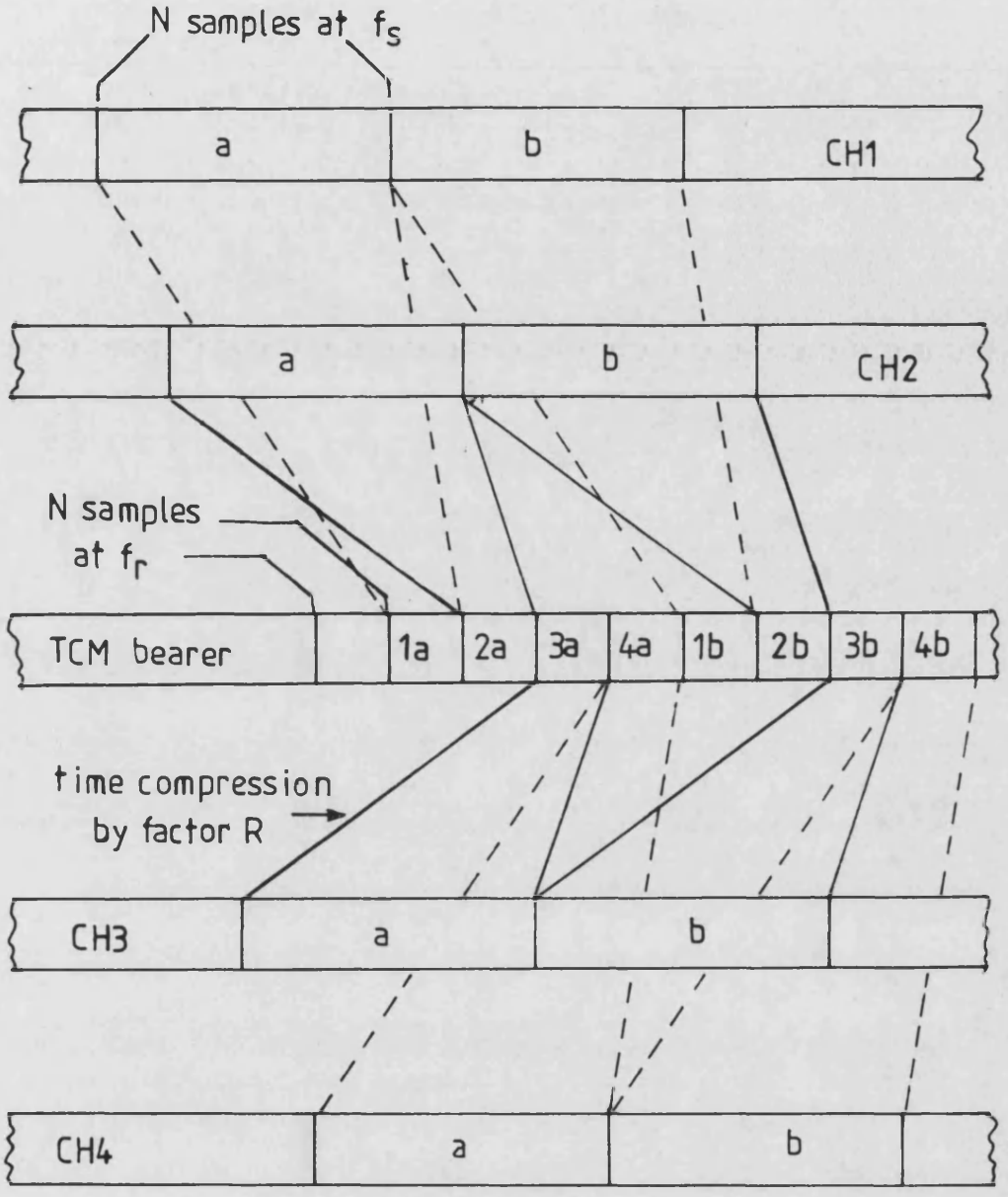

$$R = \frac{f_r}{f_s}$$

Fig.4.1 4-channel TCM system outline showing principle of time-compression and interleaving of compressed segments upon a common bearer.

$$M_s(f) = M(f) \cdot \frac{\sin\left[\frac{\pi f}{f_s}\right]}{\pi f} \qquad (4.1)$$

where M(f) is the original signal spectrum, and $M_s(f)$ is the stepped signal spectrum.

The result is to attenuate the higher frequency components in the input signal. If this effect is excessive, some form of pre-distortion before sampling or subsequent equalisation should be employed.

4.2.1.2 CHARGE-COUPLED-DEVICE IMPLEMENTATION

Time-compression multiplex systems [6,7] have been proposed which employ charge-coupled-devices (CCD's) as analogue storage elements. A full description of the technique may be found in a previous work [10]. In common with certain other time multiplexing systems, eg. TDMA with linear predictive speech coding, there is an inherent processing delay in any TCM system. For the CCD technique, the minimum delay may be determined from the clock timing diagram of fig.4.2(a). The compression delay, D_c, is equal to the original signal segment length, T, plus some fraction of the fast sampling period, ΔT_r, dependent upon the relative phasing of the two clocks. Similarly the delay, D_e, in the expansion process is the sum of the compressed segment length, Tf_s/f_r and a fraction, ΔT_s, of the slow sampling period.

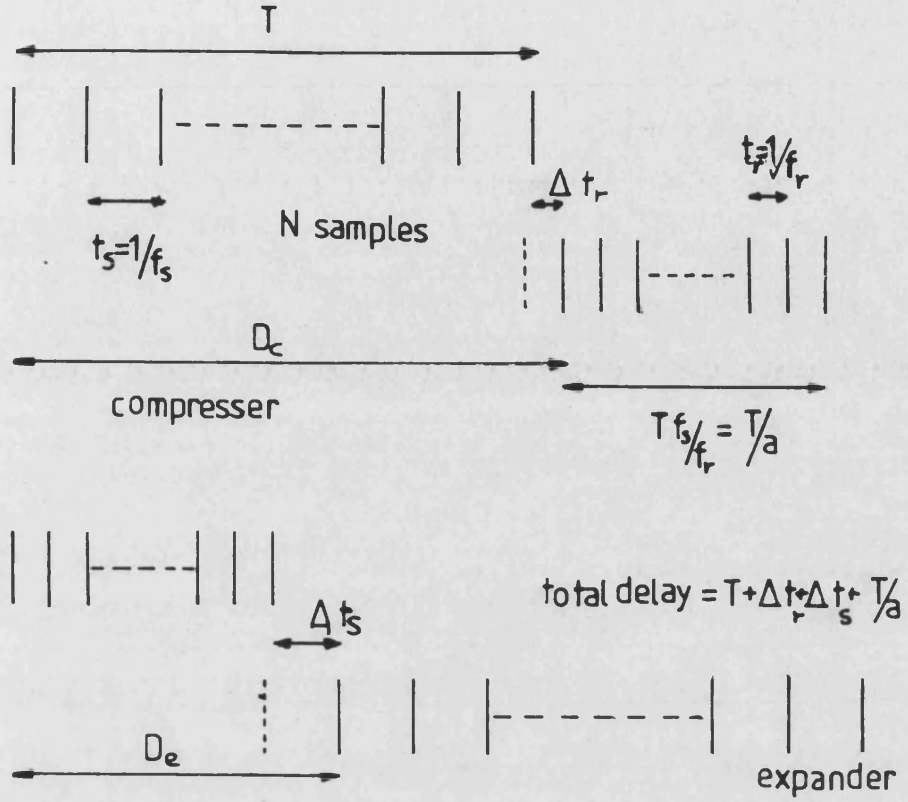

Fig. 4.2(a) Timing diagram for CCD implementation of time-companding.

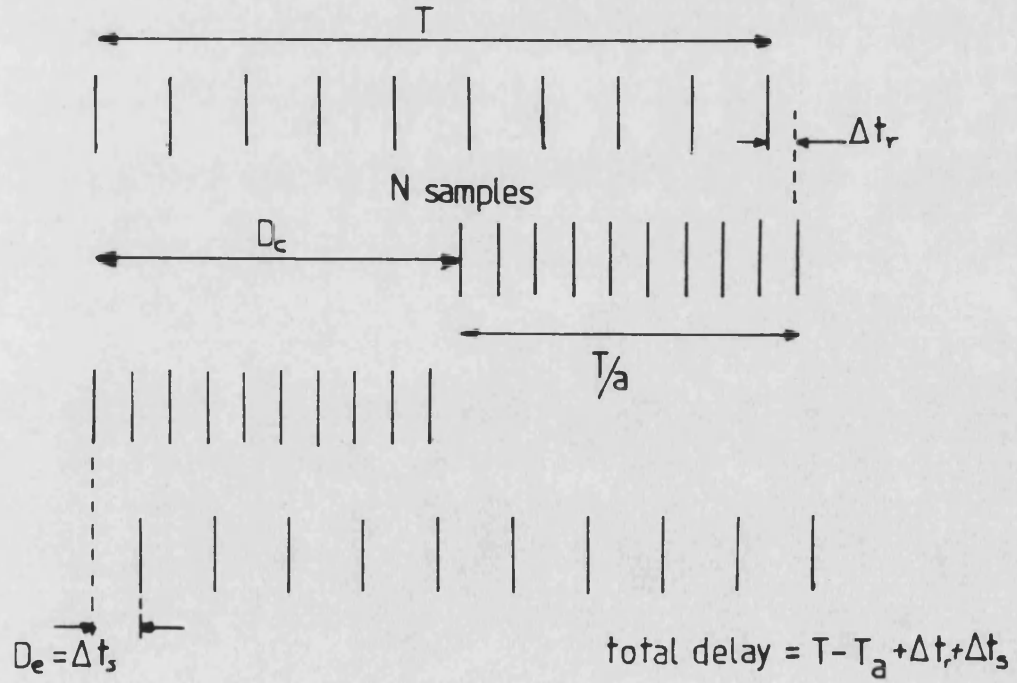

Fig. 4.2(b) Timing diagram for digital implementation of time-companding.

Therefore the total delay in the system, D, is

$$D = D_e + D_c = T + Tf_s/f_r + \Delta T_r + \Delta T_s \qquad (4.2)$$

Since the number of samples per segment, N, is normally large, ΔT_r and ΔT_s may be ignored and the expression simplifies to

$$D = T + T/a \qquad (4.3)$$

where a = companding factor = f_r/f_s

The performance of the CCD time-companding system is restricted both by the nature of the device and by the characteristics of commercially available units. The first-in first-out (FIFO) nature of the memory coupled with the limited number of sizes obtainable reduces the flexibility in the choice of sampling frequency and segment (frame) length. Typical parameters for audio [8] (MN3000 series) and video [9] (MS1000 series) CCD's are are given in Table 4.1.

The ratio of maximum-to-minimum clock frequency determines the maximum theoretical companding ratio which may achieved and is typically 10. However, the practical maximum is often much lower than this due to two factors;

(1) The maximum signal bandwidth, which must be greater than the product of the input signal bandwidth and

	MN3000 series	MS1000 series
No. stages	512,3328	851,910,1024
Min. clock frequency f_c, kHz	10	100
Max. clock frequency f_c, kHz	100	25MHz
Input bandwidth (-3dB)	12kHz at f_c =40kHz	5MHz
Total harmonic distortion	0.4% at f_c =40kHz	-
	10% at f_c =20kHz	-
Signal-to-noise ratio (typical)	80dB	40dB

Table 4.1: Parameters of commercial charge coupled devices.

the companding ratio, is typically one-quarter of the clock frequency (25kHz)

(2) The minimum usable clock frequency, f_c, may be considerably higher than the 10kHz quoted in Table 4.1 as the distortion increases rapidly from the 0.4% at f_c = 40kHz as the clock frequency decreases.

Hence, a realistic maximum compression ratio for speech signals would be less than five. The higher speed devices in general have poorer noise performance but are just fast enough for two channel video applications.

4.2.1.3 DIGITAL RANDOM-ACCESS-MEMORY IMPLEMENTATION

This process uses a digitised form of the input signal and a random access memory as the storage medium [10]. Since the digital memory is an addressable device, there is a greater degree of read/write flexibility than with the analogue technique. This has two benefits; firstly only a single RAM is required in the implementation [10] and secondly, the overall processing delay may be reduced.

The optimum timing arrangement for minimum delay both at the compressor (eqn.4.4) and at the expander (eqn.4.5) is shown in figs.4.2(b).

$$D_c = T - NT_r + \Delta T_r \qquad (4.4)$$

$$D_e = \Delta T_s \qquad (4.5)$$

Now, as with the CCD system ΔT_r and ΔT_s may be ignored and writing NT_r as T/a we get the overall delay, $D_c + D_e$;

$$D = T - T/a \qquad (4.6)$$

Comparing eqn.4.6 with the delay for the CCD system (eqn.4.3), it can be seen that for low companding ratios this technique offers appreciably less delay, whilst for large factors, the delay of both the systems approaches the frame period, T. The performance of a practical digital companding system depends primarily of the characteristics of the analogue-to-digital converter (ADC), the digital-to-analogue converter (DAC) and the memory. The two principal trade-off factors are resolution and speed. Industry standard 8-bit monolithic DAC's have access times under 100ns, whilst higher speed or greater resolution is available at extra cost. Low power RAM's are now available with access times under 50ns and they may be configured for any size and no. bits. The limiting performance of the digital companding system is ultimately determined by the performance of the ADC. Although 8-bit conversion at several tens of MHz is achievable using the newer 'flash' devices, higher resolution from a monolithic device is currently limited to to a much lower speed, e.g. 12-bit 500kHz. However, these characteristics can satisfy the

needs for most audio work with companding ratios at least an order of magnitude greater than the purely analogue technique. In general the RAM technique is preferable except for very small, eg. two channel, systems, when the extra circuit complexity and overhead is not justified.

4.2.2 TIME VARIANT DELAY TECHNIQUE

4.2.2.1 PRINCIPLE

It is possible to conceive time companding as a process achievable by passing a signal through a network whose delay varies with time. If the delay increases linearly with time then the output waveform is a linearly time expanded version of the input. Conversely a delay which decreases with time results in time compression.

Consider the hypothetical network with the linear time delay characteristic, D(t), shown in fig.4.3(a). At a time t=0, the delay is D_1 and at some time, T, it is D_2 ($D_1 > D_2$). It is assumed that the amplitude response of the network over this interval is uniform. Let the input signal to the network, x(t), be one segment of duration, T, of a single message input to the TCM system. Hence the output segment duration will be $T + D_2 - D_1$, and the compression ratio, a, is given by

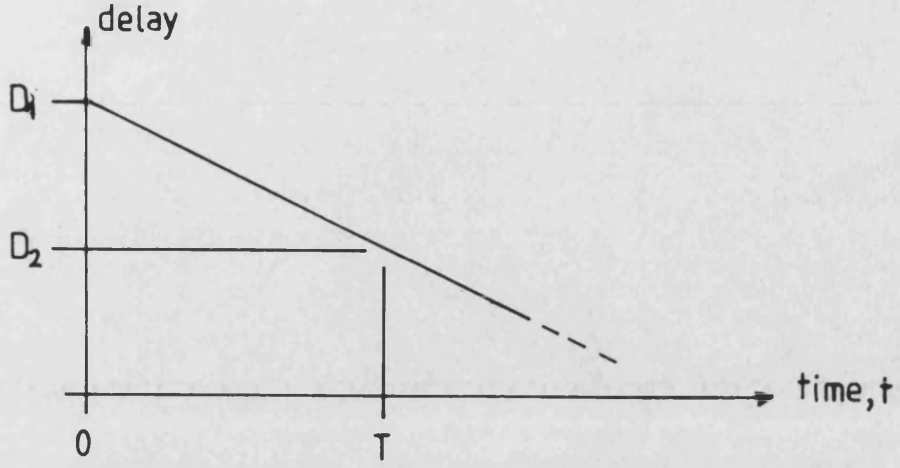

Fig. 4.3(a) Response of linear time-variant delay network.

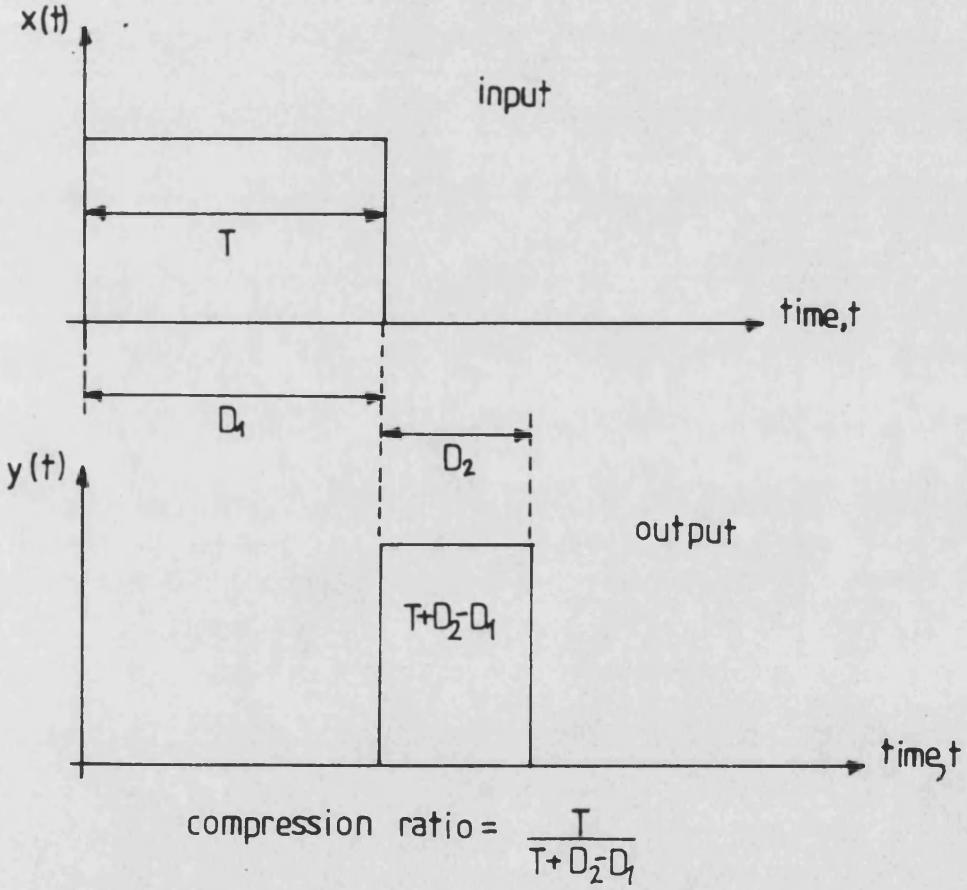

Fig. 4.3(b) Time-compression using the time-variant delay network.

$$a = \frac{T}{T + D_2 - D_1} \qquad (4.7)$$

The complementary expansion process can be obtained with a network whose delay increases with time. Let the time delay at t=0 be D_3, and that at $t=T + D_2 - D_1$, be D_4. To recover the original signal the conditions in eqn.4.8 must be satisfied.

$$T + D_2 - D_1 + D_4 - D_3 = T \qquad (4.8)$$

Therefore

$$D_1 - D_2 = D_3 - D_4 \qquad (4.9)$$

The overall time delay in the system is $D_1 + D_3$. Now, since $D_4 > D_3$, D_3 may be made zero. However, since $D_1 > D_2$ and D_2 may not be negative, D_1 can not be zero. Therefore the minimum total processing delay is D_1. Under these circumstances, $D_4 = D_1$ and the compression ratio is given by

$$a = \frac{T}{T - D_1} \qquad (4.10)$$

4.2.2.2 SURFACE-ACOUSTIC-WAVE FILTER IMPLEMENTATION

Although, in principle, the technique described above appears to be a simpler approach to time companding than the sampling system, there is no practical network which has the required response. However, the desired linear

delay-time characteristic may be synthesised using a linear dispersive filter (LDF) and a Chirp pulse.

Eng and Haskell [11] have studied this technique for possible processing of TV signals. With present-day SAW's the distortion introduced in the basic technique is too high for TV signals but may be useful for other less demanding applications. An improved technique [12] using another SAW as an equaliser can however maintain the quality of the signal for companding factors of greater than 10.

4.3 APPLICATIONS OF TIME-COMPRESSION-MULTIPLEXING

4.3.1 HIGH SPEED DATA TRANSMISSION

TCM is the key element of AT&T Bell Laboratories new Circuit Switched Digital Capability (CSDC) deployed in 1983/84 [13]. In this system time-compression-multiplexing allows full duplex data at up to 64kb/s to be transmitted over the public-switched-telephone-network; a factor of ≈6 increase over the original system.

Incoming data is partioned into 3ms segments and then compressed by a factor of about 2.25 to give a maximum data rate of 144kb/s over the interconnecting wire. This companding factor allows for guard bands of approximately 100 μs to be inserted between the send and receive blocks to allow for loop propagation delay and delay spreading. It also permits three synchronisation bits (per frame) and an additional low-speed 1.33kb/s signalling channel to be included.

The circuitry required to implement the system is relatively simple consisting primarily of two VLSI integrated circuits. An analogue circuit performs the necessary line equalisation and amplification of the signals after they have transversed the loop, whilst the entire TCM processor along with the control logic is integrated onto one CMOS digital chip [14].

4.3.2 SATELLITE TRANSMISSION OF VIDEO SIGNALS

TCM has recently been proposed [15] as a solution to the long standing problem of the transmission of multiple colour television signals via a single satellite transponder. Conventionally, FDM-FM has been used for this purpose. However, the inherent transponder non-linearity can cause serious intelligible crosstalk and intermodulation between the FM carriers unless the satellite power is backed-off considerably. The consequence of this is a reduction in received carrier-to-noise ratio and thus there exists a trade-off in overall performance.

Time-compression multiplexing does not suffer from these degradations and has the added advantage of possible compatibility with existing TDMA traffic. Eng Yue [16] have shown that for TV signals where;

(1) the signal bandwidth, B, is much greater than the reciprocal of the TCM frame period, T, (equal to one line period of 64 μs),and

(2) the signal is time-compressed by a factor, a

then virtually all the spectral power of the compressed signal is contained within a bandwidth of aB. They further demonstrated that inter-burst interference caused by bandlimiting the waveform to exactly this bandwidth

could be reduced to a negligible value by introducing a small guard time of approximately 0.5μs between bursts.

4.3.3 NARROW BAND RADIO SYSTEMS

4.3.3.1 MOBILE VHF SINGLE-SIDEBAND

The use of time-compression multiplexing for the combination of the necessary demodulation reference along with the message in 5kHz channel SSB systems has been studied in a previous work [10]. Other schemes have always relied upon the transmission of a tone somewhere in the audio band in what were essentially FDM systems. It was shown that the TCM-SSB offered potential advantages including greater tolerance to initial receiver frequency offset, reduction of spurious intermodulation, a transparent channel and an additional low speed signalling capability. These features were obtained at the expense of greater transceiver complexity and inherent TCM processing delay.

The optimum frame period in the TCM-SSB system was found to be 32ms with a companding ratio of 1.15. Sampling of the speech input at the normal PCM rate of 8kHz was found to be sufficient. With a reference burst duration of 2.5ms and guard intervals of 0.5ms the overall signal was compatible with the normal 5kHz channel spacing.

4.3.3.2 FIXED UHF-FM LINKS

Conventional point-to-point radio systems use FDM to multiplex two signals on a common FM carrier. As with the satellite transponder (section 4.3.3) it is found that attempts to gain adequate signal-to-noise ratio frequently result in severe interchannel crosstalk.

An approach to this problem utilising TCM has been investigated [6] which uses a frame period of 32ms with a compression ratio of 2.25. Four cycles of an out of band tone were used for synchronisation purposes. The results of field trials comparing the equipment performance with that of an equivalent FDM system showed the former system to be considerably better whenever the bearer was subject to non-linearities.

Research on a related system has been commissioned by the Home Office [7]. This employs the same companding ratio but a longer (45ms) frame period. Approximately 4ms remains free for synchronisation purposes and a more robust pseudorandom sequence technique was adopted, which is also suited to mobile communications as well as fixed links. The expense of the extra circuitry required by both of these systems compared to the FDM approach is largely offset by alleviating the need for time consuming alignment procedures.

4.4 REFERENCES

(1) Freebody,J.W.: 'Telegraphy', Pitman 1959, chap.2.

(2) Veaux,H.M.: 'Improvements in multi-channel pulse communication systems', British Patent no.656151.

(3) Flood,J.E., and Urquhart-Pullen,D.I.: 'Time-compression multiplex transmission', Proc.IEE, vol.III, no.4, April 1964, pp.647-68.

(4) Morgen,D.H., and Protonatarios,E.N.: 'Time-compression multiplexing for loop transmission of speech signals', IEEE Trans. on Comms., vol.COM-22, no.12, Dec.1974, pp.1932-9.

(5) Aniebona,E.N.: 'The spectrum of a time-compression multiplex (TCM) signal and its transmission bandwidth requirements', Proc. International Conference on Comms., Pt.III, Philadelphia, USA, June 1976, pp.43/1-43/6.

(6) Holbeche,R.J., and Mannings,R.T.: 'Comparison between time-compression multiplexing and frequency-division multiplexing over narrow band radio systems', Proc.IEE, vol.131, part F, no.2, April 1984.

(7) 'Time-division multiplexing of analogue channels by time compression', Home Office Directorate of Telecommunications R D Section Report prepared by Cambridge Consultants Ltd., Nov.1978, pp.79-86.

(8) RS Components data sheet no.5998, July 1986

(9) Plessey Satellite, Cable and T.V. Integrated Circuit Handbook, March 1985, pp.80,86 and 92.

(10) Skuse,B.: 'An alternative time-compression multiplexed VHF single sideband system', MSc thesis, University of Bath, 1984.

(11) Eng,K.Y., and Haskell,B.G.: 'Study of a time-compression technique for TV transmission using a Chirp filter and envelope detection ', Bell System Technical Journal, vol.60, no.10, Dec.1981, pp.2373-95.

(12) Eng,K.Y., and Yue,O.C.: 'Time-compression multiplexing of multiple television signals in satellite channels using chirp transform processors', IEEE Trans. on Comms., vol.COM-29, no.12, Dec.1981, pp.1832-40.

(13) Bosik,B.S., and Kartalopoulos,S.V.: 'A time-compression multiplexed system for a circuit switched digital capability', IEEE Trans. on Comms.,vol.COM-30, no.9, Sept.1982, pp.2046-52.

(14) Hao,C.H., and Kartalopoulos,S.V.: 'The VLSI chip of the time-compression multiplexer for the circuit switched digital capability', Proc. of IEEE Global Telecomms. Conf., USA, 29th Nov. - 2nd Dec. 1982, vol.1, pp.386-9.

(15) Eng,K.Y., Haskell,B.G., and Schmidt,R.L.: 'Time-

compression multiplexing (TCM) of three broadcast quality T.V. signals on a satellite transponder', Bell System Technical Journal, vol.62, no.10, pt.1, Dec.1983, pp.2854-55.

(16) Eng,K.Y., and Yue,O.C.: 'Spectral properties and band-limiting effects of time-compressed T.V. signals in a time-compression multiplex system', Bell System Technical Journal, vol.60, no.9, Nov.1981, pp.2167-85.

CHAPTER FIVE

TIME AND FREQUENCY DOMAIN ANALYSIS OF TIME-COMPRESSION MULTIPLEXING

5.1 INTRODUCTION

An overview of existing work on time-compression multiplexing systems was given in the previous chapter which included references to investigations of its basic characteristics. A previous work by the author [1] was concerned with the study of the properties of a single channel plus reference TCM-SSB system. In this chapter, a comprehensive mathematical treatment of multi-channel TCM systems with various classes of message signal will be developed. The analysis will be limited to those cases where there is no redundant information or guard intervals between the waveform segments, ie. when the total no. of multiplexed channels is equal to the (integer) compression ratio. The application of windowing to the TCM waveform for FM applications is considered in chapter 9.

Fundamental expressions are first considered for a general TCM system with arbitrary input signals. These equations are then developed for the special case of sinusoidal message signals only present, and certain key characteristics highlighted. Finally, the analysis is extended to cover multi-channel systems with both general

and harmonically related waveforms.

5.2 MULTI-CHANNEL TCM WITH ARBITRARY MESSAGE SIGNALS

The waveforms present in a basic multi-channel time-compression multiplex system when there is one channel active are shown in fig.5.1. There are no intervals between segments and hence the compression ratio, a, is equal to the number of multiplexed channels, R. The frame period is T, the input signal is $x_1(t)$, the output waveform is $z_1(t)$ and k is the frame number, extending from $-\infty$ to ∞, where k=0 is defined as the frame spanning $t=\pm T/2$. It has been shown in previous work that [1]

$$z_1(t) = \sum_{k=-\infty}^{\infty} x_1\left[a\left[t - k\left[\frac{a-1}{a}\right]T - \left[\frac{a+1}{2a}\right]T\right]\right] \cdot \text{rect}\left[\frac{a(t-kT-(a+1)T/2a)}{T}\right] \qquad (5.1)$$

where

$$\text{rect}(t) = \begin{cases} 1 \text{ for } |t| < 1/2 \\ 0 \text{ otherwise} \end{cases}$$

and

$$Z_1(f) = \frac{1}{a} \sum_{k=-\infty}^{\infty} X_1(f-k/T) \cdot e^{-j\pi fT\left[\frac{a+1}{a}\right]} \cdot \text{Sa}\left[\pi T(f/a - f + k/T)\right] \qquad (5.2)$$

where $\text{Sa}(x) \equiv \frac{\sin(x)}{x}$, $X_1(f)$ is the spectrum of $x_1(t)$ and $Z_1(f)$ is the spectrum of $z_1(t)$.

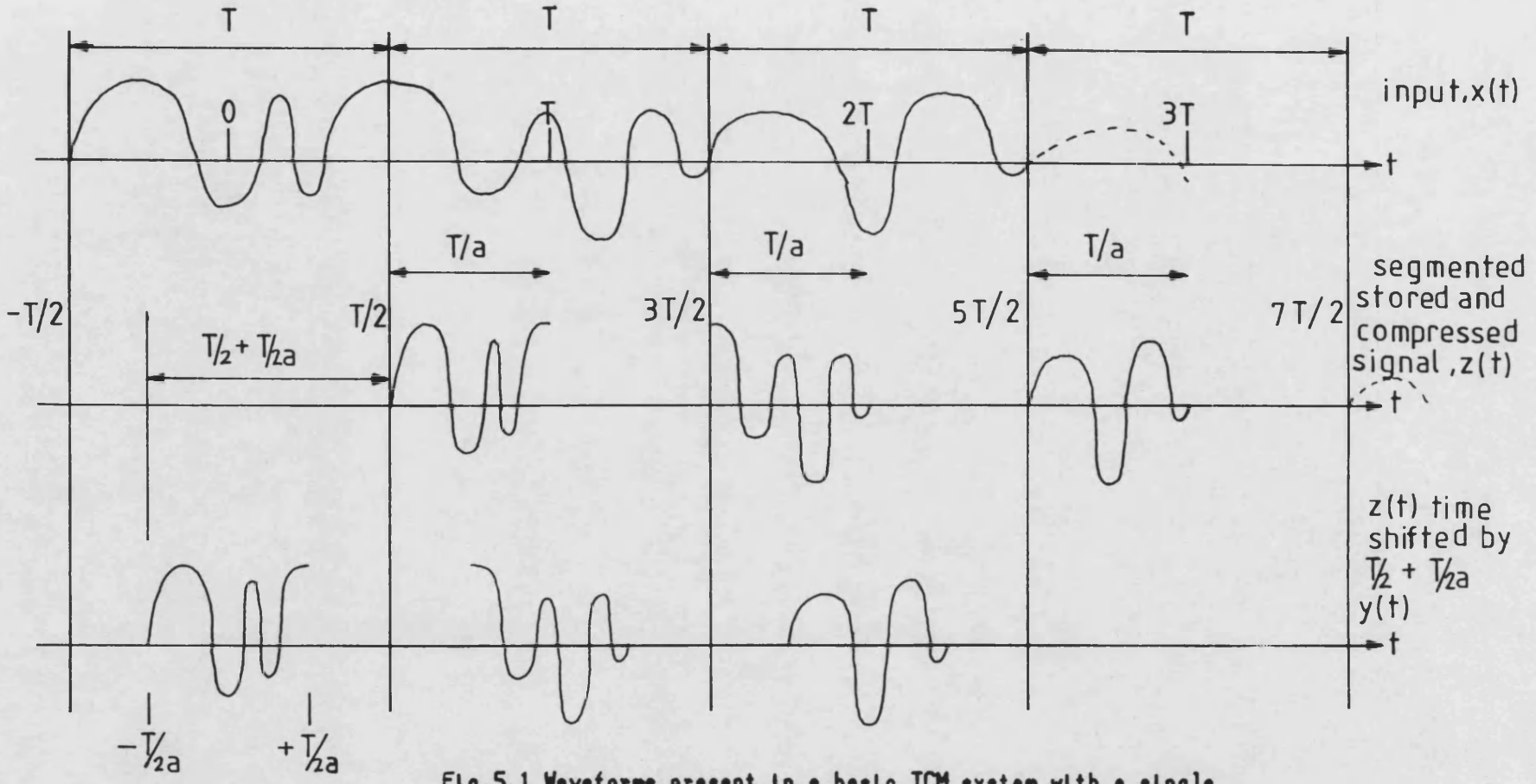

Fig.5.1 Waveforms present in a basic TCM system with a single active channel.

For subsequent analysis, the complex exponential term in $Z_1(f)$ (representing a delay of T/2+T/2a) is unimportant. Hence we define two new waveforms, $y_1(t)$ and $Y_1(f)$, such that

$$y_1(t) = \sum_{k=-\infty}^{\infty} x_1\left[a\left[t - k\left[\frac{a-1}{a}\right]T\right]\right] \cdot \text{rect}\left[\frac{a(t-kT)}{T}\right] \qquad (5.3)$$

and

$$Y_1(f) = \frac{1}{a} \sum_{k=-\infty}^{\infty} X_1(f-k/T) \cdot Sa\left[\pi T(f/a - f + k/T)\right] \qquad (5.4)$$

Two additional waveforms, $y_{TCM}(t)$ and $Y_{TCM}(f)$, are also now defined as the time and frequency domain representations respectively of the complete TCM signal.

For the case of a single active channel

$$y_{TCM}(t) = y_1(t) \qquad (5.5)$$

and

$$Y_{TCM}(f) = Y_1(f) \qquad (5.6)$$

If there is more than one channel active, then $x_r(t)$ is defined as the input from channel r and $y_r(t)$ as the corresponding time-shifted compressed output segment as shown in fig.5.2. Therefore $y_r(t)$ may be derived from

$y_1(t)$ with the addition of a time delay $(r-1)T/a$.

Now

$$y_{TCM}(t) = \sum_{r=1}^{B} y_r(t)$$

$$= \sum_{r=1}^{B} \sum_{k=-\infty}^{\infty} x_r \left[a\left[t - k\left[\frac{a-1}{a}\right]T - \left[\frac{r-1}{a}\right]T \right] \right]$$

$$\cdot \text{ rect}\left[\frac{a(t-kT-(r-1)T/a)}{T}\right] \qquad (5.7)$$

By the Fourier transform time shift theorem, [2] $Y_r(f)$ $= e^{-j2\pi f(r-1)T/a} \cdot Y_1(f)$ with appropriate change in $Y_1(f)$ for channel r waveform. Hence by superposition

$$Y_{TCM}(f) = \sum_{r=1}^{B} Y_r(f)$$

$$= \frac{1}{a} \sum_{r=1}^{B} \sum_{k=-\infty}^{\infty} X_r(f-k/T) \cdot e^{-j2\pi f(r-1)T/a}$$

$$\cdot \text{ Sa}\left[\pi T(f/a - f + k/T)\right] \qquad (5.8)$$

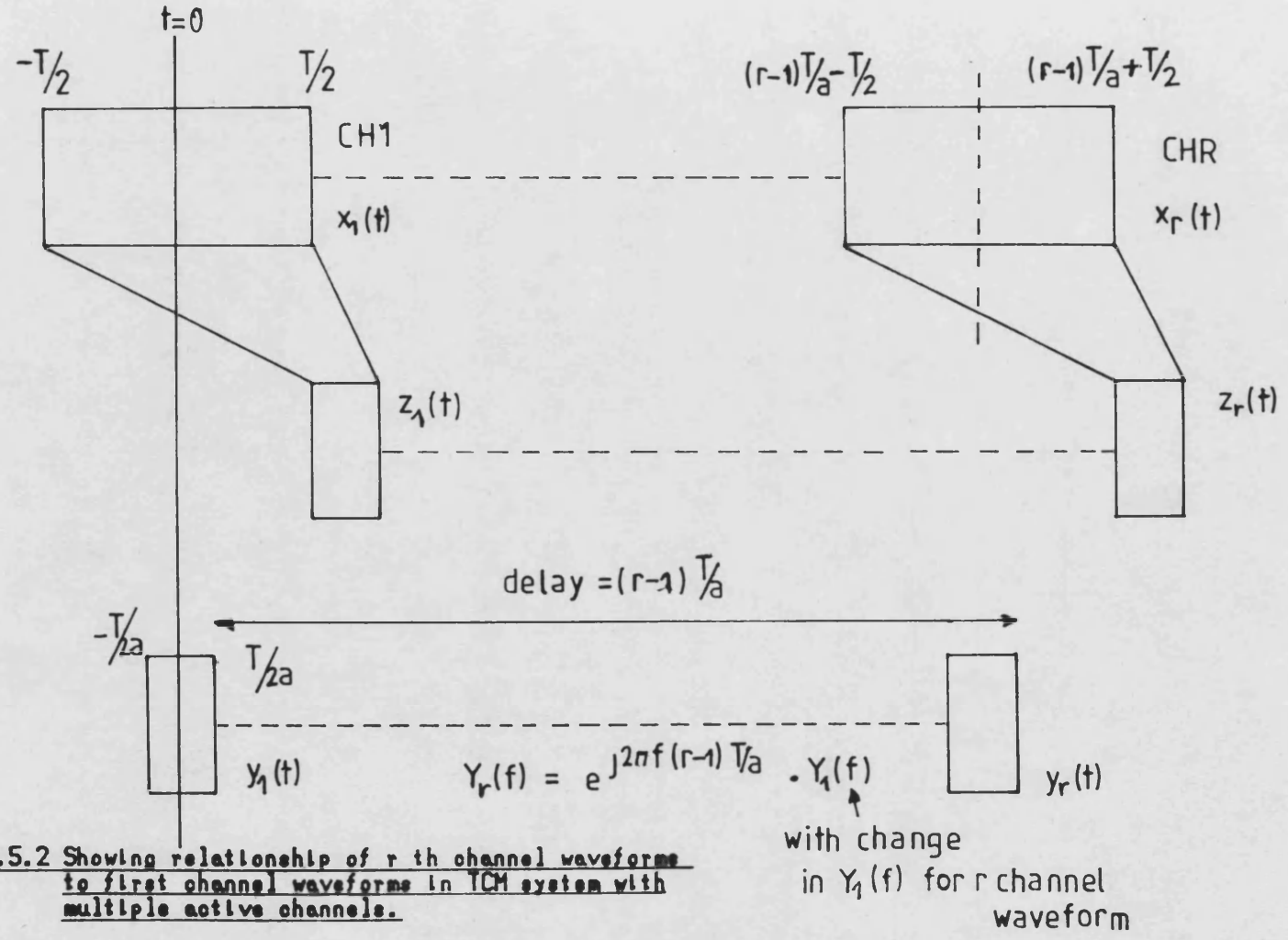

Fig.5.2 Showing relationship of r th channel waveforms to first channel waveforms in TCM system with multiple active channels.

5.3 SINUSOIDAL MESSAGE SIGNALS

5.3.1 SINGLE ACTIVE CHANNEL

Let the input signal, $x_1(t)$, be a general sinusoid of frequency, f_o, and phase, θ. Thus

$$x_1(t) = A\cos\left[2\pi f_o t + \theta\right]$$

$$= C\cos 2\pi f_o t - S\sin 2\pi f_o t \qquad (5.9)$$

where $C = A\cos\theta$, and $S = A\sin\theta$

Hence

$$X_1(f) = \pi C\left[\delta(f - f_o) + \delta(f + f_o)\right]$$

$$+ j\pi S\left[\delta(f - f_o) - \delta(f + f_o)\right] \qquad (5.10)$$

The corresponding expressions for the TCM signal may be obtained by substitution for $x_1(t)$ and $X_1(f)$ in eqns.5.5 and 5.6 respectively. Therefore

$$y_{TCM}(t) = \sum_{k=-\infty}^{\infty} \left[C\cos\left[2\pi a f_o\left[t - k\left[\frac{a-1}{a}\right]T\right]\right] \right.$$

$$\left. - S\sin\left[2\pi a f_o\left[t - k\left[\frac{a-1}{a}\right]T\right]\right] \right]$$

$$\cdot \text{rect}\left[\frac{a(t-kT)}{T}\right] \qquad (5.11)$$

$$Y_{TCM}(f) = \frac{\pi}{a} \sum_{k=-\infty}^{\infty} \Big[C\big[\delta(f - f_o - k/T) + \delta(f + f_o - k/T)\big] - jS\big[\delta(f - f_o - k/T) - \delta(f + f_o - k/T)\big]\Big] \cdot Sa\big[\pi T(f/a - f + k/T)\big] \qquad (5.12)$$

It may be seen that both the real and imaginary parts of the spectrum consist of pairs of impulse trains at frequencies $f=f_o+k/T$ and $f=k/T-f_o$. Substitution for k/T in the weighting functions provides greater insight into the shape of the spectrum. Thus

$$Y_{TCM}(f) = \frac{\pi}{a} \sum_{k=-\infty}^{\infty} (C+jS)\, \delta(f-f_o - k/T)\, Sa\big[\pi T/a\ (f-af_o)\big] + (C-jS)\, \delta(f+f_o - k/T)\, Sa\big[\pi T/a\ (f+af_o)\big] \qquad (5.13)$$

It can now be seen that the $\sin(x)/x$ weighting functions are centred on $\pm\ af_o$, and that the complex spectrum is hermitian, i.e. $Y(-f)=Y^*(f)$, where the * operator is defined as complex conjugation.

The important properties of $Y_{TCM}(f)$ will now be discussed and an alternative (Fourier) series expansion found for $y_{TCM}(t)$.

(1) There is no dc component in the TCM signal, since

for this to occur, $f_o + k/T$ and/or $k/T - f_o$ must be zero. Hence, f_oT must be an integer and both the weighting functions simplify to $Sa[\pm j\pi]$, where j is a non-zero integer ($f_o \neq 0$). Therefore, the magnitude of any component at $f=0$ is zero. This result has further been shown to be true for all types of input signals which have no dc component [1].

(2) On first examination, it would appear that time-compression of a sinusoid of frequency, f_o, by a factor 'a' would produce spectral components at $\pm af_o$. However, these only occur if a certain relationship exists between a, f_o, and T. From eqn.5.13, for there to be a component at af_o, then $f_o + k/T = af_o$, hence

$$(a-1)f_oT = \text{integer} \qquad (5.14)$$

(3) The relationship of these parameters also determines whether impulses from both sets coincide at the same frequency. From eqn.5.13, for coincident impulses, $f_o + k_1/T = k_2/T - f_o$, ie.;

$$2f_oT = k_2 - k_1 = \text{integer} \qquad (5.15)$$

The nature of the TCM spectrum, $Y_{TCM}(f)$, allows an alternative time-domain expression to be obtained in terms

of an infinite summation of cosine and sine functions, ie. a Fourier series expansion. Consider first the real spectrum, $Re\left[Y_{TCM}(f)\right]$, and let this be split into $Re\left[Y_{TCM1}(f)\right]$ and $Re\left[Y_{TCM2}(f)\right]$ as shown in fig.5.3. Time domain expressions, $y_{R1}(t)$ and $y_{R2}(t)$ respectively, corresponding to these two spectra may be written as follows where the appropriate substitution for f in the Sa(x) functions has been made.

$$y_{R1}(t) = \frac{C}{a} \sum_{k \geq k_1}^{\infty} \cos 2\pi(f_o + k/T)t \cdot Sa\left[\frac{\pi T}{a}(k/T - (a-1)f_o)\right] \qquad (5.16)$$

where k_1 is the lowest integer for which $f_o + k/T$ is non-negative, and

$$y_{R2}(t) = \frac{C}{a} \sum_{k \geq k_2}^{\infty} \cos 2\pi(f_o + k/T)t \cdot Sa\left[\frac{\pi T}{a}(k/T + (a-1)f_o)\right] \qquad (5.17)$$

where k_2 is the lowest integer for which $k/T - f_o$ is non-negative $= k_1 - 1$.

Now since cos(-f)=cos(f) and Sa(-x)=Sa(x), we can replace the summation in eqn.5.17 by a continuation of the summation in eqn.5.16 from $-\infty$ to (k_1-1). Thus

$$y_R(t) = y_{R1}(t) + y_{R2}(t)$$

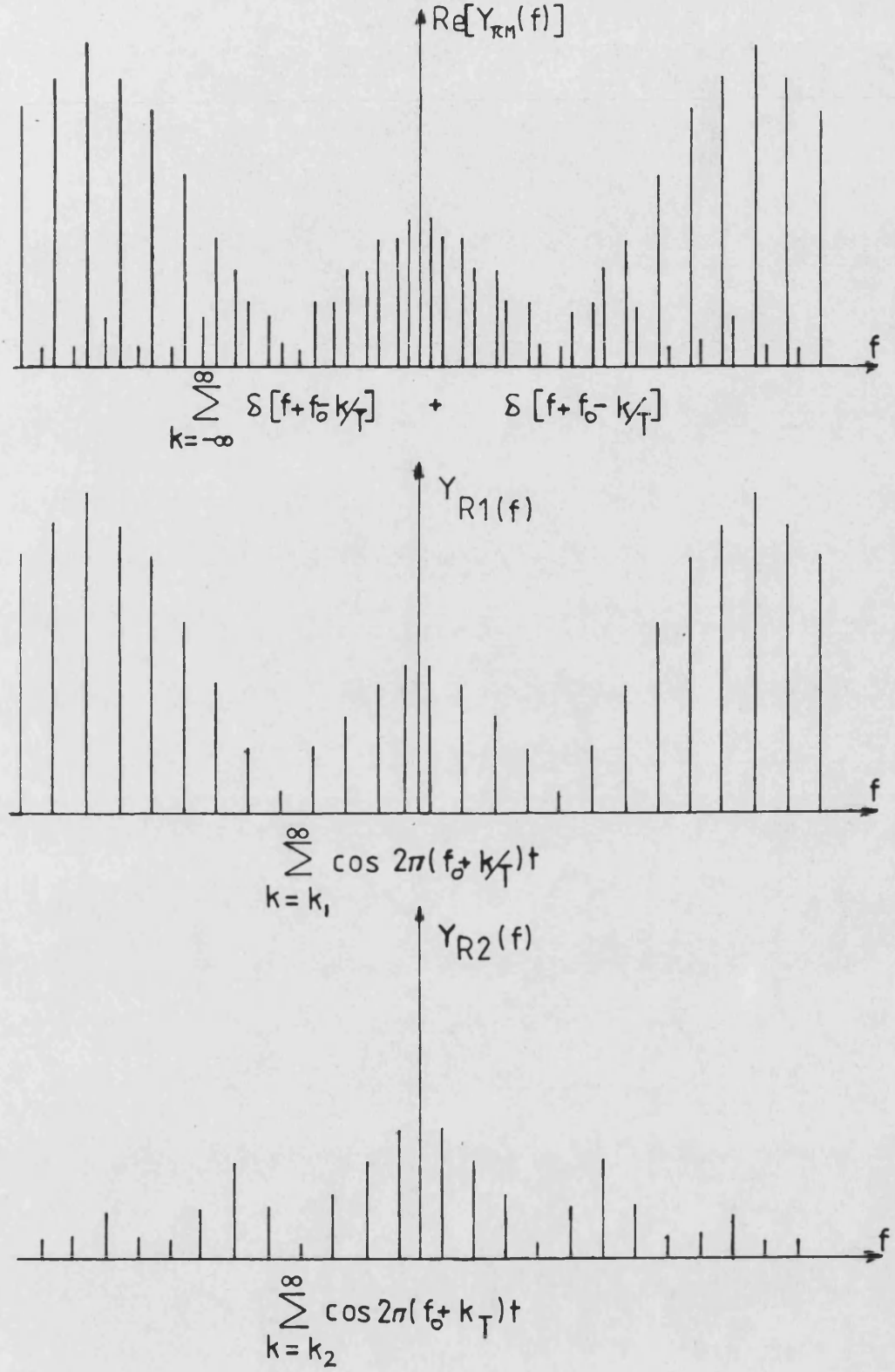

Fig.5.3 Splitting of real part of complex exponential series TCM spectrum into two cosine series.

$$= \frac{C}{a} \sum_{k=-\infty}^{\infty} \cos 2\pi(f_o + k/T)t \cdot Sa\left[\frac{\pi T}{a}(k/T - (a-1)f_o)\right]$$

(5.18)

The imaginary part, $Im\left[Y_{TCM}(f)\right]$, can be split identically, and the two time-domain expressions written as

$$y_{I1}(t) = \frac{-S}{a} \sum_{k=k_1}^{\infty} \sin 2\pi(f_o + k/T)t \cdot Sa\left[\frac{\pi T}{a}(k/T - (a-1)f_o)\right]$$

(5.19)

and

$$y_{I2}(t) = \frac{S}{a} \sum_{k=k_2}^{\infty} \sin 2\pi(f_o + k/T)t \cdot Sa\left[\frac{\pi T}{a}(k/T + (a-1)f_o)\right]$$

(5.20)

where k_1 and k_2 have the same values as before.

Again, since $\sin(-f) = -\sin(f)$, we can replace the summation in eqn.5.20 by a continuation of the summation in eqn.5.19. Thus

$$y_i(t) = \frac{-S}{a} \sum_{k=-\infty}^{\infty} \sin 2\pi(f_o + k/T)t \cdot Sa\left[\frac{\pi T}{a}(k/T - (a-1)f_o)\right]$$

(5.21)

By superposition, $y_{TCM}(t)$ is the sum of $y_R(t)$ and $y_I(t)$

$$y_{TCM}(t) = \frac{1}{a} \sum_{k=-\infty}^{\infty} A \cos 2\pi(f_o + k/T)t + \theta \cdot Sa\left[\frac{\pi T}{a}(k/T - (a-1)f_o)\right]$$

(5.22)

It is possible to re-write eqn.5.11 in terms of the original cosine function of f_o and θ as

$$y_{TCM}(t) = \sum_{k=-\infty}^{\infty} A \cos\left[2\pi a f_o t - 2\pi f_o k(a-1)T + \theta\right]$$

$$\cdot \cdot \text{rect}\left[\frac{a(t-kT)}{T}\right] \qquad (5.23)$$

Hence, a general segmented cosine waveform of frequency, f_o and phase θ, time-compressed by a factor, a, is composed of bursts of a sinusoid with frequency af_o and phase equal to $\theta - 2\pi k(a-1)f_o T$. However, for the special case when $(a-1)f_o T$= integer, the phase shift due to segmented time compression is an integer multiple of 2π for all k. Therefore eqn.5.23 simplifies to

$$y_{TCM}(t) = \sum_{k=-\infty}^{\infty} A \cos\left[2\pi a f_o t + \theta\right] \cdot \text{rect}\left[\frac{a(t-kT)}{T}\right] \qquad (5.24)$$

The waveform is now simply bursts of $\cos 2\pi a f_o t$. This is not unexpected as reference to eqn.5.14 shows that the above condition is also the requirement for spectral components at $\pm af_o$.

The period, T_{TCM}, of the TCM waveform with sinusoidal input may be found from a consideration of the spectral properties from eqn.5.12. It is also necessary for T_{TCM} to

be an integer multiple of the frame period, T. Components in $Y_{TCM}(f)$ occur at frequencies $|f_o + k/T|$, therefore the period must be the reciprocal of the highest common factor (HCF) of all these frequencies and 1/T, ie.

$$T_{TCM} = \frac{1}{HCF\left[1/T,\ f_o,\ \sum_k |f_o+k/T|\right]} \qquad (5.25)$$

At first this appears to be a complex problem, however, the HCF of 1/T and f_o is also the HCF of f_o+k/T for all k, hence

$$T_{TCM} = \frac{1}{HCF\ (f_o,\ 1/T)} = \frac{T}{HCF\ (1, f_o T)} \qquad (5.26)$$

It is now possible by using eqns.5.23 and 5.26 to define the segmented TCM signal with a single active channel and sinusoidal modulation over one complete period, ie.

$$y_{TCM_T}(t) = \sum_{k\equiv 0}^{K_T-1} A\cos\left[2\pi a f_o t - 2\pi f_o k(a-1)T + \theta\right]$$

$$\cdot\ \mathrm{rect}\left[\frac{a(t-kT)}{T}\right] \qquad (5.27)$$

where $K_T = \frac{1}{HCF(1,\ f_o T)}$

5.3.2 MULTIPLE ACTIVE CHANNELS

Let the input signal from channel r, $x_r(t)$, be;

$$x_r(t) = A_r \cos\left[2\pi f_r t + \theta_r\right] \qquad (5.28)$$

Expressing this in C cos(x)-S sin(x) form and substituting in eqn.5.7 gives;

$$y_{TCM}(t) = \sum_{r=1}^{R} y_r(t)$$

$$= \sum_{r=1}^{R} \sum_{k=-\infty}^{\infty} \text{rect}\left[\frac{a(t-kT-(r-1)T/a)}{T}\right]$$

$$\cdot \left[C_r \cos\left[2\pi a f_r\left[t - k\left[\frac{a-1}{a}\right]T - \left[\frac{r-1}{a}\right]T\right]\right]\right.$$

$$\left. - S_r \sin\left[2\pi a f_r\left[t - k\left[\frac{a-1}{a}\right]T - \left[\frac{r-1}{a}\right]T\right]\right]\right] \qquad (5.29)$$

where $C_r = A_r\cos\theta_r$ and $S_r = A_r\sin\theta_r$

The TCM spectrum is obtained similarly by substitution into eqn.5.8.

$$Y_{TCM}(f) = \frac{\pi}{a} \sum_{r=1}^{R} \sum_{k=-\infty}^{\infty} \left[C_r\left[\delta(f-f_r - k/T) + \delta(f+f_r - k/T)\right]\right.$$

$$\left. - jS_r\left[\delta(f - f_r - k/T) - \delta(f + f_r - k/T)\right]\right]$$

$$\cdot\ e^{-j2\pi f(r-1)T/a}\ \cdot\ Sa\left[\pi T(f/a - f + k/T)\right] \qquad (5.30)$$

Substitution for the values of k/T from the R pairs of impulse functions into the appropriate Sa(x) functions gives;

$$Y_{TCM}(f) = \frac{\pi}{a} \sum_{r=1}^{R} \sum_{k=-\infty}^{\infty} e^{-j2\pi f(r-1)T/a}$$

$$\cdot \Big[(C_r + jS_r)\ \delta(f - f_r - k/T)\ Sa\left[\pi T/a\ (f - af_r)\right]$$

$$+ (C_r - jS_r)\ \delta(f + f_r - k/T)\ Sa\left[\pi T/a\ (f + af_r)\right] \Big] \qquad (5.31)$$

Unlike the case for one active channel, the characteristics of the above spectrum can not be generalised due to the unknown relationship between the signals from the various channels. However, there is no dc component if there is none in the input signals and the impulses from all R positive and and negative centred sets only coincide if $2f_rT$ is an integer for all r.

The alternative Fourier series representation of $y_{TCM}(t)$ may be obtained from eqn.5.22 using eqn.5.30.

$$y_{TCM}(t) = \frac{1}{a} \sum_{r=1}^{R} \sum_{k=-\infty}^{\infty} \Big[C_r \cos\left[2\pi(f_r + k/T)(t-(r-1)T/a)\right]$$

$$- S_r \sin\left[2\pi(f_r + k/T)(t - (r-1)T/a)\right]\Big]$$

$$\cdot e^{-j2\pi f(r-1)T/a} \cdot Sa\left[\frac{\pi T}{a}(k/T - (a-1)f_r)\right]$$

$$= \frac{1}{a} \sum_{r=1}^{R} \sum_{k=-\infty}^{\infty} A_r \cos\left[2\pi(f_r + k/T)(t-(r-1)T/a)+\theta_r\right]$$

$$\cdot e^{-j2\pi f_r(r-1)T/a} \cdot Sa\left[\frac{\pi T}{a}(k/T - (a-1)f_r)\right] \quad (5.32)$$

It can be seen that eqn.5.32 is considerably more complex than the corresponding single channel expression.

Eqn.5.29 may be re-written in terms of the original cosine signals as follows

$$y_{TCM}(t) = \sum_{r=1}^{R} y_r(t)$$

$$= \sum_{r=1}^{R} \sum_{k=-\infty}^{\infty} \text{rect}\left[\frac{a(t-kT-(r-1)T/a)}{T}\right]$$

$$\cdot A_r \cos\left[2\pi a f_r t + \theta_r - 2\pi\left[k(a-1)f_r T + (r-1)f_r T\right]\right]$$

(5.33)

Thus the TCM waveform is composed of segments of the original input signals frequency scaled by the compression factor 'a' and phase shifted by $-2\pi\left[k(a-1)f_r T + (r-1)f_r T\right]$. When $(a-1)f_r T$=integer, the phase shift for segment r

(channel r) is independent of the frame number k.

Components in the spectrum occur at $|f_r + k/T|$ and the overall period of the TCM waveform, $T_{TCM}(t)$, is;

$$T_{TCM} = \frac{1}{HCF\left[1/T,\ \sum_r \sum_k |f_r + k/T|\right]} \qquad (5.34)$$

which simplifies to

$$T_{TCM} = \frac{1}{HCF\left[1/T,\ \sum_r f_r\right]} = \frac{T}{HCF\left[1,\ \sum_r f_r T\right]} \qquad (5.35)$$

Hence one period of TCM waveform with multiple active channels and sinusoidal modulation can be represented by

$$y_{TCM_T}(t) = \sum_{r=1}^{R} \sum_{k=0}^{K_T-1} \text{rect}\left[\frac{a(t - kT - (r-1)T/a)}{T}\right]$$

$$\cdot A_r \cos\left[2\pi a f_r t + \theta_r - 2\pi\left[k(a-1)f_r T + (r-1)f_r T\right]\right] \qquad (5.36)$$

where $K_T = \frac{1}{HCF\left[1,\ \sum_r f_r T\right]}$

Eqn.5.36 is the general equation for all R channels active. When there are one or more inactive channels, the appropriate values of r are simply removed from the summation.

5.4 MULTI-TONE MESSAGE SIGNALS

5.4.1 SINGLE ACTIVE CHANNEL

Let the single input signal, $x_1(t)$, consist of M sinusoidal components of frequency f_m (not necessarily harmonically related), phase θ_m and amplitude A_m.

$$x_1(t) = \sum_{m=1}^{M} A_m \cos\left[2\pi f_m t + \theta_m\right]$$

$$= \sum_{m=1}^{M} C_m \cos 2\pi f_m t + S_m \sin 2\pi f_m t \qquad (5.37)$$

where $C_m = A_m \cos\theta_m$ and $S_m = A_m \sin\theta_m$

Hence

$$X_1(f) = \pi \sum_{m=1}^{M} C_m\left[\delta(f - f_m) + \delta(f + f_m)\right]$$

$$+ jS\left[\delta(f - f_m) - \delta(f + f_m)\right] \qquad (5.38)$$

The expressions for the TCM signal may be obtained by substitution into eqns.5.5 and 5.6. Thus

$$y_{TCM}(t) = \sum_{m=1}^{M} \sum_{k=-\infty}^{\infty} \left[C_m \cos\left[2\pi a f_m\left[t - k\left[\frac{a-1}{a}\right]T\right]\right]\right.$$

$$\left. + S_m \sin\left[2\pi a f_m\left[t - k\left[\frac{a-1}{a}\right]T\right]\right]\right] \cdot \mathrm{rect}\left[\frac{a(t-kT)}{T}\right] \qquad (5.39)$$

and

$$Y_{TCM}(f) = \frac{\pi}{a} \sum_{m=1}^{M} \sum_{k=-\infty}^{\infty} \left[C_m \left[\delta(f-f_m - k/T) + \delta(f+f_m - k/T) \right] \right.$$

$$\left. - jS_m \left[\delta(f - f_m - k/T) - \delta(f + f_m - k/T) \right] \right]$$

$$. \; Sa\left[\pi T(f/a - f + k/T) \right] \qquad (5.40)$$

Both the real and imaginary spectra are similar to those for sinusoidal signals, except that each now consists of M pairs of impulse trains centred on $f_m + k/T$ and $k/T - f_m$. Hence the Fourier series representation of $T_{TCM}(t)$ may be easily found using eqn.5.22 as

$$y_{TCM}(t) = \frac{1}{a} \sum_{m=1}^{M} \sum_{k=-\infty}^{\infty} A_m \cos 2\pi(f_m + k/T)t$$

$$. \; Sa\left[\frac{\pi T}{a}(k/T - (a-1)f_m) \right] \qquad (5.41)$$

Now, eqn.5.39 may be re-written in terms of the original cosine functions as

$$y_{TCM}(t) = \sum_{m=1}^{M} \sum_{k=-\infty}^{\infty} A_m \cos\left[2\pi a f_m t - 2\pi k(a-1) f_m T + \theta_m \right]$$

$$. \; \mathrm{rect}\left[\frac{a(t-kT)}{T} \right] \qquad (5.42)$$

Hence, for a general multi-tone input, the segmented TCM output signal consists of bursts of an identical signal but with all components frequency scaled by a factor 'a' with a frame dependent phase shift of $-2\pi f_m k(a-1)T$. Since this latter phase shift is proportional to signal frequency, no phase distortion occurs. For the special case when $(a-1)f_m T$=integer, for all m, the above equation reduces to;

$$y_{TCM}(t) = \sum_{m=1}^{M} \sum_{k=-\infty}^{\infty} A_m \cos\left[2\pi a f_m t + \theta_m\right] \cdot \text{rect}\left[\frac{a(t-kT)}{T}\right] \qquad (5.43)$$

The TCM waveform is now simply a frequency scaled version of the input.

When all the signal components are successive harmonics of a certain fundamental frequency, ie $f_m = m f_f$, then the condition for eqn.5.43 to hold reduces to $(a-1)f_f T$ = integer. This latter class of signal, when the input phase angles, θ_m, are random but with uniform distribution and all the amplitudes, A_m, are equal is representative of a band of white noise and is of considerable importance in chapters 8 and 9.

Components in the TCM spectrum occur at $|f_m + k/T|$ and hence the TCM signal period is given by;

$$T_{TCM}(t) = \frac{1}{HCF\left[1/T,\ \sum_m \sum_k |f_m + k/T|\right]}$$

$$= \frac{1}{HCF\left[1/T,\ \sum_m f_m\right]} \quad \text{for general signals} \qquad (5.44)$$

and

$$T_{TCM}(t) = \frac{1}{HCF\left[1/T,\ f_f\right]} \quad \text{for harmonic signals} \qquad (5.45)$$

Hence one period of the waveform for a general multitone input can be represented by

$$y_{TCM_T}(t) = \sum_{m=1}^{M} \sum_{k=0}^{K_I-1} A_m \cos\left[2\pi a f_m t + \theta_m - 2\pi(a-1) f_m T\right]$$

$$\cdot \text{rect}\left[\frac{a(t - kT)}{T}\right] \qquad (5.46)$$

$$\text{where } K_T = \frac{1}{HCF\left[T,\ \sum_m f_m T\right]}$$

and

$$y_{TCM_T}(t) = \sum_{m=1}^{M} \sum_{k=0}^{K_I-1} A_m \cos\left[2\pi a m f_f t + \theta_m - 2\pi(a-1) m f_f T\right]$$

$$\cdot \text{rect}\left[\frac{a(t - kT)}{T}\right] \qquad (5.47)$$

where $K_T = \frac{1}{HCF(T, f_f T)}$, for an input whose components are harmonically related.

5.4.2 MULTIPLE ACTIVE CHANNELS

The relevant expressions for this final, most general category of signals may be obtained in a straightforward manner by pertinent substitution using previous results. Let the input signal from channel r be;

$$x_r(t) = \sum_{m_r=1}^{M_r} A_{rm} \cos\left[2\pi f_{rm} t + \theta_{rm}\right] \qquad (5.48)$$

Expressing eqn.5.48 in C cos(x)-S sin(x) form and using eqn.5.29 gives the segmented TCM signal as;

$$\begin{aligned} y_{TCM}(t) &= \sum_{r=1}^{B} y_r(t) \\ &= \sum_{r=1}^{B} \sum_{m_r=1}^{M_r} \sum_{k=-\infty}^{\infty} \text{rect}\left[\frac{a(t-kT-(r-1)T/a)}{T}\right] \\ &\quad \cdot \left[C_{rm} \cos\left[2\pi a f_{rm}\left[t - k\left[\frac{a-1}{a}\right]T - \left[\frac{r-1}{a}\right]T\right]\right]\right. \\ &\quad \left. - S \sin\left[2\pi a f_{rm}\left[t - k\left[\frac{a-1}{a}\right]T - \left[\frac{r-1}{a}\right]T\right]\right]\right] \end{aligned} \qquad (5.49)$$

The alternative Fourier series expansion is obtained by a similar substitution in eqn.5.32

$$y_{TCM}(t) = \frac{1}{a} \sum_{r=1}^{B} \sum_{m_r=1}^{M_r} \sum_{k=-\infty}^{\infty} \cdot e^{-j2\pi f_{rm}(r-1)T/a}$$

$$\cdot A_{rm} \cos\left[2\pi(f_{rm} + k/T)(t-(r-1)T/a) + \theta_{rm}\right]$$

$$\cdot Sa\left[\frac{\pi T}{a}\left[k/T - (a-1)f_{rm}\right]\right] \qquad (5.50)$$

The expression for the TCM spectrum is a modified form of eqn.5.30. Thus

$$Y_{TCM}(f) = \frac{\pi}{a} \sum_{r=1}^{B} \sum_{m_r=1}^{M_r} \sum_{k=-\infty}^{\infty} e^{-j2\pi f(r-1)T/a}$$

$$\cdot \Big[C_{rm}\left[\delta(f-f_{rm} - k/T) + \delta(f+f_{rm} - k/T)\right]$$

$$- jS_{rm}\left[\delta(f - f_{rm} - k/T) - \delta(f + f_{rm} - k/T)\right]\Big]$$

$$\cdot Sa\left[\pi T(f/a - f + k/T)\right] \qquad (5.51)$$

Components in the spectrum occur at frequencies of $|f_{rm} + k/T|$ and hence the overall period of the TCM waveform is

$$T_{TCM}(t) = \frac{1}{HCF\left[1/T,\ \sum_r \sum_{m_r} \sum_k |f_{rm}+k/T|\right]} \qquad (5.52)$$

As with the other classes of signal, this simplifies to;

$$T_{TCM}(t) = \frac{1}{HCF\left[1/T,\ \sum_r \sum_{m_r} f_{rm}\right]} \qquad (5.53)$$

Writing eqn.5.49 in terms of the original cosine functions and using the above result allows one period of the multi-channel, multi-tone message TCM signal to be written as

$$y_{TCM_T}(t) = \sum_{r=1}^{B} \sum_{m_r=1}^{M_r} \sum_{k=0}^{K_T-1} \text{rect}\left[\frac{a(t-kT-(r-1)T/a)}{T}\right]$$

$$A_{rm} \cos\left[2\pi a f_{rm} t + \theta_{rm} - 2\pi\left[k(a-1)f_{rm}T + (r-1)f_{rm}T\right]\right] \qquad (5.54)$$

$$\text{where } K_T = \frac{1}{HCF\left[1,\ \sum_r \sum_{m_r} f_{rm}T\right]}$$

5.5 CONCLUSIONS

Expressions describing the TCM waveform in both the time- and frequency domains for various classes of message signal have been developed. For the case of a single active channel with a sinusoidal input at frequency, f_o, and TCM frame period of T (seconds), the TCM signal spectrum is composed of two infinite trains of impulses. These are centred around $\pm af_o$, where a is the compression ratio. However, there is not necessarily a component at these frequencies unless $(a-1)f_oT$ is an integer. Similarly, the impulses from the two trains do not coincide at every frequency unless $2f_o T$ is an integer. Each additional input frequency (from either the same or from another message channel) adds another pair of impulse trains to the composite spectrum with the appropriate frequency and phase shift. Hence, due to the many combinations of parameters, it is not possible to draw general conclusions as to the spectral characteristics with arbitrary signals.

Alternative expressions have also been derived representing the TCM signal in periodic form. These are of a form suitable for subsequent analysis using a numerical technique such as the discrete Fourier transform. The application of such a technique with the further complication of modulation of the TCM signal on to an FM bearer is considered in chapter 8.

Due to the large number of combinations of variables in the above expressions, it is not possible to make general statements about either the time or frequency domain characteristics of the TCM signal, except for the case of a single sinusoid. However, although many of the expressions are complex, numerical techniques may be employed for their solution. This will be investigated for the application of TCM for frequency modulation in chapters 8 and 9. In this respect, the equations describing the periodic form of the TCM signal will be of particular importance.

5.6 REFERENCES

(1) Skuse,B.: 'An alternative time-compression multiplexed VHF single sideband system', MSc thesis, Chapter 5, University of Bath, 1984.

(2) Papoulis,A.: 'The Fourier integral and its applications', Mc Graw-Hill, 1962.

(3) Beauchamp,K.G. and Yuen,C.K.: 'Digital methods for signal analysis', chapter 3.4, George Allen and Unwin, 1979.

CHAPTER SIX

THEORETICAL ANALYSIS OF ANGLE MODULATION

6.1 INTRODUCTION

The basic equations describing general angle modulation with both sinusoidal and general multi-tone modulating signals are derived. Expressions are then found for the frequency spectra using a Fourier series expansion involving Bessel functions. It is shown that unlike the case for sinusoidal signals, the calculation of spectra for other baseband waveforms is far from straightforward involving the tedious solution of Diophantine equations. The bandwidths of equivalent phase and frequency modulation systems with sinusoidal signals are compared. The reduced bandwidth requirement of the latter has caused it to be universally adopted for mobile radio, and hence it is the system upon which the majority of subsequent analysis is based.

The noise characteristics of an ideal phase or frequency demodulator are complex. However, with an ideal rectangular IF filter under conditions of good carrier-to-noise ratio, the output noise is approximately white for a phase detector whereas it rises at about 6dB per octave for a frequency discriminator. This has led to the adoption of +6dB/octave transmitter pre-emphasis in

practical FM systems in an attempt to normalise the recovered signal-to-noise ratio across the audio band.

An expression is derived for the output of an FM detector with sinusoidal modulation in the presence of an IF filter, using the vector summation or Fourier technique. The suitability of this and also the asymptotic method of Carson and Fry [4] is considered for more complex modulating signals. The work of Rice and others concerning random (noise) modulation is also discussed. Finally the performance of FM in the presence of general interferering signals is considered.

6.2 FUNDAMENTAL EXPRESSIONS

A general equation describing an angle modulated carrier, $e_{\phi M}(t)$, of frequency, f_c, and amplitude, A_c, is

$$e_{\phi M}(t) = A_c \cos\left[2\pi f_c t + \phi(t) + \theta_c\right]$$

$$= \mathrm{Re}\left[A_c e^{j\left[2\pi f_c t + \theta_c\right]} \cdot e^{j\phi(t)}\right] \qquad (6.1)$$

where $\phi(t)$ is related to the message signal,

For phase modulation $\phi(t)$ is directly proportional to the message signal m(t). For the sinusoidal signal

$$m(t) = A_m \sin\left[2\pi f_m t + \theta_m\right] \qquad (6.2)$$

$$e_{PM}(t) = \mathrm{Re}\left[A_c e^{j\left[2\pi f_c t + \theta_c\right]} \cdot e^{j\beta \sin\left[2\pi f_m t + \theta_m\right]}\right] \qquad (6.3)$$

where β is the peak phase deviation = $k_d A_m$ (radians) and k_m is a modulation constant.

The peak frequency deviation, Δf, is the maximum value of $\left[\frac{1}{2\pi} d\phi(t)/dt\right] = \beta f_m$, ie. proportional to the modulating frequency.

For the complex message signal, m(t), consisting of M sinusoidal components

$$m(t) = \sum_{m=1}^{M} A_m \sin\left[2\pi f_m t + \theta_m\right] \qquad (6.4)$$

then

$$e_{PM}(t) = \mathrm{Re}\left[A_c e^{j\left[2\pi f_c t + \theta_c\right]} \cdot \prod_{m=1}^{M} e^{j\beta_m \sin\left[2\pi f_m t + \theta_m\right]}\right] \qquad (6.5)$$

The rms phase deviation, β_{rms}, is $\left[\frac{\sum_{m=1}^{M} \beta_m^2}{2}\right]^{1/2}$ whilst the rms frequency deviation, Δf_{rms}, is $\left[\frac{\sum_{m=1}^{M} (\beta_m f_m)^2}{2}\right]^{1/2}$.

For frequency modulation, $\dot{\phi}(t)$, is proportional to m(t). For the purpose of comparison with PM in section 6.3.1, the components in m(t) will now be phase shifted by 90^{o}. Hence for the sinusoidal signal

$$\phi(t) = k_d \int_0^t \omega(\tau)\, d\tau$$

$$= \int_0^t 2\pi A_m \cos\left[2\pi f_m \tau + \theta_m\right] \qquad (6.6)$$

the FM waveform is

$$e_{FM}(t) = \mathrm{Re}\left[A_c\, e^{j\left[2\pi f_c t + \theta_c'\right]} \cdot e^{j \frac{k_d A_m}{f_m} \sin\left[2\pi f_m t + \theta_m\right]} \right] \tag{6.7}$$

where $\theta_c' = \theta_c - \frac{k_d A_m}{f_m} \sin\theta_m$

The peak frequency deviation, Δf, is $k_d A_m$, whilst the peak phase deviation is $\frac{k_d A_m}{f_m} = \frac{\Delta f}{f_m}$.

For the multitone signal

$$e_{FM}(t) = \mathrm{Re}\left[A_c\, e^{j\left[2\pi f_c t + \theta_c'\right]} \cdot \prod_{m=1}^{M} e^{j \frac{k_d A_m}{f_m} \sin\left[2\pi f_m t + \theta_m\right]} \right] \tag{6.8}$$

where $\theta_c' = \theta_c - \sum_{m=1}^{M} \frac{k_d A_m}{f_m} \sin\theta_m$

Thus the rms frequency deviation is $\left[\frac{\sum_{m=1}^{M} \left[k_d A_m\right]^2}{2} \right]^{1/2}$. The rms phase deviation is $\left[\frac{\sum_{m=1}^{M} \left[\frac{k_d A_m}{f_m}\right]^2}{2} \right]^{1/2}$. Thus, in contrast to PM the peak (or rms) frequency deviation is con-

stant while the phase deviation is inversely proportional to the modulation frequency.

6.3 SPECTRAL ANALYSIS USING A FOURIER SERIES EXPANSION

6.3.1 SINUSOIDAL MODULATION

Eqns.6.3 and 6.7 may be expanded in terms of a Fourier series using the following identity

$$e^{j\beta\sin\left[2\pi f_m t + \theta_m\right]} = \sum_{n=-\infty}^{\infty} J_n(\beta) e^{jn\left[2\pi f_m t + \theta_m\right]} \qquad (6.9)$$

where $J_n(\beta)$ is the Bessel function of the first kind of order n and argument β, and is defined as

$$J_n(\beta) = \sum_{k=0}^{\infty} \frac{(-1)^k \beta^{(n+2k)}}{2^{(n+2k)}\, k!\,(n+k)!} \qquad (6.10)$$

thus

$$e_{PM}(t) = \mathrm{Re}\left[A_c\, e^{j\left[2\pi f_c t + \theta_c\right]} \cdot \sum_{m=1}^{M} J_n(\beta)\, e^{jn\left[2\pi f_m t + \theta_m\right]} \right] \qquad (6.11)$$

and

$$e_{FM}(t) = \mathrm{Re}\left[A_c\, e^{j\left[2\pi f_c t + \theta_c\right]} \cdot \sum_{m=1}^{M} J_n\left[\frac{\Delta f}{f_m}\right] e^{jn\left[2\pi f_m t + \theta_m\right]} \right] \qquad (6.12)$$

Comparison of the latter equations shows that the PM and FM spectra are identical if $\Delta F = \beta f_m$ and the modulating signal in the FM case is phase shifted by 90^o. Thus the general øM spectrum for a sinusoidal modulating signal of frequency, f_m, consists of a carrier plus an infinite number of sidebands spaced at frequencies of $\pm f_m$, $\pm 2f_m$ etc. whose amplitudes are determined by the appropriate Bessel function.

A well known rule of thumb guide used to estimate bandwidths in øM systems is Carson's rule [1]. This states that, for sinusoidal modulation, approximately $2(\beta+1)$ sidebands in addition to the carrier are required to transmit 98% of the total power. Thus the approximate bandwidths are $2f_m(\beta+1)$ and $2(\Delta f+f_m)$ for phase and frequency modulation respectively. Hence, over the audio frequency range of 300-3000Hz, the PM bandwidth increases by a factor of ten whereas the FM bandwidth shows appreciably less variation, particularly when Δf is large. It is predominantly for this reason that FM is employed in preference to PM in practical 'fixed' bandwidth communication systems. However, when pre-emphasis is employed (section 6.4) the distinction between the two systems becomes less clear.

For the special case when β (or $\Delta f/f_m$) $<<1$, the following approximations may be applied

$$J_0(\beta) \simeq 1 - \left|\frac{\beta}{2}\right|^2 \qquad (6.13)$$

$$J_n(\beta) \simeq \frac{1}{n!}\left|\frac{\beta}{2}\right|^n \; ; \; n \neq 0 \qquad (6.14)$$

Hence, $J_0(\beta) = 1$, $J_1(\beta) = \beta/2$ and $J_1(\beta) = -\beta/2$, with all others orders negligible. Under these circumstances, the øM spectrum consists of just one pair of sidebands, rather like AM but with the lower sideband phase reversed, and may be deemed 'linear' modulation. However, in general, angle modulation is a non-linear (exponential) process, and it is not possible to relate the modulated spectrum to the original signal spectrum.

6.3.2 COMPLEX MODULATION

It is also possible to expand eqns.6.4 and 6.8 for complex modulation using the identity of eqn.6.9. Hence, for PM

$$e_{PM}(t) = \mathrm{Re}\left[A_c\, e^{j\left[2\pi f_c t + \theta_c\right]} \cdot \prod_{m=1}^{M} \sum_{n_m=-\infty}^{\infty} J_{n_m}(\beta) \cdot e^{jn\left[2\pi f_m t + n\theta_n\right]}\right] \qquad (6.15)$$

whilst for FM

$$e_{FM}(t) = \mathrm{Re}\left[A_c\, e^{j\left[2\pi f_c t + \theta'_c\right]}\right.$$

$$\prod_{m=1}^{M} \sum_{n_m=-\infty}^{\infty} J_{n_m}\left[\frac{\Delta f_m}{f_m}\right] e^{jn\left[2\pi f_m t + n\theta_n\right]} \qquad (6.16)$$

Unlike sinusoidal modulation, the PM and FM spectra are only identical if $\beta_m = \frac{\Delta f_m}{f_m}$ for all m, and all components in the FM baseband signal are phase shifted by 90^o. Since a constant phase shift distorts the time waveform, it can be said that the PM and FM spectra of a common complex message signal are dissimilar. The sidebands in both spectra occur at frequencies f_s given by

$$f_s = f_c + \sum_{m=1}^{M} n_m f_m \qquad (6.17)$$

where n_m may take any value from $-\infty$ to ∞.

The magnitude, M_s', of one particular component at the sideband frequency, f_s, is given by the product of A_c and the M Bessel coefficients, whose orders, n_m, are one set of solutions to eqn.6.17. This equation is of linear Diophantine type [2] and has an infinite number of solutions for any particular value of f_s. Hence each sideband is generally composed of an infinite number of components, and the total magnitude M_s is given by

$$M_s = \sum M_s' = A_c \sum \prod_{m=1}^{M} J_{n_m}(x) \qquad (6.18)$$

where the summation is carried out for all values of

n_m satisfying eqn.6.17, and $x=\beta_m$ for PM and $\Delta f_m/f_m$ for FM.

In practice, there will only be a finite set of solutions to eqn.6.17 which produce components of appreciable amplitude due to the diminishing nature of the high order Bessel coefficients. This is especially true for narrow deviations. However, in general the determination of spectra by this method is tedious.

6.4 SIGNAL-TO-NOISE CHARACTERISTICS

In AM systems, the signal-to-noise ratio (SNR) at the output of an ideal product demodulator bears a linear relationship to the received carrier-to-noise ratio (CNR) under all conditions. However in angle modulation systems, an ideal phase or frequency detector is characterised by two distinct regions of operation. When the received CNR is high, the output SNR bears an approximately linear relationship to the input and depending upon the deviation, they may be an improvement over an equivalent AM system. However, when the CNR falls below a certain threshold, the signal-to-noise ratio deteriorates rapidly.

Taub and Schilling [1] have shown that for an ideal frequency discriminator with a perfect rectangular IF filter that the output SNR is related to the received CNR by

$$SNR(FM) = \frac{3\Delta f^2 \, f_m \, CNR(FM)}{B_{IF} + 24 \, CNR(FM) \, \Delta f \, . \exp\left[\frac{-f_m \, CNR(FM)}{B_{IF}\left[1 + \frac{\Delta f}{f_m}\right]}\right]} \qquad (6.19)$$

where CNR(FM) is measured in the IF bandwidth of $2B_{IF}$

Under conditions of good carrier-to-noise ratio with arbitrary modulation, the output noise spectral densities are

given by the simple expressions [3]

$$S(f)_{PM} = \frac{S(f+f_c)}{A_c^2} \tag{6.20}$$

and

$$S(f)_{FM} = 4\pi^2 \frac{S(f+f_c)}{A_c^2} \tag{6.21}$$

for PM and FM systems respectively, where A_c is the carrier amplitude and $S(f+f_c)$ is the noise spectral density after the IF filter.

Hence, the noise power is flat (white) in PM systems, while in FM it is proportional to the square of the baseband frequency. The corresponding output signal-to-noise ratios under the above conditions, for sinusoidal modulation and an ideal rectangular baseband filter with cut-off at f_m, are [3]

$$SNR(PM) = \beta^2 \left|\frac{B_{IF}}{f_m}\right| CNR(PM) \; ; \; CNR \text{ large} \tag{6.22}$$

and

$$SNR(FM) = 3\left|\frac{\Delta f_m}{f_m}\right|^2 \left|\frac{B_{IF}}{f_m}\right| CNR(FM) \; ; \; CNR \text{ large} \tag{6.23}$$

where the input CNR is measured in the IF bandwidth of $2B_{IF}$.

It has been shown above that the signal-to-noise ratio in FM systems under good C/N conditions and with a rectangular IF filter decreases at a rate of 6dB per octave. In practical systems, an attempt is made to remedy this situation by using pre- and de-emphasis networks in the transmitter and receiver respectively. The signal is passed through a filter with a +6dB per octave (high-pass cut-off) characteristic before transmission, with an inverse (-6dB,low-pass cut-off) filter after demodulation. Hence there is no net effect on the wanted signal, but demodulator output noise is attenuated by 6dB per octave, leading to a uniform SNR across the audio band.

6.5 FILTERING AND DEMODULATION

6.5.1 SINUSOIDAL MODULATION

Let the FM signal with sinusoidal modulation be represented by

$$e_{FM}(t) = \sum_{n=-\infty}^{\infty} J_n\left[\frac{\Delta f}{f_m}\right] \cdot \cos 2\pi(f_c + nf_m)t \qquad (6.24)$$

Let this signal be passed through an arbitrary filter which has amplitude and phase coefficients A_n, ϕ_n respectively at the sideband frequencies, $f_c + nf_m$. Therefore the output, $e'_{FM}(t)$, is

$$e'_{FM}(t) = \sum_{n=-\infty}^{\infty} A_n\, J_n\left[\frac{\Delta f}{f_m}\right] \cdot \cos\left[2\pi(f_c + nf_m)t + \phi_n\right] \qquad (6.25)$$

This can be re-written in terms of in-phase and quadrature components as

$$e'_{FM}(t) = \sum_{n=-\infty}^{\infty} A_n\, J_n\left[\frac{\Delta f}{f_m}\right] \cdot \Big[\cos(2\pi n f_m t + \phi_n)\cos(2\pi f_c t) - \sin(2\pi n f_m t + \phi_n)\sin(2\pi f_c t)\Big] \qquad (6.26)$$

Hence the resultant phase, $\theta(t)$, is;

$$\theta(t) = \tan^{-1}\left[\frac{\sum_{n=-\infty}^{\infty} A_n \cdot J_n\left[\frac{\Delta f}{f_m}\right] \sin(2\pi n f_m t + \phi_n)}{\sum_{n=-\infty}^{\infty} A_n \cdot J_n\left[\frac{\Delta f}{f_m}\right] \cos(2\pi n f_m t + \phi_n)}\right] \qquad (6.27)$$

and the output, $e_o(t)$, from a frequency demodulator is

$$e_o(t) = \frac{d}{dx}(\tan^{-1}x) \cdot \frac{dx}{dt}$$

$$= \frac{S_1 \cdot S_2 + S_3 \cdot S_4}{S_1^2 \cdot S_3^2} \qquad (6.28)$$

where

$$S_1 = \sum_{n=-\infty}^{\infty} J_n\left[\frac{\Delta f}{f_m}\right] A_n \cos(2\pi n f_m t + \phi_n)$$

$$S_2 = \sum_{n=-\infty}^{\infty} J_n\left[\frac{\Delta f}{f_m}\right] 2\pi n f_m A_n \cos(2\pi n f_m t + \phi_n)$$

$$S_3 = \sum_{n=-\infty}^{\infty} J_n\left[\frac{\Delta f}{f_m}\right] A_n \sin(2\pi n f_m t + \phi_n)$$

$$S_4 = \sum_{n=-\infty}^{\infty} J_n\left[\frac{\Delta f}{f_m}\right] 2\pi n f_m A_n \sin(2\pi n f_m t + \phi_n)$$

and

$$x = \frac{S_3}{S_1}$$

Although eqn.6.28 may be simplified in practice due to a finite filter bandwidth and by the nature of high order Bessel functions, evaluation of the demodulated signal is still cumbersome and extremely laborious. In addition, eqn.6.28 does not give the harmonics of f_m in explicit form, these must subsequently be obtained by Fourier

analysis. However, it has been shown [3] that when the filter amplitude characteristic is even and the phase characteristic is odd, such that $A_{-n}=A_n$ and $\phi_{-n}=-\phi_n$, then only odd harmonics are present.

6.5.2 COMPLEX MODULATION

Although the vector summation process above can be used for complex modulation, the final result is likely to be lost in the enormous number of computations that are necessary. A simpler approach is to use the dynamic or asymptotic method of Carson and Fry [4] which approximates the filter characteristics by a moderate number of terms of a power series. Unfortunately, the number of terms required to represent a rectangular type of response is large, resulting in a loss of accuracy, and hence this technique is really only applicable to filters with fairly gentle roll-off characteristics.

6.5.3 RANDOM MODULATION

Rice [5] has analysed the distortion produced by filtering an FM signal where the modulation is a zero mean, gaussian random process with the two sided power spectrum

$$N(f) = \begin{cases} N & |f| \leq B \\ 0 & |f| > B \end{cases} \qquad (6.29)$$

where B is the highest baseband frequency.

Both ideal rectangular and Gaussian filters were analysed. However, the resulting expressions were derived using first-order approximations which are only valid for small rms frequency deviations. Shimbo and Loo [6] have used Rice's work to calculate actual distortion figures using numerical techniques. Anuff and Liou [7] have derived the following empirical formula relating bandlimiting distortion due to a rectangular filter of bandwidth, B_N, to rms deviation, σ, in an FDM-FM system

$$B_N = 2f_h \left[1 + 0.065\log_{10}(S/D) + \sigma \log_{10}(S/D)\right] \qquad (6.30)$$

where S/D is the signal-to-distortion at the highest baseband frequency of f_h.

6.6 INTERFERENCE DUE TO UNWANTED SIGNALS

6.6.1 GENERAL RESULT FOR A SINGLE INTERFERER AND SINUSOIDAL MODULATION

Interference arises in FM systems when signals other than that desired are present in the receiver IF. The interfering signal may or may not be modulated and can be of the same nominal carrier frequency (co-channel interference) or offset by the channel spacing (adjacent channel interference).

Let the wanted signal with sinusoidal modulation, $e_1(t)$, be represented in the usual way by;

$$e_1(t) = \cos\phi_1(t)$$

$$= \cos\left[2\pi f_1 t + \frac{\Delta f_1}{f_{m1}}\sin 2\pi f_{m1} t\right] \qquad (6.31)$$

Consider a single interferer, $e_2(t)$, with carrier frequency, f_2, and phase, ϕ_o, modulated by a sinusoid at frequency, f_{m2},;

$$e_2(t) = \cos\phi_2(t)$$

$$= x\cos\left[2\pi f_2 t + \phi_o + \frac{\Delta f_2}{f_{m2}}\sin 2\pi f_{m2} t\right] \qquad (6.32)$$

where $|x| < 1$

The resultant phase angle, $\theta(t)$, is given by;

$$\theta(t) = \phi_1(t) + \tan^{-1}\left[\frac{z \sin\phi(t)}{1 + x \cos\phi(t)}\right] \qquad (6.31)$$

where $\phi(t) = \phi_2(t) - \phi_1(t)$

The output of an FM detector, $e_o(t)$, is proportional to the instantaneous frequency of the resultant. Therefore

$$e_o(t) = \frac{1}{2\pi}\frac{d\theta(t)}{dt}$$

$$= f_1 + \Delta f_1 \cos 2\pi f_{m1} t + \frac{d}{dx}\left[\tan^{-1}(x)\right] \cdot \frac{dx}{d\phi(t)} \cdot \frac{d\phi(t)}{dt} \qquad (6.33)$$

where $x = \dfrac{z \sin\phi(t)}{1 + z \cos\phi(t)}$

Evaluation of the functions in x gives

$$e_o(t) = f_1 + \Delta f_1 \cos 2\pi f_{m1} t + \frac{z^2 + z \cos\phi(t)}{1 + 2z \cos\phi(t) + z^2} \cdot \frac{d\phi(t)}{dt} \qquad (6.34)$$

The first terms represent the output in the absence of interference, whilst the remainder represents the distortion components.

It has been shown by Corrington [8] that $e_o(t)$ can be represented by the Fourier series

$$e_o(t) = f_1 + \Delta f_1 \cos 2\pi f_{m1} t - \sum_{s=1}^{\infty} \frac{(-1)^s z^s}{s} \sum_{m=-\infty}^{\infty} J_m\left[\frac{s\Delta f_1}{f_{m1}}\right]$$

$$\cdot \sum_{n=-\infty}^{\infty} J_n\left[\frac{s\Delta f_2}{f_{m2}}\right] \cdot \left[sf_2 - sf_1 - mf_{m1} + nf_{m2}\right]$$

$$\cdot \cos\left[\pi\left[sf_2 - sf_1 - mf_{m1} + nf_{m2}\right]t + s\phi_o\right] \qquad (6.35)$$

This is the general expression for a single interferer. It can be seen from eqn.6.35 that if $f_2 \neq f_1$, the demodulated output signal does not in general contain the frequency f_{m2}, i.e. the interference is un-intelligible. When it is desired to find the level of interference falling within a given audio frequency band 0-f_B, eqn.6.36 must be solved for all values of s, m and n, and these values then inserted into eqn.6.35 to find the component amplitudes.

$$|s(f_2 - f_1) - mf_{m1} + nf_1| \leq f_B \qquad (6.36)$$

This equation is of Diophantine [2] form with three variables, for which there exist an infinite number of solutions, although the distortion components for which |m| and |n| are large are of small magnitude due to the nature of Bessel functions.

6.6.2 OTHER CONDITIONS

For each additional unwanted signal the complexity of the above equations would be further increased by the inclusion of another Bessel function summation and an additional variable inside the cosine function. If both

the wanted and interfering signal had complex modulation consisting of M sinusoidal components, then both the Bessel coefficients in eqn.6.35 would be replaced by a product of M Bessel coefficients. The products nf_{m1} and mf_{m2} would also be replaced by series of the form $\sum_{m=1}^{M} n_m f_m$ etc. and the whole equation would have to be evaluated for all sets of n_m, m_m and s satisfying a Diophantine equation.

6.7 CONCLUSIONS

The non-linear nature of angle modulation has been shown to make analysis using classical techniques extremely complex unless considerable over-simplifications are made. Hence it is extremely difficult to predict the signal degradation in practical systems due to bandlimiting and co-channel interference for anything but the simplest sinusoidal modulating signal. Hence, in order to be able to make detailed comparisons between the likely performance of a conventional narrow-band FM and a yet more complex TCM-FM system, a radically different analysis technique is required, preferably one which lends itself to computer simulation.

6.8 REFERENCES

(1) Taub,H.T. and Schilling,D.L.:'Principles of communication systems' , chapter 4, Mc Graw-Hill, 1982.

(2) Mordell, L.J.:'Diophantine equations', chapter 5, Academic Press, 1965.

(3) Panter,P.F.:'Modulation, noise and spectral analysis', chapters 7 and 14, Mc Graw-Hill, 1965.

(4) Carson,J.R. and Fry,T.C.:'Variable-frequency electric circuit theory', Bell System Technical Journal, vol.16, pp.513-540, Oct.1937.

(5) Rice,S.O.:'Distortion produced by band limitation of an FM wave', BSTJ, vol.52, no.5, pp.605-625, May 1973.

(6) Shimbo,O. and Loo, C.:'Digital computation of FM distortion due to linear systems', IEEE Int. Comms. Conf., pp.482-486, 1968.

(7) Anuff,A. and Liou,M.L.:'A note on necessary bandwidth in FM systems' Proceedings IEEE (Letters), vol.59, no.10, pp.1552-53, Oct.1971.

(8) Corrington, M.S.:'Frequency modulation distortion caused by common- and adjacent-channel interference', RCA Review, vol.17, pp.522-560, Dec.1946.

CHAPTER SEVEN

ANALYSIS OF ANGLE MODULATION USING THE DISCRETE FOURIER TRANSFORM

7.1 INTRODUCTION

The application of the discrete Fourier transform (DFT) and its derivative, the fast Fourier transform (FFT), to the analysis of frequency modulation with both sinusoidal and complex message signals is considered. It is shown that computer implementations of the techniques are eminently suited to spectral analysis and to the determination of intermodulation distortion due to bandlimiting and co-channel interference. The techniques are then extended to cover noise-like modulating signals by employing a Monte Carlo procedure [1] with pseudo-random noise samples.

For versatility, separate specialised computer sub-routines (listed in Appendices A to F) were developed for each area of analysis. Extensive results are presented which are shown to be in very good agreement with other published work and practical measurements. These confirm the validity of the techniques and provide confidence in the extended application with time-compression multiplexed baseband signals, as described in chapters 8 and 9.

7.2 SPECTRAL ANALYSIS

7.2.1 DETERMINISTIC SIGNALS

The conventional Fourier transform, Y(f), of the FM waveform

$$e_{FM}(t) = Re\left[A_c\, e^{j2\pi f_c t + \frac{\Delta f}{f_m}\sin 2\pi f_m t}\right] \qquad (7.1)$$

may be readily obtained by using the standard result for $e^{j2\pi f_o t}$. Hence

$$Y(f) = \pi A_c \sum_{n=-\infty}^{\infty} J_n\left[\frac{\Delta f}{f_m}\right] \cdot \left[\delta\left[f-(f_c+nf_m)\right]+\delta\left[f+(f_c+nf_m)\right]\right] \qquad (7.2)$$

Eqn.7.2 is the direct frequency domain equivalent of the Fourier series expansion derived in chapter 6. Therefore, use of the conventional transform does not aid the spectral analysis problem since the Bessel coefficients are still present, and indeed if the transform for complex modulation is derived, the result will be seen to involve a Diophantine equation.

However, it is possible to evaluate the Fourier transform of an FM waveform numerically without the use of Bessel functions using a set of N equally spaced samples taken in the time domain over a single period of the sig-

nal, T. This technique, known as the discrete Fourier transform (DFT), is detailed in Appendix A along with a Fortran 77 subroutine listing. The Appendix also describes a modified technique based upon the fast Fourier transform (FFT) which offers improved efficiency.

For a sinusoidally modulated signal, the period, T, of the waveform is simply the reciprocal of the highest common factor (HCF) of f_m and f_c. However, it is shown in Appendix A that for optimum use of the available samples, f_c should be made equal to N/4T, and that then when N/4 is an integer, the period, T, is simply $1/f_m$, For a complex modulating signal composed of M sinusoids, the period is given by

$$T = \frac{1}{\mathrm{HCF}\left[\sum_m f_m \right]} \qquad (7.3)$$

where the same conditions on N and f_c apply.

Although the period for complex modulation is always at least as great as for any single component, spectral analysis using the DFT is far less laborious than the classical Fourier series approach involving Diophantine equations.

7.2.2 RANDOM SIGNAL TECHNIQUES

Spectral analysis with various deterministic modulating signals is invaluable in the comparison of FM systems. However, since the majority of practical systems are intended for voice communication, analysis with some form of speech like signal would be preferable. Due to its aperiodicity, speech is not, however, suitable for the type of DFT analysis cited previously, Although it is possible to characterise short segments of speech (eg. a single utterance), such a process requires a detailed knowledge of speech characteristics and statistics.

In fdm systems, if the number of speech channels is sufficiently large, the statistical properties of the multiplexed signal become similar to those of random noise [1]. Hence, it has become common practice to evaluate such systems using a random noise test signal. Although random noise does not truly represent a speech signal in a single channel system, noise loading tests have still been used for FM systems [2], principally due to the lack of any other easily handled signal.

The use of a random noise signal instead of speech still does not overcome the aperiodicity problem preventing the use of the discrete Fourier transform. However, Bennett [3] has shown that it is quite legitimate to

represent a narrow band of gaussian noise by a sufficiently large number, M, of constant amplitude, equally frequency spaced tones of random but uniformly distributed phase. If the bandwidth of the noise signal is W (Hz), then the waveform is repetitive with period M/B (sec.). However, two problems remain:

(1) A true gaussian instantaneous amplitude distribution requires an infinite number of tones,

(2) This technique of noise representation requires that the results be averaged over all possible combinations of initial random phases in order to obtain absolute accuracy.

Medhurst and Roberts [1] have plotted the instantaneous amplitude distribution for various numbers of randomly phased equal amplitude tones. Whereas a value of M=100 produces a very good approximation to gaussian, there is only a small error (equal to about a 1dB reduction in the instantaneous amplitude reached for less than 0.00001% of the time) for M=20. Hence a value within this range would seem to represent a good compromise between accuracy and complexity. It has also been shown by Ruthroff [2] that the average of the results of a number of initial random phase sets normally shows good convergence after only a modest number of runs, however, this should be verified

for each particular application. Techniques which exploit these two approximations for random analysis are known as Monte Carlo procedures. Results of sufficient accuracy can generally be achieved with only a moderate amount of effort, with further improvement only obtainable after a great deal more work.

7.2.3 MONTE CARLO RESULTS

A subroutine, SPEC.for, invoking the FFT.for subroutine, for Monte Carlo analysis of FM spectra with pseudo-random noise modulation is given in Appendix B. An efficient method of calculating the required trigonometric series is used [3], with pseudo-random phases angles from RAND.for (Appendix C).

The period of the waveform for DFT analysis with the carrier set to N/4T and N=kT, where k is an integer, is simply the period of the pseudo-random noise signal, W/B. To simulate both 12.5 and 25kHz conventional narrow-band FM systems, a noise bandwidth of 3kHz was used with rms frequency deviations of 1.5kHz and 3kHz respectively. Monte Carlo processes were performed using M=30 and 60 tones, corresponding to periods of 10 and 20ms respectively. The final spectra, averaged over 100 independent runs, and shown in figs.7.1 and 7.2. There is excellent correlation between the respective spectra for M=30 and

M=60 tones, with only a marginal increase of less than 5% in the -100dB bandwidth for the latter system.

For noise modulation, Carson's rule has been expressed as [2]

$$B = 2W(1 + 4\frac{\sigma}{W}) \qquad (7.4)$$

where W is the noise bandwidth, and the peak frequency deviation is assumed to be four times the rms deviation, σ. The average peak-to-rms value of the pseudo-random noise signal above with M=30 tones, over 100 runs, was measured as 2.51; a figure somewhat less than Carson's formula. To verify, the rule with this new figure, 98, 99, 99.5 and 99.75% spectral power bandwidths were calculated for a range of rms deviations and the results plotted in fig.7.3. It can be seen that the bandwidth estimated from Carson's formula with the revised figure is a very good approximation to the computed results.

The convergence of the above bandwidth figures against number of runs averaged is plotted for deviations of 2.7kHz and 3kHz in figs.7.4(a) and (b) respectively. The figures indicate excellent accuracy after 100 runs, whilst acceptable accuracy is obtained after only some 50 runs.

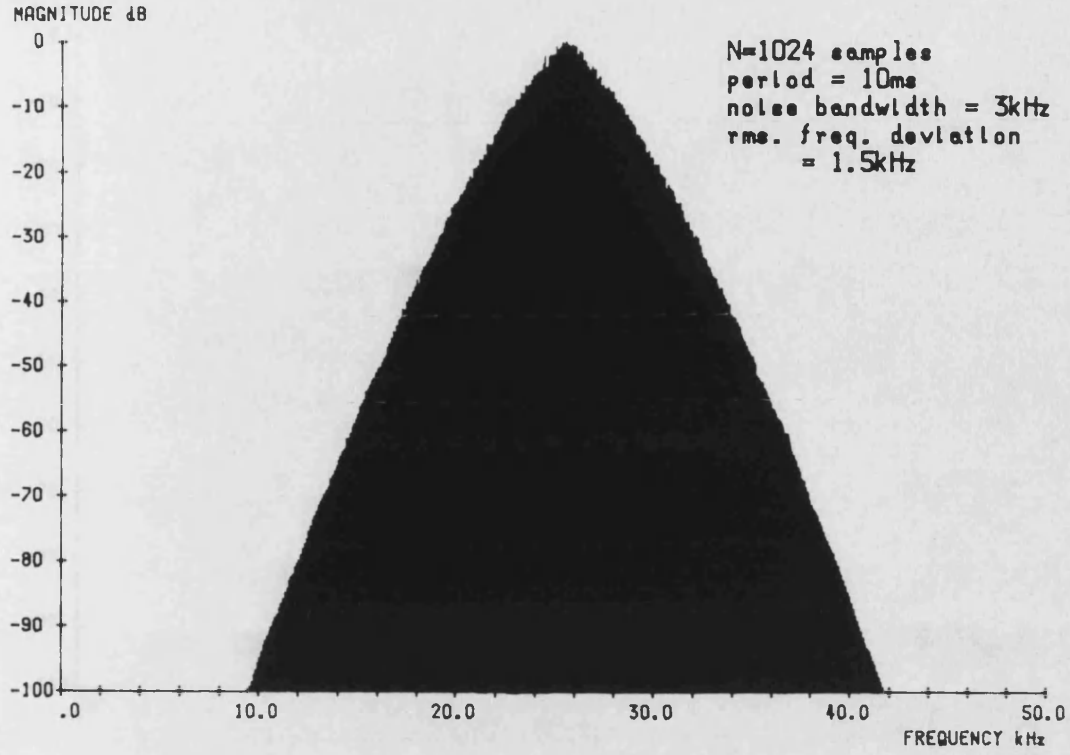

Fig. 7.1(a) Spectrum of an FM signal with pseudo-random noise modulation using a Monte Carlo Process with 30 sinusoids.

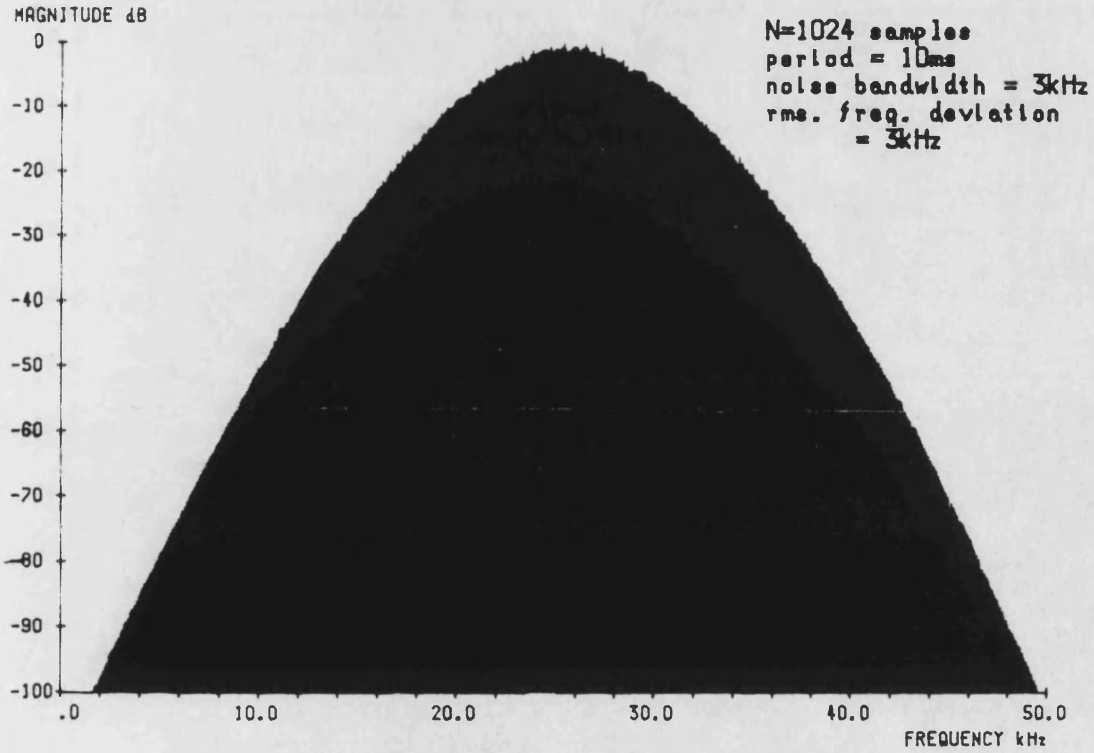

Fig. 7.1(b) Spectrum of an FM signal with pseudo-random noise modulation using a Monte Carlo Process with 30 sinusoids.

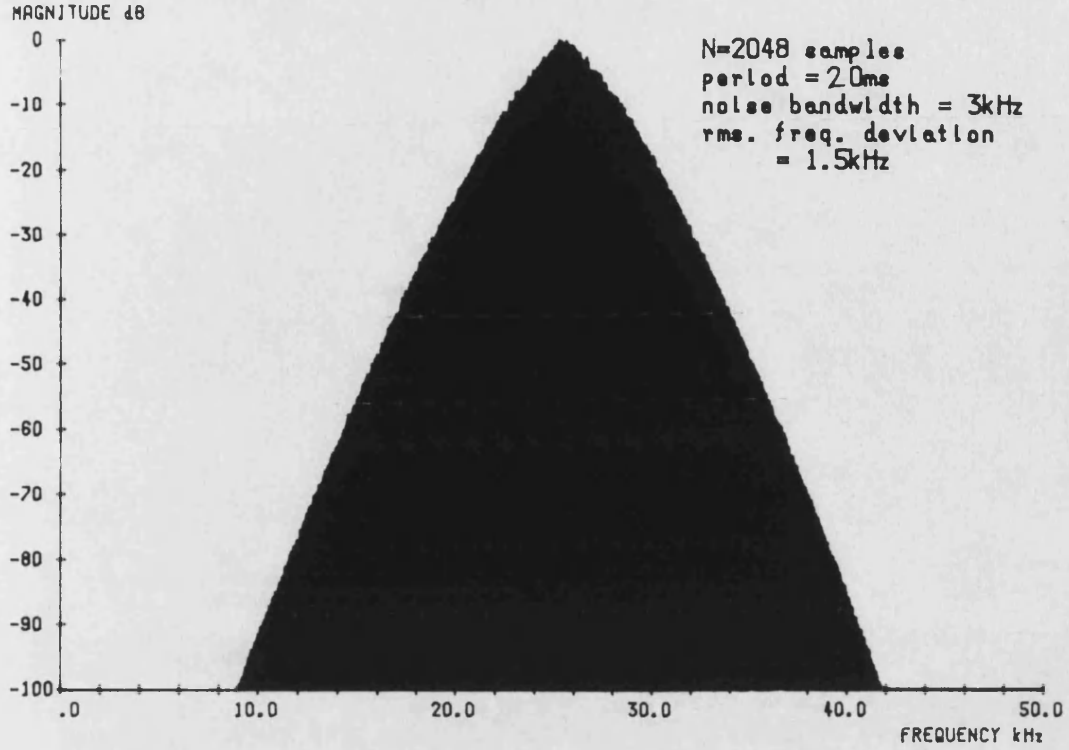

Fig. 7.2(a) Spectrum of an FM signal with pseudo-random noise modulation using a Monte Carlo Process with 60 sinusoids.

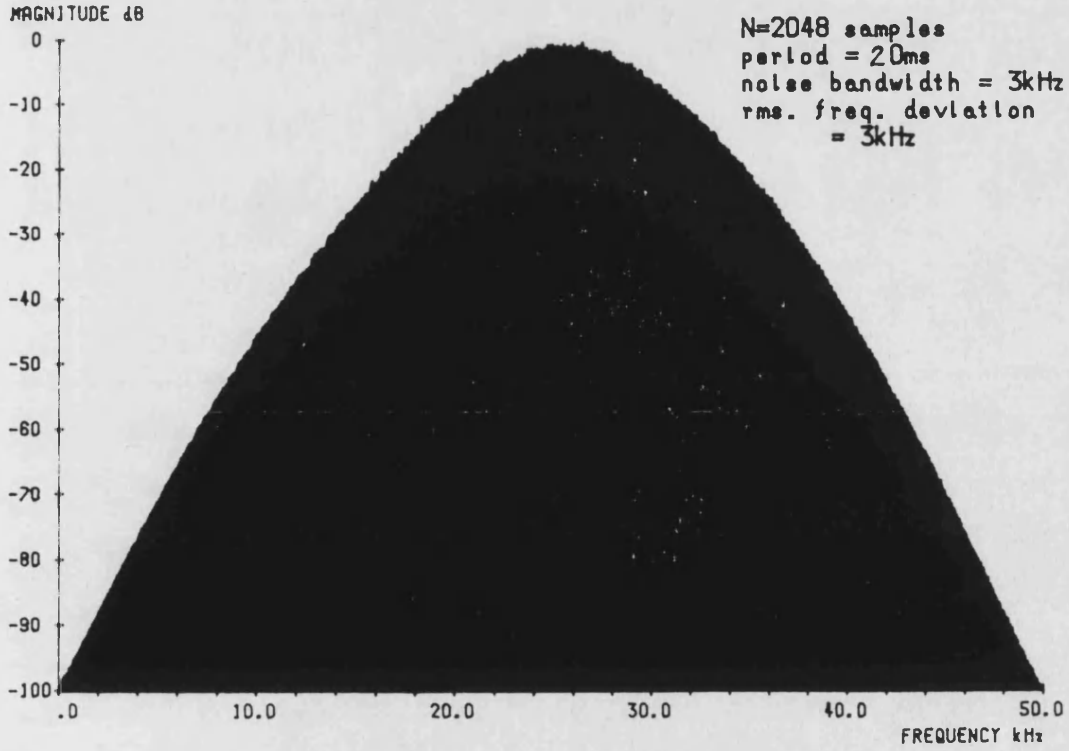

Fig. 7.2(b) Spectrum of an FM signal with pseudo-random noise modulation using a Monte Carlo Process with 60 sinusoids.

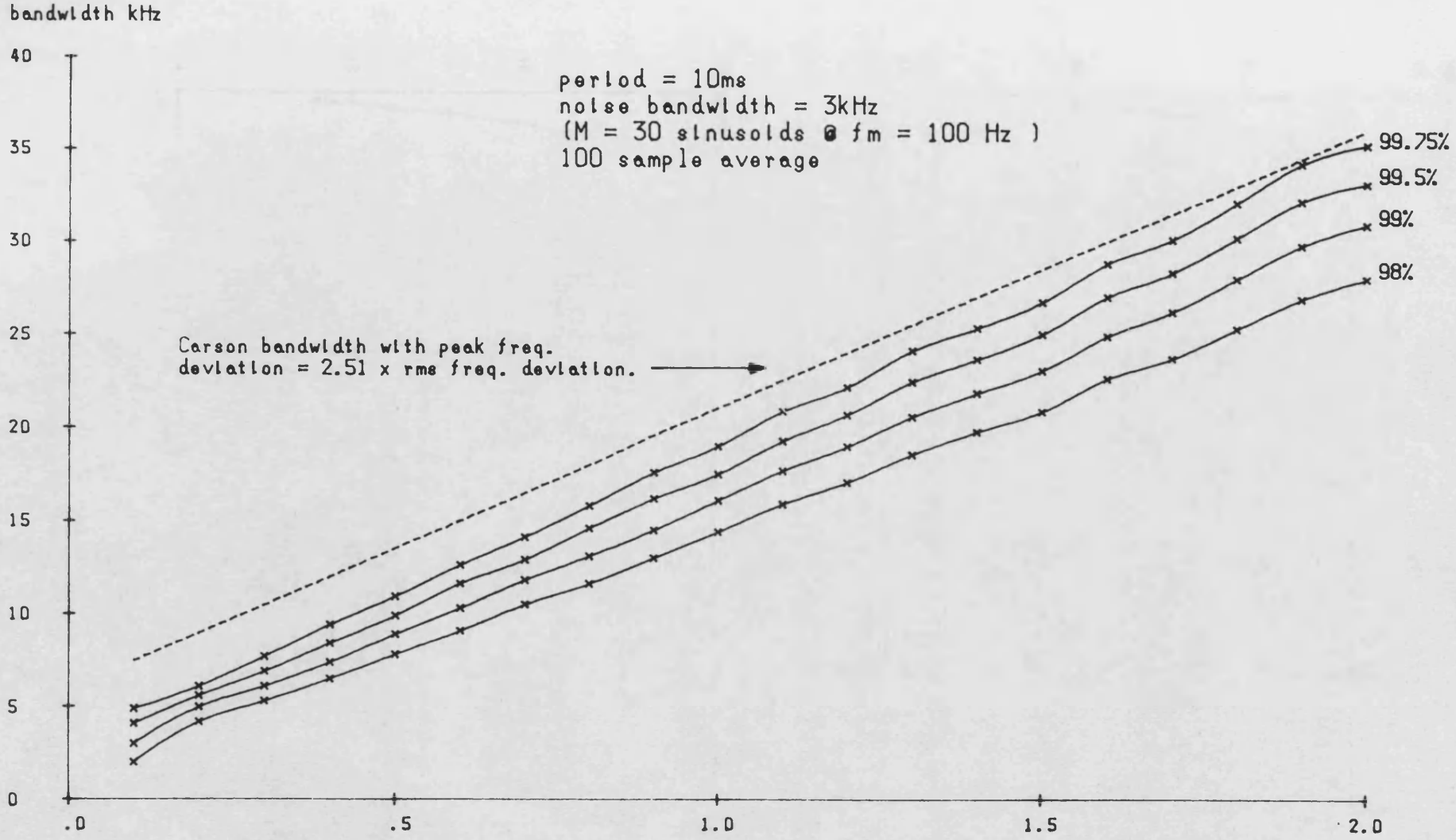

Figure. 7.3 Bandwidth of FM signal with pseudo-random noise modulation using a Monte Carlo process.

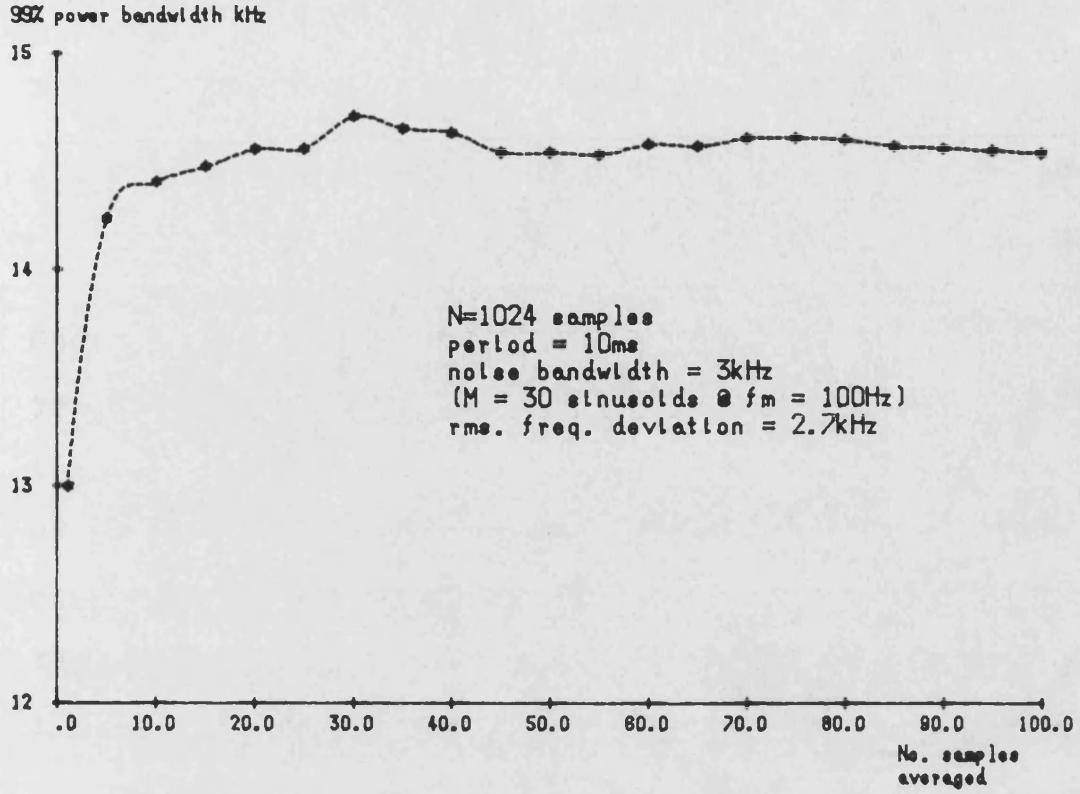

Fig. 7.4(a) Convergence of Monte Carlo results for 99% power bandwidth of FM signal with pseudo-random noise modulation.

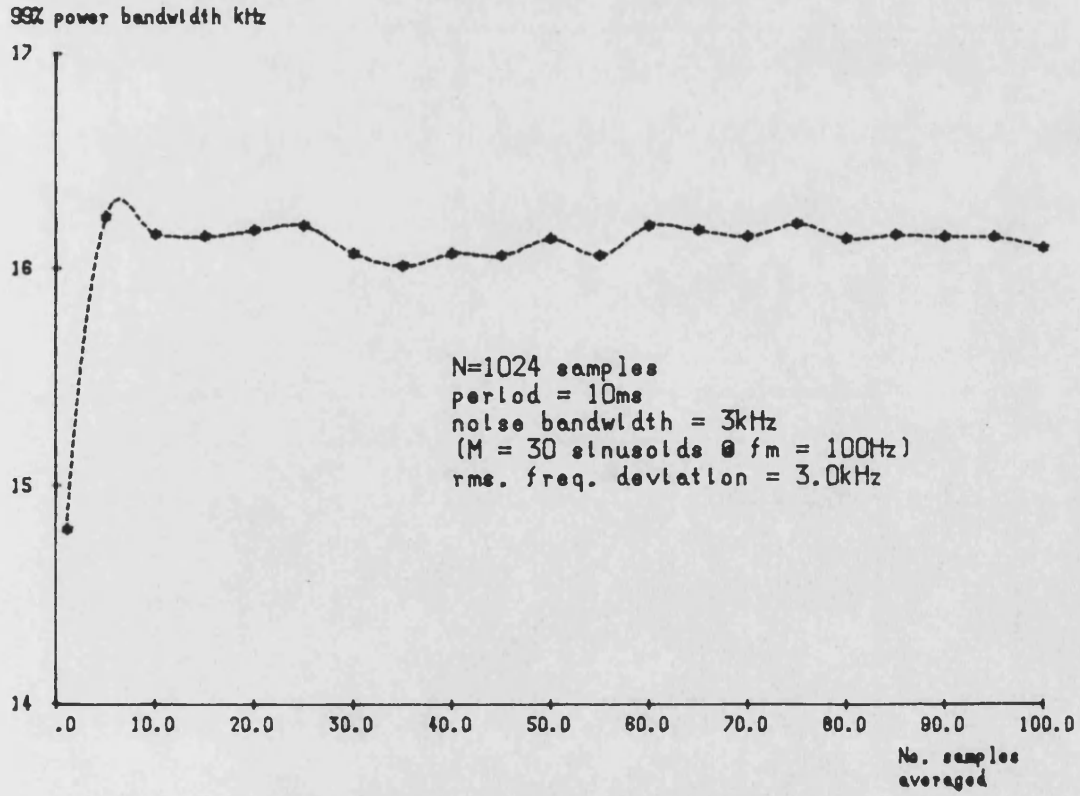

Fig. 7.4(b) Convergence of Monte Carlo results for 99% power bandwidth of FM signal with pseudo-random noise modulation.

7.3 FILTERING AND DEMODULATION ANALYSIS

7.3.1 PRINCIPLES

It has been shown in section 7.2 how the discrete Fourier transform and in particular the Fast Fourier transform, can be used for spectral analysis of FM. The technique may be readily extended to include the effects of bandlimiting simply by multiplying the complex spectral components by the corresponding filter coefficients. Taking the inverse discrete transform then yields a sampled time-domain waveform from which the instantaneous frequency and hence the output from an ideal limiting frequency discriminator may be derived. Finally, a second discrete transform may be taken to yield the demodulated signal spectrum. A detailed description of the algorithms, especially the demodulation process, along with a subroutine FILDEM1.for for sinusoidal signals is given in Appendix D.

With sinusoidal modulation, the resulting distortion may either be expressed as the level of a particular harmonic or as the ratio of the average distortion occurring in a given bandwidth to the fundamental. Both of these methods can produce misleading results when the frequency in question is at either extreme of the audio passband. At low frequencies, there are many possible in-band distor-

tion products, hence quoting the level of say, the third-harmonic, does not give a true representation of signal quality. Conversely, at frequencies above about 1.5kHz, the average in-band distortion figure will be zero.

A superior method of assessing the signal degradation due to filtering may be obtained using a pseudo-random test signal. A discrete equivalent of the fdm noise loading technique with a notch at the measurement frequency can be implemented. The component at the desired frequency is removed from the baseband signal before modulation. Then after filtering and demodulation, the signal power occurring in this frequency 'slot' relative to the average wanted signal power is a measure of the total signal degradation due to both intermodulation and harmonic mechanisms. By employing Monte Carlo techniques and repeating the measurement over a range of baseband frequency 'slots', a characteristic for the particular filter under examination may be produced. A subroutine, FILDEM2.for, to perform these processes is given in Appendix E.

7.3.2 SINGLE POLE BANDPASS FILTER

Although this class of filter finds little practical application in FM systems, it was included to permit comparison of the results with those obtained from practical

measurements by Bodtmann [5] and from Bedrosian and Rice's third order approximation [5]. The continuous filter frequency response, Y(f), is given by

$$Y(f) = \frac{1}{1+j\left|\frac{f - f_c}{f_B}\right|} \qquad (7.5)$$

where B is the bandwidth at the -6dB points.

The corresponding discrete complex filter coefficients, Y(i)=(a+jb), are defined using the usual notation by

$$Y(i) = \left[\frac{1}{1+\left[\frac{T(i-N/4-1)}{f_B}\right]^2} , \frac{\left[\frac{T(i-N/4-1)}{f_B}\right]}{1+\left[\frac{T(i-N/4-1)}{f_B}\right]^2} \right]$$

$$\text{for } 1 \leq i \leq (N/2+1)$$

$$= \left[\frac{1}{1+\left[\frac{T(3N/4+1-i)}{f_B}\right]^2} , - \frac{\left[\frac{T(3N/4+1-i)}{f_B}\right]}{1+\left[\frac{T(3N/4+1-i)}{f_B}\right]^2} \right]$$

$$\text{for } N/2+1 < i \leq N \qquad (7.6)$$

where the filter centre frequency is N/4T and the complex conjugate of eqn.7.5 is used for negative frequencies (i > N/2+1).

Bodtmann's filter had a half-bandwidth (B) of

1.223MHz and the tests were performed for modulating frequencies of 84kHz, 360kHz and 1MHz for various rms frequency deviations up to 2MHz. To permit comparison with results for audio systems, the above parameters were scaled such that the modulating frequencies become 252Hz,1080Hz and 3kHz. The filter half-bandwidth then becomes 3669Hz and the maximum peak deviation $\pm$8.48kHz for sinusoidal signals. The levels of third harmonic distortion computed using FILDEM1.for along with Bodtmann's results are compared in fig.7.5. There is generally good agreement between the two sets of results, with the greatest discrepancy at 3kHz. For rms frequency deviations less than the filter half-bandwidth, the distortion at all baseband frequencies increases at about 12dB per octave of frequency deviation. At low deviations, the distortion rises with baseband frequency up to about 1kHz, where upon it decreases slightly with further increase in frequency.

For random modulation, Bodtmann used noise bandlimited to 1MHz. Monte Carlo runs were performed using FILDEM2.for with M=30 and 100 runs, using the same frequency scaling factor as above. Bodtmann's scaled measurement frequencies of 252Hz, 1080Hz and 3KHz correspond to slot positions of 2/3, 10/11 and 30 respectively. Results at these and other slot positions are compared with Bodtmann's data and Bedrosian and Rice's approxima-

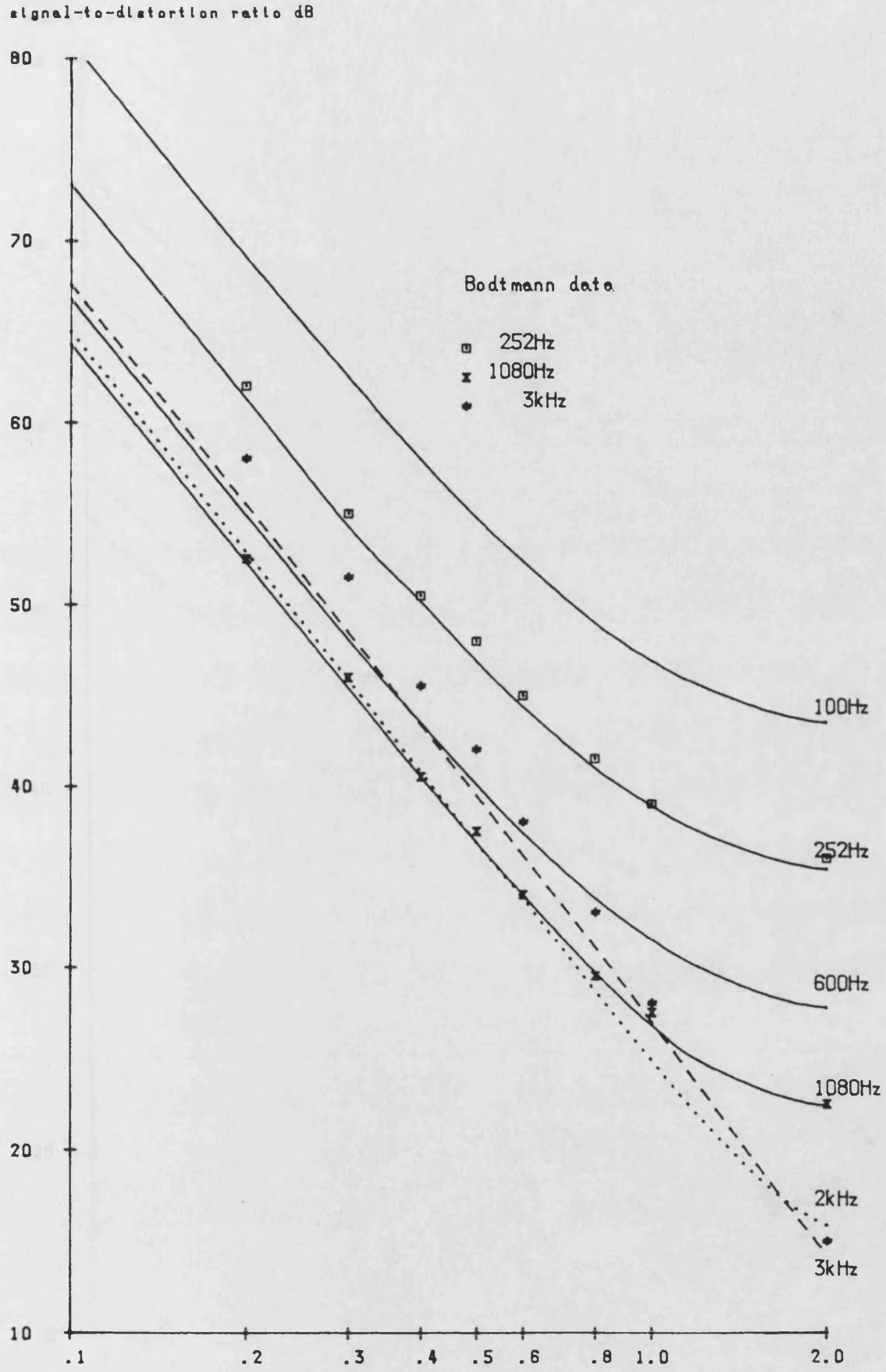

Fig.7.5 Computed third harmonic distortion in single pole filter (-6dB BW=+/-3,669kHz) compared with scaled Bodtmann experimental data.

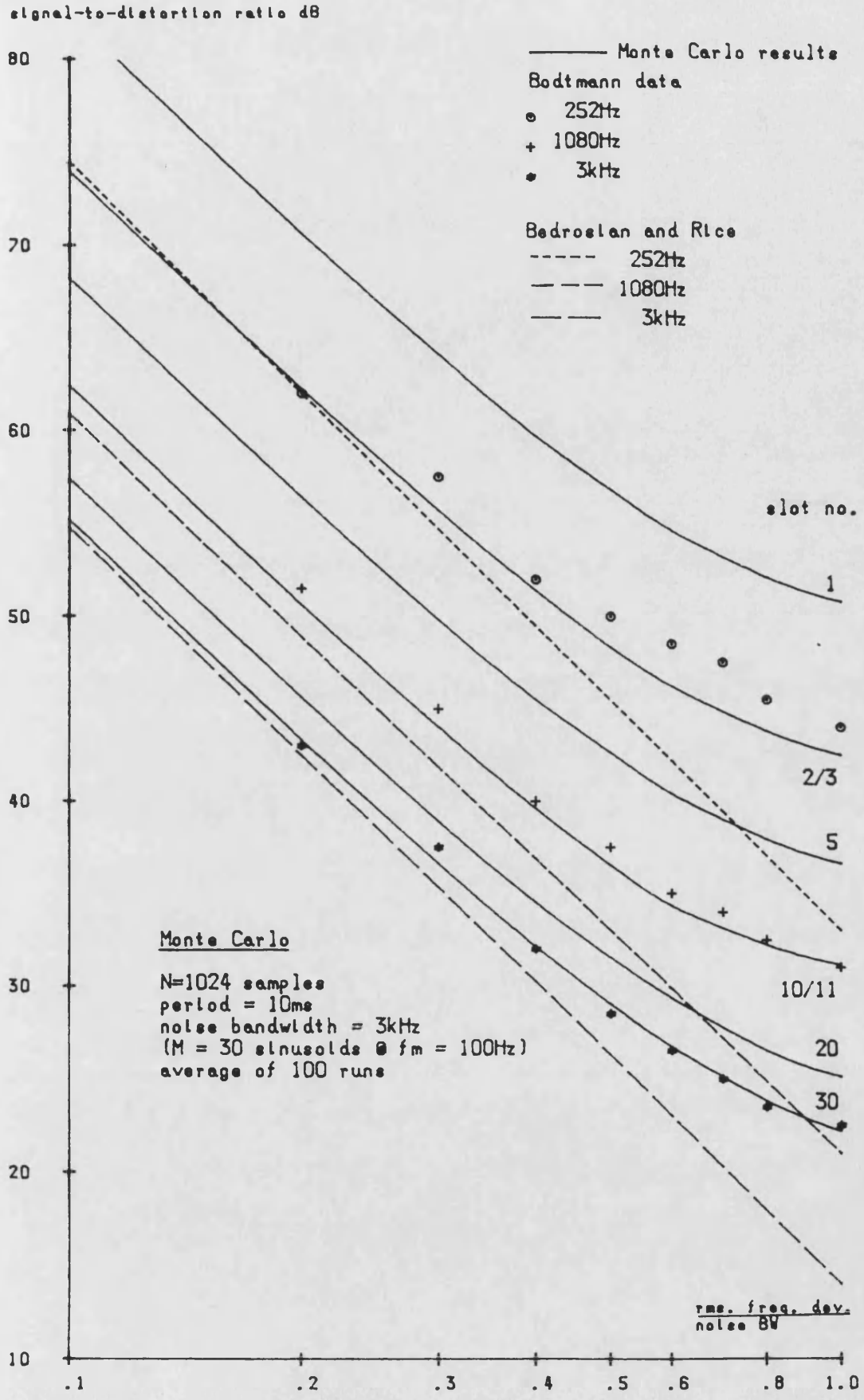

Fig.7.6 Computed intermodulation distortion in single pole filter for pseudo-random modulation compared with scaled Bodtmann experimental data and theoretical results of Bedrosian and Rice.

tion in fig.7.6. There is excellent correlation between the Monte Carlo results and Bodtmann's results with the third-order approximation (12dB per octave of deviation) only really being applicable for low frequency deviations.

7.3.3 RECTANGULAR FILTER

Due to the discontinuities at the band edges, the ideal rectangular filter is not readily amenable to an exact simulation. However, an arbitrary close Fourier series approximation can be obtained with a finite number of terms, K. Let B and -B be the band edges of the filter, then a cosine series representation, Y(f), over the interval -2B to 2B is given by

$$Y(f) = \sum_{j=1}^{K} \frac{\sin \frac{j\pi}{2}}{\frac{j\pi}{2}} \cdot \cos j\pi f/2B \qquad (7.8)$$

To avoid the Gibbs overshoot problem due to taking only a finite number of terms, all the terms were truncated using the method of Anuff and Liou [5] with K=64. Hence Y(f) becomes

$$Y(f) = \sum_{j=1}^{32} \frac{2\left[(64-j)^3 - 4(32-j)^3\right] \cdot \sin j\pi/2 \cdot \cos j\pi f/2B}{64^3 \pi j/2}$$

$$+ \sum_{j=33}^{64} \frac{2\left[(64-j)^3\right] \cdot \sin j\pi/2 \cdot \cos j\pi f/2B}{64^3 \pi j/2} \qquad (7.8)$$

The final response is shown in fig.7.7.

The intermodulation distortion in a ±7.5kHz pseudo-rectangular filter at slot positions 1,5,10,15,20 and 30 calculated using FILDEM2.for after 100 runs with M=30 tones is shown in fig.7.8. For the majority of the curves, the distortion increases at greater then 30dB per octave of frequency deviation. The curves are also characterised by relatively constant signal-to-distortion ratio (S/D) at low deviations, and very abrupt deterioration as the normalised rms deviation approaches unity. The limiting values of S/D at very low deviations are probably caused by rounding errors in the trigonometric series and FFT algorithms.

The variation in the signal-to-distortion ratio with filter bandwidth, measured at 1kHz and 3kHz is shown in figs.7.9 and 7.10 respectively. The increase in the slope of the curves with rising filter bandwidth is clearly shown. In addition, the S/D is constant for a major proportion of the curves for the larger bandwidths. The information from the above diagrams is plotted as contours of constant signal-to-distortion ratio in figs.7.11 and 7.12. Except for small normalised rms frequency deviations below about 0.2, a very good linear fit is obtained to the former with

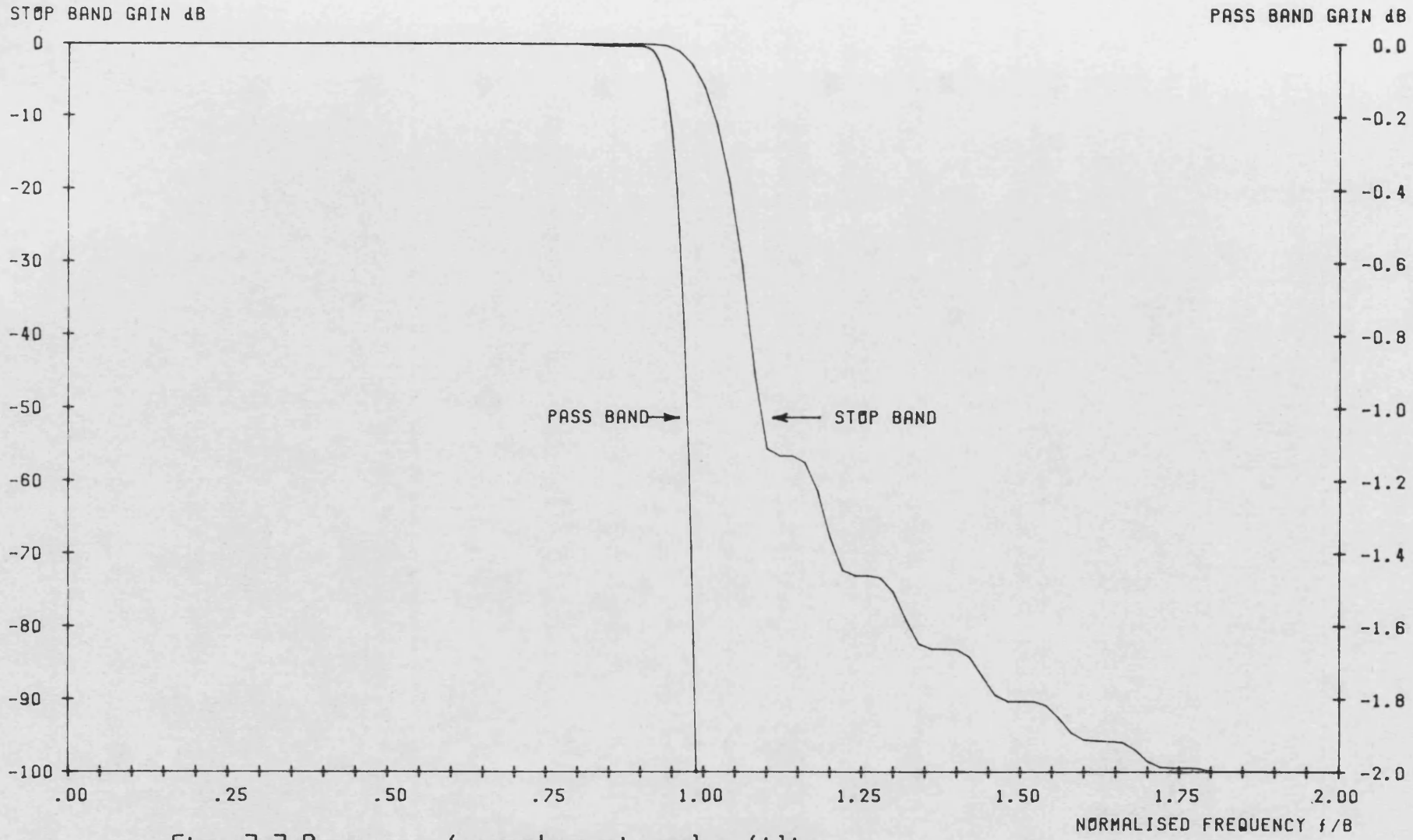

Fig. 7.7 Response of pseudo-rectangular filter of Anuff and Liou.

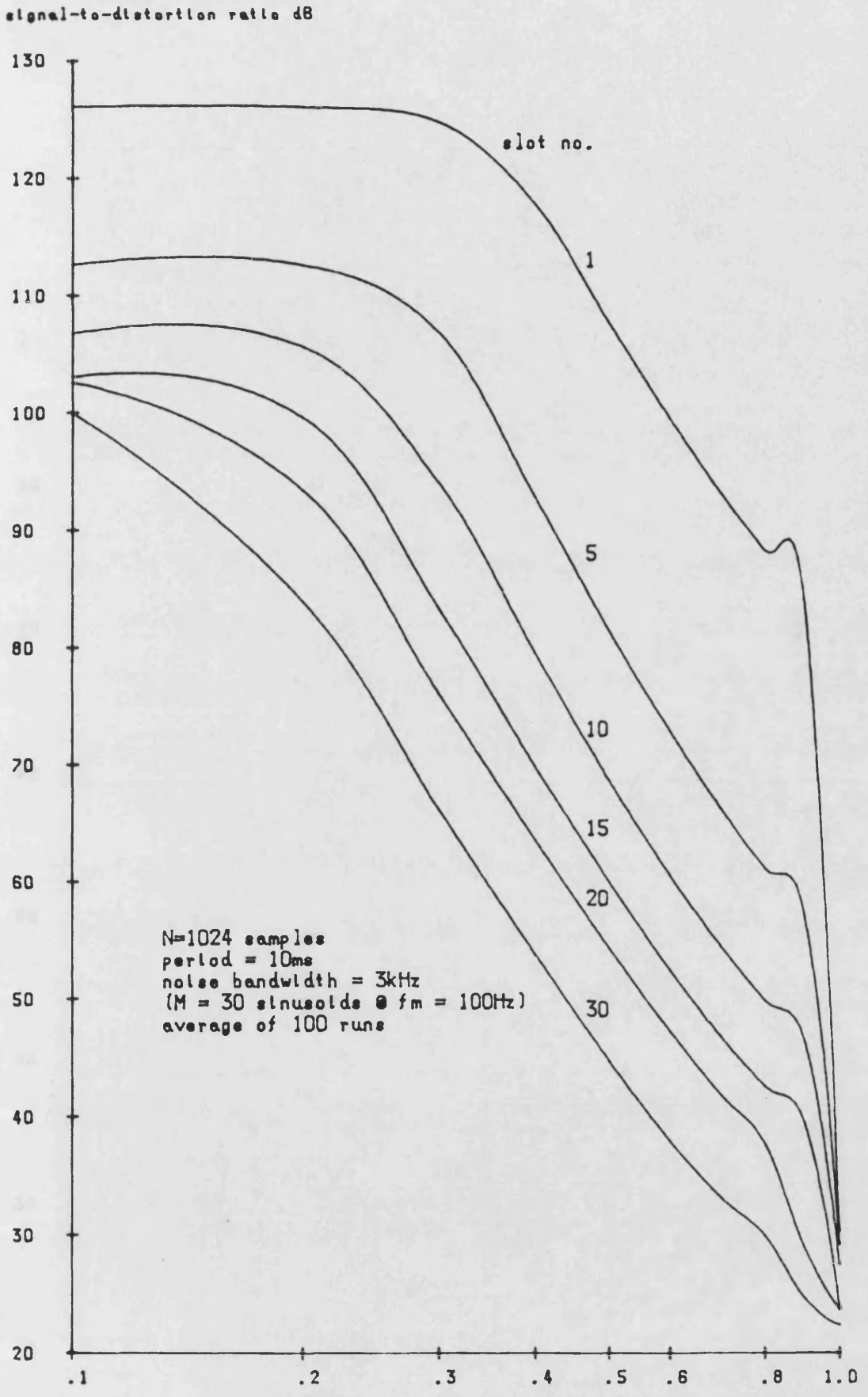

Fig.7.8 Computed intermodulation distortion in pseudo-rectangular filter of +/-7.5kHz -6dB bandwidth with pseudo-random noise modulation.

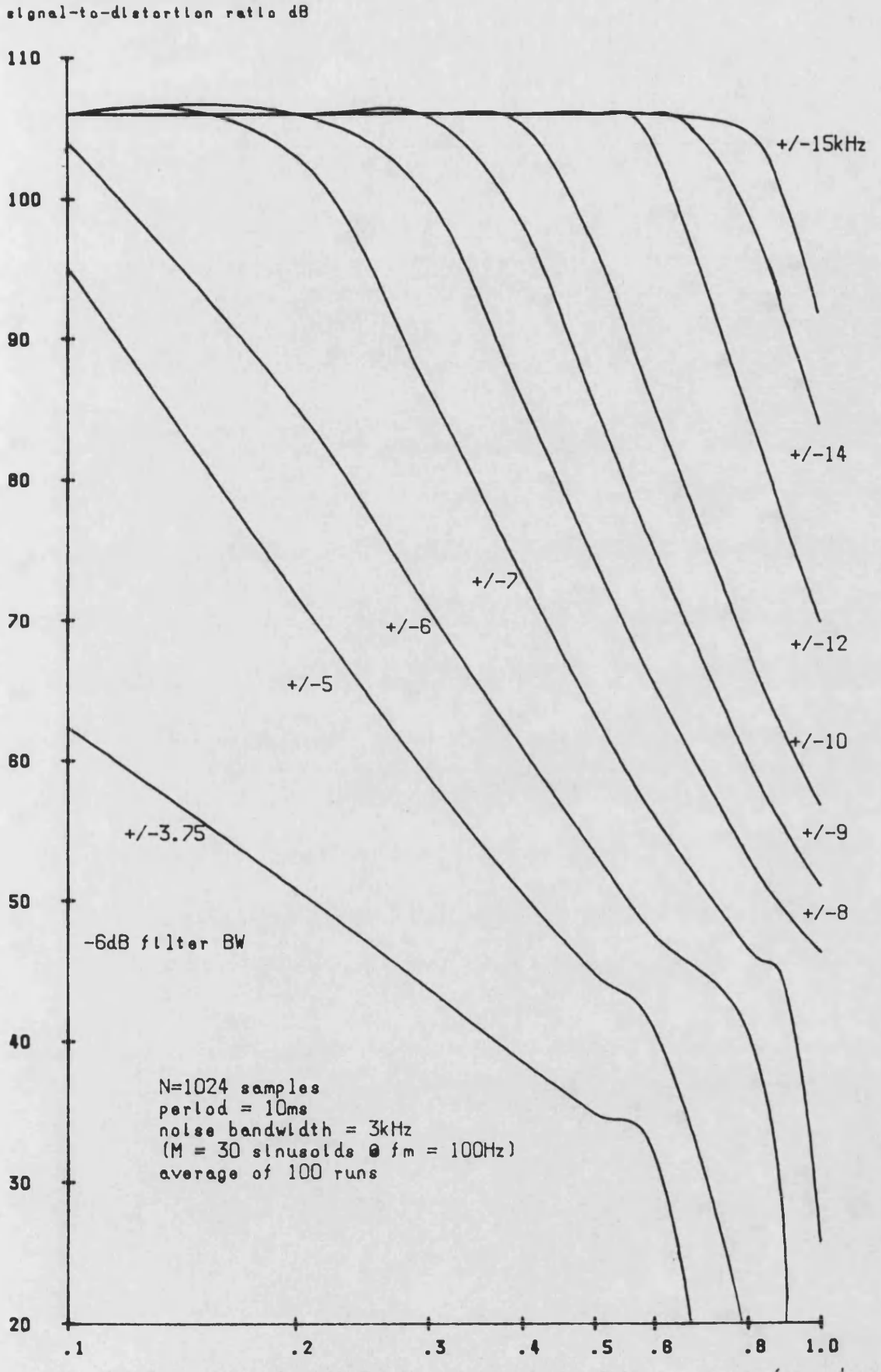

Fig.7.9 Computed intermodulation distortion at 1kHz in pseudo- rectangular filter with pseudo-random noise modulation.

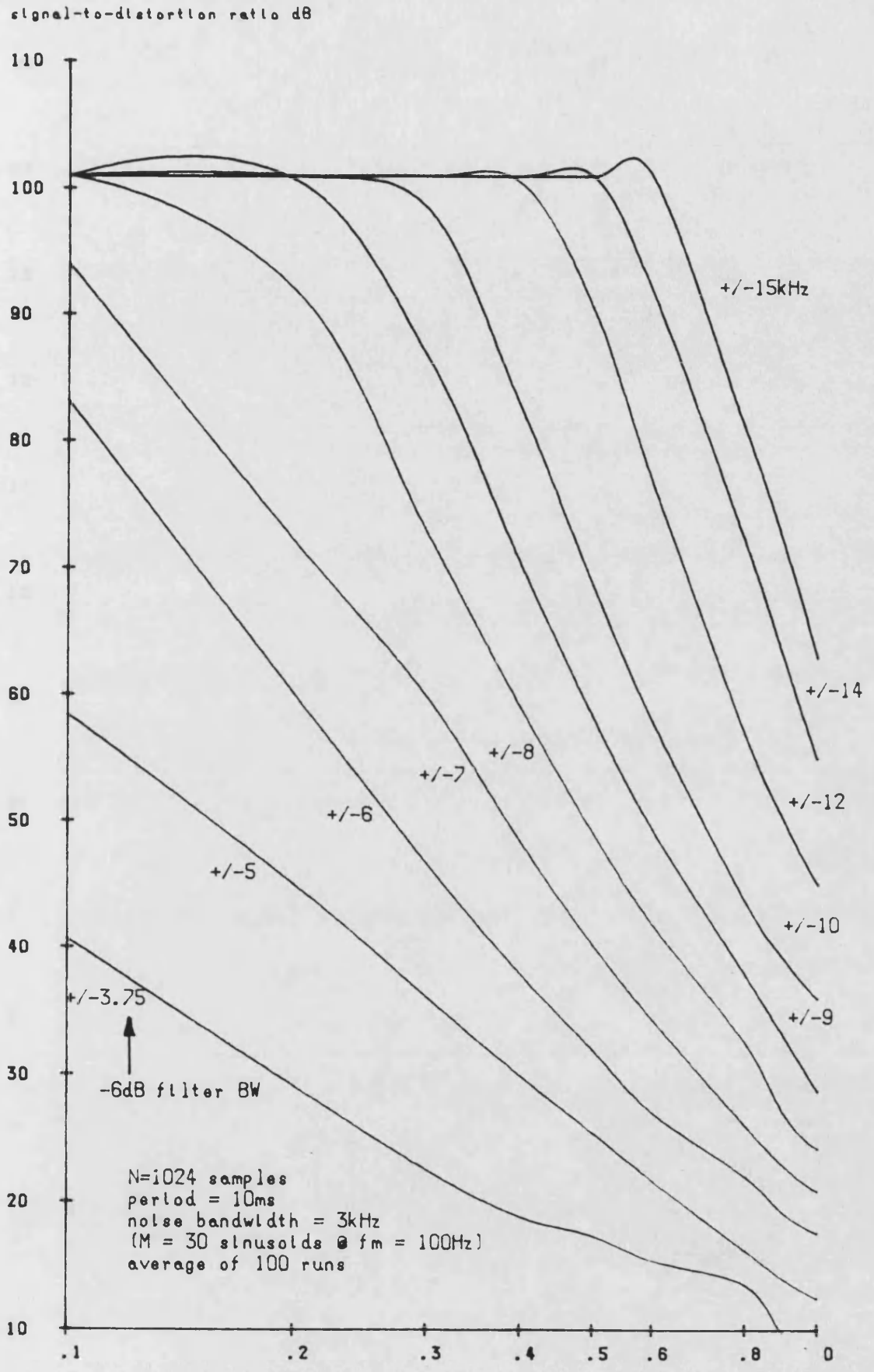

Fig.7.10 Computed intermodulation distortion at 3kHz in pseudo- rectangular filter with pseudo-random noise modulation.

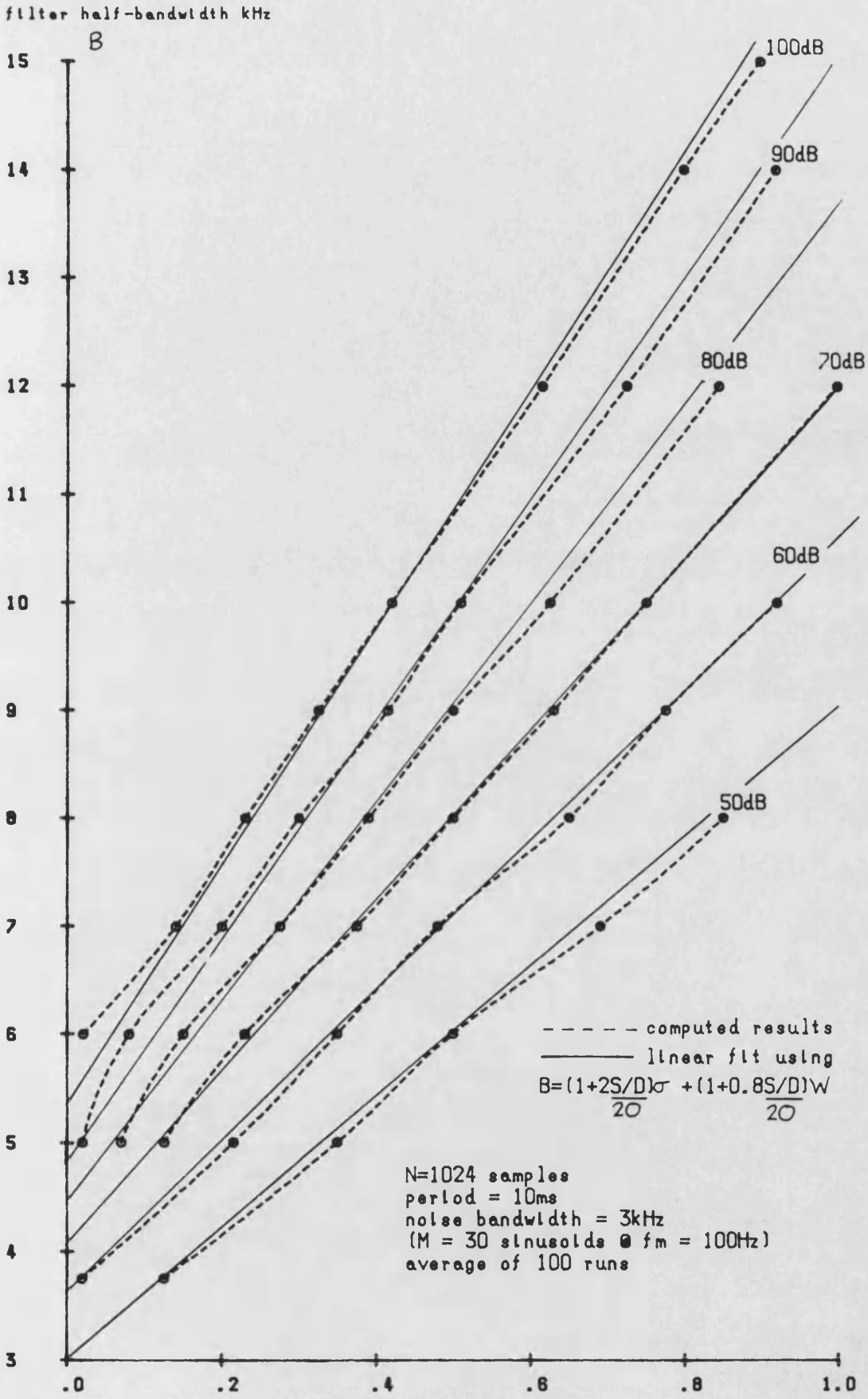

Fig.7.11 Necessary filter bandwidth for given signal-to-distortion ratio versus normalised rms freq. dev. Baseband frequency = 1kHz.

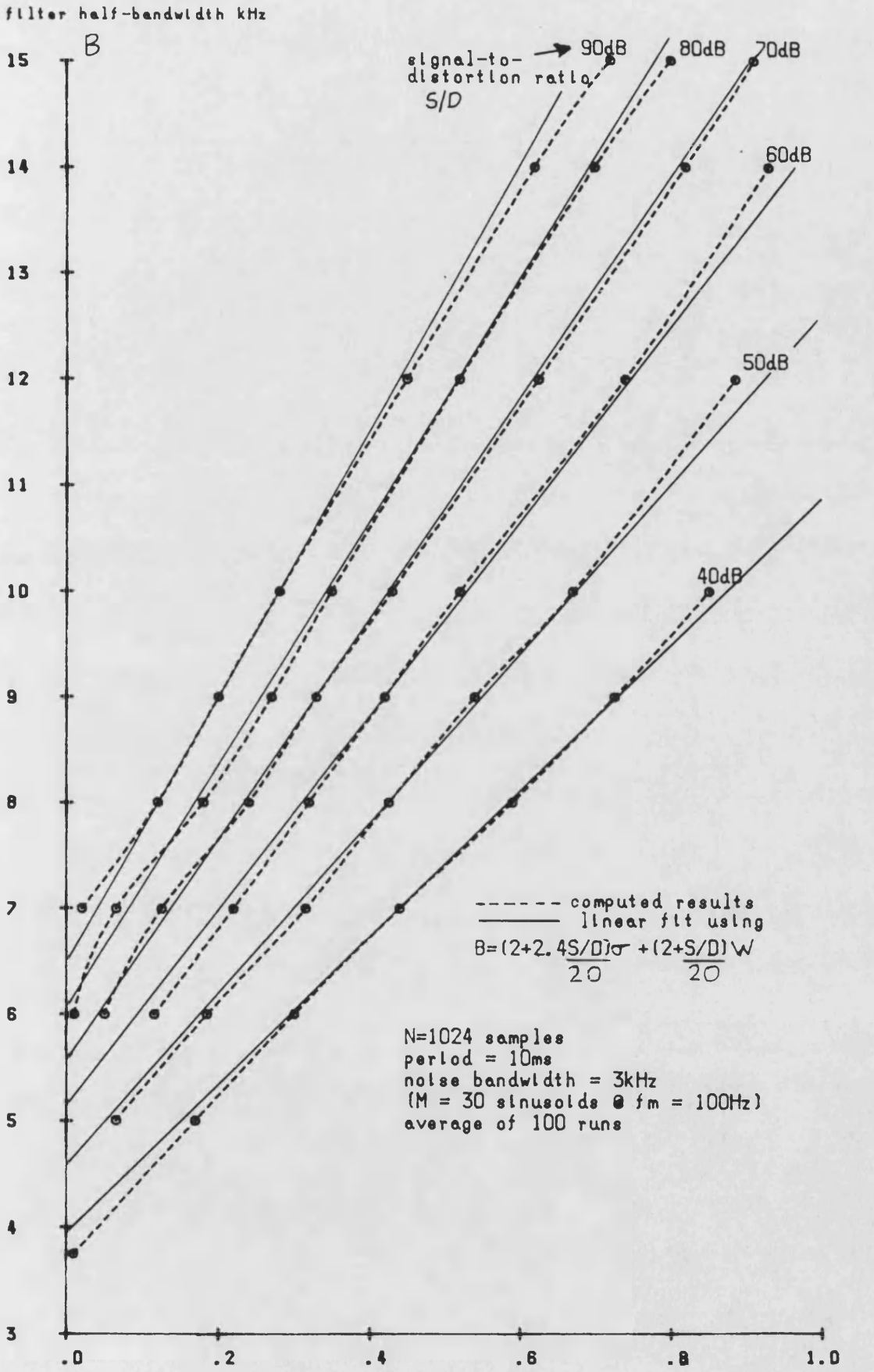

Fig.7.12 Necessary filter bandwidth for given signal-to-distortion ratio versus normalised rms freq. dev. Baseband frequency = 3kHz.

$$B = \left[1 + 2\left[\frac{S/D}{20}\right]\right]\sigma + \left[1 + 0.8\left[\frac{S/D}{20}\right]\right]W \qquad (7.9)$$

and to the latter with

$$B = \left[2 + 2.4\left[\frac{S/D}{20}\right]\right]\sigma + \left[2 + \left[\frac{S/D}{20}\right]\right]W \qquad (7.10)$$

where σ =rms freq. dev., W= noise bandwidth, and $\frac{S/D}{20}$ =log (true signal-to-distortion ratio).

These equations are of very similar format to that obtained by Anuff and Liou for pre-emphasised FDM-FM systems (eqn.6.30).

7.3.4 CRYSTAL FILTER

In existing narrowband FM communications equipment, crystal filters are employed at the IF stage to provide the bulk of the receiver selectivity. However, these filters also introduce considerable distortion into the signal due not only to the attenuation of components outside the filter passband, but also due to the non-linear phase response in the passband. It is desirable to be able to assess the effects of the amplitude and phase characteristics separately, which is obviously not possible by practical measurement.

Although the response of a real crystal filter can not be defined in the same way as previous filters, it is

still possible to use the discrete Fourier transform approach using a set of measured parameters. The filters chosen were 10.7MHz ITT Types 024DC and 024BC intended for ±12.5kHz and ±25kHz channel spacing systems respectively. These filters are 7-pole types with nominal -6dB bandwidths of ±3.75kHz and ±7.5kHz and a maximum quoted peak passband amplitude ripple of ±2dB. Both filters have identical input and output impedances of 910 Ω in parallel with 25pF. A standard single LC network was used to match this to the measurement impedance of 50Ω at 10.7MHz.

The harmonic distortion at 1kHz with a peak deviation of ±5kHz for the ±7.5kHz filter obtained from practical measurement is shown in fig.7.14(a). Excellent correlation was achieved with computed results shown in fig.7.14(b). Results for pseudo-random modulation for M=30 tones averaged over 100 runs were obtained from a modified version of FILDEM2.for. Slots 1,5,10,15,20 and 30 were analysed using both the full filter response (figs.7.15 and 7.17) and the linear-phase amplitude only response (fig.7.16 and 7.18). In all cases the S/D for slot 1 is appreciably greater then for any other slot. For the ±3.75kHz filter, the linearisation of the phase response increases the S/D by anything from 15 to 25dB, and the performance for slots 1,5,10 and 15 is maintained for higher rms frequency deviations. For the higher slot

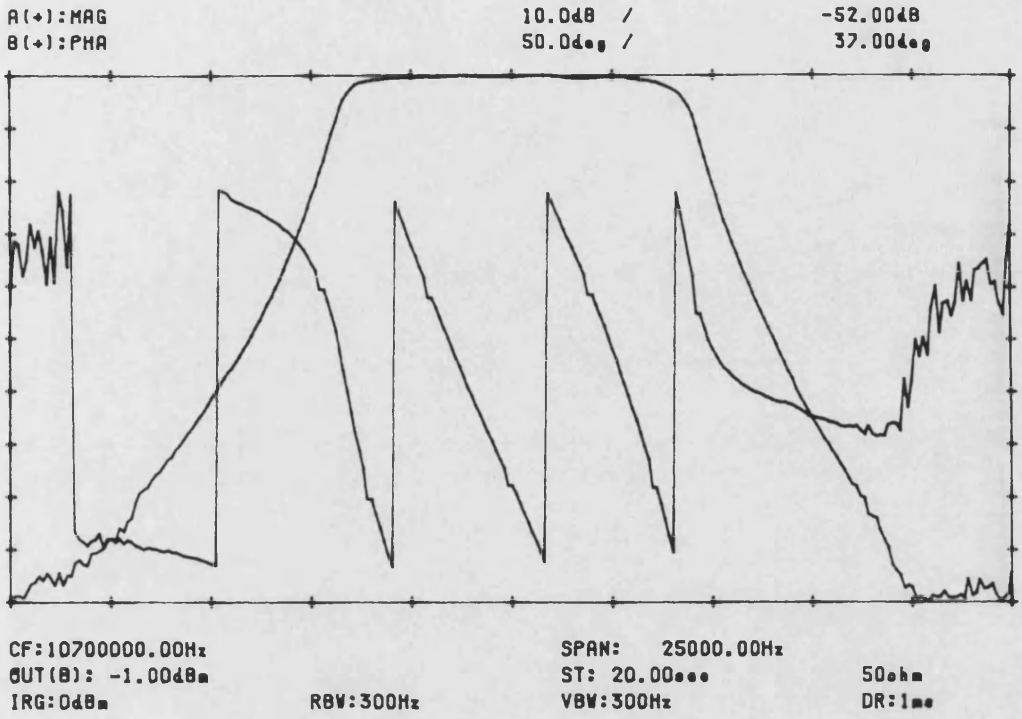

Fig. 7.13(a) Magnitude and phase response of +/-3.75kHz crystal filter type ITT 02400.

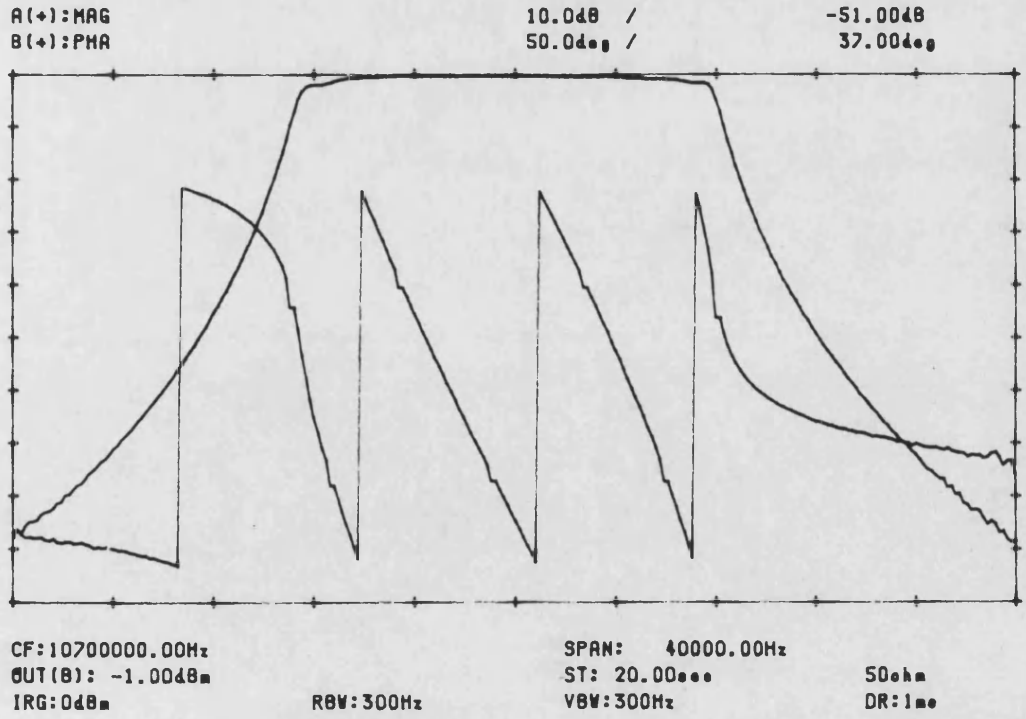

Fig. 7.13(b) Magnitude and phase response of +/- 7.5kHz crystal filter type ITT 0248C.

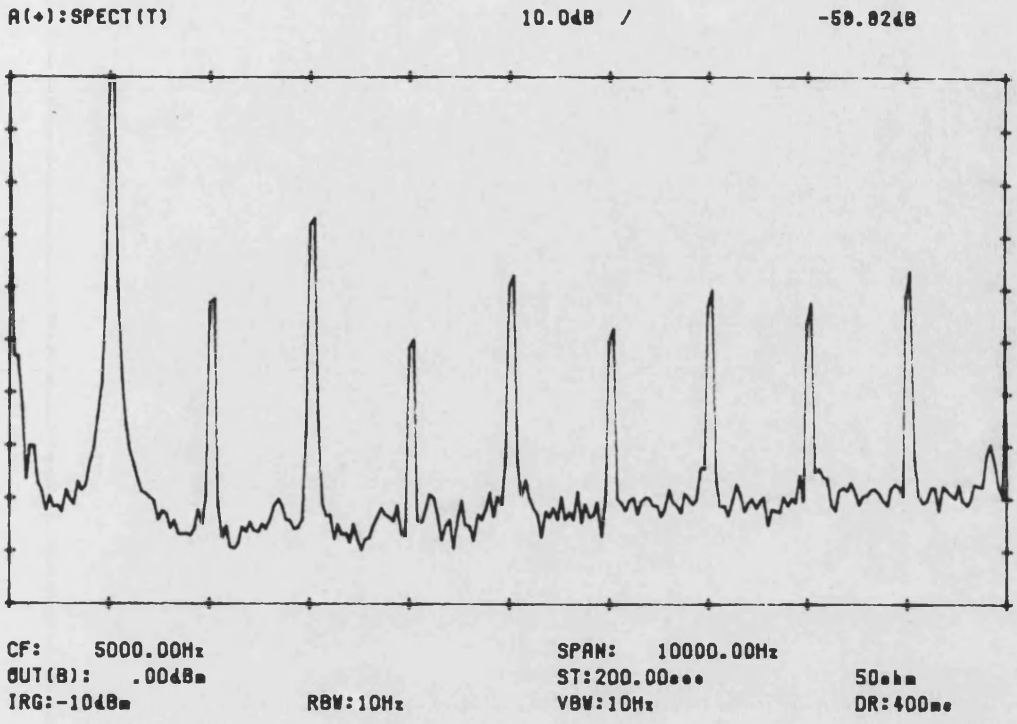

Fig. 7.14(a) Measured distortion in +/-7.5kHz crystal filter with 1kHz sinusoidal modulation at +/-5kHz peak deviation.

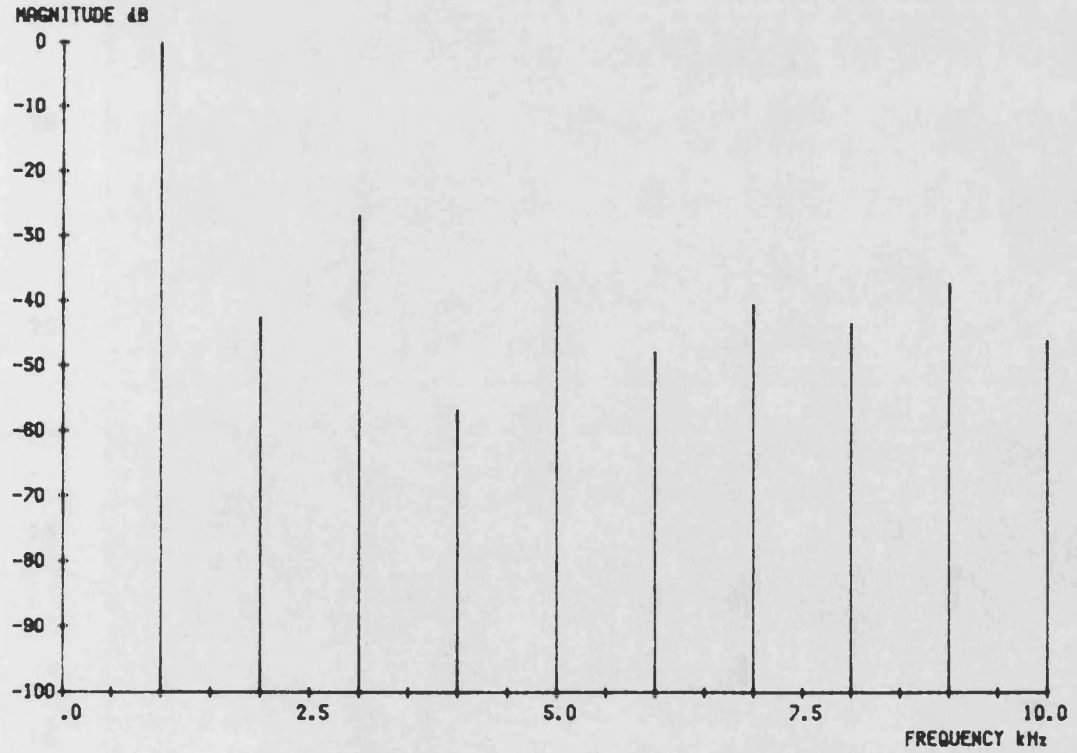

Fig. 7.14(b) Computed distortion in +/-7.5kHz crystal filter with 1kHz sinusoidal modulation and +/-5kHz peak deviation.

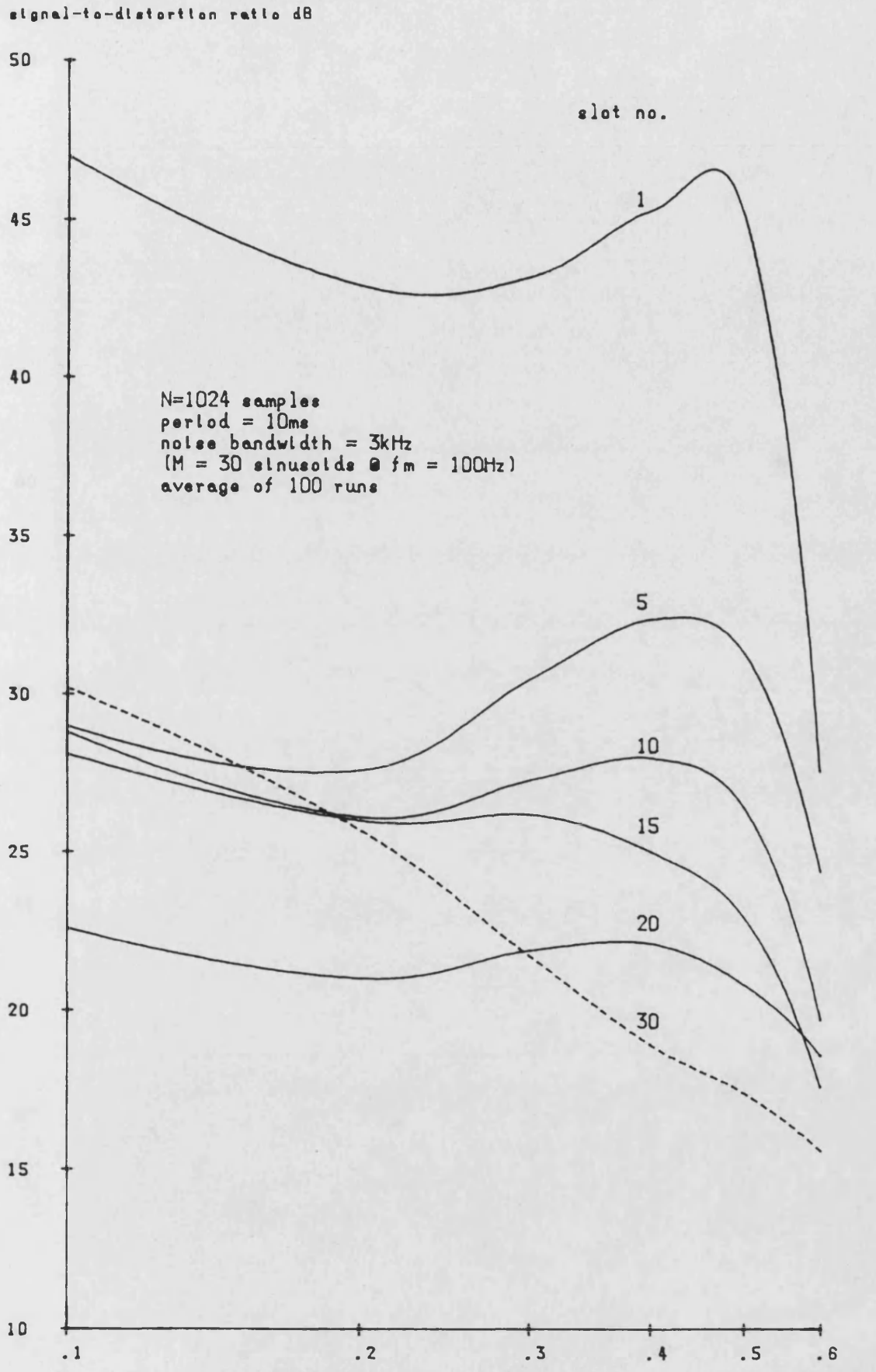

Fig.7.15 Computed intermodulation distortion in +/-3.75kHz crystal filter for pseudo-random modulation using a Monte Carlo process.

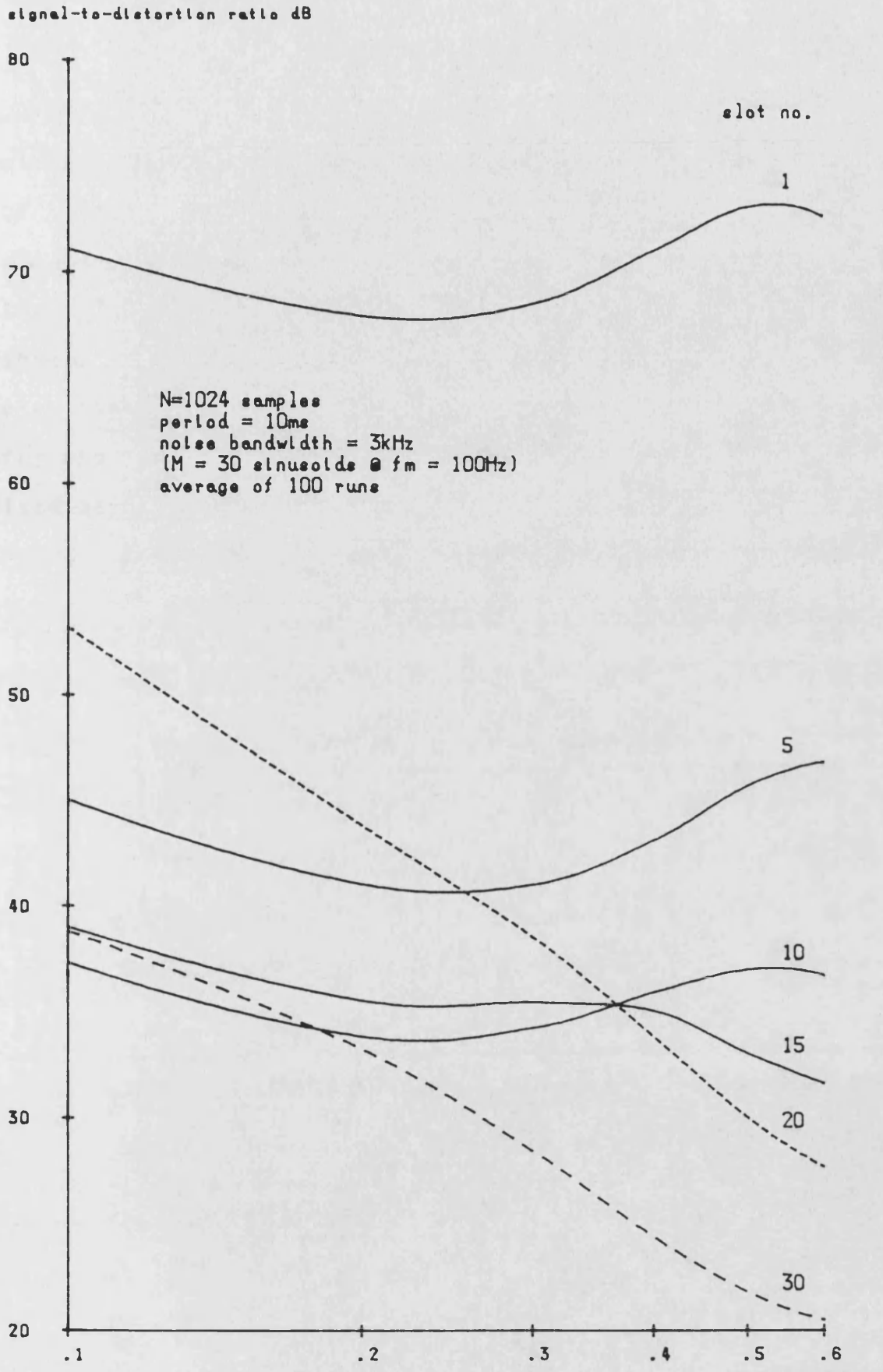

Fig.7.16 Computed intermodulation distortion in +/-3.75kHz crystal filter with artificial linear phase response.

positions (20 and 30), the performance falls off rapidly with increasing deviation, due primarily to the bandwidth of the filter being insufficient to pass the second order sidebands at these frequencies. The characteristics with the ±7.5kHz filter are not dissimilar to those discussed above, although the average signal-to-distortion levels are higher. There is also a pronounced dip in the curve for slot 30 with the linear phase filter around a normalised deviation of 0.4.

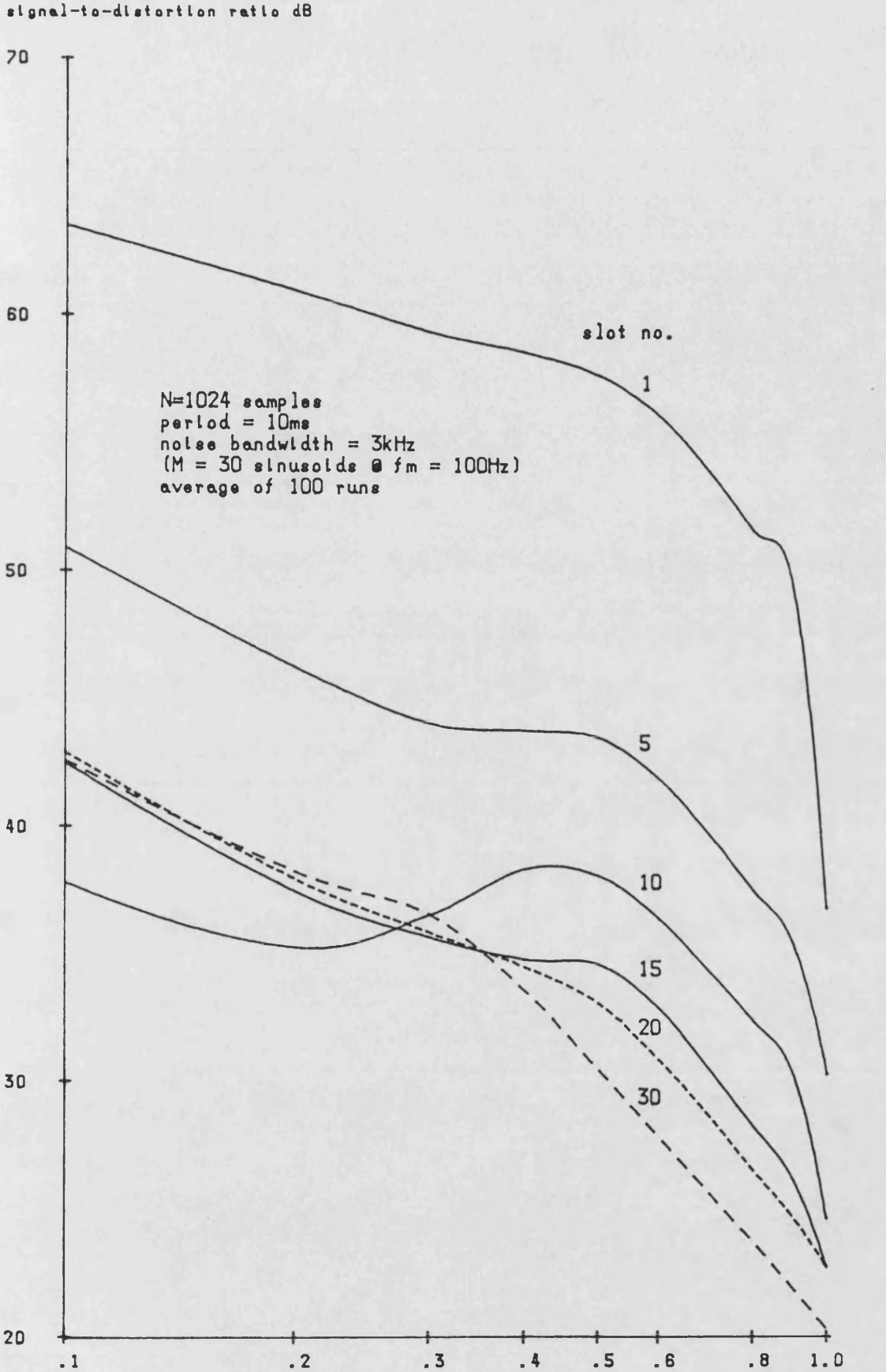

Fig.7.17 Computed intermodulation distortion in +/-7.5kHz crystal filter for pseudo-random modulation using a Monte Carlo process.

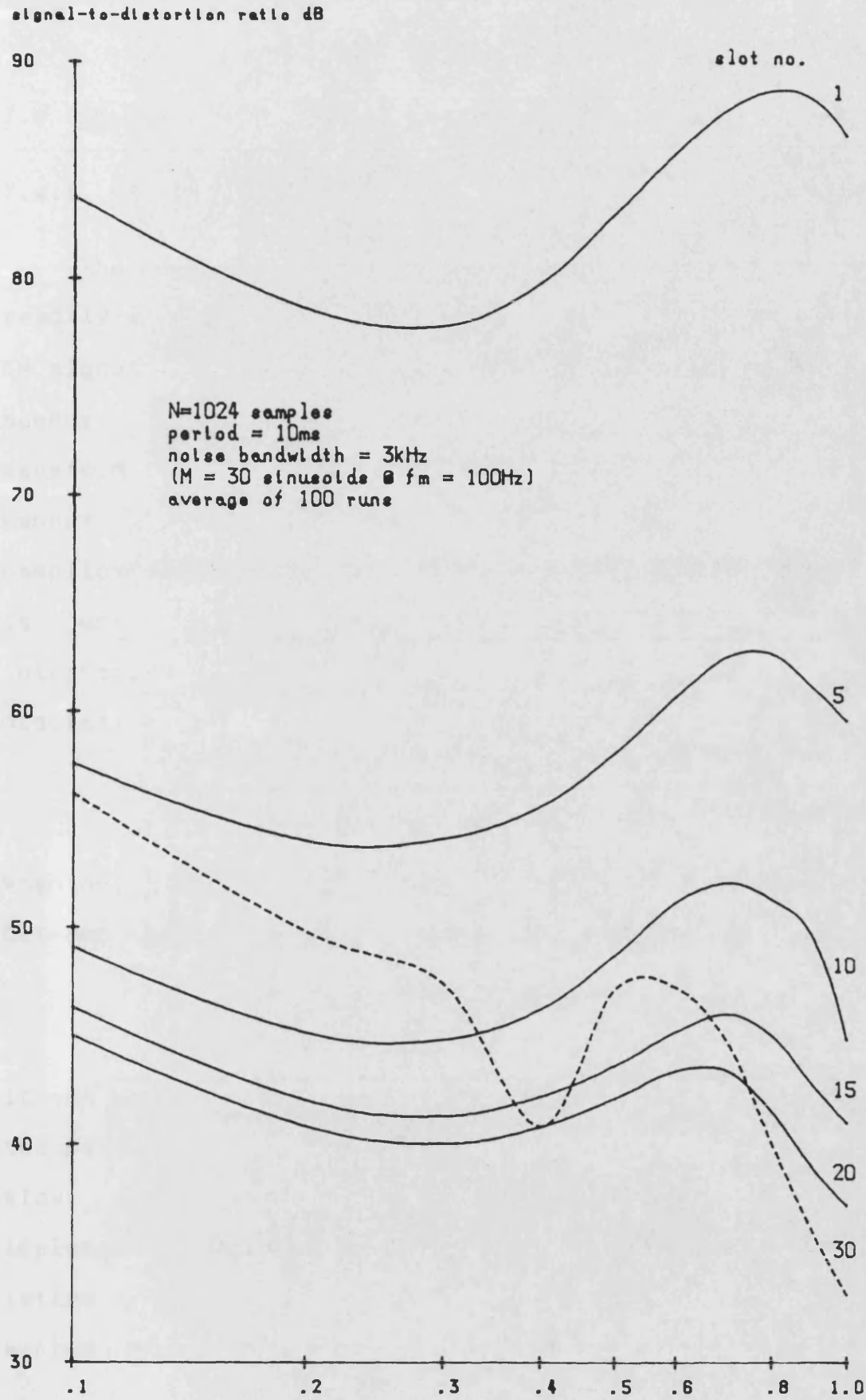

Fig.7.18 Computed intermodulation distortion in +/-7.5kHz crystal filter with artificial linear phase response.

7.4 CO-CHANNEL INTERFERENCE

7.4.1 PRINCIPLES

The presence of an unwanted co-channel signal may be readily analysed by summing the interferer with the wanted FM signal in the time domain, without recourse to frequency domain transformation. The demodulated signal waveform and its spectrum may then be found in the normal manner using just one DFT process. The algorithm is only complicated by the need to ensure that the correct period is used for the composite waveform. For a single interferer, and carrier frequencies of f_{c1} and f_{c2}, with modulating signals of period T_1 and T_2, this is given by

$$T = \frac{1}{HCF(f_{c1},\ f_{c2},\ 1/T_1,\ 1/T_2)} \qquad (7.11)$$

When one carrier frequency is N/4T ($N \geq 4$) and the offset between the two carriers is f_o, this simplifies to

$$T = \frac{1}{HCF(f_o,\ 1/T_1,\ 1/T_2)} \qquad (7.12)$$

It can be seen that when the offset is small but not zero, the period is very long, and hence the computation is very slow. The subroutine, COCHAN1.for, listed in Appendix F, implements the algorithms required to calculate intermodulation distortion due to a single interferer, when both wanted and un-wanted signals are modulated by pseudo-

random noise.

7.4.2 RESULTS WITH A SINGLE INTERFERER

Monte Carlo results for slots 1,5,10,15,20 and 30 with the co-channel interferer at a level of -60dB relative to the wanted signal and zero carrier offset are shown in fig.7.19. Each slot position has the same general characteristic, with the highest immunity to interference being displayed by slot 1. The benefit of increased freq. deviation (above a normalised value of about 0.25) is clearly visible, with an abrupt change in the slope of all curves. Results at other un-wanted signal levels up to -10dB below wanted, indicated a linear relationship of signal-to-distortion with interferer magnitude. Further results with carrier offsets of 100 and 200Hz in fig.7.20 show little variance from those in fig.8.19. Hence the signal-to-distortion (at constant interferer level) with pseudo-random noise modulation is primarily dependent upon frequency deviation and the measurement (slot) frequency.

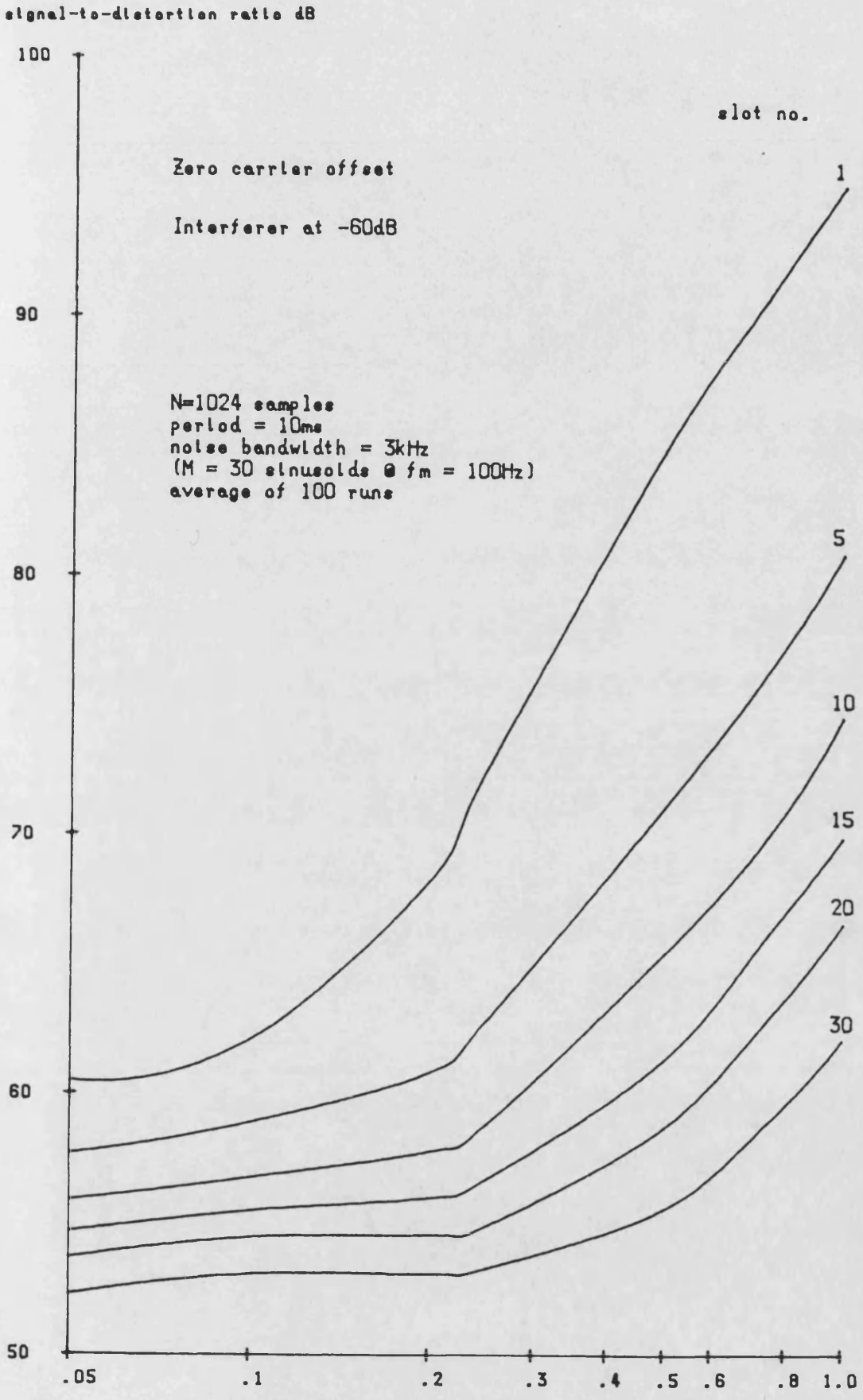

Fig.7.19 Computed intermodulation distortion with a single co-channel interferer. Both signals modulated with pseudo-random noise with equal deviation.

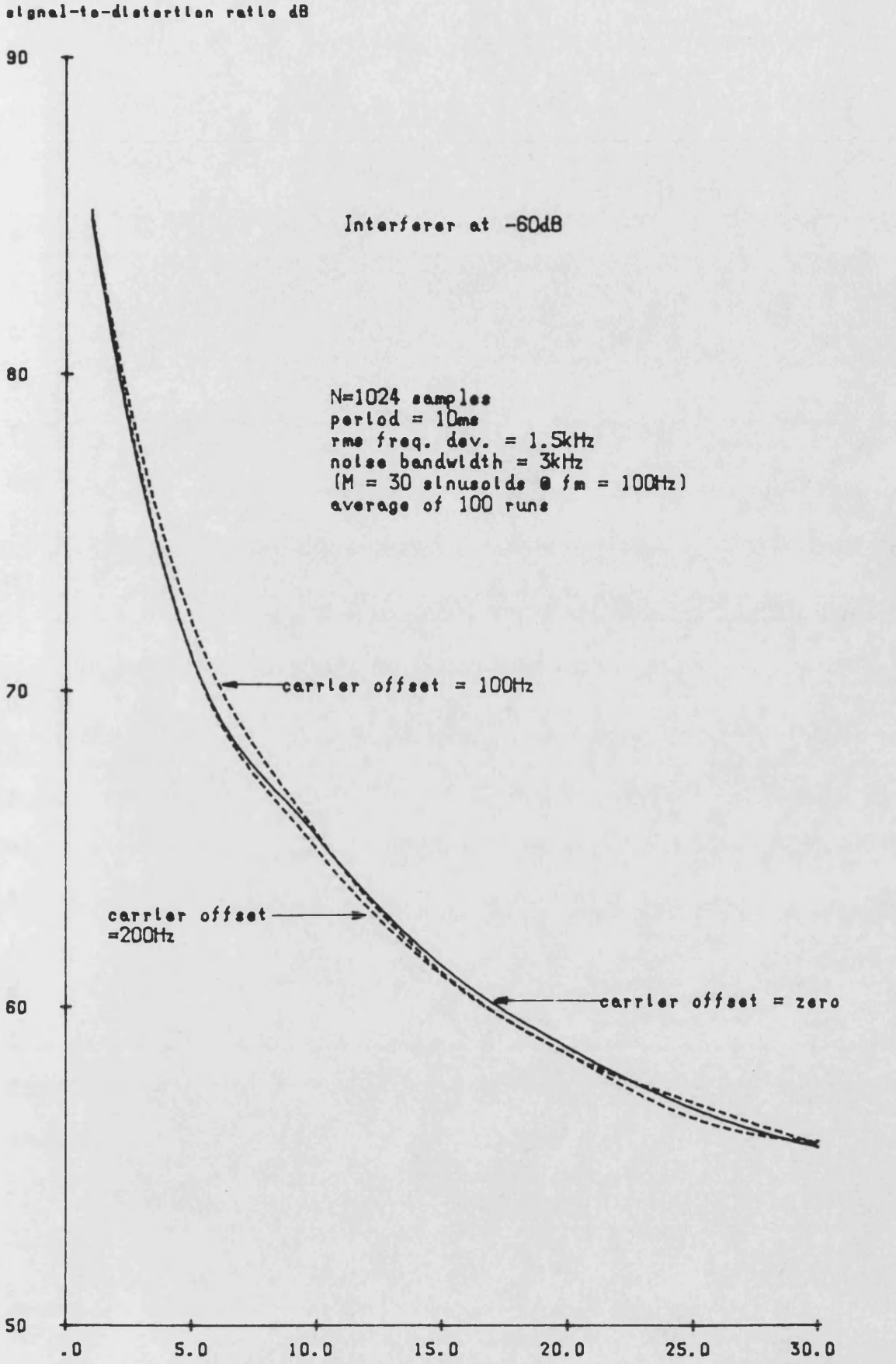

Fig.7.20 Computed intermodulation distortion with a single co-channel interferer with baseband slot frequency and carrier offset.

7.5 CONCLUSIONS

The discrete Fourier transform has been shown to be eminently suitable for the spectral analysis and assessment of message signal degradation due to bandlimiting and co-channel interference in angle modulation systems. The approach was extended to include more realistic pseudo-random noise-like modulation by the use of Monte Carlo methods. The validity of these techniques was verified by the excellent correlation observed with both practical measurements and the work of others.

It was shown that the bandwidth of the FM signal with pseudo-random modulation containing 99% of the spectral power can be predicted by a simple modification to Carsons rule to allow for the reduced peak-to-rms value of the waveforms analysed. The effects of bandlimiting using single-pole, crystal and pseudo-rectangular responses were investigated. Excellent agreement was obtained between the results for the single-pole filter and those from practical measurements by Bodtmann. For the pseudo-rectangular filter, empirical formulas were derived relating the necessary bandwidth at a given frequency deviation to the required signal-to-distortion ratio. These were an excellent fit to the calculated data over a wide range of parameter variations. Finally the results for the crystal filters demonstrated the importance of the group delay

characteristic in the filters specification.

The degradation of the the FM signal with pseudo-random noise modulation due to a single co-channel interferer was found to decrease with increasing frequency deviation as expected. However, there was considerable variation in the results across the audio band, with as much as a 35dB increase in the measured signal-to-distortion ratio from 100Hz to 3kHz. The effect of a moderate carrier offset was found to be negligible.

7.6 REFERENCES

(1) Medhurst,R.G.:'Evaluation of distortion in FM trunk radio systems by a Monte Carlo method', Proc.IEE, vol.113, no.4, pp.570-580, April 1966.

(2) Ruthroff, C.L.:'Computation of FM distortion in linear networks for bandlimited periodic signals', Bell System Tech. Journal, vol.47, no.7, pp.1043-1063, July 1968.

(3) Bennett, W.R.'Distribution of the sum of randomly phased components', Quart. Appl. Math. , vol.5, no.1, pp.385-393, April 1947.

(4) Watt, J.M.:'A note on the evaluation of trigonometric series', Computer Journal, vol.1, p.161, 1959.

(5) Anuff, A. and Liou, M.L.:'A note on necessary bandwidth in FM systems', IEEE Proc. (Letters), vol.59, no.10, pp.1522-3, Oct. 1971.

(6) Roberts, J.H.:'FM distortion: A comparison of theory and measurement', IEEE Proc. (Letters), vol.57, no.4, pp.728-732, April 1969.

CHAPTER EIGHT

ANGLE MODULATION WITH TIME-COMPRESSION MULTIPLEXED SIGNALS

8.1 INTRODUCTION

The fundamental expressions describing an angle modulated carrier with a time-compression multiplexed modulating signal are derived. Certain characteristics are then revealed using classical Fourier analysis, however, it is shown that further theoretical treatment is only of very limited value as the solution of the resulting Diophantine equations is particular tedious, even with computer aid.

By using the periodic form of the general multichannel TCM signal developed in chapter 5, relatively straightforward expressions describing TCM-PM and TCM-FM suitable for application of the discrete Fourier transform are derived. It is then shown qualitatively, that the usual increased bandwidth requirement of phase modulation systems over equivalent frequency modulation systems is emphasised with TCM. This leads to TCM-FM being adopted in favour of the alternative for the remainder of the work.

Typical spectra for TCM-FM with both sinusoidal and pseudo-random noise modulation are presented, and comparisons made with non-multiplexed systems. A comprehen-

sive range of results are then given for the performance of TCM-FM with RF filtering using the pseudo-rectangular response developed in chapter 7. Finally, results are presented for the intermodulation distortion in a TCM-FM system due to co-channel interference.

8.2 FUNDAMENTAL EXPRESSIONS FOR TIME-COMPRESSION MULTIPLEXED FM

The general expression for an R channel TCM signal , $y_{TCM}(t)$, with complex baseband signals composed of M_r sinusoids is, from eqn.5.50

$$y_{TCM}(t) = \frac{1}{a} \sum_{r=1}^{R} \sum_{m_r=1}^{M_r} \sum_{k=-\infty}^{\infty} A_{rm} \cdot Sa\left[\frac{\pi T}{a}(k/T - (a-1)f_{rm})\right]$$

$$\cdot \cos\left[2\pi(f_{rm} + k/T)(t - (r-1)T/a) + \theta_{rm}\right]$$

$$\cdot e^{-j2\pi f_{rm}(r-1)T/a} \qquad (8.1)$$

where T is the TCM frame period and a is the compression ratio

Thus the expression for the corresponding phase modulated waveform, $e_{PM}(t)$, with the usual notation is

$$e_{PM}(t) = Re\left[A_c \cdot e^{j2\pi f_c t + \theta_c} \cdot \prod_{r=1}^{R} \prod_{m_r=1}^{M_r} \prod_{k=-\infty}^{\infty} e^{j\beta_{rmk}} \cdot \cos\left[2\pi(f_{rm} + k/T)(t - (r-1)T/a) + \theta_{rm}\right]\right]$$

(8.2)

where

$$\beta_{rmk} = \frac{k_d A_{rm} \cdot Sa\left[\frac{\pi T}{a}(k/T - (a-1)f_{rm})\right] \cdot e^{-j2\pi f_{rm}(r-1)T/a}}{a}$$

Thus the rms phase deviation is

$$\Delta\phi_{rms} = \left[\sum_{r=1}^{R}\sum_{m_r=1}^{M_r}\sum_{k=-\infty}^{\infty}\frac{\beta_{rmk}^2}{2}\right]^{1/2} \qquad (8.3)$$

and the rms frequency deviation is

$$\Delta f_{rms} = \left[\sum_{r=1}^{R}\sum_{m_r=1}^{M_r}\sum_{k=-\infty}^{\infty}\frac{(f_{rm} + k/T)^2\,\beta_{rmk}^2}{2}\right]^{1/2} \qquad (8.4)$$

Integrating eqn.8.1 to find the expression for frequency modulation gives

$$e_{FM}(t) = Re\left[A_c \cdot e^{j2\pi f_c t + \theta_c'} \cdot \prod_{r=1}^{R}\prod_{m_r=1}^{M_r}\prod_{k=-\infty}^{\infty} e^{\frac{j\Delta f_{rmk}}{f_{rm} + k/T}} \cdot \sin\left[2\pi(f_{rm} + k/T)(t-(r-1)T/a) + \theta_{rm}\right]\right] \qquad (8.5)$$

where

$$\theta_c' = \theta_c - \sum_{r=1}^{R}\sum_{m_r=1}^{M_r}\sum_{k=-\infty}^{\infty} A_{rm} \cdot Sa\left[\frac{\pi T}{a}(k/T - (a-1)f_{rm})\right]$$

$$\cdot \sin\left[-2\pi(f_{rm} + k/T)(r-1)T/a + \theta_{rm}\right]$$

and

$$\Delta f_{rmk} = \frac{k_d A_{rm} \cdot Sa\left[\frac{\pi T}{a}(k/T - (a-1)f_{rm})\right] \cdot e^{-j2\pi f_{rm}(r-1)T/a}}{a}$$

Thus the rms phase deviation is

$$\Delta\phi_{rms} = \left[\sum_{r=1}^{R}\sum_{m_r=1}^{M_r}\sum_{k=-\infty}^{\infty}\frac{\left[\frac{\Delta f_{rmk}}{f_{rm} + k/T}\right]^2}{2}\right]^{1/2} \qquad (8.6)$$

and the rms frequency deviation is

$$\Delta f_{rms} = \left[\sum_{r=1}^{R}\sum_{m_r=1}^{M_r}\sum_{k=-\infty}^{\infty}\frac{\Delta f_{rmk}^2}{2}\right]^{1/2} \qquad (8.7)$$

The above expressions are not dissimilar to those for non-multiplexed ØM with multi-tone modulation (eqns.6.5 and 6.8). However, the complexity is greatly increased due to the large number of components in the TCM baseband signal. In addition, since the frequency deviation in PM is proportional to the baseband frequency (eqn.8.4) this leads to wide spectra for TCM-PM. Hence, just as practical narrow-band systems employ FM in preference to PM, TCM-FM is vastly superior to TCM-PM for the same reasons of bandwidth conservation.

Using the identity of eqn.6.9 to expand eqn.8.5 as a Fourier series and neglecting the time independent carrier phase, θ_c', gives

$$e_{FM}(t) = \mathrm{Re}\left[A_c \cdot e^{j2\pi f_c t} \cdot \prod_{r=1}^{R} \prod_{m_r=1}^{M_r} \prod_{k=-\infty}^{\infty} \sum_{n_{rmk}=-\infty}^{\infty} J_{n_{rmk}}\left[\frac{\Delta f_{rmk}}{f_{rm}+k/T}\right] \cdot e^{jn\left[2\pi(f_{rm}+k/T)(t-(r-1)T/a)+\theta_{rm}\right]}\right] \tag{8.8}$$

Hence the TCM-FM spectrum consists of sidebands at frequencies, f_s, given by

$$f_s = f_c + \sum_{r=1}^{R} \sum_{m_r=1}^{M_r} \sum_{k=-\infty}^{\infty} n_{rmk}\,(f_{rm} + k/T) \tag{8.9}$$

where n_{rmk} is an integer.

The magnitude, A_s, of the sideband at f_s is

$$A_s = \sum A_c \prod_{r=1}^{R} \prod_{m_r=1}^{M_r} \prod_{k=-\infty}^{\infty} J_{n_{rmk}}\left[\frac{\Delta f_{rmk}}{(f_{rm} + k/T)}\right] \tag{8.10}$$

where the summation is performed for all sets of n_{rmk} satisfying eqn.8.9

The above Diophantine equations are extremely tedious to solve even with computer aid. Hence it may be concluded

that there is little to be gained from any further theoretical analysis of TCM-ØM. However, the following section will consider the application of the discrete Fourier transform to this class of angle modulated signals.

8.3 APPLICATION OF THE DISCRETE FOURIER TRANSFORM

From eqn.5.54, one period of the general R channel TCM signal, $y_{TCM_T}(t)$, is given by

$$y_{TCM_T}(t) = \sum_{r=1}^{R} \sum_{m_r=1}^{M_r} \sum_{k=0}^{K_T-1} A_{rm} \cdot \text{rect}\left[\frac{a(t - kT - (r-1)T/a)}{T}\right]$$

$$\cdot \cos\left[2\pi a f_{rm}\left[t - k\left[\frac{a-1}{a}\right]T - \left[\frac{r-1}{a}\right]T\right] + \theta_{rm}\right] \quad (8.11)$$

where

$$K_T = \frac{1}{\text{HCF}\left[1, \sum_r \sum_m f_{rm}T\right]}$$

Thus, one period of the corresponding PM signal, $e_{PM_T}(t)$, may be written as

$$e_{PM_T}(t) = \text{Re}\left[A_c \exp\left[j2\pi f_c t + j\theta_c + jk_d A_{rm} \sum_{r=1}^{R} \sum_{m_r=1}^{M_r} \sum_{k=0}^{K_T-1}\right.\right.$$

$$\left.\left. \cdot \cos\phi_{rmk} \cdot \text{rect}\left[\frac{a(t - kT - (r-1)T/a)}{T}\right]\right]\right] \quad (8.12)$$

where

$$\phi_{rmk} = \left[2\pi a f_{rm}\left[t - k\left[\frac{a-1}{a}\right]T - \left[\frac{r-1}{a}\right]T\right] + \theta_{rm}\right]$$

providing f_c is an integer multiple of the reciprocal of the composite period, $\frac{1}{T_{TOTAL}} = \frac{1}{K_T T}$.

Eqn.8.12 may be readily converted into a form suitable for DFT or FFT analysis by replacing the real part of the exponential with a cosine function and introducing limits on t, therefore

$$e_{PM_T}(t) = A_c \cos\left[2\pi f_c t+\theta_c+k_d A_{rm} \sum_{r=1}^{B} \sum_{m_r=1}^{M_r} \sum_{k=0}^{K_I-1} \cos\phi_{rmk}\right]$$

$$\left[-T/2a<t\leq -T/2a+T.K_T\right]$$

for

$$kT+(r-1)T/a-T/2a\leq t\leq kT+(r-1)T/a+T/2a$$

$$= A_c \cos\left[2\pi f_c t + \theta_c\right] \quad \text{otherwise} \qquad (8.13)$$

The above equation applies providing the carrier frequency is set to $N/4T_{TOTAL}$ and N=4i where i = integer.

For frequency modulation, the situation is complicated by the need to integrate eqn.8.11 to produce an expression for the instantaneous phase, $\phi(t)$, ie.

$$\phi(t) = \int_{-\infty}^{t} \omega_i(\tau)\, d\tau = \int_{-\infty}^{t} 2\pi y_{TCM_T}(\tau)\, d\tau \qquad (8.14)$$

Splitting the integral in two and using the product rule gives

$$\phi(t) = \left[\sum_{r=1}^{B} \sum_{m_r=1}^{M_r} \sum_{k=0}^{K_I-1} \frac{A_{rm}}{af_{rm}} \text{ rect}\left[\frac{a(\tau - kT - (r-1)T/a)}{T}\right]\right.$$

$$\cdot \sin\left[2\pi a f_{rm}\left[\tau - k\left[\frac{a-1}{a}\right]T - \left[\frac{r-1}{a}\right]T\right] + \theta_{rm}\right]\Bigg]_{\tau=-\infty}^{t}$$

$$- \int_{-\infty}^{t} \left[\sum_{r=1}^{B} \sum_{m_r=1}^{M_r} \sum_{k=0}^{K_I-1} \frac{A_{rm}}{a f_{rm}}\left[\delta\left[\tau - kT - \left[\frac{r-1}{a}\right]T + T/2a\right]\right.\right.$$

$$\left.\left. - \delta\left[\tau - kT - \left[\frac{r-1}{a}\right] - T/2a\right]\right]\right.$$

$$\cdot \sin\left[2\pi a f_{rm}\left[\tau - k\left[\frac{a-1}{a}\right]T - \left[\frac{r-1}{a}\right]T\right] + \theta_{rm}\right]\Bigg] \, d\tau$$

(8.15)

Assuming the order of integration and summation may be interchanged, the integral becomes

$$\phi(t) = \sum_{r=1}^{B} \sum_{m_r=1}^{M_r} \frac{A_{rm}}{a f_{rm}} \left[\sum_{k=0}^{K_I-1} \text{rect}\left[\frac{a(t - kT - (r-1)T/a)}{T}\right]\right.$$

$$\cdot \sin\left[2\pi a f_{rm}\left[t - k\left[\frac{a-1}{a}\right]T - \left[\frac{r-1}{a}\right]T\right] + \theta_{rm}\right]$$

$$+ \sum_{k_1=0}^{K_1} \sin\left[\pi f_{rm} T(2k_1+1) + \theta_{rm}\right]$$

$$\left. - \sum_{k_2=0}^{K_2} \sin\left[\pi f_{rm} T(2k_2-1) + \theta_{rm}\right]\right] \qquad (8.16)$$

since both the rect(x) and $\delta(x)$ functions are zero at

the lower limit, and where

$$K_1 = \text{largest integer} \leq \left[\frac{t-(r-1)T/a-T/2a}{T}\right]$$

and

$$K_2 = \text{largest integer} \leq \left[\frac{t-(r-1)T/a+T/2a}{T}\right]$$

The first term in eqn.8.16 is the TCM modulating signal and the remainder are offsets which serve to remove the instantaneous phase changes that would otherwise occur at the segment edges. Hence, unlike TCM-PM there are no impulsive instantaneous frequency transitions at the segment edges, resulting in a much narrower spectrum. The complete FM expression may then be found by substitution for $\phi(t)$ in

$$e_{FM_T}(t) = \text{Re}\left[A_c\, e^{j2\pi f_t + \theta_c + k_d\phi(t)}\right] \qquad (8.17)$$

An example will serve to illustrate the application of eqn.8.16. With T=5ms, a=4 and sinusoidal signals of 100Hz and 200Hz on two active channels (R=2, M_1=1, M_2=1), then $T_{TOTAL} = \dfrac{T}{\text{HCF}[\,1,\ 0.5,\ 1]} = 10\text{ms}$ and K_T=2. Hence $\phi(t)$ is defined by

$$\phi(t) = A_1 \sin\left[2\pi a f_1 t + \theta_1\right]$$

$$- A_1 \sin\left[-\pi f_1 T + \theta_1\right] \quad \text{for} \quad -T/2a < t \leq T/2a$$

$$= A_2 \sin\left[2\pi a f_2(t-T/a) + \theta_2\right]$$

$$+ A_1\left[\sin\left[\pi f_1 T + \theta_1\right] - \sin\left[-\pi f_1 T + \theta_1\right]\right]$$

$$- A_2 \sin\left[-\pi f_2 T + \theta_2\right] \quad \text{for} \quad T/2a < t \leq 3T/2a$$

$$= A_1 \sin\left[2\pi a f_1(t-T+T/a) + \theta_1\right]$$

$$+ A_1\left[\sin\left[\pi f_1 T + \theta_1\right] - \sin\left[-\pi f_1 T + \theta_1\right]\right]$$

$$+ A_2\left[\sin\left[\pi f_2 T + \theta_2\right] - \sin\left[-\pi f_2 T + \theta_2\right]\right]$$

$$- A_1 \sin\left[(2a-1)\pi f_1 T + \theta_1\right] \quad \text{for} \quad T-T/2a < t \leq T+T/2a$$

$$= A_2 \sin\left[2\pi a f_2(t-T) + \theta_2\right]$$

$$+ A_1\left[\sin\left[\pi f_1 T + \theta_1\right] - \sin\left[-\pi f_1 T + \theta_1\right]\right]$$

$$+ A_2\left[\sin\left[\pi f_2 T + \theta_2\right] - \sin\left[-\pi f_2 T + \theta_2\right]\right]$$

$$+ A_1\left[\sin\left[(2a+1)\pi f_1 T + \theta_1\right] - \sin\left[(2a-1)\pi f_1 T + \theta_1\right]\right]$$

$$- A_2 \sin\left[(2a-1)\pi f_2 T + \theta_2\right] \quad \text{for} \quad T+T/2a < t \leq T+3T/2a$$

$$= 0 \qquad \text{otherwise} \qquad (8.18)$$

8.4 SPECTRAL ANALYSIS USING THE DFT

A subroutine, TCMSIN.for, (listed in Appendix G) was developed from eqn.8.6 to evaluate TCM-FM spectra with a single active channel and sinusoidal modulation. Fig.8.1(a) shows the result for a 2-channel system with a 10ms frame period, and 1kHz modulation with a peak frequency deviation of 10kHz. The principle sidebands occur at intervals of the compressed modulating frequency (2kHz) with minor sidebands spaced at the reciprocal of the frame period (100Hz) as expected. The spectrum for a 4-channel system with a frame period of 20ms is illustrated in fig.8.1(b), with a modulating frequency of 2kHz. The sideband spacing is now 50Hz, with peaks at every 8kHz.

Appendix H contains a listing of SPECTCM.for, developed from eqn.8.6 for pseudo-random noise modulation on all channels using the Monte Carlo process described in chapter 7. The effects on the spectra of varying both the compression ratio and frame period are illustrated in figs.8.2 to 8.4. All the results were calculated using noise signals comprising of 30 tones and were averages of 100 independent Monte Carlo runs. The spectra are all characterised by a main lobe, resembling that for non-multiplexed FM (figs.7.1 and 7.2), with a relatively poor asymptotic roll-off. Furthermore, when the frequency axis is normalised by the compression ratio, the spectra are

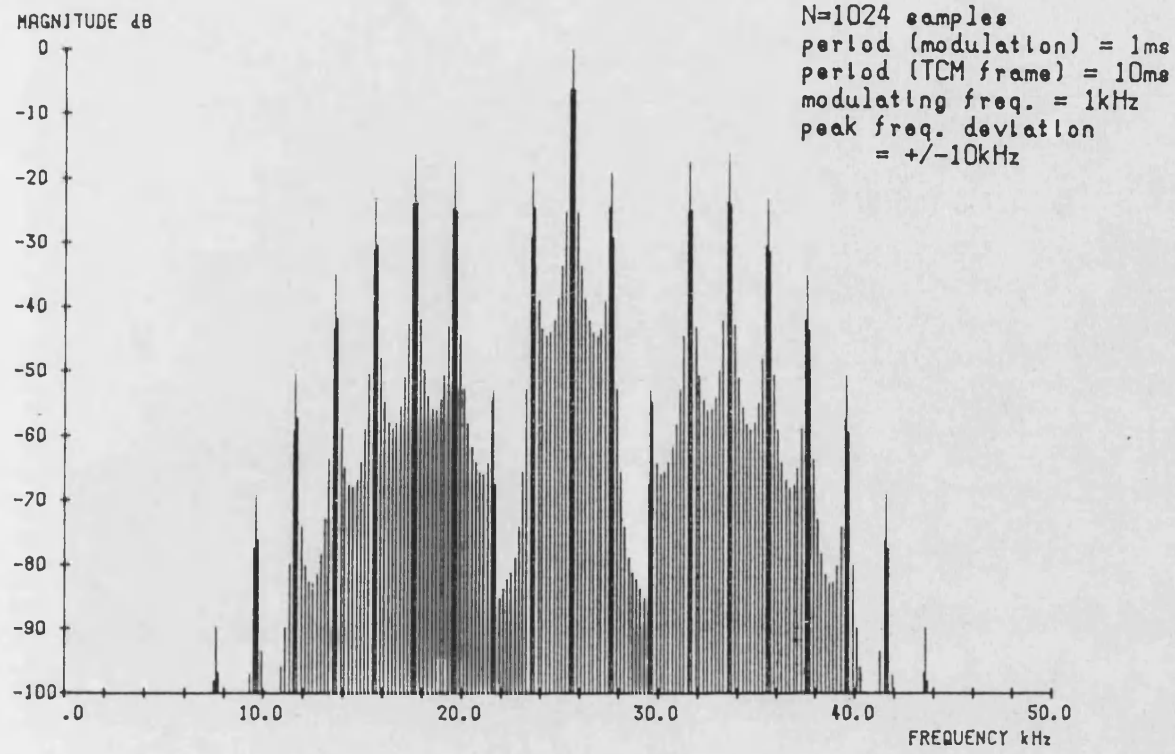

Fig. 8.1(a) Spectrum of a 2-channel TCM-FM signal with a single active channel with sinusoidal modulation at 1kHz.

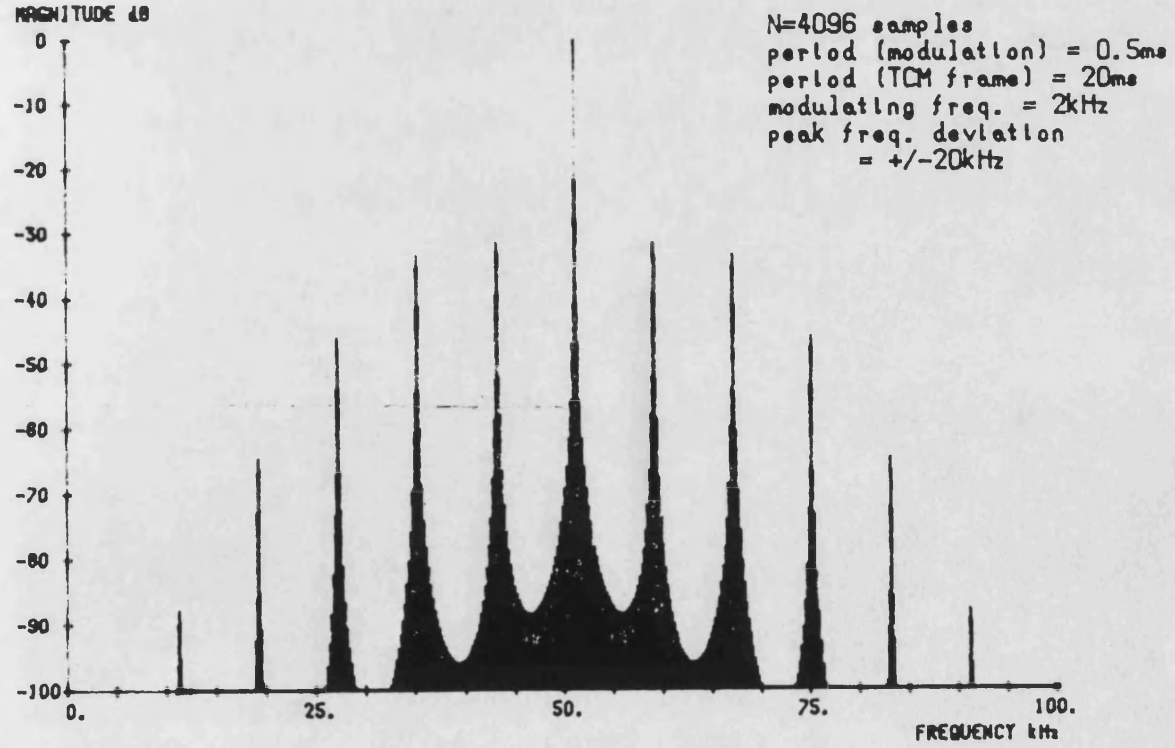

Fig. 8.1(b) Spectrum of a 4-channel TCM-FM signal with a single active channel with sinusoidal modulation at 2kHz.

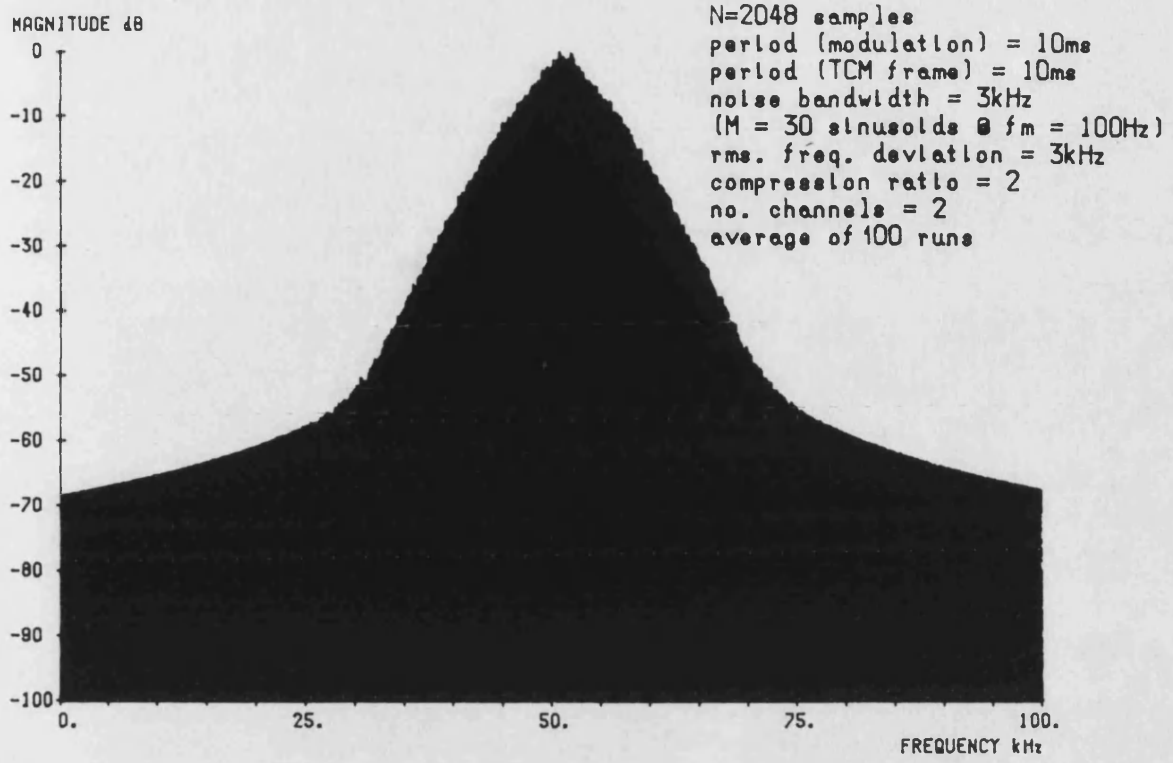

Fig. 8.2(a) Spectrum of a 2-channel TCM-FM signal with all channels active and pseudo-random noise modulation using a Monte Carlo process.

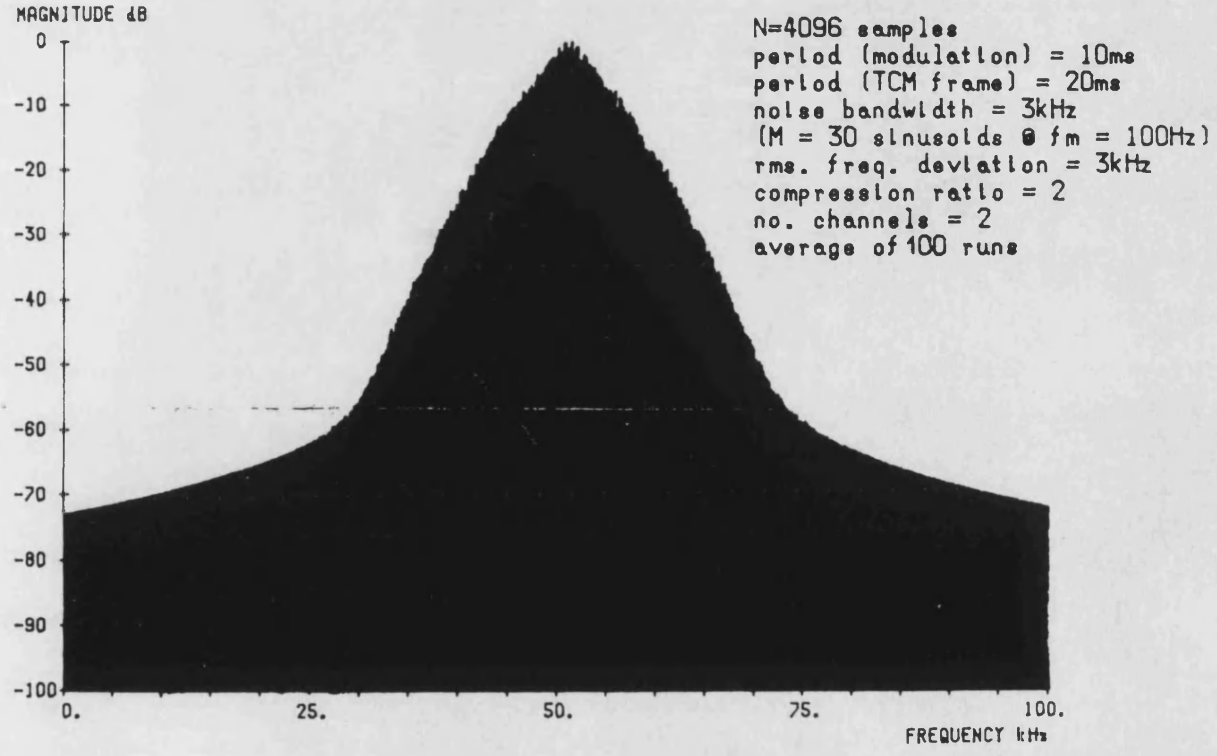

Fig. 8.2(b) Spectrum of a 2-channel TCM-FM signal with all channels active and pseudo-random noise modulation using a Monte Carlo process.

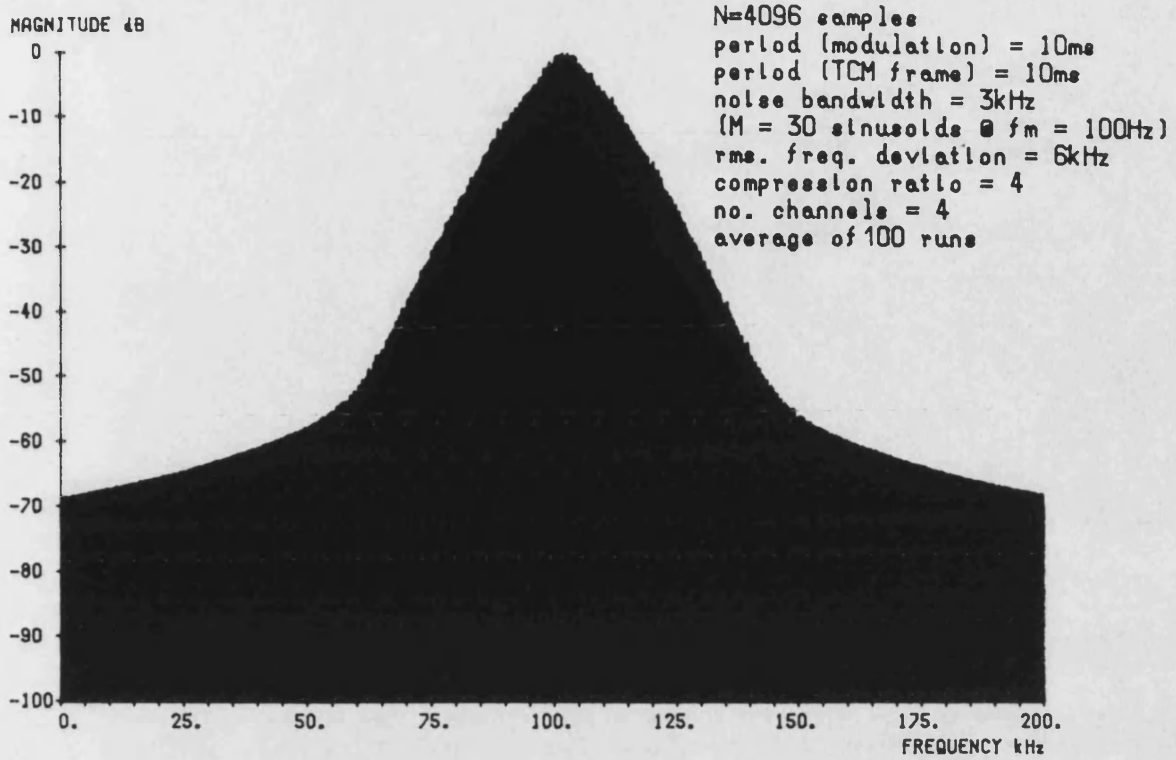

Fig. 8.3(a) Spectrum of a 4-channel TCM-FM signal with all channels active and pseudo-random noise modulation using a Monte Carlo process.

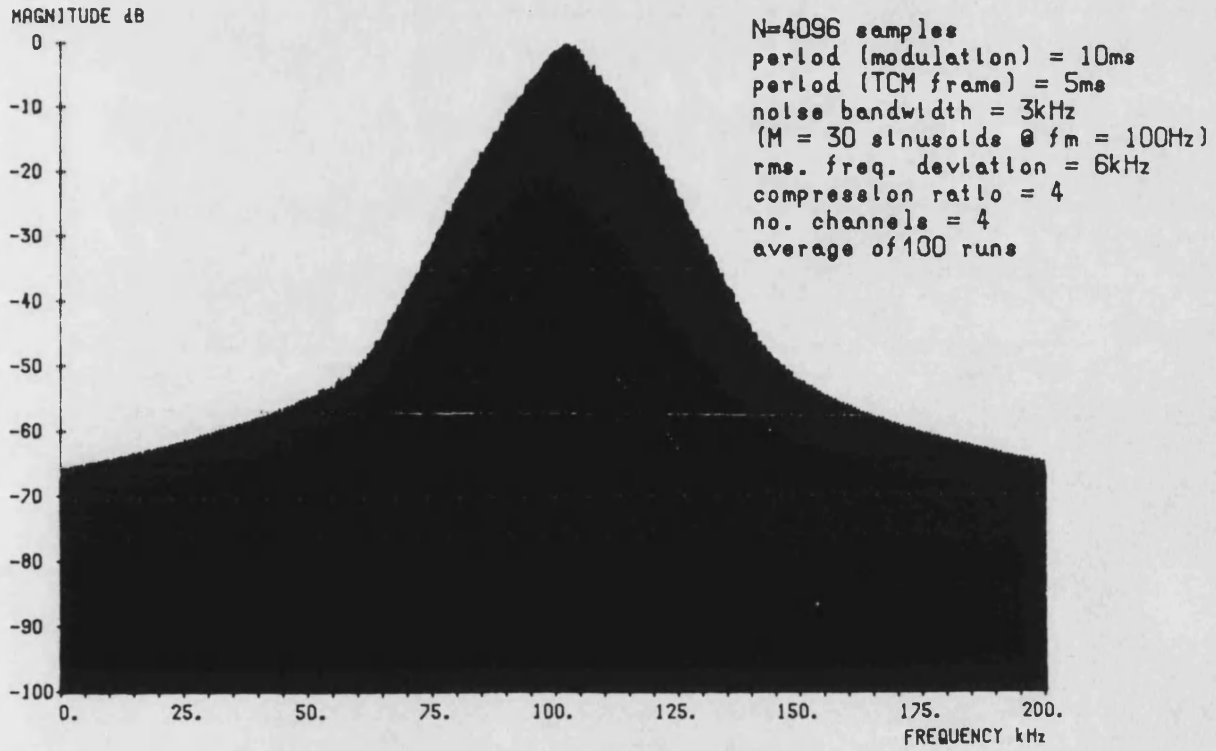

Fig. 8.3(b) Spectrum of a 4-channel TCM-FM signal with all channels active and pseudo-random noise modulation using a Monte Carlo process.

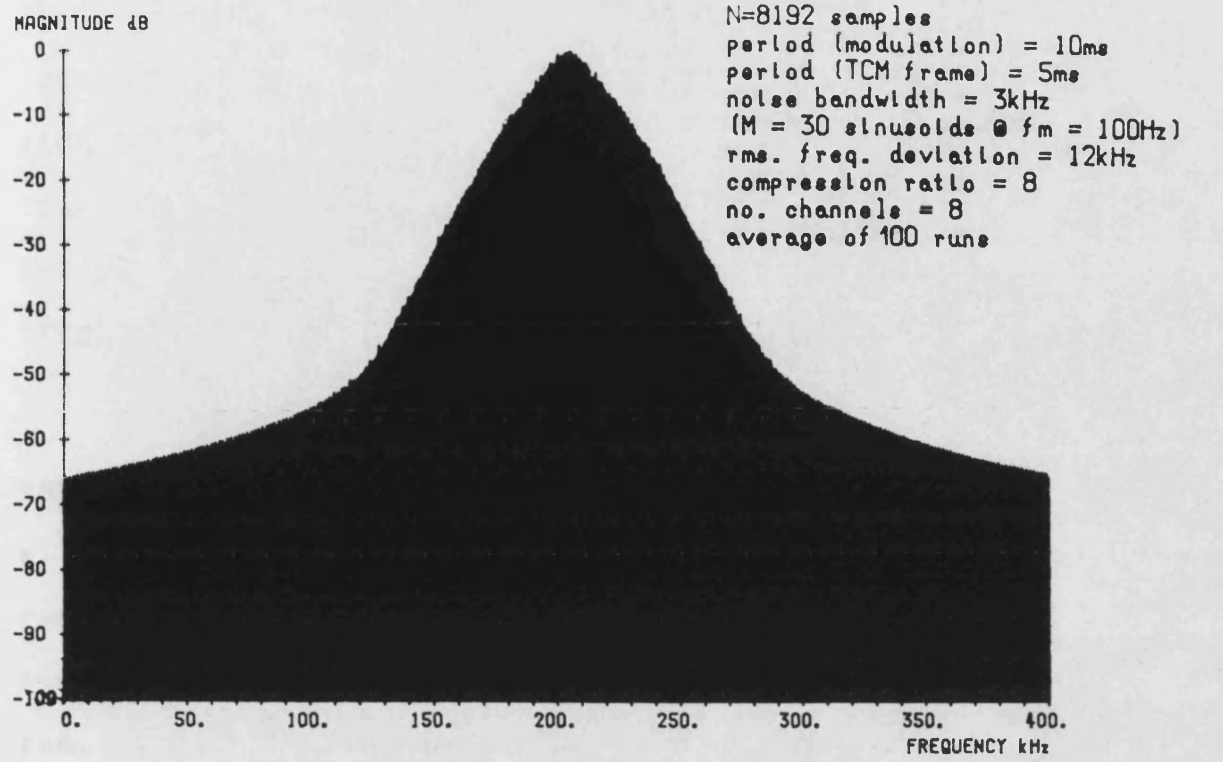

Fig. 8.4(a) Spectrum of a 8-channel TCM-FM signal with all channels active and pseudo-random noise modulation using a Monte Carlo process.

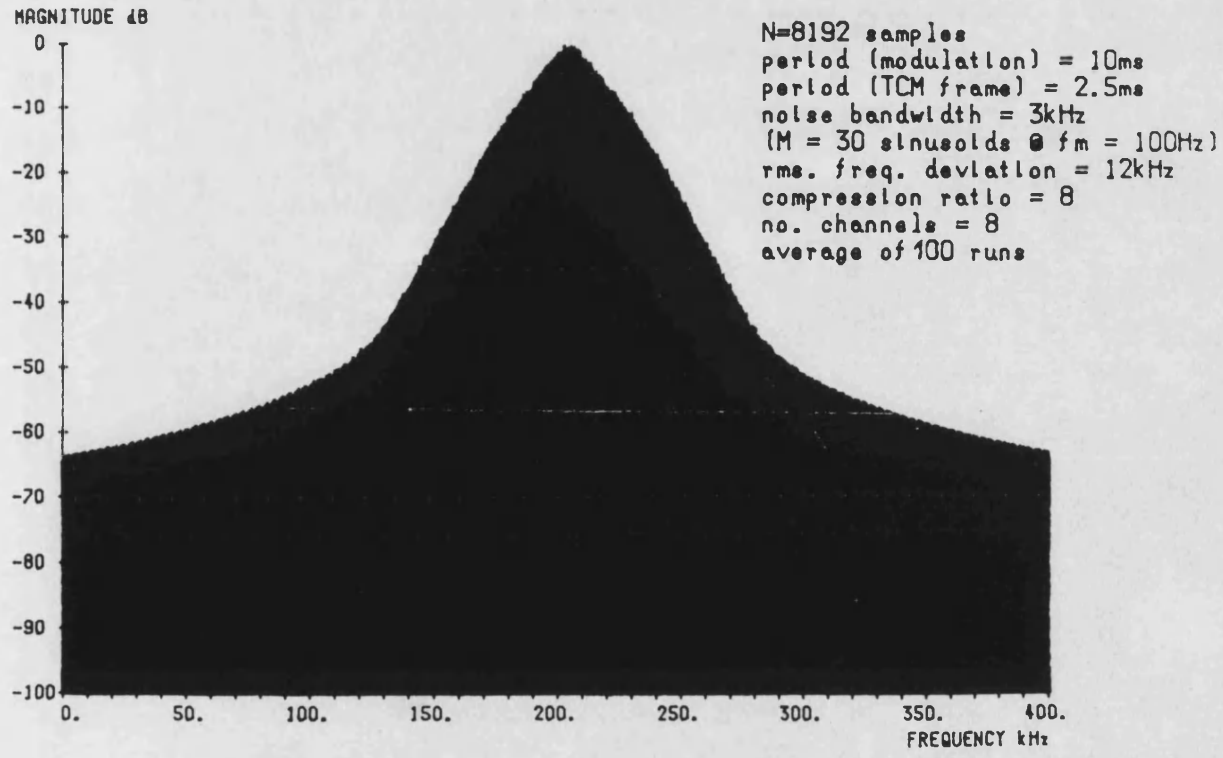

Fig. 8.4(b) Spectrum of a 8-channel TCM-FM signal with all channels active and pseudo-random noise modulation using a Monte Carlo process.

seen to be largely identical, with the magnitude of the sidebands at the edges of the plots varying slightly with frame period. This value ranges from -63dB for a frame period of 2.5ms (fig.8.4(b)) to -72dB for 20ms (fig.8.2(b)).

As for non-multiplexed FM, the bandwidths containing 98% and 99% of the spectral power in the TCM-FM signal with pseudo-random noise modulation were calculated. The results for compression ratios of 2,4,8 and 16 with just a single active channel are shown in fig.8.5. The bandwidth requirement is approximately linearly related to the rms deviation normalised to the compression ratio times the noise bandwidth, except for small values of the latter. Of particular significance is the appreciable difference between the curves for 98% and 99% power indicating poor spectral roll-off. More meaningful results when all channels are active are shown in fig.8.6. Again the same linear relationship of bandwidth to normalised frequency deviation is found. Comparison with fig.7.3 shows that the 98%/99% bandwidth requirement for TCM-FM is increased from that of an equivalent ordinary FM system by a factor equal to the compression ratio. However, as will be confirmed in section 8.5, the spectral efficiency is not as good due to the poor asymptotic roll-off.

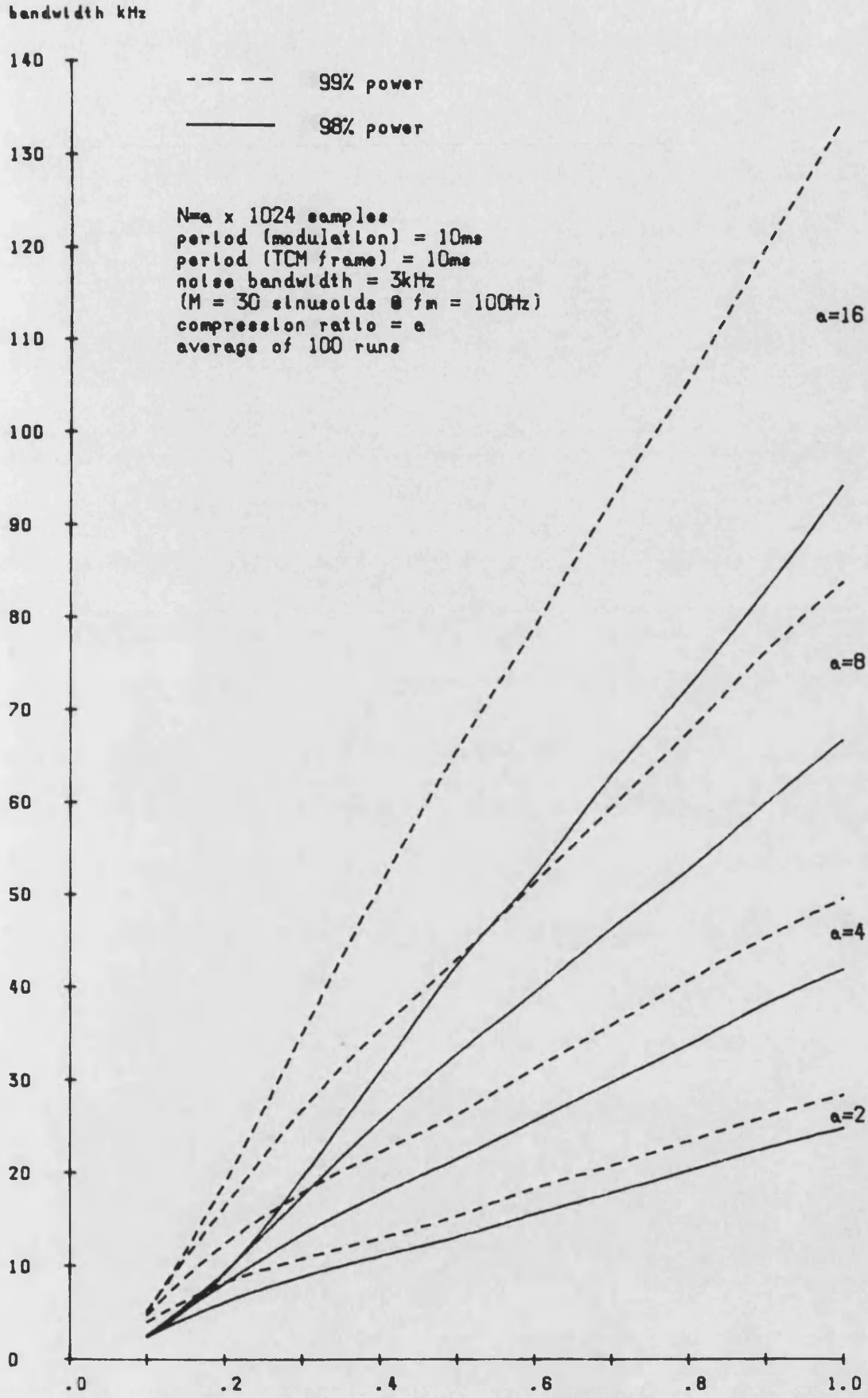

Fig.8.5 98/99% spectral power bandwidths of TCM-FM signal with single active channel with pseudo-random noise modulation.

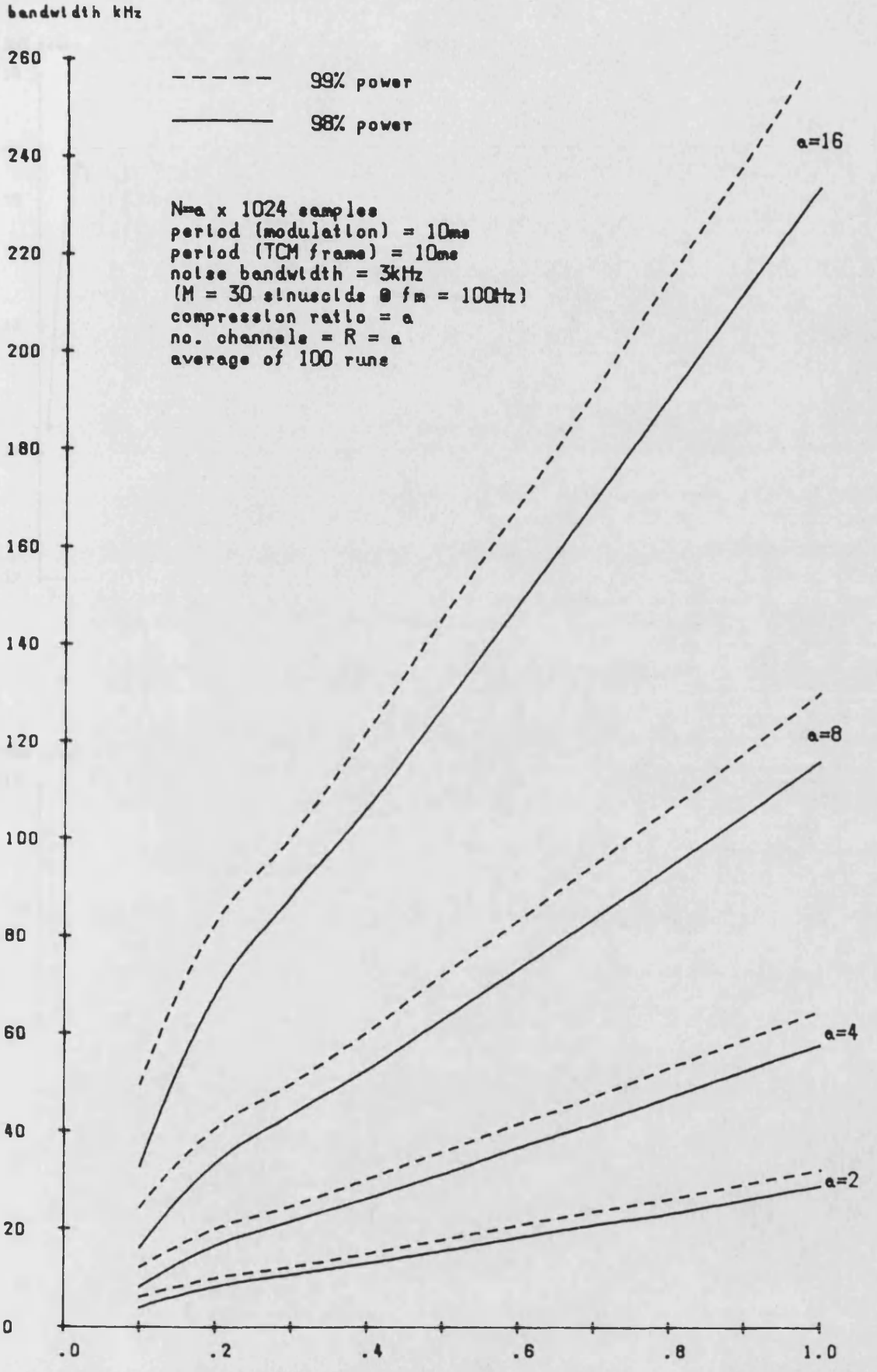

Fig.8.6 98/99% spectral power bandwidths of TCM-FM signal with all channels active with pseudo-random noise modulation.

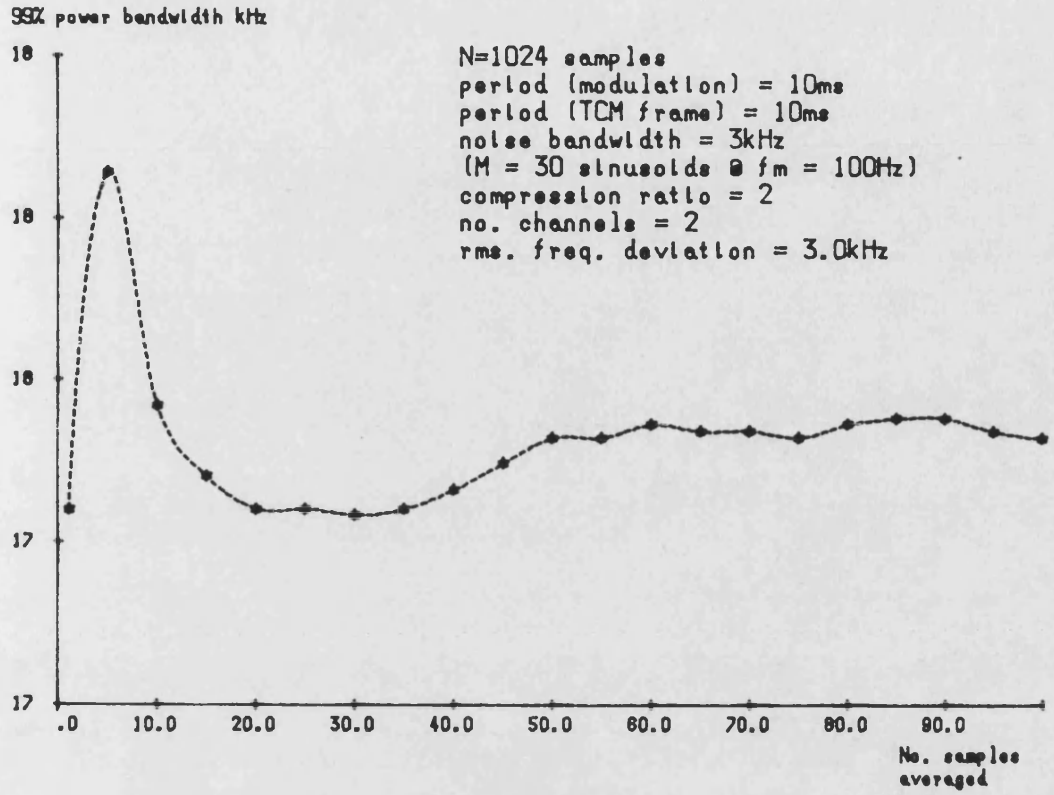

Fig. 8.7(a) Convergence of Monte carlo results for 99% spectral power bandwidth of TCM-FM signal with pseudo-random noise modulation.

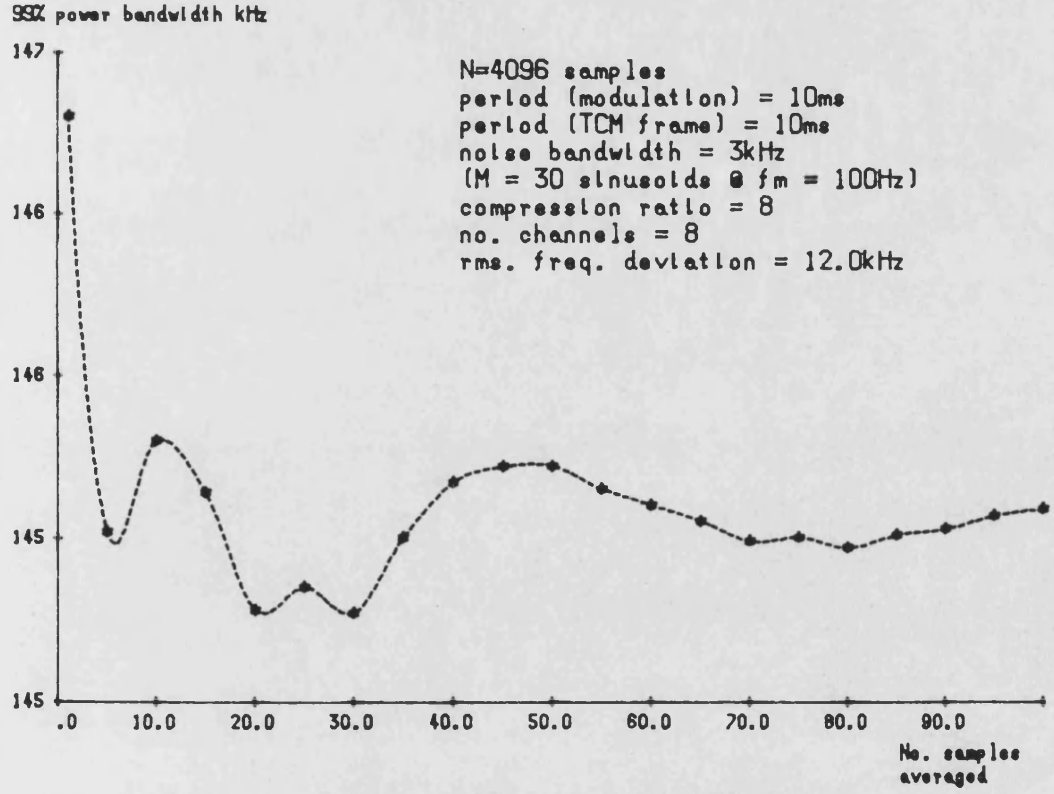

Fig. 8.7(b) Convergence of Monte carlo results for 99% spectral power bandwidth of TCM-FM signal with pseudo-random noise modulation.

In order to confirm the convergence of the Monte Carlo technique for TCM-FM, the 99% power bandwidth from above was plotted against number of runs averaged. The results for compression ratios of two (rms deviation =3kHz) and eight (rms deviation =12kHz) are illustrated in figs.8.7(a) and (b) respectively. In both examples, the convergence after 100 runs is excellent, whilst there is only a minor decrease in accuracy from using 50-60 runs. In view of this, to provide some economies in the amount of computer time needed, all subsequent analysis is based on 60 run averages rather than the previous 100.

8.5 FILTERING, DEMODULATION AND TIME-EXPANSION

A subroutine, FILDEM3.for, to permit the analysis of TCM-FM with RF filtering, and perform the necessary frequency demodulation, time-expansion and signal-to-distortion measurements is listed in Appendix I. Pseudo-random noise with a slot at the measurement frequency is used as the test signal. The Monte Carlo process used closely follows that for non-multiplexed FM described in chapter 7. The time-expansion of the demodulated signal is readily accomplished using the sampled signal approach providing the compression ratio is 2,4,8 etc. such that the number of samples representing a single channel is itself a power of 2. This allows the FFT subroutine to be used for the derivation of the final signal spectrum. The RF filter chosen has the same pseudo-rectangular response as for ordinary FM, but with the bandwidth suitably increased. It was not possible to perform tests using crystal filter responses, due to the lack of devices of sufficiently wide bandwidth for even 2-channel systems unless unreasonably low frequency deviations are employed.

The signal-to-distortion ratios (S/D) at several slot frequencies for a 2-channel system with a 10ms frame period using a $\pm$15kHz filter bandwidth are shown in fig.8.8. The same characteristics as for non-multiplexed FM (equivalent filter BW=$\pm$7.5kHz) in fig.7.8 are apparent

except that the region of constant S/D for each slot frequency is extended. The maximum values of S/D attained for each slot are significantly reduced, indicating that the performance is degraded by a process other than in-channel intermodulation. Reference to fig.8.2(a) and 8.6 at a normalised deviation of 0.5 shows that the filter bandwidth of ±15kHz is sufficient to pass most of the sidebands in the main lobe but not others. Hence, it may be concluded that the increase in distortion over a non-multiplexed FM system is due to inter-channel intermodulation caused by time spreading of the signal into adjacent time slots. Due to the poor asymptotic spectral roll-off, this effect would be expected to remain significant unless a very wide filter bandwidth was used.

The effect of varying the filter bandwidth at baseband frequencies of 1kHz and 3kHz (slots 10 and 30) with the same TCM system parameters is shown in figs.8.9 and 8.10 respectively. Comparison with figs.7.9 and 7.10 shows that the S/D at higher deviations (distortion primarily due to in-channel intermodulation) is largely the same as for ordinary FM with an equivalent filter bandwidth. However, at other deviations, the distortion is appreciably worse, even with a ±35kHz bandwidth. The contours of constant signal-to-distortion for slots 10 and 30 are drawn in figs.8.11 and 8.12. The same general trend of

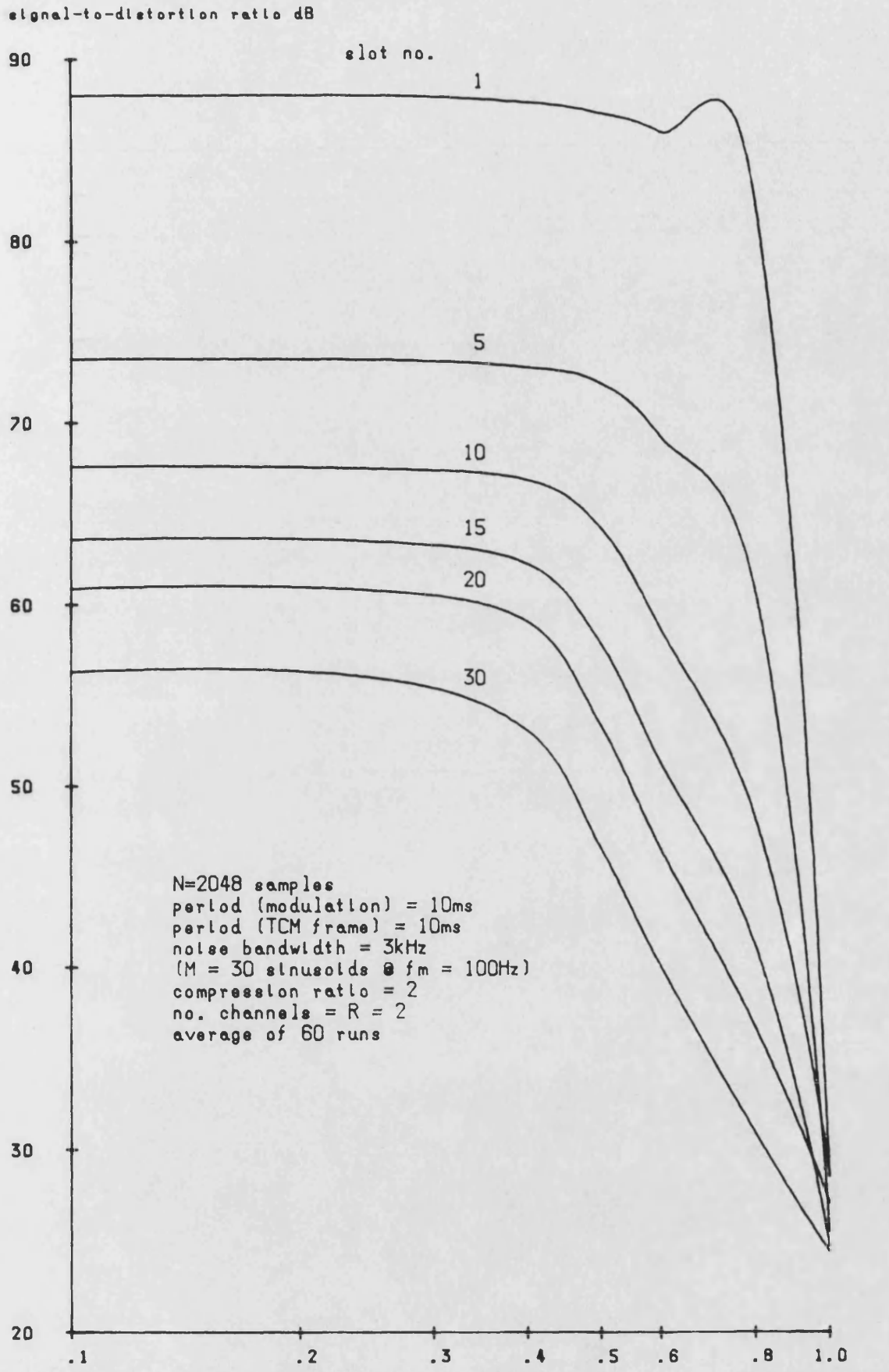

Fig.8.8 Computed intermodulation distortion with 2-channel TCM-FM signal and pseudo-rectangular filter of +/-15kHz -6dB bandwidth

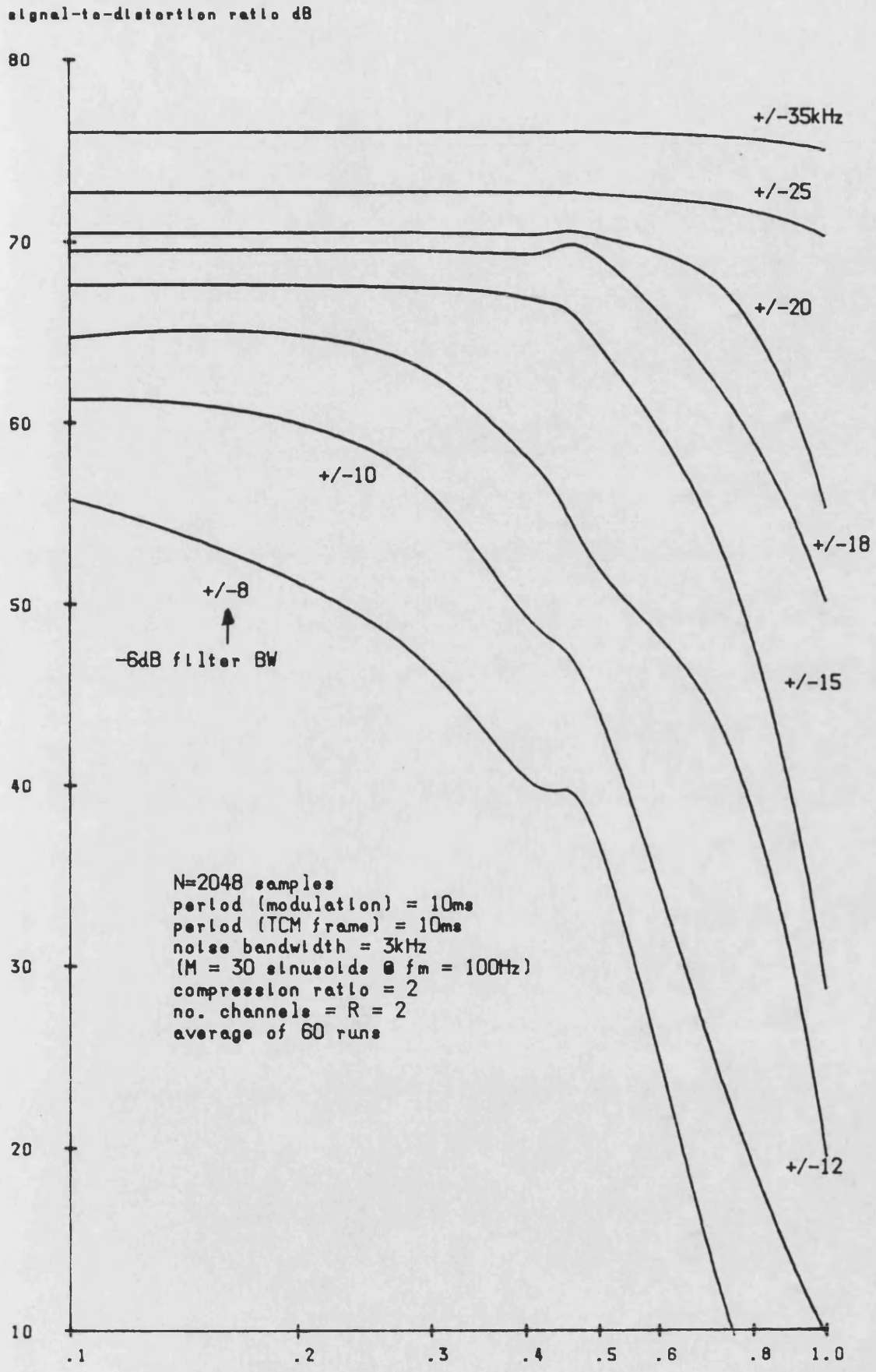

Fig.8.9 Computed intermodulation distortion at 1kHz in 2-channel TCM-FM system with pseudo-rectangular filter.

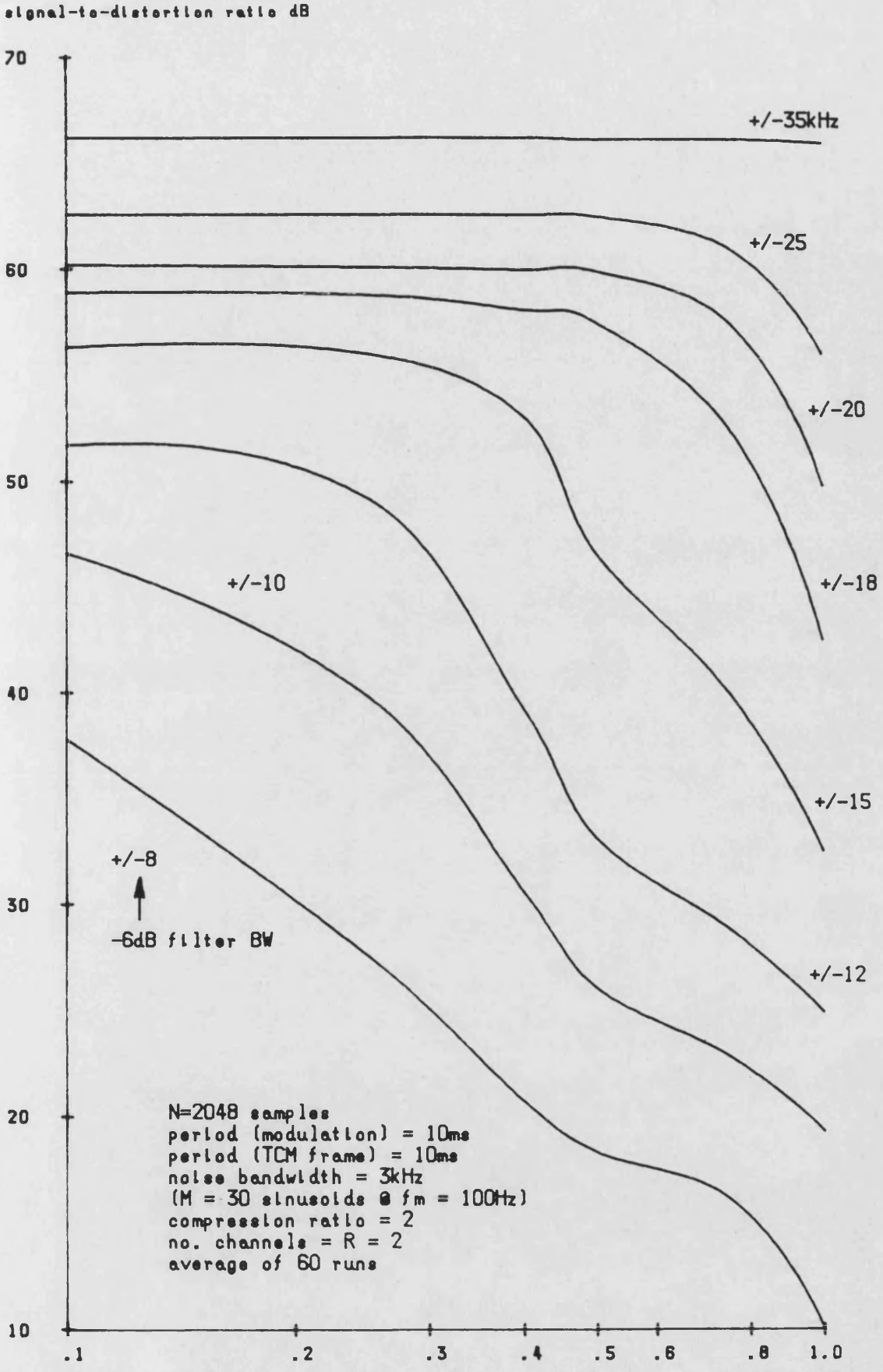

Fig.8.10 Computed intermodulation distortion at 3kHz in 2-channel TCM-FM system with pseudo-rectangular filter.

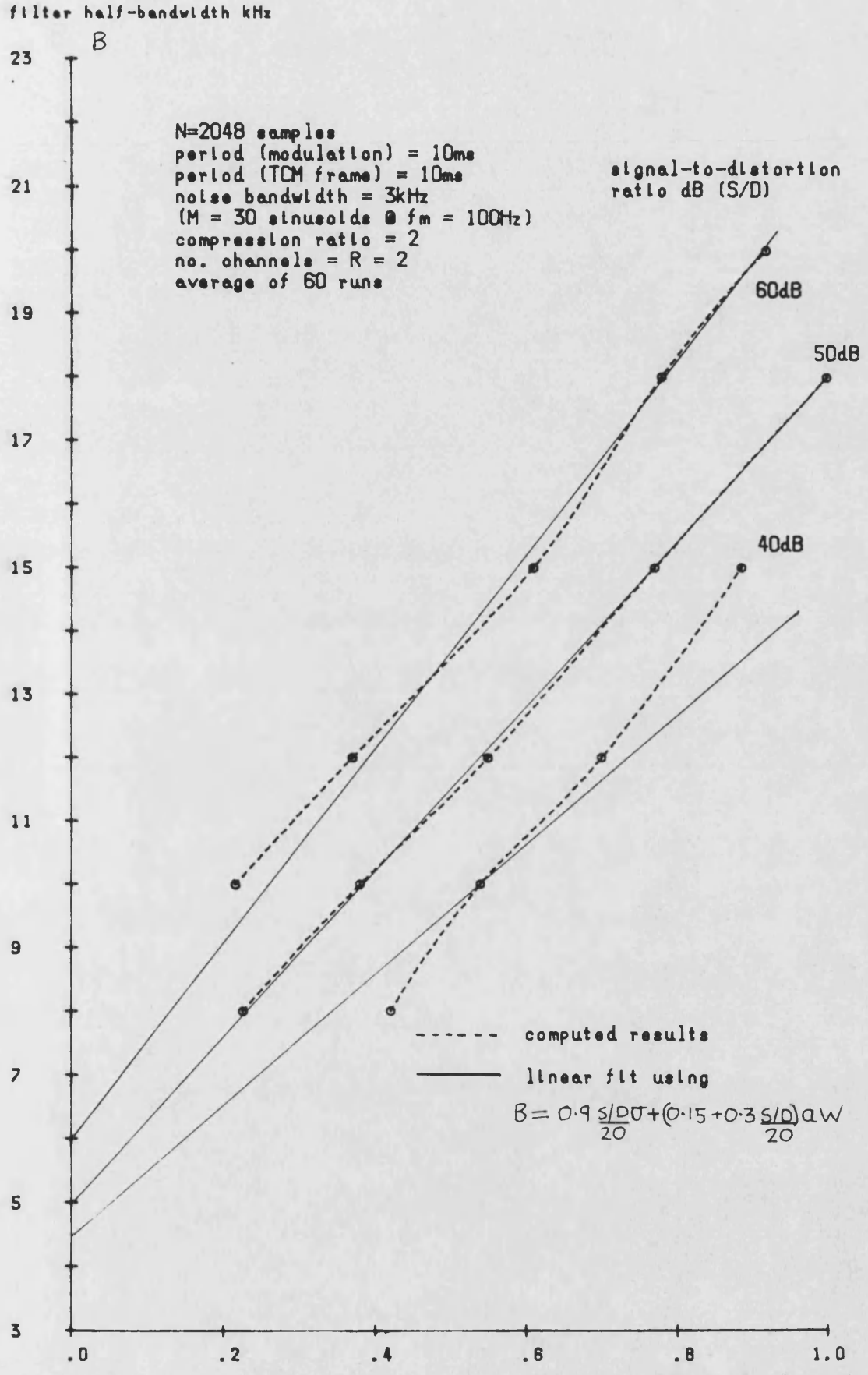

Fig. 8.11 Necessary filter bandwidth in 2-channel TCM-FM system for given signal-to- distortion ratio v. normalised freq. dev. Baseband frequency = 1kHz.

rms. freq. dev. / a x noise BW

$\frac{\sigma}{aW}$

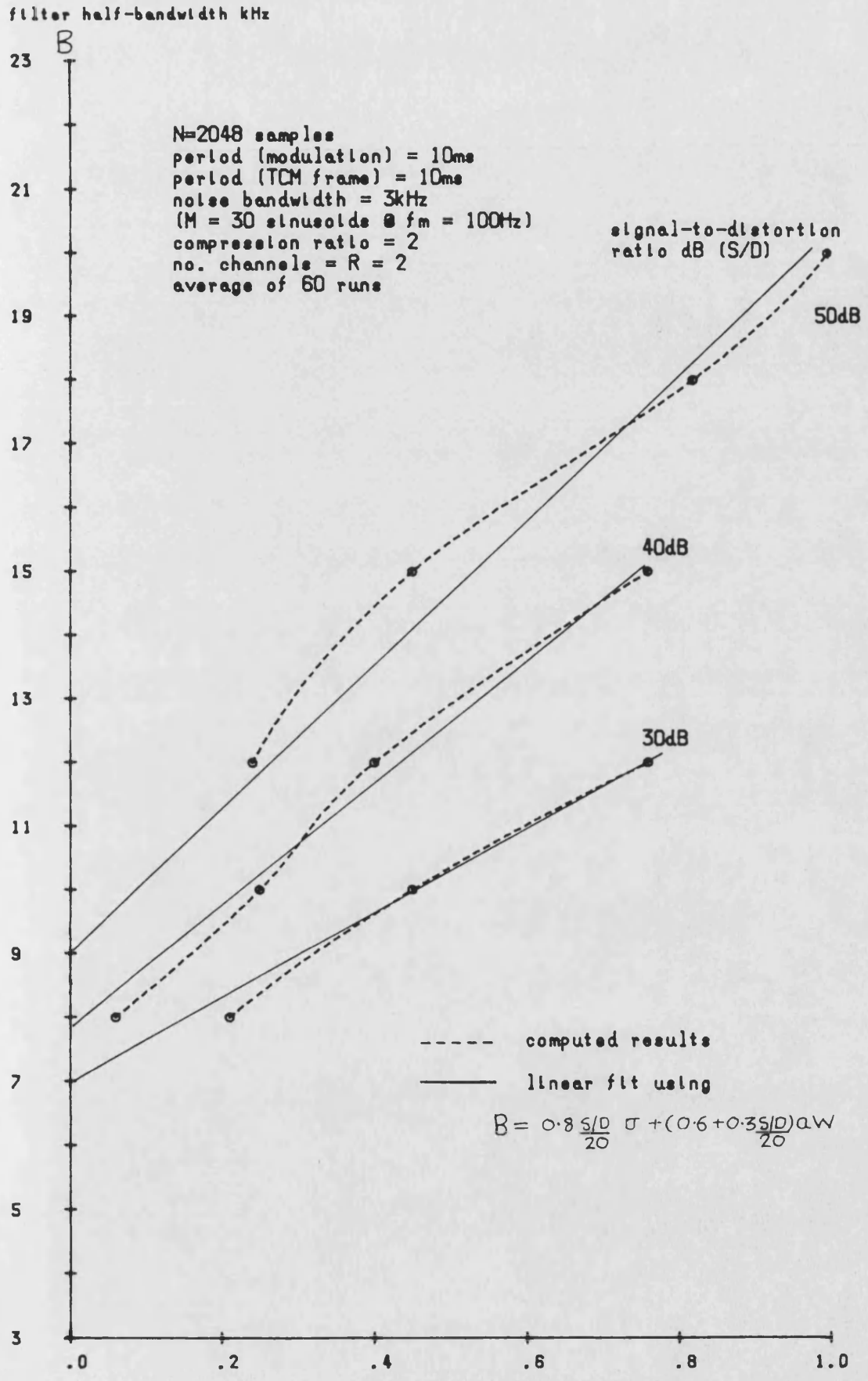

Fig.8.12 Necessary filter bandwidth in 2-channel TCM-FM system for given signal-to-distortion ratio v. normalised freq. dev. Baseband frequency = 3kHz.

increasing slope with higher S/D as in figs.7.11 and 7.12 is observed, but the departure from a linear fit is more pronounced, especially at lower signal-to-distortion levels. The range of contours is also reduced, since higher S/D ratios are impossible to achieve with filter bandwidths less than ±35kHz. An approximate linear fit for slots 10 is given by

$$B = 0.9\left[\frac{S/D}{20}\right]\sigma + \left[0.15 + 0.3\left[\frac{S/D}{20}\right]\right]aW \qquad (8.19)$$

and for slot 30

$$B = 0.8\left[\frac{S/D}{20}\right]\sigma + \left[0.6 + 0.3\left[\frac{S/D}{20}\right]\right]aW \qquad (8.20)$$

where σ is the rms frequency deviation, a is the compression ratio, W is the noise BW and $\frac{S/D}{20}$ is log10(true signal-to-noise ratio).

The equivalent results for a 4-channel TCM system, again with a 10ms frame, are shown in figs.8.13 to 8.17. A marginal increase of around 2dB in the signal-to-distortion ratio at each slot frequency is observed in fig.8.13 compared to the equivalent 2-channel results (fig.8.8). A similar increase is also found in the curves for other filter bandwidths. Generally, the results for the 4-channel system in figs.8.14 and 8.15 resemble those for non-multiplexed FM more than those for the 2-channel

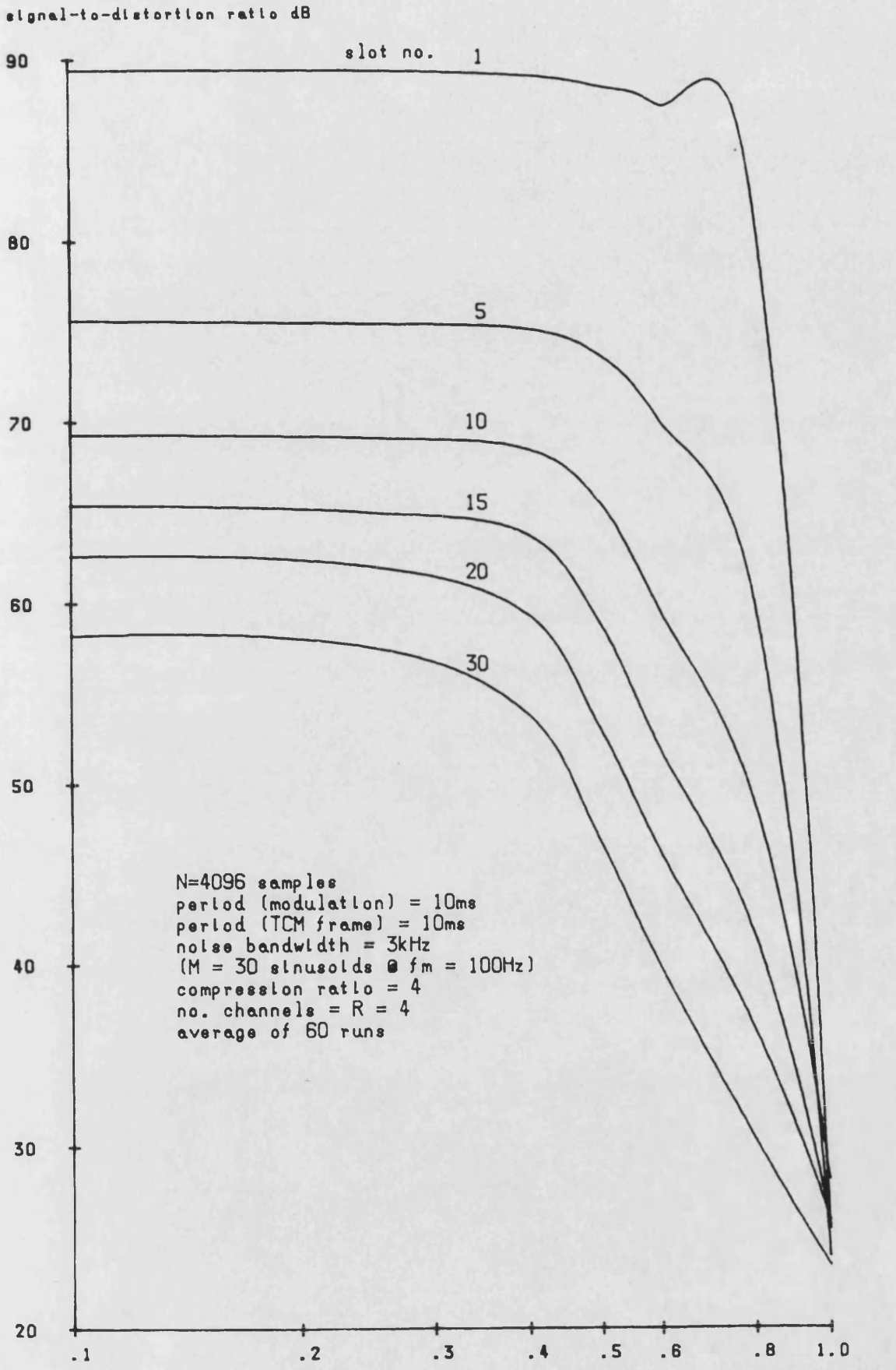

Fig.8.13 Computed intermodulation distortion with 4-channel TCM-FM signal and pseudo-rectangular filter of +/-30kHz -6dB bandwidth

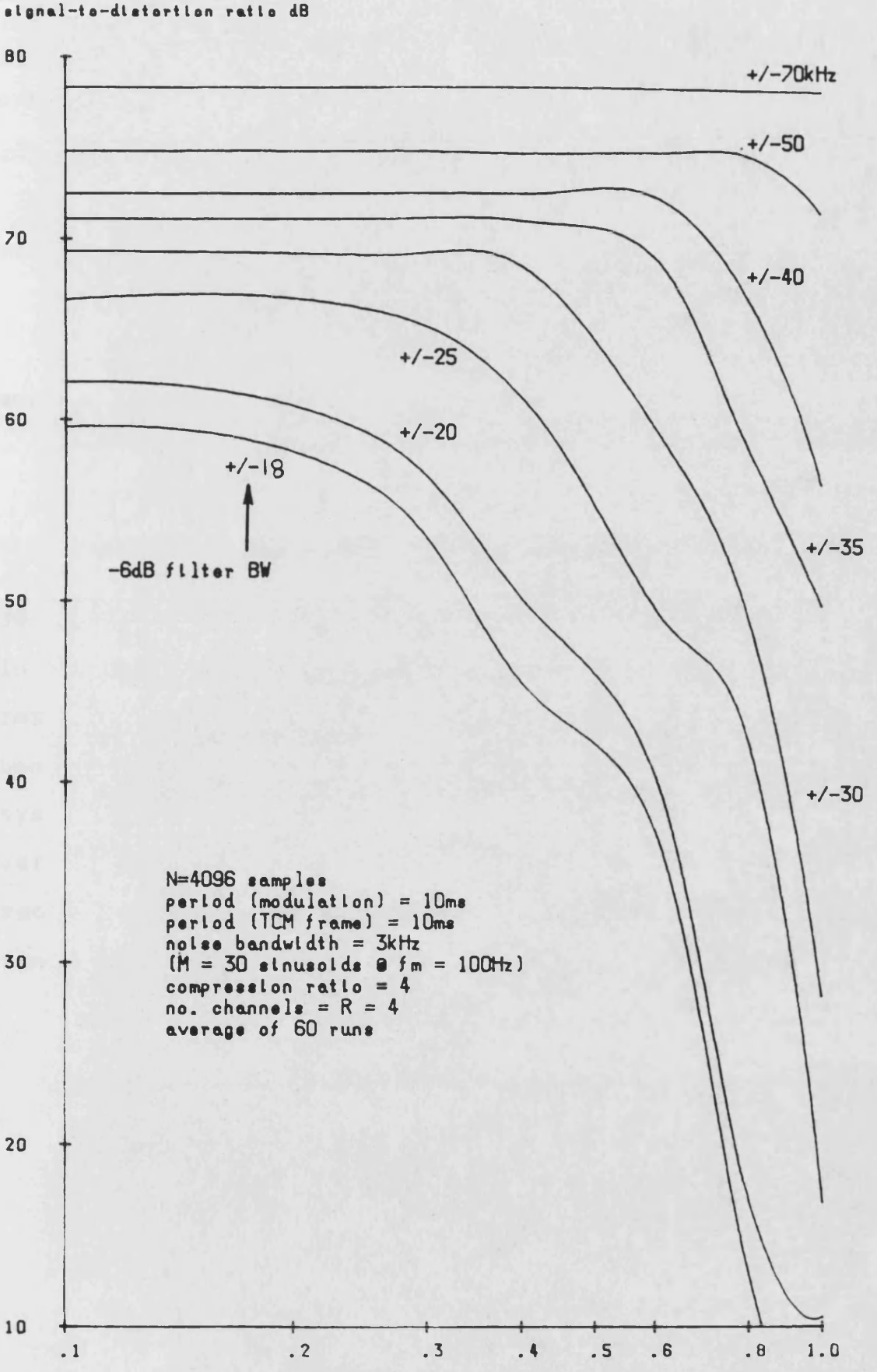

Fig.8.14 Computed intermodulation distortion at 1kHz in 4-channel TCM-FM system with pseudo-rectangular filter.

system. They are also more well-behaved, with fewer irregularities. This is confirmed by the significantly better fit of the contours of constant S/D in figs.8.16 and 8.17 to the following linear approximations. For slot 10

$$B = 0.8\left[\frac{S/D}{20}\right]\sigma + 0.3\left[\frac{S/D}{20}\right]aW \qquad (8.21)$$

and for slot 30

$$B = 1.3\left[\frac{S/D}{20}\right]\sigma + \left[0.3 + 0.3\left[\frac{S/D}{20}\right]\right]aW \qquad (8.22)$$

The variation in signal-to-distortion for slots 1 and 30 with frame period and compression ratio is illustrated in fig.8.18. All calculations were made with a normalised rms frequency deviation of 0.5, with equivalent filter bandwidths of $\pm$10, 20 and 40kHz for the 2, 4 and 8-channel systems respectively. It can be seen that there is little variance in the results, with the total deviation being some 8dB for slot 1 and only 1.5dB for slot 30 across the range of parameters.

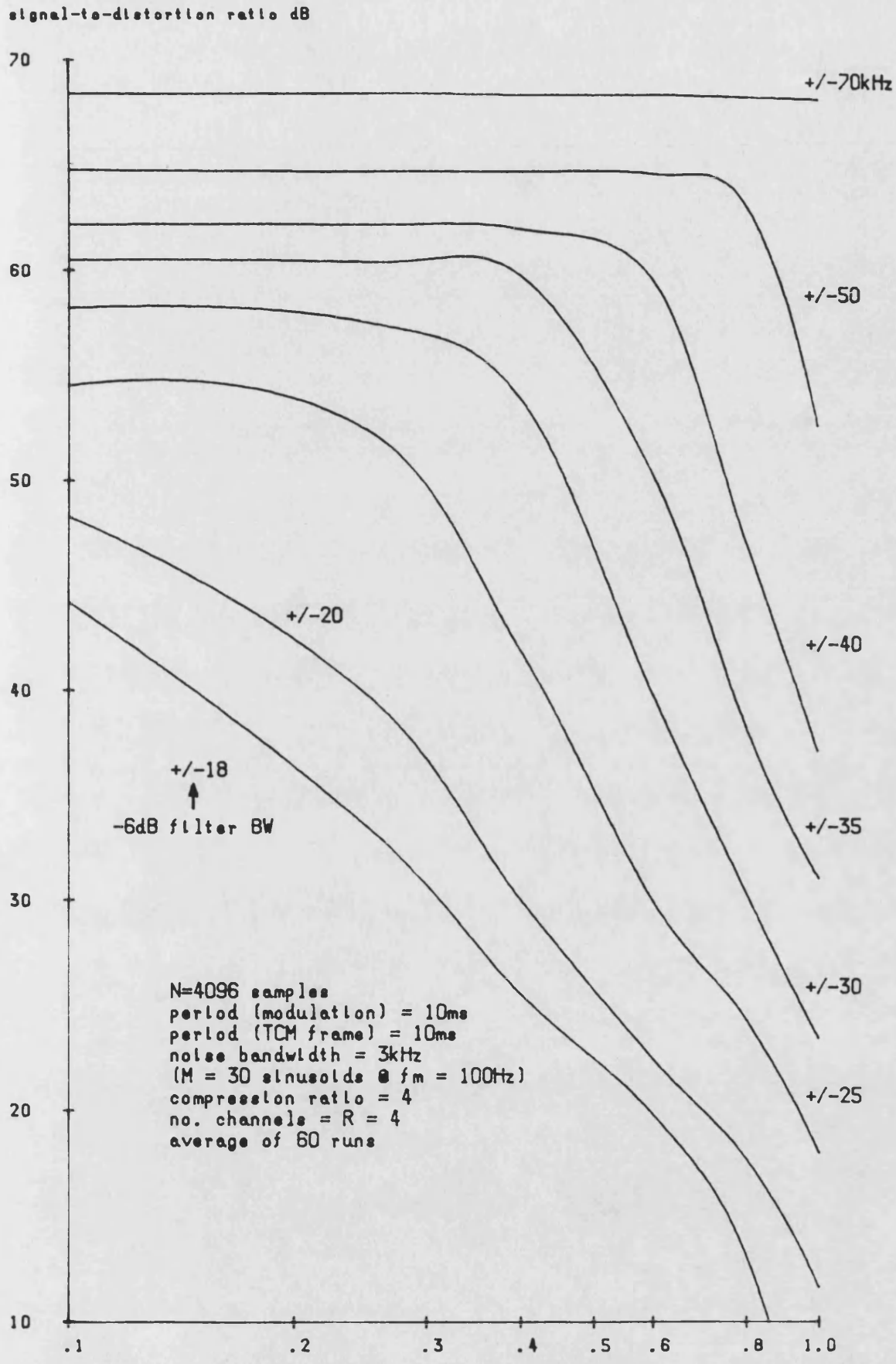

Fig.8.15 Computed intermodulation distortion at 3kHz in 4-channel TCM-FM system with pseudo-rectangular filter.

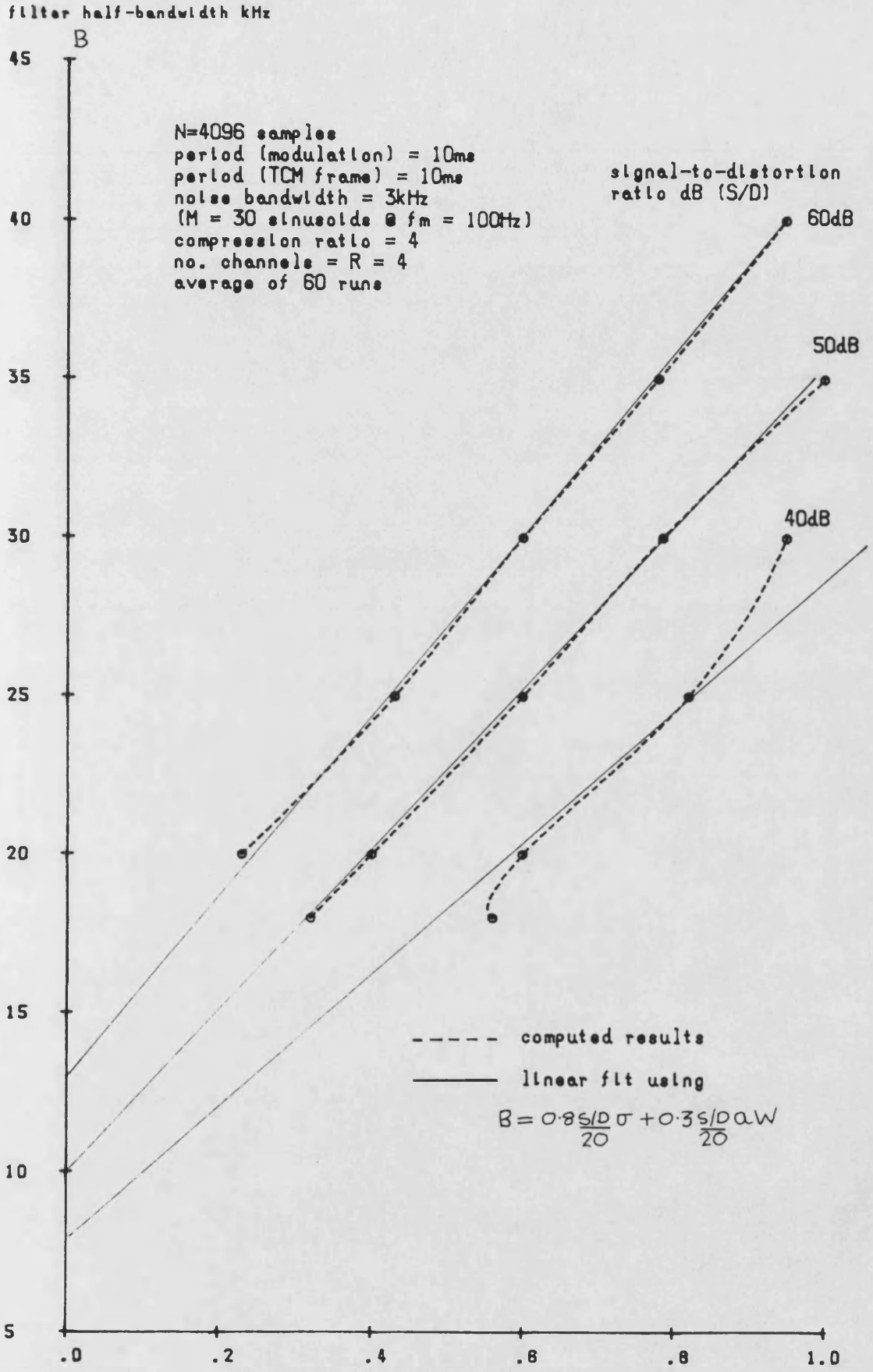

Fig.8.16 Necessary filter bandwidth in 4-channel TCM-FM system for given signal-to- distortion ratio v. normalised freq. dev. Baseband frequency = 1kHz.

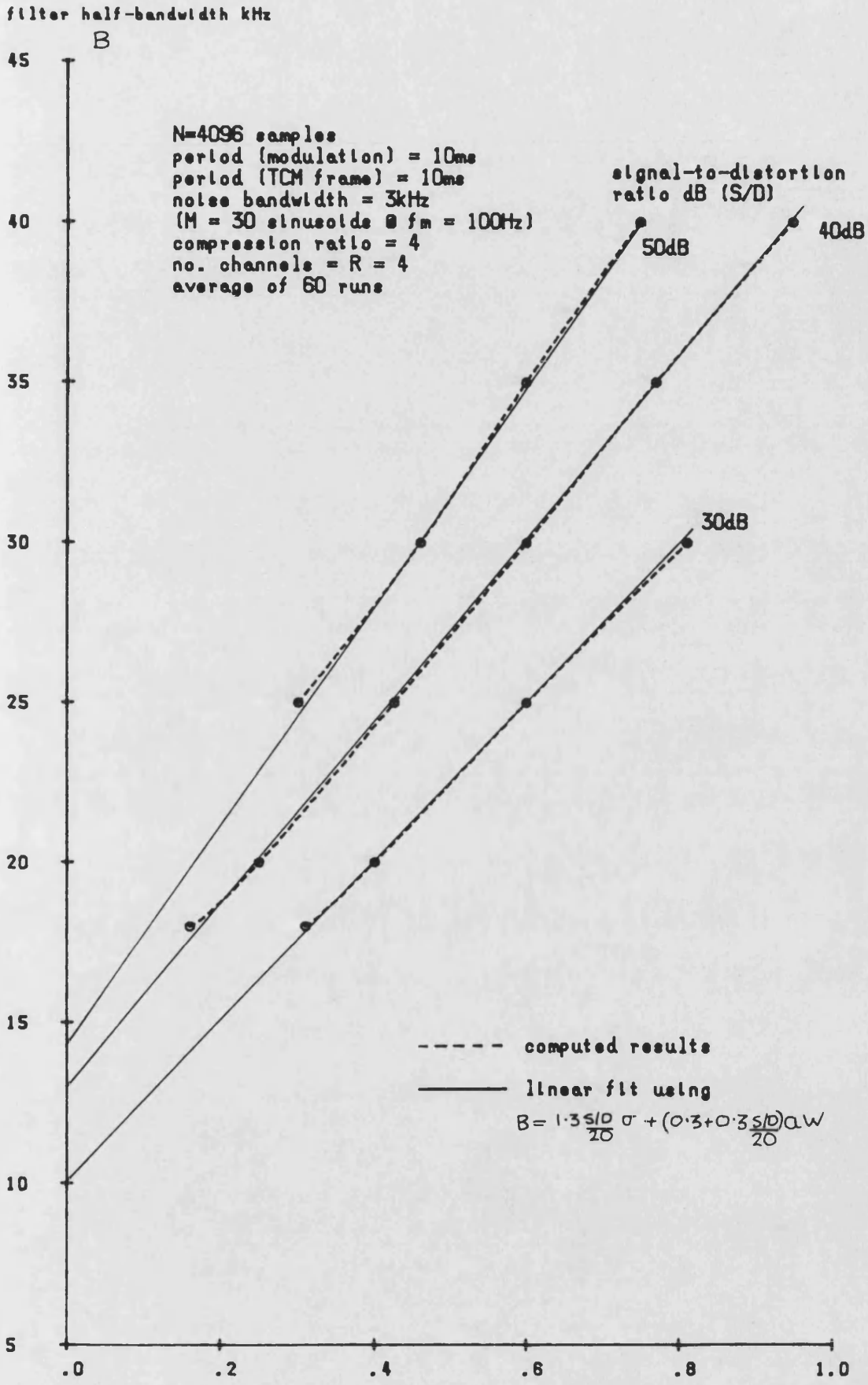

Fig.8.17 Necessary filter bandwidth in 4-channel TCM-FM system for given signal-to-distortion ratio v. normalised freq. dev. Baseband frequency = 3kHz.

$\frac{\text{rms. freq. dev.}}{\text{a x noise BW}}$

$\frac{\sigma}{aW}$

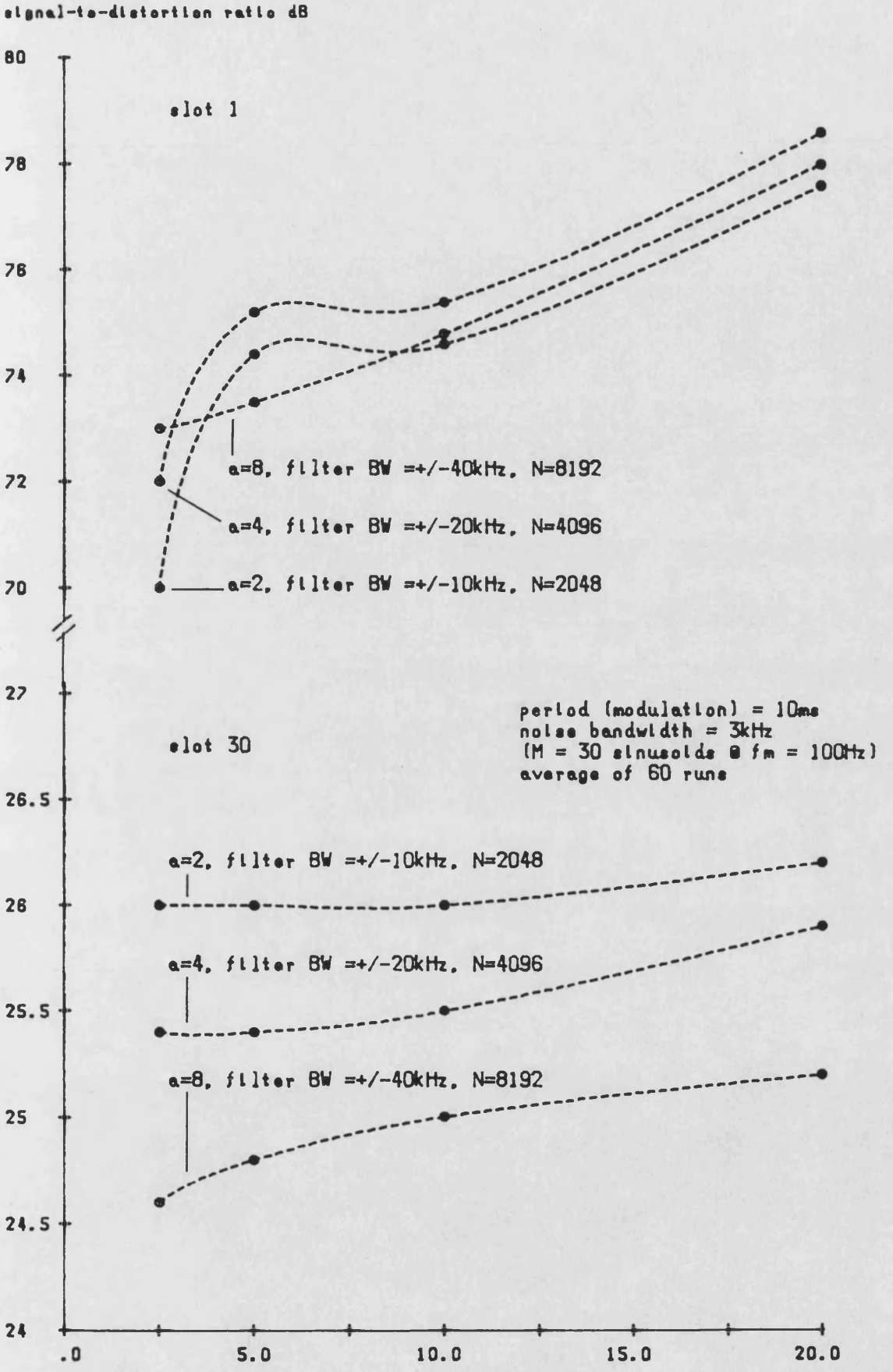

Fig.8.18 Variation of intermodulation distortion in TCM-FM system with compression ratio and frame period.

8.6 CO-CHANNEL INTERFERENCE

The subroutine COCHAN2.for, listed in Appendix J, evaluates the intermodulation distortion due to a single co-channel TCM-FM signal. Both wanted and un-wanted signals are modulated with independent pseudo-random noise signals, with a slot at the measurement frequency in the former. The results are derived over a number of independent runs using a Monte Carlo process. Fig.8.19 shows the signal-to-distortion ratio in a 2-channel TCM-FM system with a frame period of 10ms. The interfering signal level is -60dB relative to the wanted signal with no carrier offset. The increasing resistance to interference with frequency deviation for all slot frequencies can be clearly seen. The results show considerable agreement with those for non-multiplexed FM (fig.7.19), with an overall general improvement in the S/D figures of a few dB.

The equivalent curves for a 4-channel system, again with a TCM frame period of 10ms are shown in fig.8.20. There is remarkable similarity between these results and those above, although there is now only a marginal improvement over the ordinary FM system. Hence, it may be concluded that the co-channel performance depends principally on the frequency deviation and upon the measurement frequency, and that there is little difference between TCM-FM and non-multiplexed FM. This was confirmed by

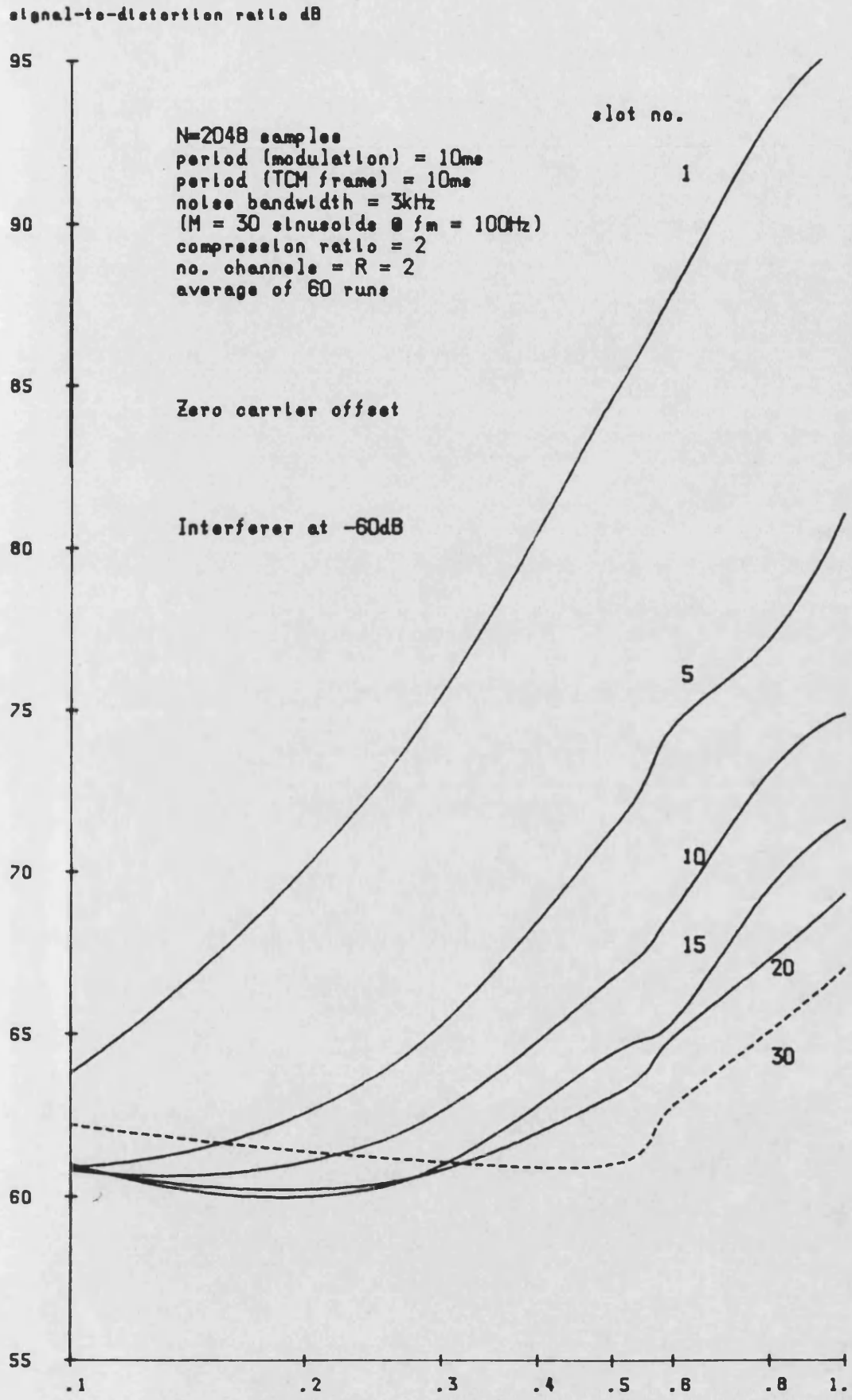

Fig.8.19 Computed intermodulation distortion in 2-channel TCM-FM system with a single co-channel interferer. Both signals modulated with pseudo-random noise.

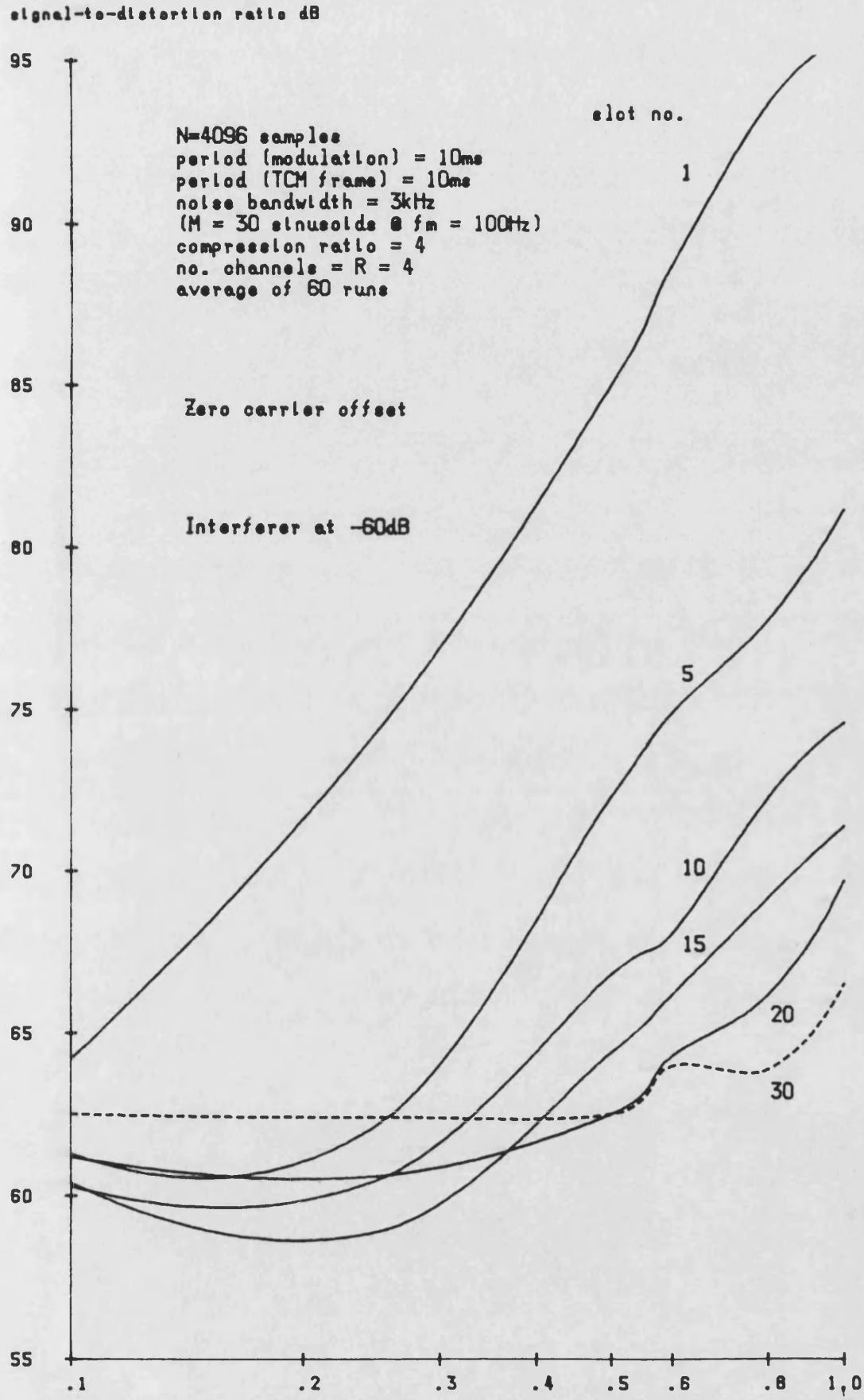

Fig.8.20 Computed intermodulation distortion in 4-channel TDM-FM system with a single co-channel interferer. Both signals modulated with pseudo-random noise.

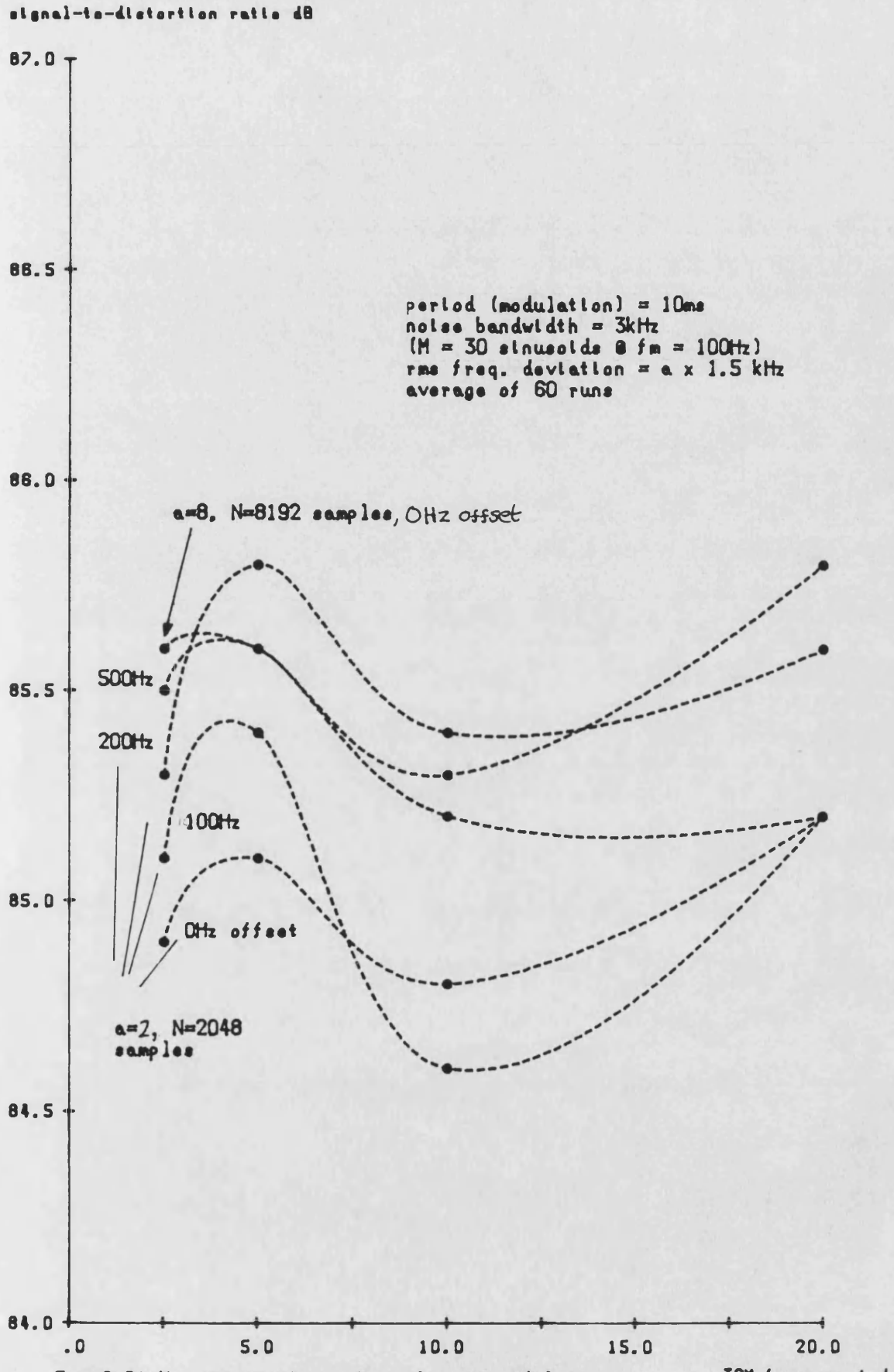

Fig.8.21 Variation of co-channel intermodulation distortion in TCM-FM system with compression ratio, frame period and carrier offset.

further measurements at other compression ratios, frame periods and co-channel offsets shown in fig.8.21. There is excellent agreement between these results and those in figs.8.19 and 8.20, with the greatest deviation being of the order of 1.5dB for slot 1.

8.7 CONCLUSIONS

The application of time-compression multiplexing to angle modulation has been considered. The non-linearity of the process and the complexity of the TCM spectrum allow few significant characteristics of TCM-FM to be obtained from theoretical analysis. However, the suitability of the discrete Fourier transform with both sinusoidal and pseudo-random signals has been confirmed.

The spectra of TCM-FM signals with pseudo-random modulation have a characteristic main lobe which may be closely likened to that of non-multiplexed FM with suitable frequency scaling. The 98/99% spectral power bandwidths of TCM-FM were found to very nearly equal to those for equivalent ordinary FM, when normalised by the compression ratio. However, the asymptotic spectral roll-off is poor due to the discontinuities at segment boundaries caused by simple rectangular windowing. This latter effect was found to worsen slightly as the frame period was decreased.

The poor spectral roll-off causes inter-channel crosstalk when the TCM-FM signal is bandlimited, even when the filter bandwidth is several times greater than the width of the main lobe. This is shown to be distinct from in-channel intermodulation which occurs, as with non-

multiplexed FM, when sidebands inside the main lobe are attenuated. Hence, the signal-to-distortion performance of TCM-FM with equivalent filtering is significantly worse than that of simple FM. Moreover, substantially the same results were achieved as both the compression ratio and frame period were varied. However, it was possible to derive empirical formulas relating the necessary bandwidth for a required signal-to-distortion ratio for both 2- and 4-channel TCM-FM systems. In this respect, the agreement with the computed results was best for the latter system. Overall, the spectral efficiency of the TCM-FM system is reduced from that of non-multiplexed FM due to the poor spectral roll-off.

The co-channel performance of TCM-FM was found to be substantially similar to that of simple FM, with an overall improvement in the signal-to-distortion figures for both 2- and 4-channel systems of 2-3dB. Furthermore, the performance was maintained over a range of TCM frame periods, compression ratios and interferer carrier offset. Hence, the TCM-FM system retains the important co-channel advantages of existing FM systems; an important requirement for cellular applications.

CHAPTER NINE

ANGLE MODULATION WITH WINDOWED TIME-COMPRESSION MULTIPLEXED SIGNALS

9.1 INTRODUCTION

The TCM systems considered in previous chapters were based upon straightforward time-compression and interleaving of signal segments to form the composite waveform, producing inevitable discontinuities at the segment edges. Hence, although the majority of spectral power in a TCM-FM signal is contained within a reasonable bandwidth, the asymptotic roll-off rate is poor, leading to reduced overall spectral efficiency.

This chapter investigates the use of time-domain windowing techniques to smooth the inter-segment transitions and so improve overall spectral efficiency of the TCM-FM system. It is shown qualitatively, that simple techniques operating on the instantaneous phase waveform of the TCM-FM signal can actually worsen the transition in the instantaneous frequency waveform, and thus are of little benefit. However, a class of straightforward functions are identified , which although not optimal, effectively remove all transitions when applied directly to the instantaneous frequency waveform.

Two windowed TCM-FM systems are considered; the first in which the weighting is applied to the simple TCM signal with equalisation at the receiver, and the second in which over-compression is employed such that the weighted segments are redundant and can be ignored at the receiver. The amplitude of the message signal at the transitions is effectively reduced to zero by the windowing, hence any perturbation of the received signal in these regions is emphasised in the former system by equalisation. Furthermore, other practical problems are shown to make this system impractical, hence subsequent emphasis is placed on the over-compressed system.

Spectra and intermodulation performance curves are presented for a variety of TCM system parameters and weighting functions. Little variation is observed between the functions investigated, with the well-known raised cosine having marginally the best performance. A substantial overall improvement in performance over a simple TCM-FM system is confirmed for the over-compressed windowed TCM-FM system, with moderate weighting intervals equal to about 5% of the TCM segment period. A worthwhile spectral improvement is also obtained with only 1% windowing intervals.

9.2 PRINCIPLES OF WINDOWED TCM

9.2.1 OVERVIEW

The original TCM expression (in periodic form) from eqn.5.54 is

$$y_{TCM_T}(t) = \sum_{r=1}^{B} \sum_{m_r=1}^{M_r} \sum_{k=0}^{K_T-1} A_{rm} \cdot \text{rect}\left[\frac{a(t - kT - (r-1)T/a)}{T}\right] \cdot \cos\left[2\pi a f_{rm}\left[t - k\left[\frac{a-1}{a}\right]T - \left[\frac{r-1}{a}\right]T + \theta_{rm}\right]\right] \quad (9.1)$$

where

$$K_T = \frac{1}{HCF\left[1, \sum_r \sum_m f_{rm}T\right]}$$

Each segment of the waveform is formed from the product of the appropriate signal waveform and a rectangular window of duration T/a. Hence there are generally step discontinuities in the composite signal amplitude at the segment edges as shown in fig.9.1(a). For TCM-FM, these are transformed into steps in the instantaneous carrier frequency, $f_i(t)$. This produces a poor spectral roll-off in the modulated signal spectrum which becomes more pronounced as the TCM frame period decreases, ie. as the effective frequency of the transitions increases (chapter 8). Hence, the spectral efficiency of the basic TCM-FM system is somewhat worse than an equivalent non-

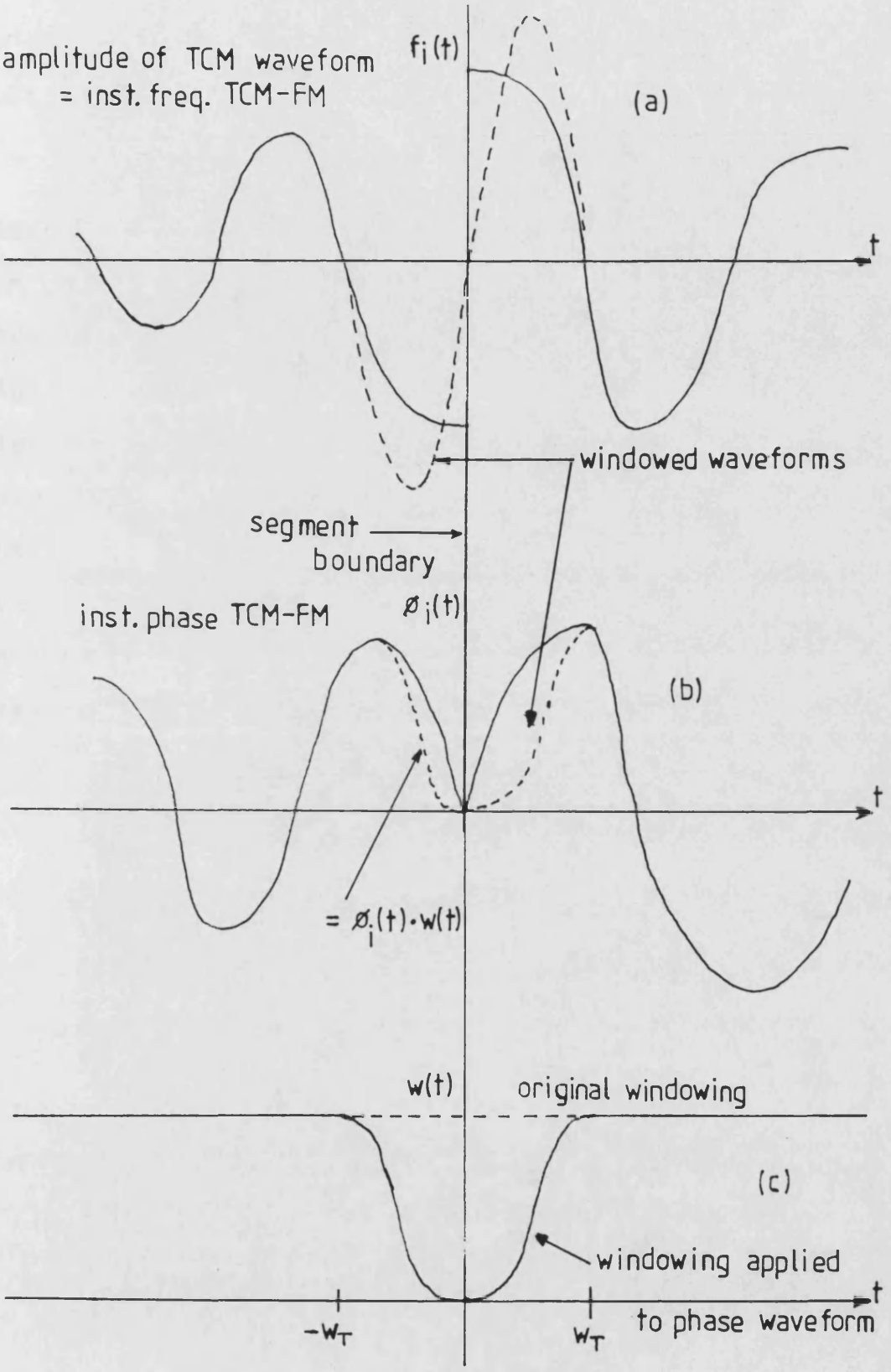

Fig.9.1 Instantaneous freq. of TCM-FM signal (a), instantaneous phase (b), windowing waveform (c) and its effect when applied to instantaneous phase waveform.

multiplexed system.

The spectral efficiency may be improved if the discontinuities in the instantaneous frequency waveform can be removed or at least made less abrupt. Fig.9.1(b) shows the corresponding phase, $\phi_i(t)$, of the basic TCM-FM signal in the vicinity of a segment boundary. It is feasible to remove the phase discontinuity by multiplying the waveform by, for example, an inverted raised-cosine pulse, w(t), of duration $-w_T$ to w_T as shown in fig.9.1(c). However, the instantaneous frequency waveform, although no longer containing a step, is in fact more transitory than previously. Hence this approach would not generally result in any significant improvement in spectral roll-off.

An alternative approach is to multiply the instantaneous frequency waveform by the weighting pulse as shown in fig.9.2(a), resulting in the phase waveform of fig.9.2(b). It can be seen that the transition is made appreciably smoother, with the best waveform obtained when the final level at the boundary is made equal to the average, av, of the extremes of the discontinuity rather than zero. This is accomplished by first subtracting the average transition value (av) from $f_i(t)$, multiplying by the windowing function and finally adding back the average value.

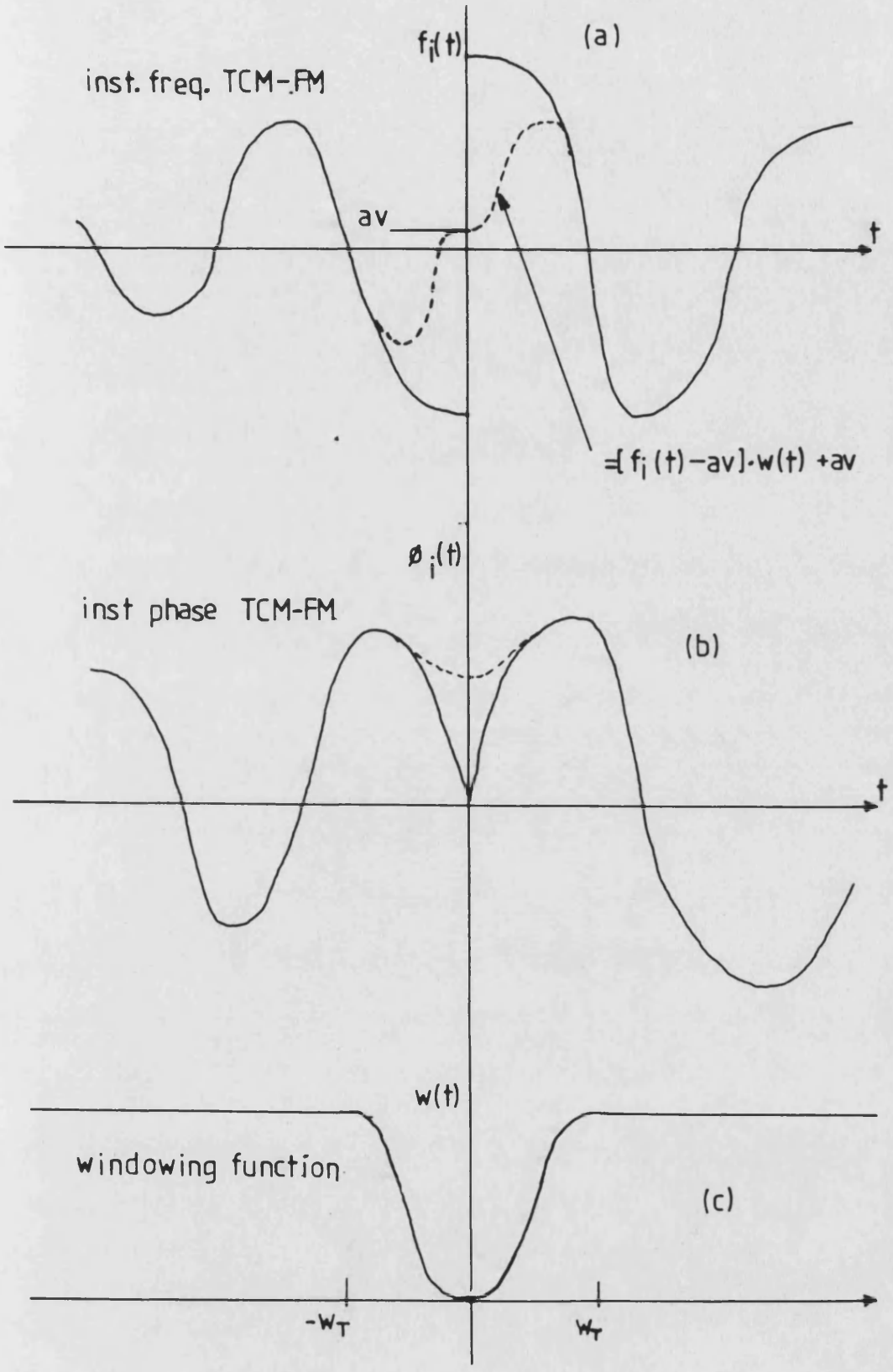

Fig.9.2 Instantaneous freq. of TCM-FM signal (a), instantaneous phase (b), windowing waveform (c) and its effect when applied to instantaneous frequency waveform.

In order to avoid distortion in the received signal when non-rectangular windowing is employed, either some form of receiver equalisation must be employed or redundant information must be transmitted during the weighted segments which can subsequently be neglected.

For the first approach, windowing is applied directly to the otherwise unaltered TCM signal. However, an exact inverse of the weighting function is required at the receiver and both the amplitude and dc offset of the recovered signal must be identical to the pre-processed signal if a distortionless output is to be achieved. In addition, since the effective amplitude of the message signal (ie. without any level shift) near to the segment boundaries is small (actually zero at the boundary), there is a high susceptibility to intermodulation distortion in this region. Thus, although the spectral characteristics will be improved, the effect of bandlimiting and/or co-channel interference may well be intolerable.

In the second system, the compression ratio of the TCM signal must be increased such that the information during a weighted interval is repeated (without weighting) in either the previous or following segment of the same channel as shown in fig.9.3. The windowing is then performed as in the basic system. If the weighting interval is w_T and the segment length T/R (R = no. multiplexed

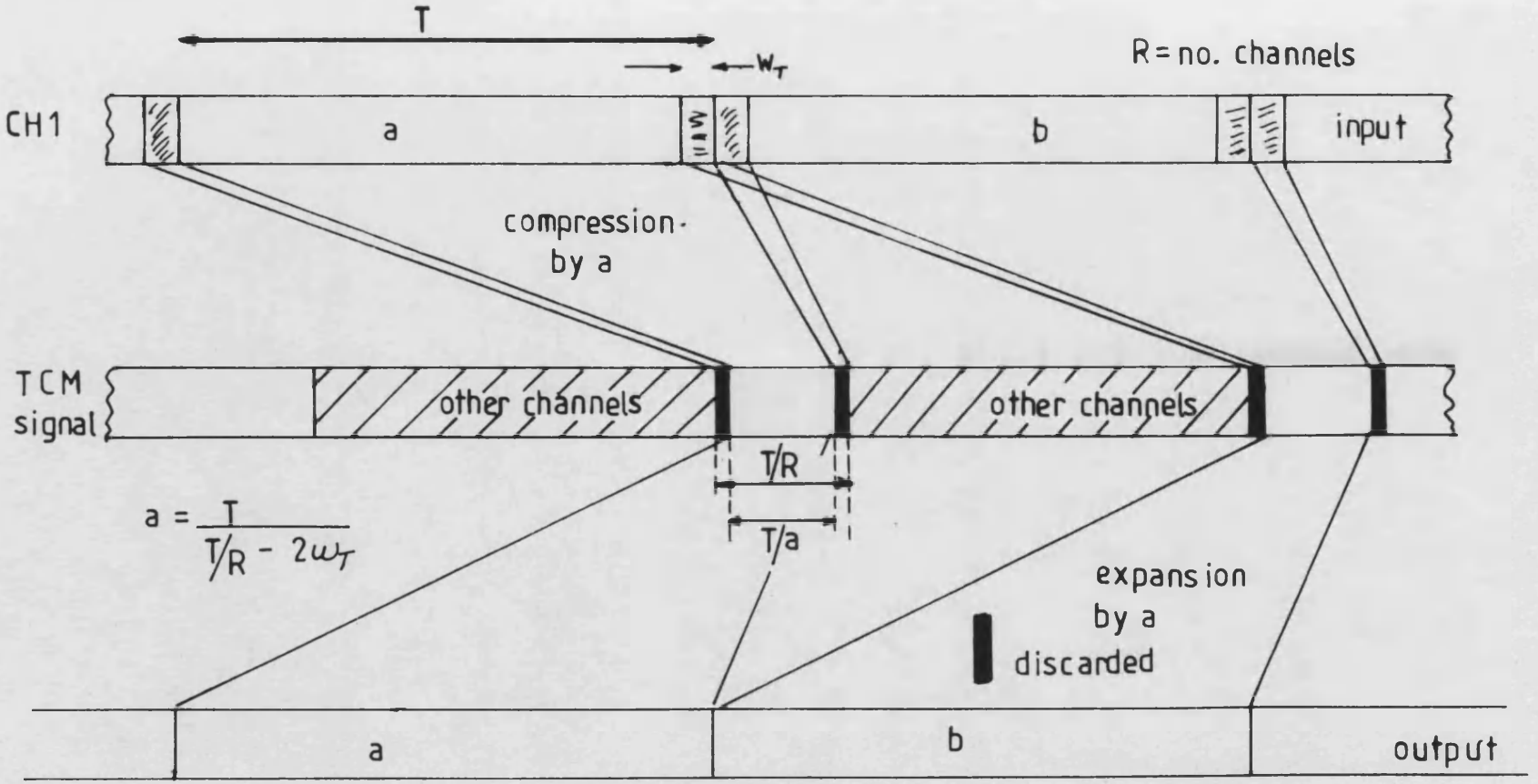

Fig.9.3 Illustrating principle of over-compression in TCM system to create redundant information at ends of segment.

channels) then the minimum compression ratio to satisfy this requirement is

$$a \geq \frac{RT}{T - 2w_T R} \qquad (9.2)$$

ie. the compression ratio is now generally a non-integer.

Although, a slightly wider overall bandwidth results, no equalisation is required thus simplifying receiver circuitry, since the removal of the redundant segments is readily accomplished using a digital companding technique (chapter 4.1.2.3). However, there is an important additional feature in that the sections of signal likely to contain the highest levels of time-spread interference (crosstalk) are neglected. Hence the signal degradation with reasonable bandlimiting is likely to be minimal.

9.2.2 REQUIREMENTS OF THE WINDOWING FUNCTION

Numerous windowing functions have been investigated for the related application of reducing the sidelobes present when short-term signals are analysed using discrete Fourier transform techniques [1]. The type and characteristics of the optimum function in each case is determined by the nature of the signal under analysis. It is very difficult, however, to find an optimum function which will produce the smoothest inter-segment transition (and hence best asymptotic spectral roll-off) for any ran-

dom TCM-FM waveform. However, a class of simple weighting functions may be defined which eliminate the boundary discontinuities and provide acceptable roll-off with a reasonable windowing interval. These are real, non-negative functions characterised by having first derivatives which are zero both at the segment boundaries ($t = kT+(r-1)T/a \pm T/2a$), and at the ends of the windowing intervals ($t = kT+(r-1)T/a \pm T/2a + w_T$) and ($t = kT+(r-1)T/a \pm T/2a - w_T$). A selection satisfying these requirements are defined in Table 9.1 and illustrated in fig.9.4 for the interval $kT + (r-1)T/a + T/2a - w_T < t \leq kT + (r-1)T/a + T/2a$.

The Hann and Blackman windows are special cases of a versatile 3-coefficient window (eqn.9.3) due to Geckinli and Yavuz [1] with $\lambda = 0$ and 0.04 respectively.

$$w(t) = \frac{1 - 4\lambda}{2} + 0.5\cos\left[\frac{\pi}{w_T}\left[t - kT - \left[\frac{r-1}{a}\right]T - \frac{T}{2a} + w_T\right]\right] + 2\lambda\cos\left[\frac{2\pi}{w_T}\left[t - kT - \left[\frac{r-1}{a}\right]T - \frac{T}{2a} + w_T\right]\right] \qquad (9.3)$$

Using this function, expressions will be derived in the following section enabling discrete Fourier transform analysis to be performed on the windowed TCM-FM signal.

Raised Cosine (Hann) $\frac{1}{2} + \frac{1}{2}\cos\left[\frac{\pi}{w_T}\left[t - kT - \left[\frac{r-1}{a}\right]T - \frac{T}{2a} + w_T\right]\right]$
Papoulis $\frac{1}{\pi}\sin\left[\frac{\pi}{w_T}\left[t - kT - \left[\frac{r-1}{a}\right]T - \frac{T}{2a} + w_T\right]\right]$ $+ \left[1 - 2(t - kT - (r-1)T/a - T/2a + w_T)\right]$ $\cos\left[\frac{\pi}{w_T}\left[t - kT - \left[\frac{r-1}{a}\right]T - \frac{T}{2a} + w_T\right]\right]$
Parzen $\left[1-24(t-kt-(r-1)T/a-T/2a+w_T)^2\right]\left[1-2(t-kT-(r-1)T/a+w_T)\right]$ for $t < kT - (r-1)T/a - T/2a+w_T/2$ $2\left[1 - 2(t - kT - (r-1)T/a - T/2a+w_T)\right]^3$ for $t \geq kT - (r-1)T/a - T/2a + w_T/2$
Blackman $0.42 + 0.5\cos\left[\frac{\pi}{w_T}\left[t - kT - \left[\frac{r-1}{a}\right]T - \frac{T}{2a} + w_T\right]\right]$ $+ 0.08\cos\left[\frac{2\pi}{w_T}\left[t - kT - \left[\frac{r-1}{a}\right]T - \frac{T}{2a} + w_T\right]\right]$

Table 9.1: Windowing functions for TCM-FM.

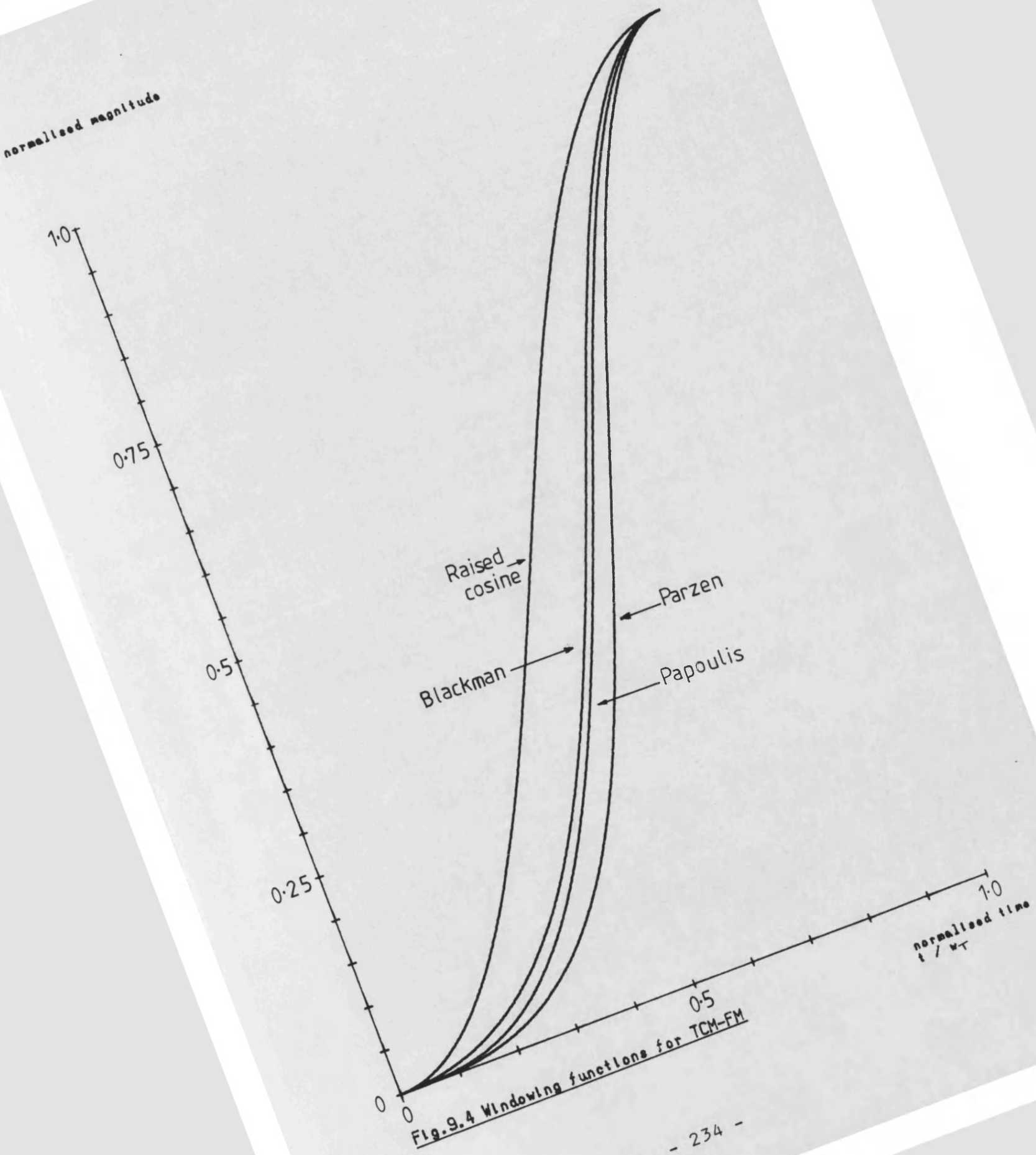

Fig.9.4 Windowing functions for TCM-FM

9.3 ANALYSIS

The analysis here will be concerned only with the over-compressed windowed TCM-FM system since the basic equalised system is unlikely to be practically viable. However, expressions for the latter system may be obtained by substitution with R=a.

Let windowing be applied to the over-compressed TCM signal (eqn.9.1) over an interval ,w_T, at the beginning and end of each segment using the 3-coefficient weighting function, w(t), defined in eqn.9.3. Hence the new compression ratio is

$$a = \frac{RT}{T - 2w_T R} \tag{9.4}$$

The expression of eqn.9.1 is still valid providing the appropriate substitution for a is made. Hence the windowed TCM signal in periodic form, $y_{WTCM_T}(t)$, is

$$y_{WTCM_T}(t) = \sum_{r=1}^{R} \sum_{m_r=1}^{M_r} \sum_{k=0}^{K_I-1} A_{rm} \cdot \text{rect}\left[\frac{R(t - kT - (r-1)T/R)}{T - 2Rw_T}\right]$$

$$\cdot \cos\left[2\pi a f_{rm}\left[t - k\left[\frac{r-1}{R}\right]T - \left[\frac{r-1}{R}\right]T\right] + \theta_{rm}\right]$$

$$+ \left[\left[A_{rm} \cos\left[2\pi a f_{rm}\left[t-k\left[\frac{r-1}{R}\right]T-\left[\frac{r-1}{R}\right]T\right]+\theta_{rm}\right]-C(kR+r)\right]\right.$$

$$
\cdot \left[\frac{1-4\lambda}{2} + \frac{1}{2} \cos\left[\frac{\pi}{w_T} \left[t - kT - \left[\frac{r-1}{R}\right] T + \frac{T}{2R} - w_T \right] \right] \right.
$$

$$
\left. + 2\lambda \cos\left[\frac{2\pi}{w_T} \left[t - kT - \left[\frac{r-1}{R}\right] T + \frac{T}{2R} - w_T \right] \right] \right] + C(kR+r) \Bigg]
$$

$$
\cdot \operatorname{rect}\left[\frac{t - kT - (r-1)T/R + T/2R - w_T/2}{w_T} \right]
$$

$$
+ \left[\left[A_{rm} \cos\left[2\pi a f_{rm} \left[t - k\left[\frac{r-1}{R}\right] T - \left[\frac{r-1}{R}\right] T \right] + \theta_{rm} \right] \right] \right.
$$

$$
\left. - C(kR+r+1, \bmod K_T.R) \right]
$$

$$
\cdot \left[\frac{1-4\lambda}{2} + \frac{1}{2} \cos\left[\frac{\pi}{w_T} \left[t - kT - \left[\frac{r-1}{R}\right] T - \frac{T}{2R} + w_T \right] \right] \right]
$$

$$
+ 2\lambda \cos\left[\frac{2\pi}{w_T} \left[t - kT - \left[\frac{r-1}{R}\right] T - \frac{T}{2R} + w_T \right] \right] \Bigg]
$$

$$
+ C(kR+r+1, \bmod K_T.R) \Bigg]
$$

$$
\cdot \operatorname{rect}\left[\frac{t - kT - (r-1)T/R - T/2R + w_T/2}{w_T} \right] \qquad (9.5)
$$

where C(kR+r) is the 'average' value of the composite TCM waveform at the discontinuity at the start of segment k,r (ie. at t=kT+(r-1)T/R-T/2R). Thus

$$C(kR+r) = \frac{1}{2}\left[\sum_{m_r=1}^{M_r} A_{rm}\cos\left[2\pi a f_{rm}\left[kT - T/2R\right] + \theta_{rm}\right] + \sum_{m_{r1}=1}^{M_{r1}} A_{r1\,m}\cos\left[2\pi a f_{r1m}\left[k1T + T/2R\right] + \theta_{r1\,m}\right]\right] \quad (9.6)$$

where k1 = k-1 if r=1 otherwise k1 = k

and r1 = (r-1) modulo R

Only frequency modulation will be considered, hence $f_i = k_d\, w_{TCM_T}(t)$ and $\phi_i = \int_{-\infty}^{t} 2\pi f_i\, d\tau$. The integration of eqn.9.3 to yield ϕ follows along the lines of chapter 8.2. Hence

$$\phi = k_d \sum_{r=1}^{R}\sum_{m_r=1}^{M_r}\sum_{k=0}^{K_I-1} \frac{A_{rm}}{af_{rm}} \sin\left[2\pi a f_{rm}\left[t-k\left[\frac{r-1}{R}\right]T-\left[\frac{r-1}{R}\right]T\right]+\theta_{rm}\right]$$

$$\cdot\ \mathrm{rect}\left[\frac{R(t - kT - (r-1)T/R)}{T - 2Rw_T}\right]$$

$$+\left[A_{rm}\left[\frac{1-4\lambda}{2af_{rm}}\sin\left[2\pi a f_{rm}\left[t - k\left[\frac{r-1}{R}\right]T - \left[\frac{r-1}{R}\right]T\right] + \theta_{rm}\right]\right.\right.$$

$$+\frac{1}{4\left[af_{rm} + \frac{1}{2w_T}\right]}\sin\left[2\pi a f_{rm}\left[t - k\left[\frac{r-1}{R}\right]T - \left[\frac{r-1}{R}\right]T\right]\right.$$

$$\left.\left.\left.+\frac{\pi}{w_T}\left[t-kT-\left[\frac{r-1}{R}\right]T + \frac{T}{2R} - w_T\right] + \theta_{rm}\right]\right]$$

$$+ \frac{1}{4\left[af_{rm} - \frac{1}{2w_T}\right]} \sin\left[2\pi af_{rm}\left[t - k\left[\frac{r-1}{R}\right]T - \left[\frac{r-1}{R}\right]T\right]\right.$$

$$\left. - \frac{\pi}{w_T}\left[t-kT-\left[\frac{r-1}{R}\right]T + \frac{T}{2R} - w_T\right] + \theta_{rm}\right]$$

$$+ \frac{\lambda}{\left[af_{rm} + \frac{1}{w_T}\right]} \sin\left[2\pi af_{rm}\left[t - k\left[\frac{r-1}{R}\right]T - \left[\frac{r-1}{R}\right]T\right]\right.$$

$$\left. + \frac{2\pi}{w_T}\left[t-kT-\left[\frac{r-1}{R}\right]T + \frac{T}{2R} - w_T\right] + \theta_{rm}\right]$$

$$+ \frac{\lambda}{\left[af_{rm} - \frac{1}{w_T}\right]} \sin\left[2\pi af_{rm}\left[t - k\left[\frac{r-1}{R}\right]T - \left[\frac{r-1}{R}\right]T\right]\right.$$

$$\left.\left. - \frac{2\pi}{w_T}\left[t-kT-\left[\frac{r-1}{R}\right]T + \frac{T}{2R} - w_T\right] + \theta_{rm}\right]\right]$$

$$+ C(kR+r)\left[(1+4\lambda)\pi t - w_T \sin\left[\frac{\pi}{w_T}\left[t-kT-\left[\frac{r-1}{R}\right]T+\frac{T}{2R}-w_T\right]\right]\right.$$

$$\left.\left. - 2\lambda w_T \sin\left[\frac{2\pi}{w_T}\left[t - kT - \left[\frac{r-1}{R}\right]T + \frac{T}{2R} - w_T\right]\right]\right]\right]$$

$$\cdot \operatorname{rect}\left[\frac{t - kT - (r-1)T/R + T/2R - w_T/2}{w_T}\right]$$

$$+ \left[A_{rm}\left[\frac{1-4\lambda}{2af_{rm}} \sin\left[2\pi af_{rm}\left[t - k\left[\frac{r-1}{R}\right]T - \left[\frac{r-1}{R}\right]T\right] + \theta_{rm}\right]\right.\right.$$

$$+ \frac{1}{4\left[af_{rm} + \frac{1}{2w_T}\right]} \sin\left[2\pi af_{rm}\left[t - k\left[\frac{r-1}{R}\right]T - \left[\frac{r-1}{R}\right]T\right]\right.$$

$$\left. + \frac{\pi}{w_T}\left[t-kT-\left[\frac{r-1}{R}\right]T - \frac{T}{2R} + w_T\right] + \theta_{rm}\right]$$

$$+ \frac{1}{4\left[af_{rm} - \frac{1}{2w_T}\right]} \sin\left[2\pi af_{rm}\left[t - k\left[\frac{r-1}{R}\right]T - \left[\frac{r-1}{R}\right]T\right]\right.$$

$$\left. - \frac{\pi}{w_T}\left[t-kT-\left[\frac{r-1}{R}\right]T - \frac{T}{2R} + w_T\right] + \theta_{rm}\right]$$

$$+ \frac{\lambda}{\left[af_{rm} + \frac{1}{w_T}\right]} \sin\left[2\pi af_{rm}\left[t - k\left[\frac{r-1}{R}\right]T - \left[\frac{r-1}{R}\right]T\right]\right.$$

$$\left. + \frac{2\pi}{w_T}\left[t-kT-\left[\frac{r-1}{R}\right]T - \frac{T}{2R} + w_T\right] + \theta_{rm}\right]$$

$$+ \frac{\lambda}{\left[af_{rm} - \frac{1}{w_T}\right]} \sin\left[2\pi af_{rm}\left[t - k\left[\frac{r-1}{R}\right]T - \left[\frac{r-1}{R}\right]T\right]\right.$$

$$\left.\left. - \frac{2\pi}{w_T}\left[t-kT-\left[\frac{r-1}{R}\right]T - \frac{T}{2R} + w_T\right] + \theta_{rm}\right]\right]$$

$$+ \left[(1+4\lambda)\pi t - w_T \sin\left[\frac{\pi}{w_T}\left[t-kT-\left[\frac{r-1}{R}\right]T - \frac{T}{2R} + w_T\right]\right]\right]$$

$$- 2\lambda w_T \sin\left[\frac{2\pi}{w_T}\left[t-kT-\left[\frac{r-1}{R}\right]T-\frac{T}{2R}+w_T\right]\right]\Bigg] . C(kR+r+1, \text{mod } K_T.R)\Bigg]$$

$$. \text{rect}\left[\frac{t - kT - (r-1)T/R - T/2R + w_T/2}{w_T}\right]$$

$$+ k_d \sum_{r=1}^{R} \sum_{m_r=1}^{M_r} \left[-X_1 + X_2 - X_3 + X_4\right] \qquad (9.7)$$

where X_1 etc. are the integration constants, and are given by

$$X_1 = \sum_{k_1=0}^{K_1} A_{rm} \sin\left[\pi f_{rm} T(2k_1-1)+\theta_{rm}\right] . \Bigg[-\frac{1}{4\left[af_{rm} + \frac{1}{2w_T}\right]}$$

$$+ \frac{1-4\lambda}{2af_{rm}} + \frac{\lambda}{af_{rm} + \frac{1}{w_T}} + \frac{\lambda}{af_{rm} - \frac{1}{w_T}} - \frac{1}{4\left[af_{rm} - \frac{1}{2w_T}\right]}\Bigg]$$

$$+ C(kR+r).\left[(1+4\lambda)\pi\left[k_1 T+(r-1)T/R-T/2R\right]\right] \qquad (9.8)$$

$$X_2 = \sum_{k_2=0}^{K_2} A_{rm} \sin\left[2\pi af_{rm}(2k_2 T-T/2R+w_T)+\theta_{rm}\right]$$

$$.\Bigg[\frac{1-4\lambda}{2af_{rm}} + \frac{\lambda}{af_{rm} + \frac{1}{w_T}} + \frac{\lambda}{af_{rm} - \frac{1}{w_T}} + \frac{1}{4\left[af_{rm} + \frac{1}{2w_T}\right]}$$

$$+ \frac{1}{4\left[af_{rm} - \frac{1}{2w_T}\right]} - \frac{1}{af_{rm}}\Bigg]$$

$$+ C(kR+r).\left[(1+4\lambda)\pi\left[k_2T+(r-1)T/R-T/2R+w_T\right]\right] \qquad (9.9)$$

$$X_3 = \sum_{k_3=0}^{K_3} A_{rm} \sin\left[2\pi af_{rm}(2k_3T+T/2R-w_T)+\theta_{rm}\right]$$

$$\cdot\Bigg[\frac{1-4\lambda}{2af_{rm}} + \frac{\lambda}{af_{rm}+\frac{1}{w_T}} + \frac{\lambda}{af_{rm}-\frac{1}{w_T}} + \frac{1}{4\left[af_{rm}+\frac{1}{2w_T}\right]}$$

$$+ \frac{1}{4\left[af_{rm} - \frac{1}{2w_T}\right]} - \frac{1}{af_{rm}}\Bigg]$$

$$+ C(kR+r+1,\text{mod } K_T.R).\left[(1+4\lambda)\pi\left[k_3T+(r-1)T/R+T/2R-w_T\right]\right]$$

(9.10)

$$X_4 = \sum_{k_4=0}^{K_4} A_{rm} \sin\left[\pi f_{rm}T(2k_4+1)+\theta_{rm}\right] \cdot \Bigg[\frac{1-4\lambda}{2af_{rm}} + \frac{\lambda}{af_{rm}+\frac{1}{w_T}}$$

$$+ \frac{\lambda}{af_{rm}-\frac{1}{w_T}} - \frac{1}{4\left[af_{rm}+\frac{1}{2w_T}\right]} - \frac{1}{4\left[af_{rm}-\frac{1}{2w_T}\right]}\Bigg]$$

$$+ C(kR+r+1,\text{mod } K_T.R).\left[(1+4\lambda)\pi\left[k_4T+(r-1)T/R+T/2R\right]\right] \qquad (9.11)$$

where

$$K_1 = \text{largest integer} \leq \left\lfloor \frac{t - (r-1)T/R + T/2R}{T} \right\rfloor$$

$$K_2 = \text{largest integer} \leq \left\lfloor \frac{t - (r-1)T/R + T/2R - w_T}{T} \right\rfloor$$

$$K_3 = \text{largest integer} \leq \left\lfloor \frac{t - (r-1)T/R - T/2R + w_T}{T} \right\rfloor$$

$$K_4 = \text{largest integer} \leq \left\lfloor \frac{t - (r-1)T/R - T/2R}{T} \right\rfloor$$

Eqns. 9.5 to 9.11 may be readily configured for other windowing functions if required.

9.4 SPECTRAL ANALYSIS USING THE DFT

The subroutine, WTCM1.for, listed in Appendix K was written to evaluate the spectra of both basic (equalised) and over-compressed windowed TCM-FM signals using the expressions derived in the previous section and the discrete Fourier transform. Papoulis, Parzen or 3-coefficient weighting functions may be applied. As with non-multiplexed FM and TCM-FM, choosing 2^N samples and a 2,4 or 8 channel system allows the computational efficient fast fourier transform (FFT) to be used. In addition, a pseudo-random baseband modulating signal was employed consisting of 30 tones at a frequency spacing of 100Hz using proven Monte Carlo techniques.

Fig.9.5(a) and (b) show the spectra for a 4-channel basic windowed TCM-FM signal with Papoulis weighting applied over intervals of approximately 1% and 5% of the segment duration respectively. An rms frequency deviation of 6kHz and a TCM frame period of 10ms were used. Comparison with the equivalent simple TCM-FM spectrum (fig.8.3(a)) shows that a substantial increase in spectral roll-off is achieved, particularly with a 5% period. With only 1% windowing, the magnitude of the sidebands at the plot edges has been reduced from around -70dB to -95dB. With 5% windowing there is no discernible spectral spreading due to the segmentation of the TCM signal. This is

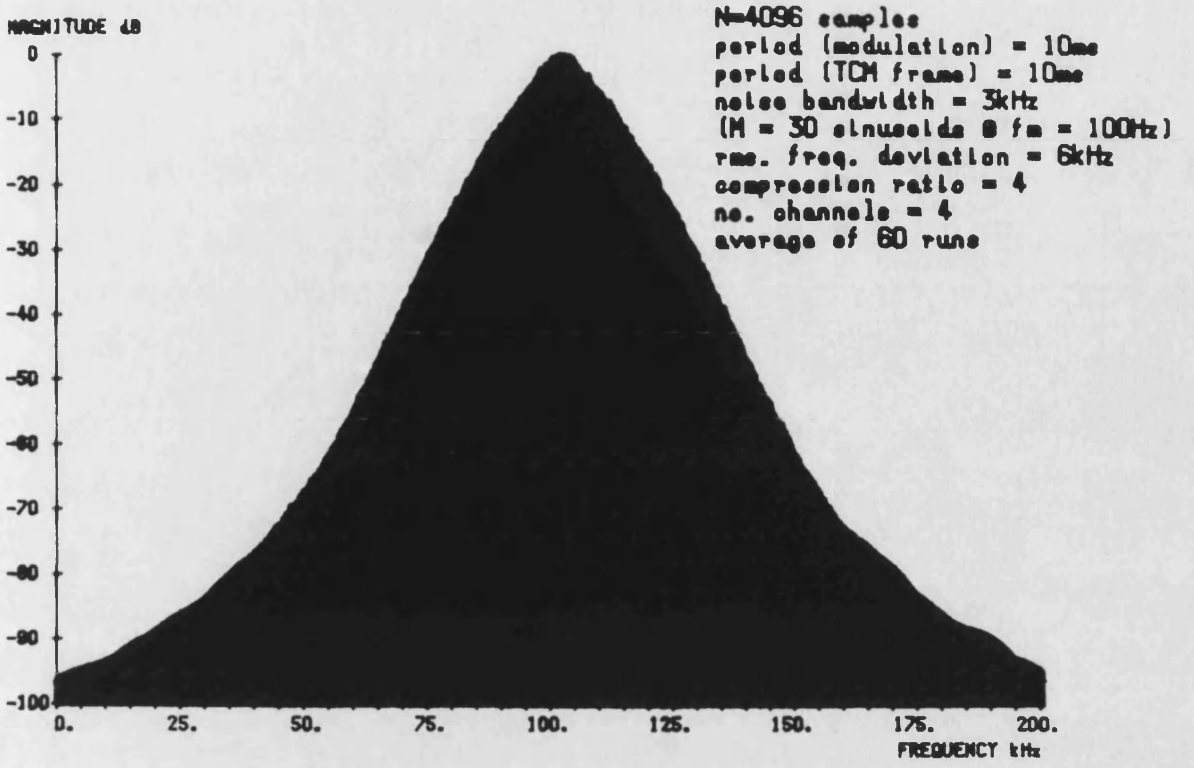

Fig. 9.5(a) Spectrum of a 4-channel windowed TDM-FM signal with pseudo-random noise modulation. Weighting interval =1% of segment duration using Papoulis function.

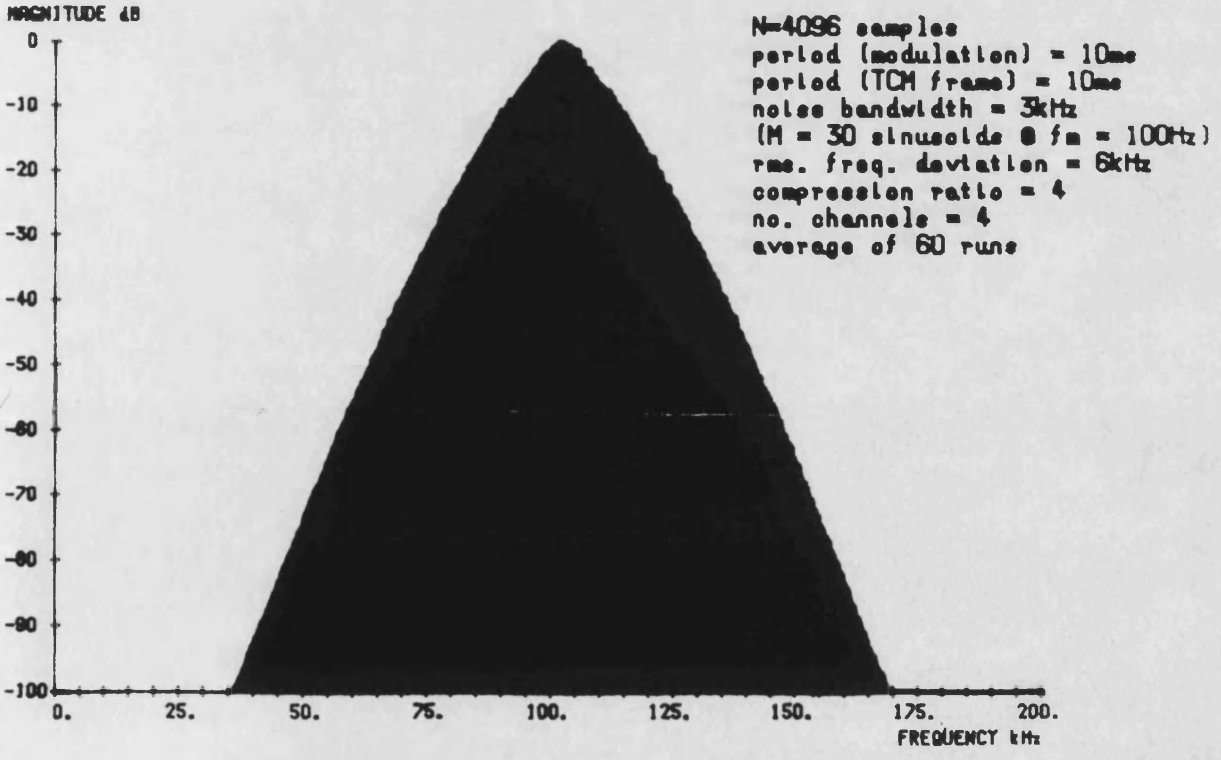

Fig. 9.5(b) Spectrum of a 4-channel windowed TDM-FM signal with pseudo-random noise modulation. Weighting interval =5% of segment duration using Papoulis function.

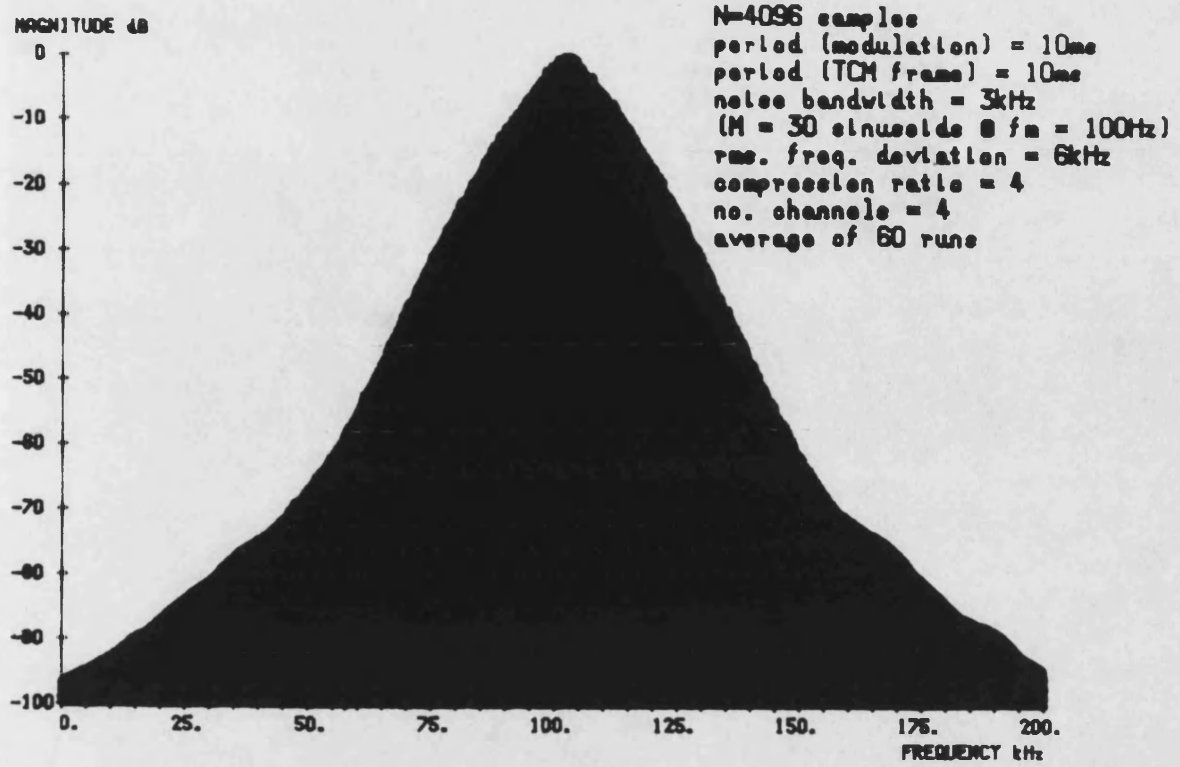

Fig. 9.6(a) Spectrum of a 4-channel windowed TCM-FM signal with pseudo-random noise modulation. Weighting interval =1% of segment duration using Parzen function.

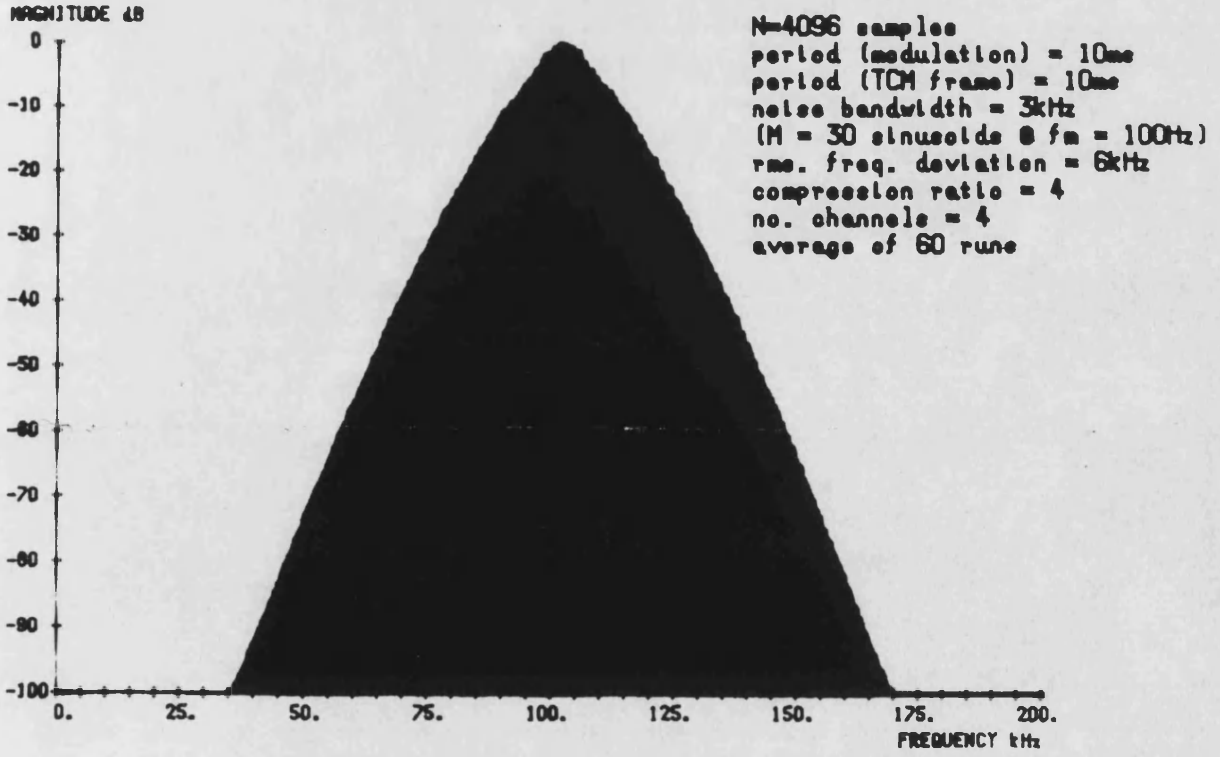

Fig. 9.6(b) Spectrum of a 4-channel windowed TCM-FM signal with pseudo-random noise modulation. Weighting interval =5% of segment duration using Parzen function.

confirmed by the excellent correlation with the equivalent non-multiplexed FM spectrum (fig.7.1(a)). Indeed, the two spectra are identical when the frequency axis is scaled by the number of multiplexed channels.

The corresponding spectra using Parzen, raised cosine and Blackman windowing functions are shown in fig.9.6 to 9.8. All the functions produce similar spectra, particularly with 5% windowing. There are however minor differences in the 1% spectra for sideband magnitudes less than -60dB, with the raised cosine function producing the lowest (-100dB) sideband magnitude at the plot edges. Hence this latter function is adopted for subsequent analysis.

Fig.9.9(a) and (b) illustrate the spectra for a 4-channel windowed TCM-FM system with over-compression and raised cosine weighting applied over intervals of approximately 1% and 5% of the segment period. An rms frequency deviation of 6kHz and a TCM frame period of 10ms was employed as above. The compression ratios required were increased from the simple system by about 2% and 10% to 4.08 and 4.43 respectively. Comparison of fig.9.9(a) with fig.9.7(a) shows little variation as expected from the marginal increase in compression ratio. However, there is an increase of around 10% in the -100dB BW of the spectrum of fig.9.9(b) compared to that of fig.9.7(b), as expected.

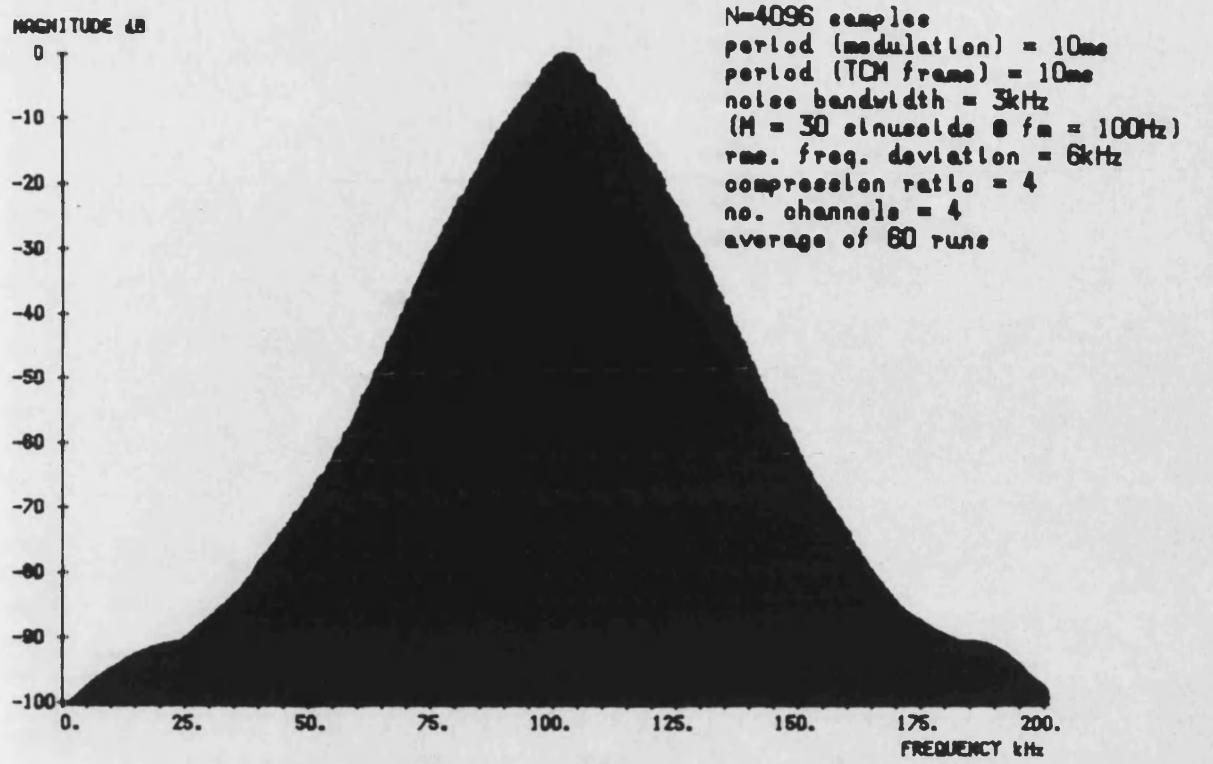

Fig. 9.7(a) Spectrum of a 4-channel windowed TDM-FM signal with pseudo-random noise modulation. Weighting interval =1% of segment duration using raised cosine function.

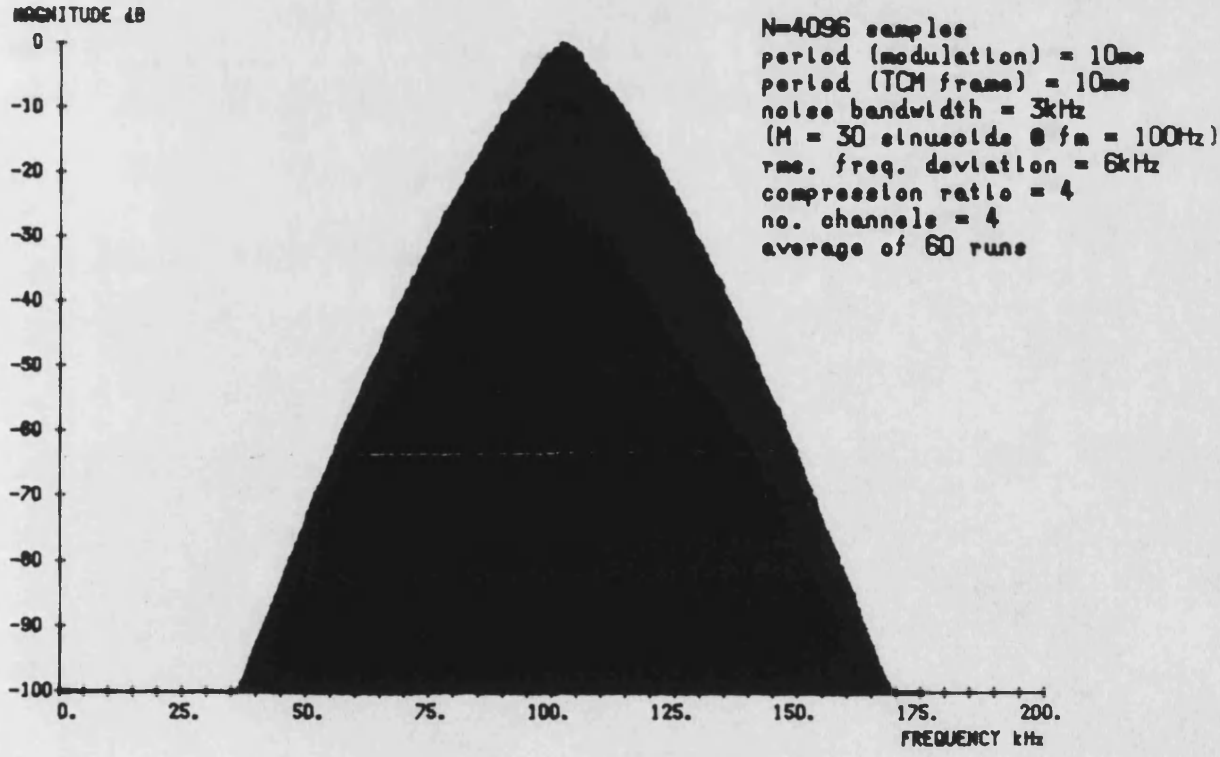

Fig. 9.7(b) Spectrum of a 4-channel windowed TDM-FM signal with pseudo-random noise modulation. Weighting interval =5% of segment duration using raised cosine function.

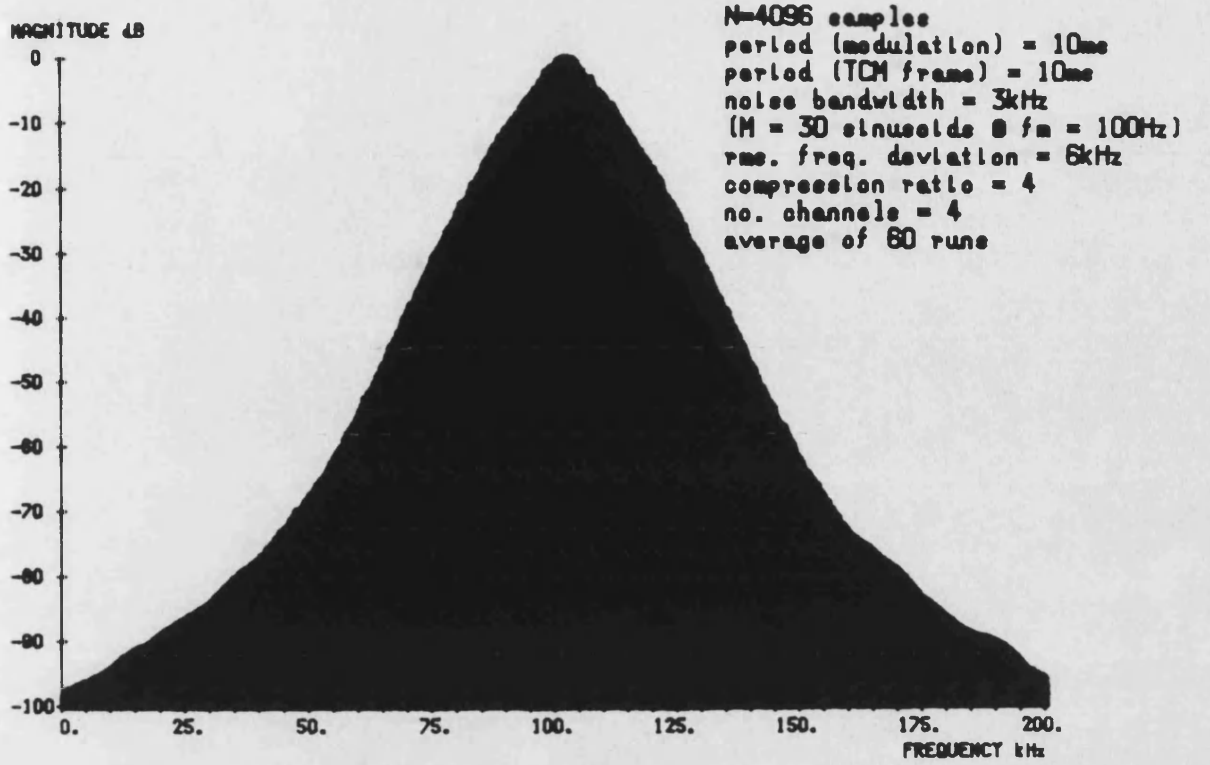

Fig. 9.8(a) Spectrum of a 4-channel windowed TDM-FM signal with pseudo-random noise modulation. Weighting interval =1% of segment duration using Blackman function.

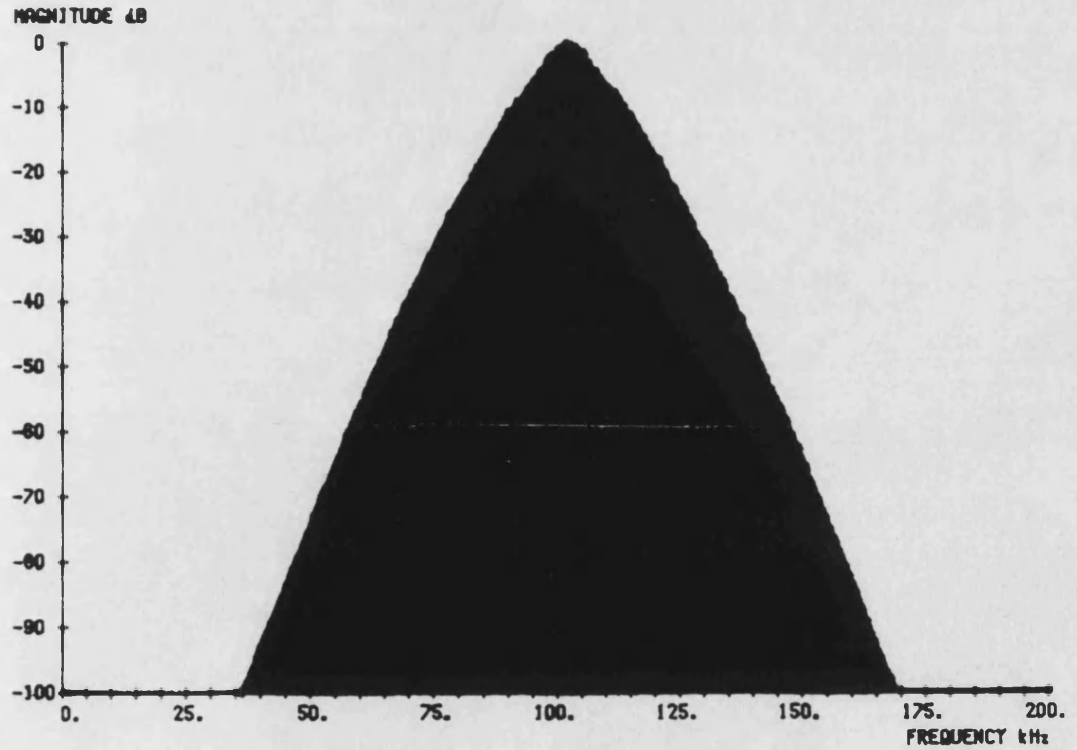

Fig. 9.8(b) Spectrum of a 4-channel windowed TDM-FM signal with pseudo-random noise modulation. Weighting interval =5% of segment duration using Blackman function.

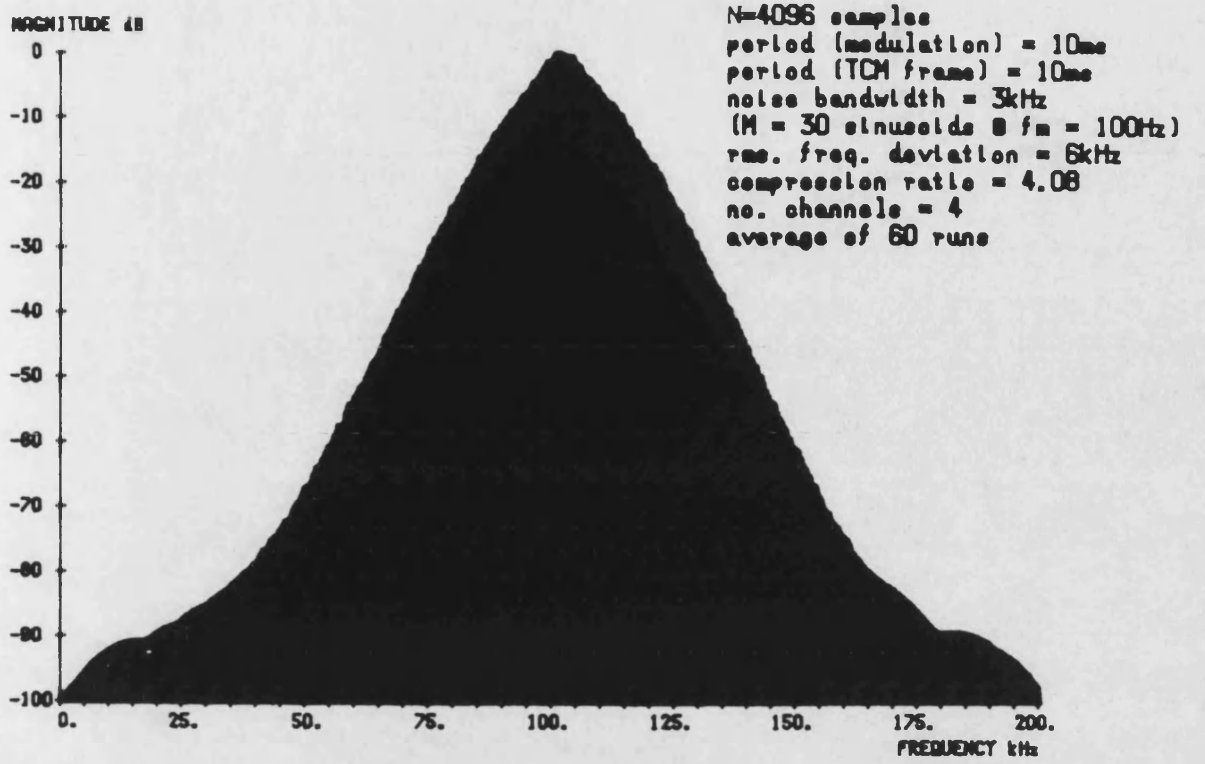

Fig. 9.9(a) Spectrum of a 4-channel windowed and over-compressed TDM-FM signal with pseudo-random noise modulation. Weighting interval =1% of segment duration using raised cosine function.

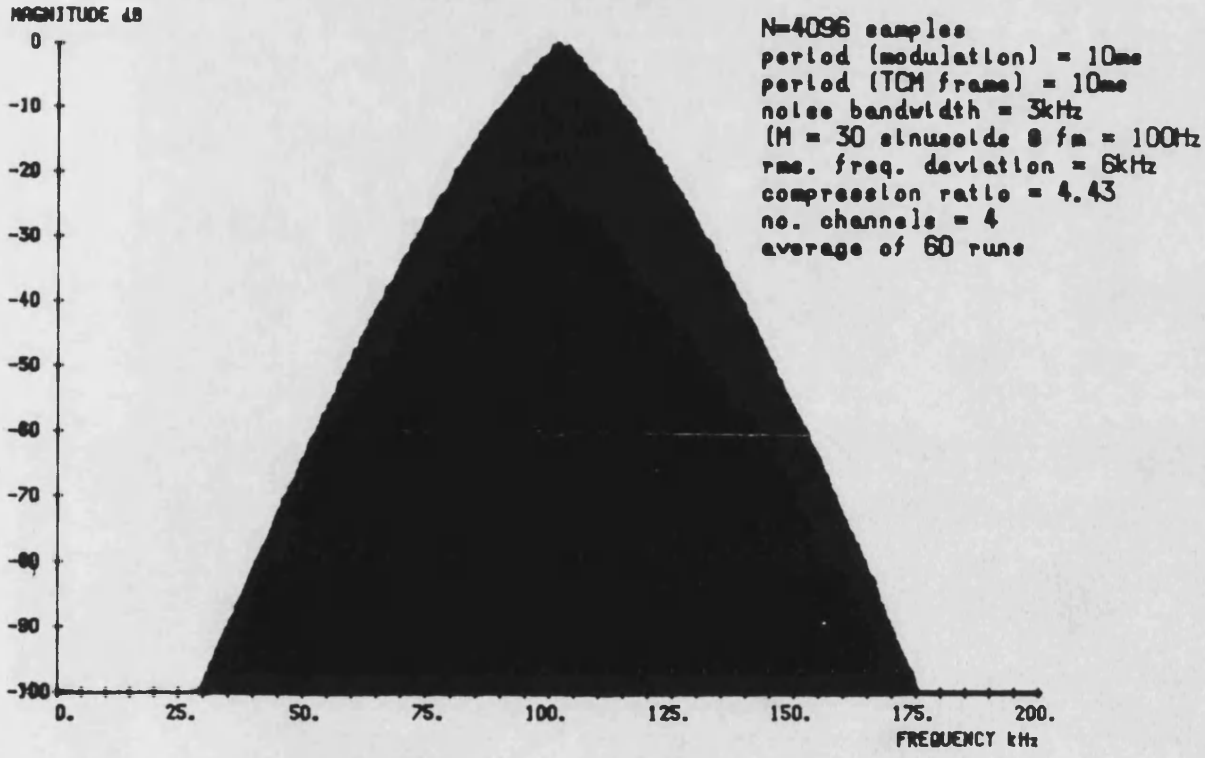

Fig. 9.9(b) Spectrum of a 4-channel windowed and over-compressed TDM-FM signal with pseudo-random noise modulation. Weighting interval =5% of segment duration using raised cosine function

This is confirmed by the same percentage increases measured in the 98%/99% spectral power bandwidths from 31.8 and 36.6kHz to 34.8 and 40.2kHz respectively.

The spectra for a 2-channel over-compressed system with frame periods of 5 and 2.5ms are shown in figs.9.10(a) and (b) respectively. Windowing was applied for approximately 10% and 20% of the segment duration respectively. The same excellent spectral roll-off is obtained although the larger ratio of modulation period to TCM frame period necessitates a considerable increase in the compression ratios to 2.49 and 3.28 respectively and hence produces wider main spectral lobes. Finally, an 8-channel system with frame periods of 10 and 2.5ms was assessed and the results illustrated in fig.9.11(a) and (b). The bandwidth of the former is approximately 10% greater than eight times the equivalent non-multiplexed FM system (from fig.7.1(a)), as expected from the 5% windowing interval. In addition the same observations regarding the small TCM frame period are made as for the 2-channel system.

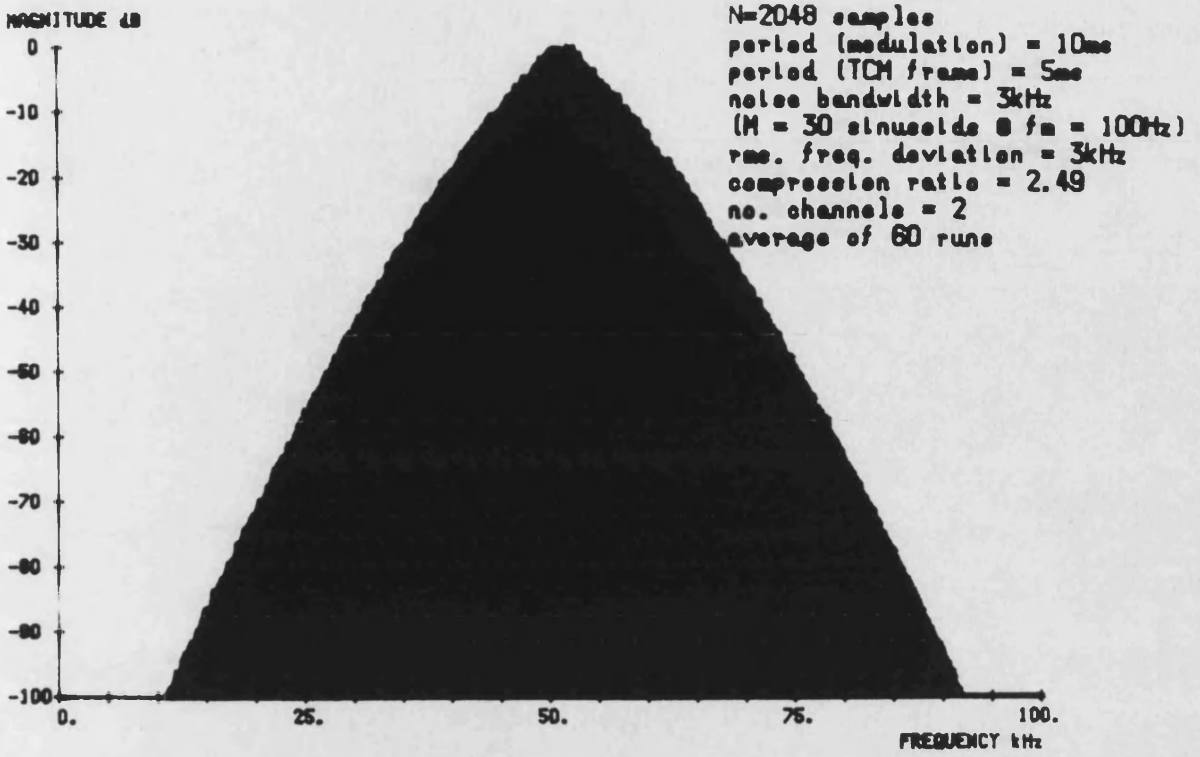

Fig. 9.10(a) Spectrum of a 2-channel windowed and over-compressed TCM-FM signal with pseudo-random noise modulation. Weighting interval =10% of segment duration using raised cosine function.

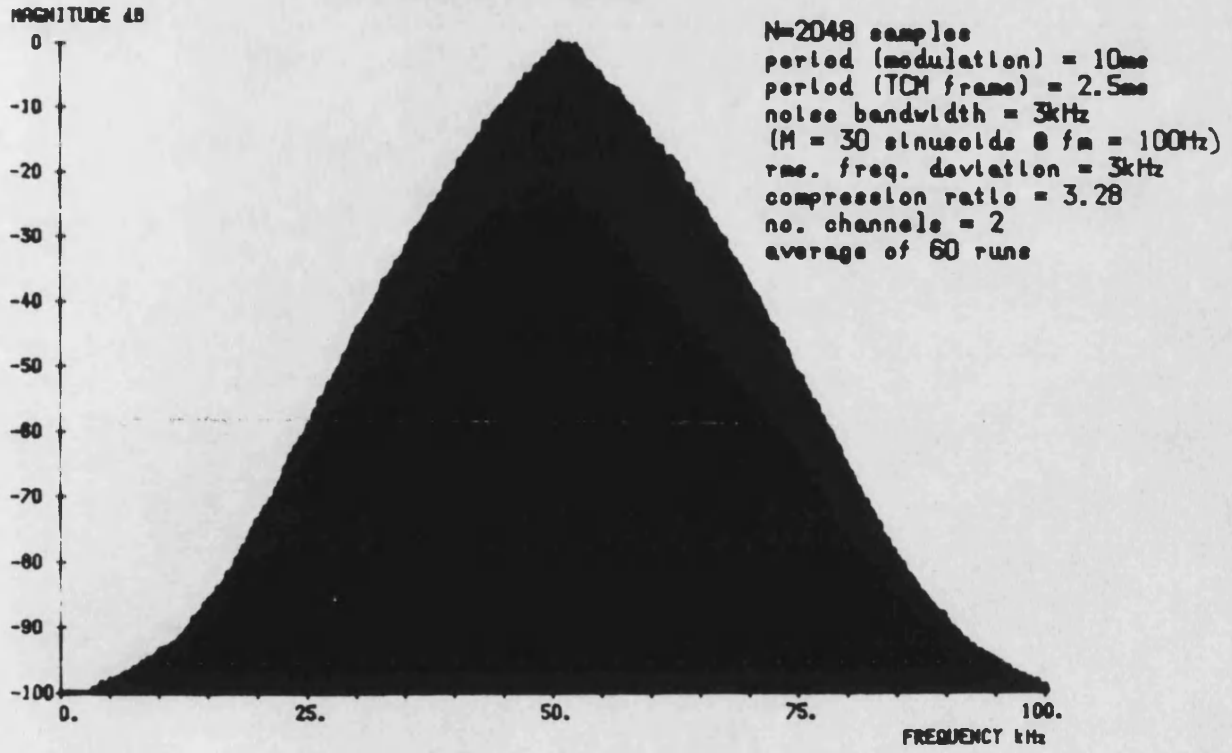

Fig. 9.10(b) Spectrum of a 2-channel windowed and over-compressed TCM-FM signal with pseudo-random noise modulation. Weighting interval =20% of segment duration using raised cosine function

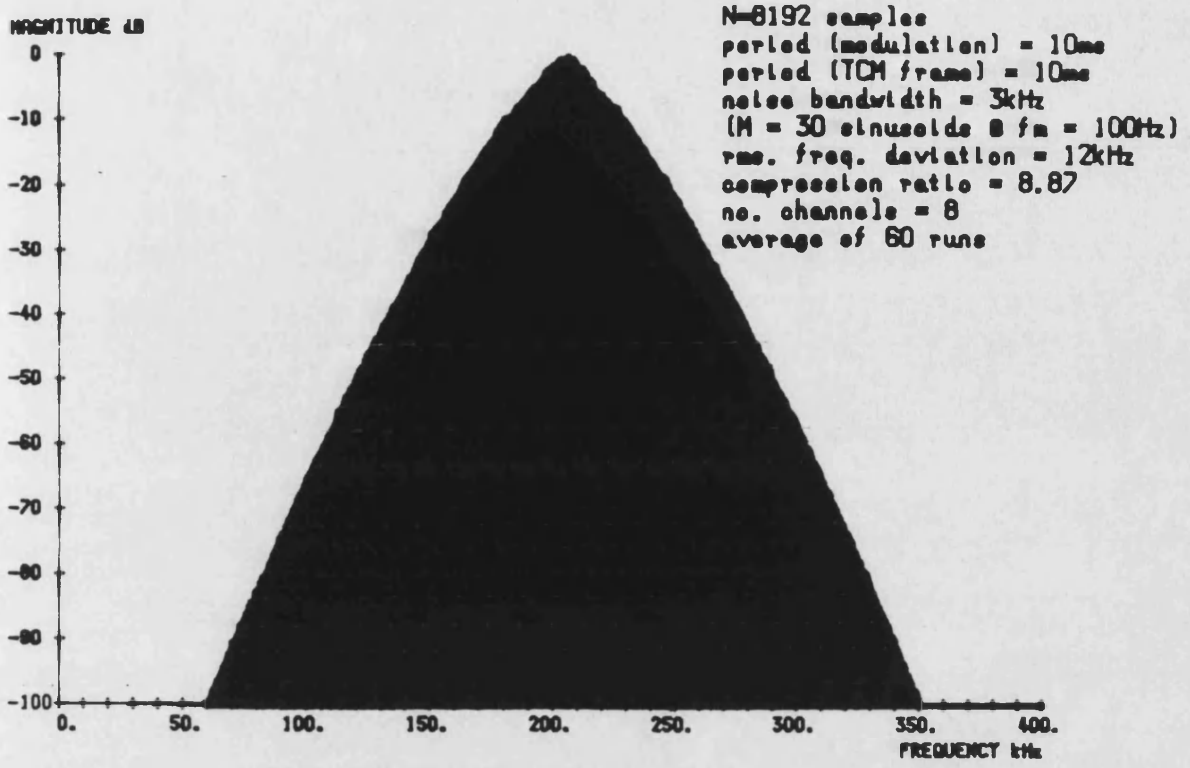

Fig. 9.11(a) Spectrum of an 8-channel windowed and over-compressed TDM-FM signal with pseudo-random noise modulation. Weighting interval =5% of segment duration using raised cosine function.

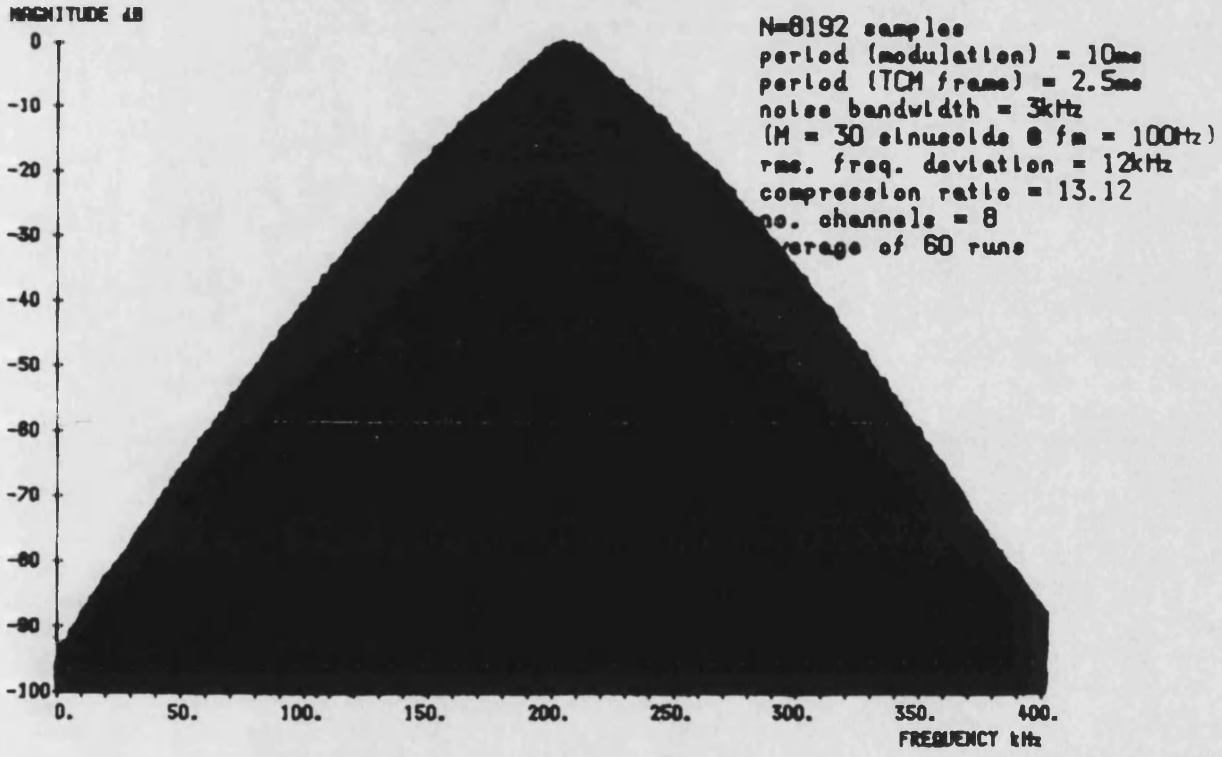

Fig. 9.11(b) Spectrum of an 8-channel windowed and over-compressed TDM-FM signal with pseudo-random noise modulation. Weighting interval =20% of segment duration using raised cosine function

9.5 FILTERING, DEMODULATION AND TIME-EXPANSION

The subroutine FILDEM4.for listed in Appendix L was written to evaluate the intermodulation distortion due to pseudo-rectangular bandlimiting of a windowed TCM-FM signal. Only over-compressed signals are considered since the basic (equalised) system is unlikely to be practically viable. The modulated signal spectrum and demodulation processes are based on 2^N samples and hence the FFT may be used. However, the spectrum of the final expanded signal requires the use of the DFT since a number of samples (representing the redundant intervals) must be ignored leading to a total which is no longer a power of two. Hence, computation is slow and although FILDEM4.for caters for 3-coefficient weighting, only raised cosine was evaluated due to limits on available computer time. However, it was shown previously that there are only marginal differences between the chosen functions.

Fig.9.12 shows the intermodulation distortion for a 2-channel TCM-FM system with approximately 5% raised cosine windowing for a selection of filter bandwidths. A TCM frame period of 10ms was used and the measurement was performed at 1kHz. Comparison with the equivalent curves for simple TCM-FM (fig.8.9) shows an overall improvement of typically 20dB for the larger filter bandwidths. However, the increased compression ratio required (2.28)

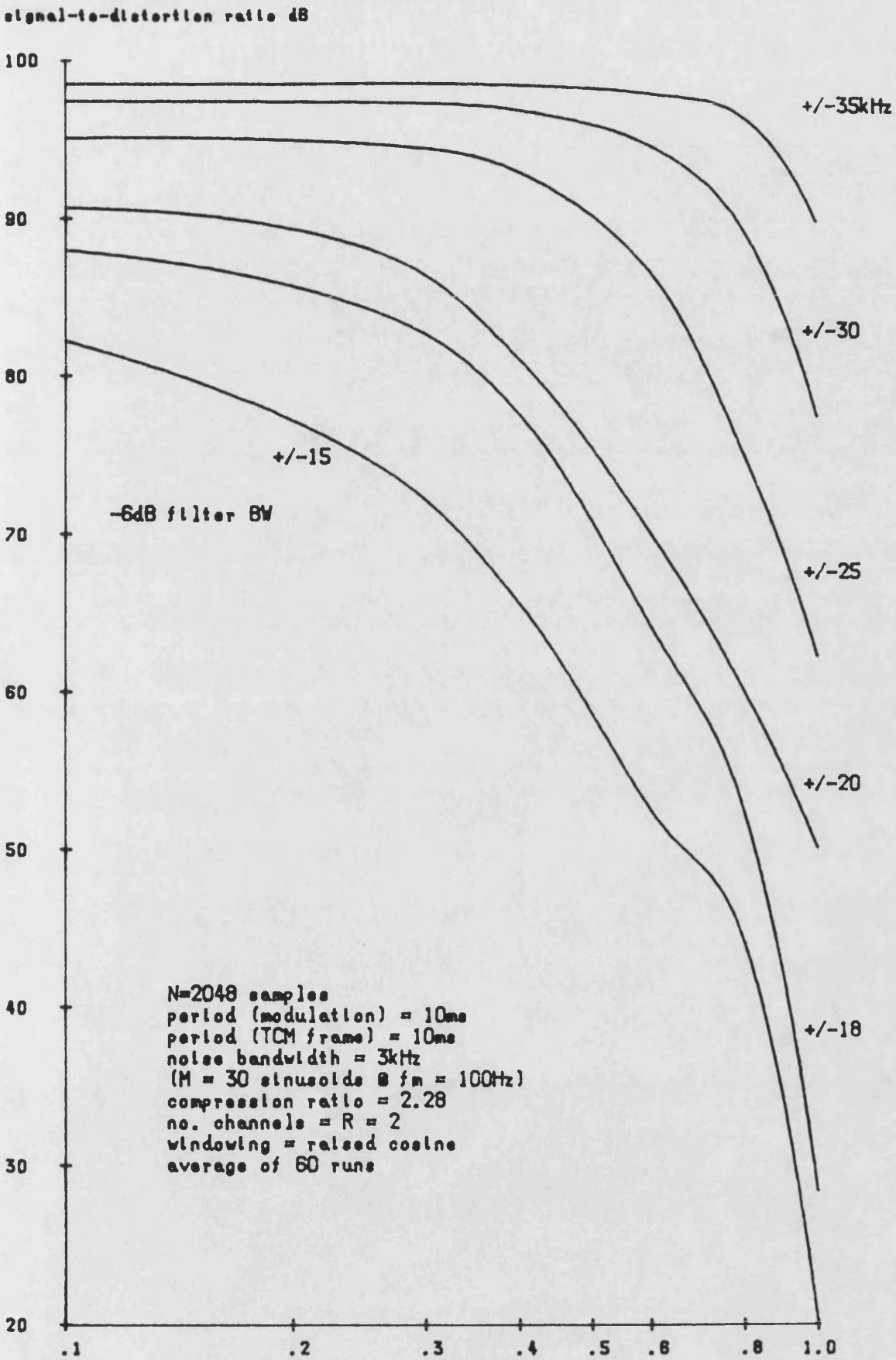

Fig.9.12 Computed intermodulation distortion at 1kHz in 2-channel raised-cosine windowed TCM-FM system with pseudo-rectangular filter.

reduces the advantage of the windowed system for smaller bandwidths. At a typical normalised frequency deviation of 0.5, a signal-to-distortion ratio of 97dB is achieved with a ±30kHz filter. This compares to around 74dB for an equivalent simple TCM-FM system, and 106dB for a non-multiplexed FM system (±15kHz from fig.7.9). The equivalent results measured at 3kHz illustrated in fig.9.13 show a slightly increased improvement over simple TCM-FM at large filter bandwidths. With a normalised frequency deviation of 0.5, signal-to-distortion ratios of 98dB(32dB improvement), 66dB and 102dB are obtained at ±30kHz for the windowed TCM-FM system, simple TCM-FM system (fig.8.10) and non-multiplexed FM system (fig.7.10) respectively.

Contours of constant signal-to-distortion against frequency deviation are shown in figs.9.14 and 9.15 for 1kHz and 3kHz baseband frequencies respectively. A good fit is obtained to the following linear approximations

$$B = \left\lfloor 0.9 + 0.6\left\lceil \frac{S/D}{20} \right\rceil \right\rfloor \sigma + 0.5\left\lceil \frac{S/D}{20} \right\rceil aW \qquad (9.12)$$

for 1kHz, and

$$B = \left\lfloor 2 + 0.5\left\lceil \frac{S/D}{20} \right\rceil \right\rfloor \sigma + 0.5\left\lceil \frac{S/D}{20} \right\rceil aW \qquad (9.13)$$

for 3kHz.

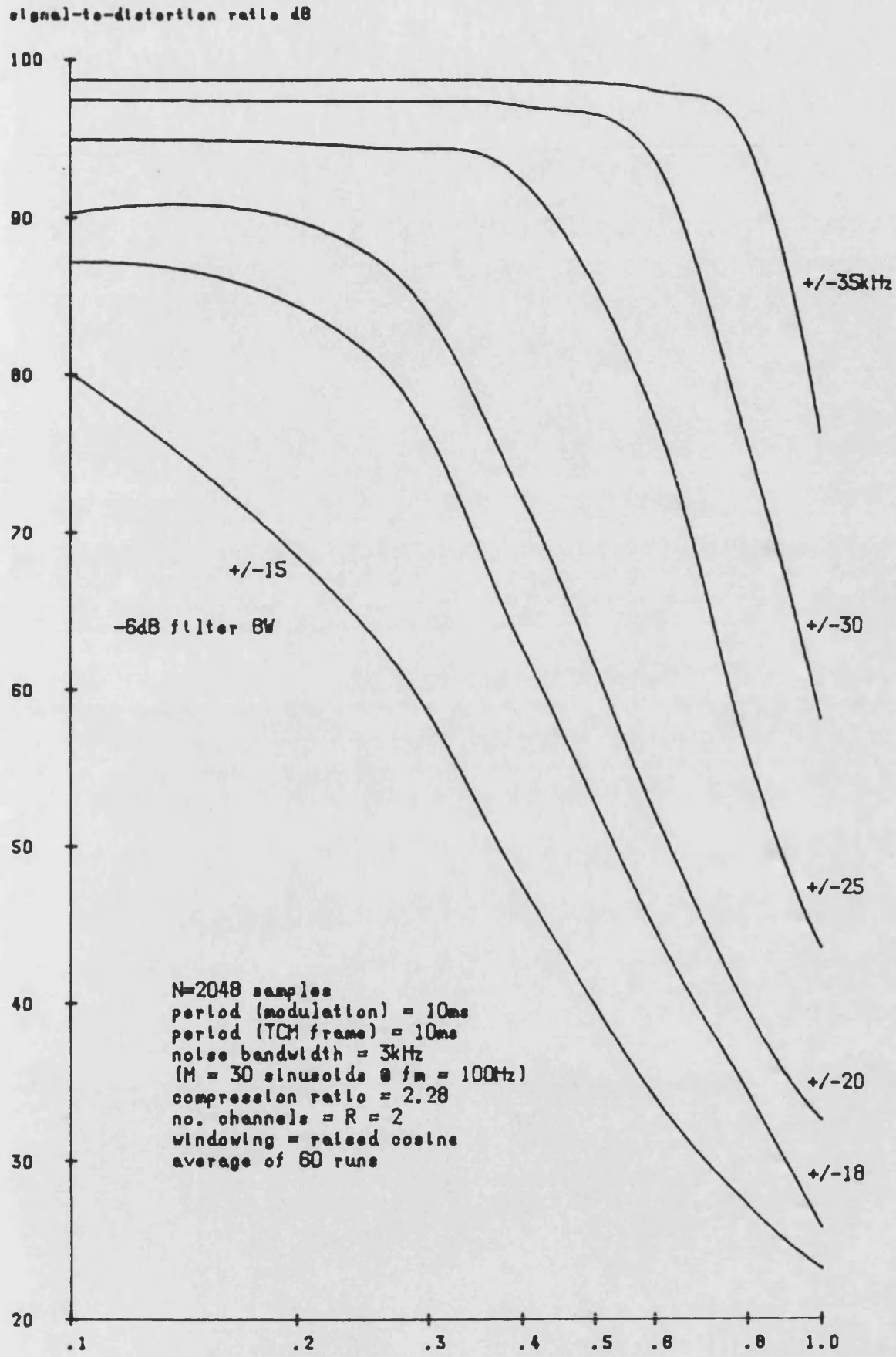

Fig.9.13 Computed intermodulation distortion at 3kHz in 2-channel raised-cosine windowed TCM-FM system with pseudo-rectangular filter.

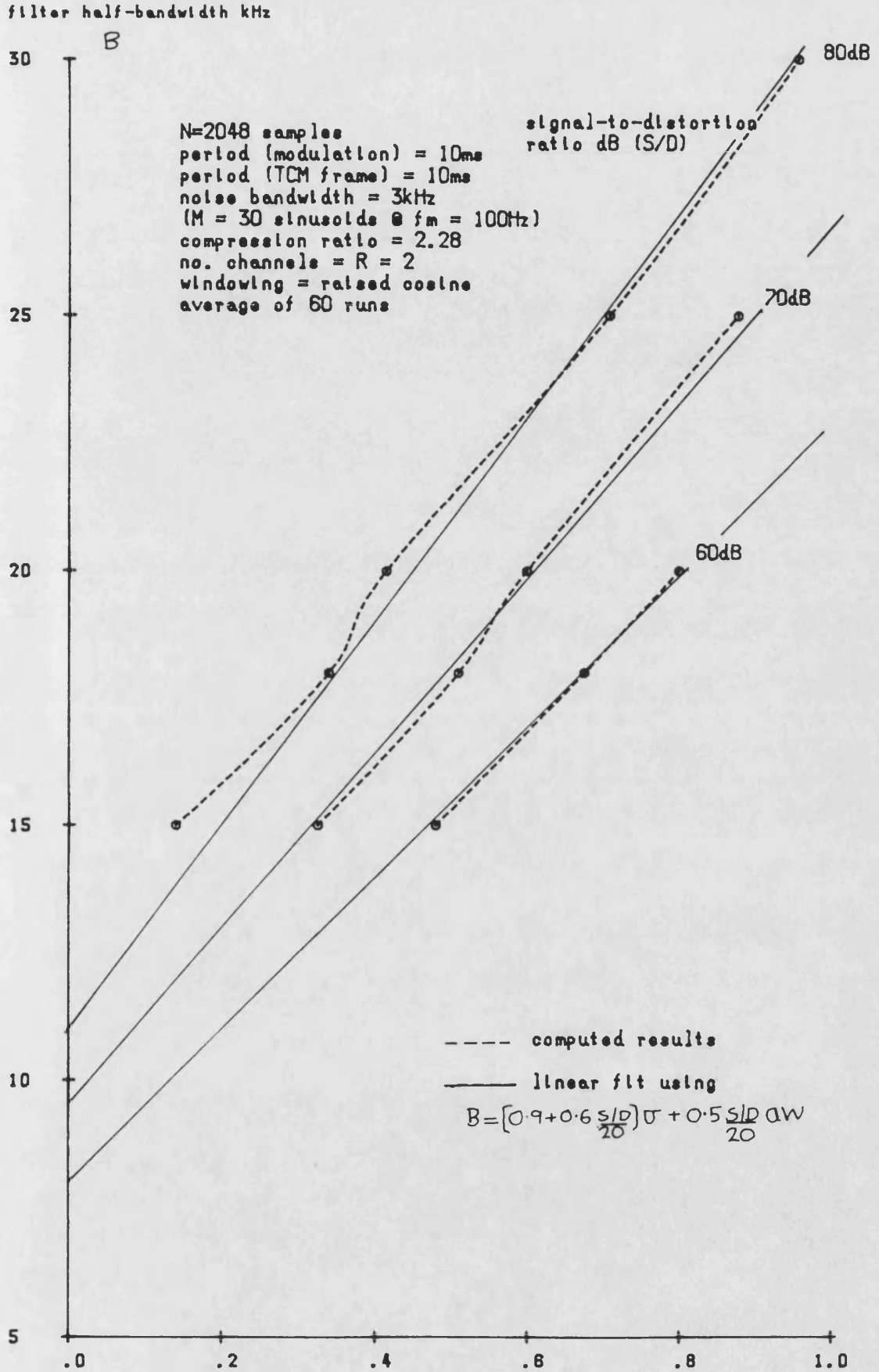

Fig.9.14 Necessary filter bandwidth in 2-channel windowed TCM-FM system for given signal-to- distortion ratio v. normalised freq. dev. Baseband frequency = 1kHz. $\frac{\text{rms. freq. dev.}}{\alpha \times \text{noise BW}}$, $\frac{\sigma}{\alpha_W}$

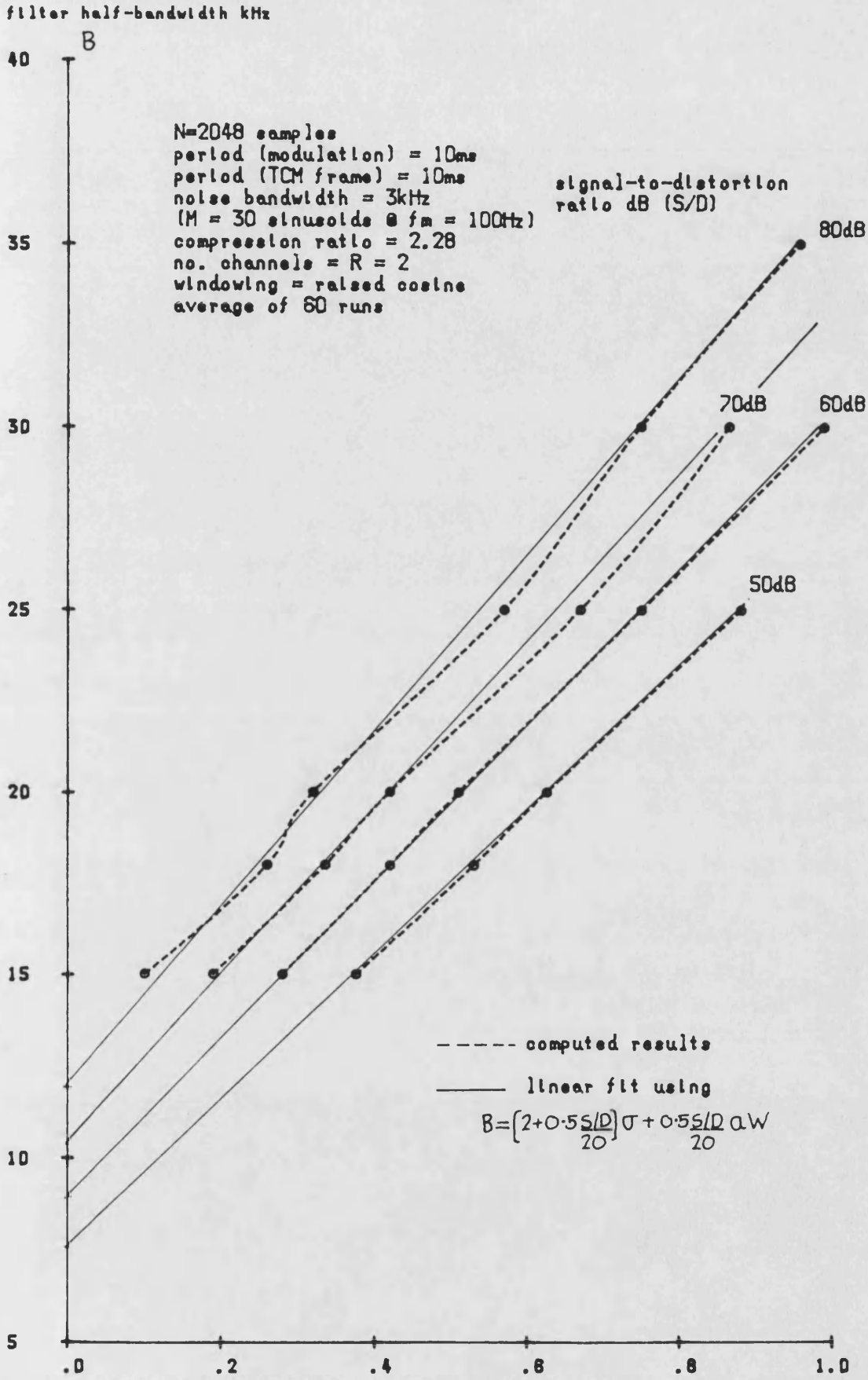

Fig.9.15 Necessary filter bandwidth in 2-channel windowed TCM-FM system for given signal-to- distortion ratio v. normalised freq. dev. Baseband frequency = 3kHz.

The similarity of the equations confirms the near identical performance figures for 1kHz and 3kHz obtained above. This is especially true for large S/D ratios (ie. wide filter bandwidths) as expected.

Figs.9.16 and 9.17 illustrate the equivalent results for a 4-channel windowed TCM-FM system, again with weighting intervals equal to approximately 5% of the segment period (compression ratio=4.43). Again improvements over simple TCM-FM systems (figs.8.14 and 8.15) are observed at large bandwidths. Typical S/D figures at 0.5 normalised deviation for a $\pm$60kHz filter are 95dB and 96dB for 1kHz and 3kHz respectively. The corresponding figures for ordinary TCM-FM are 68dB (27dB improvement) and 47dB(49dB improvement) respectively. The results for are nearly identical to the 2-channel system, with again little variation between 1kHz and 3kHz.

The contours of constant signal-to-distortion ratio for the 4-channel system are shown in figs.9.18 and 9.19. A very good fit is obtained to the following linear approximations for 1kHz and 3kHz respectively.

$$B = \left[2 + 0.3\left[\frac{S/D}{20}\right]\right]\sigma + \left[0.8\left[\frac{S/D}{20}\right] - 1.5\right]aW \quad (9.14)$$

$$B = \left[0.8 + 0.8\left[\frac{S/D}{20}\right]\right]\sigma + \left[0.5 + 0.5\left[\frac{S/D}{20}\right]\right]aW \quad (9.15)$$

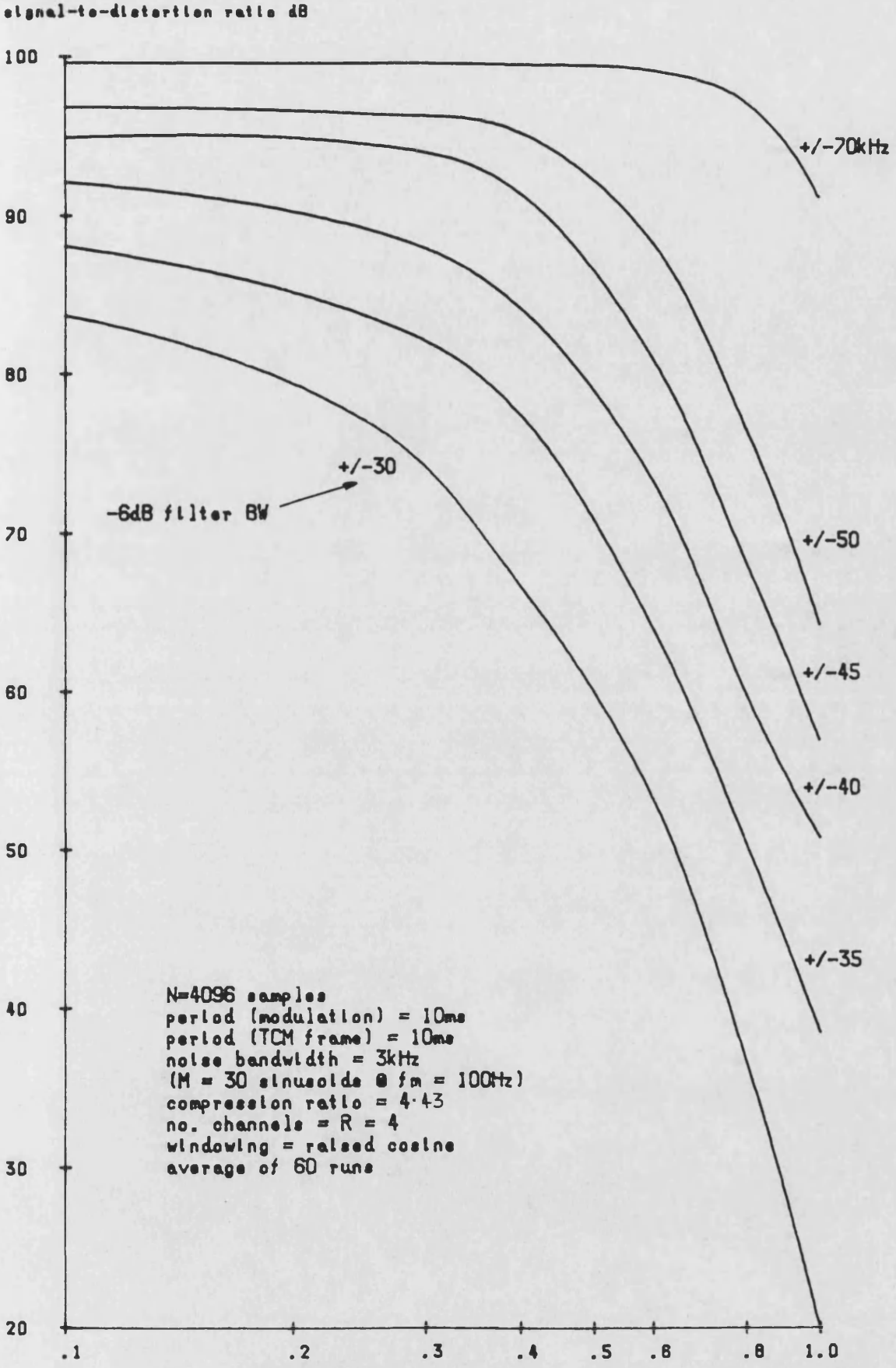

Fig.9.16 Computed intermodulation distortion at 1kHz in 4-channel raised-cosine windowed TCM-FM system with pseudo-rectangular filter.

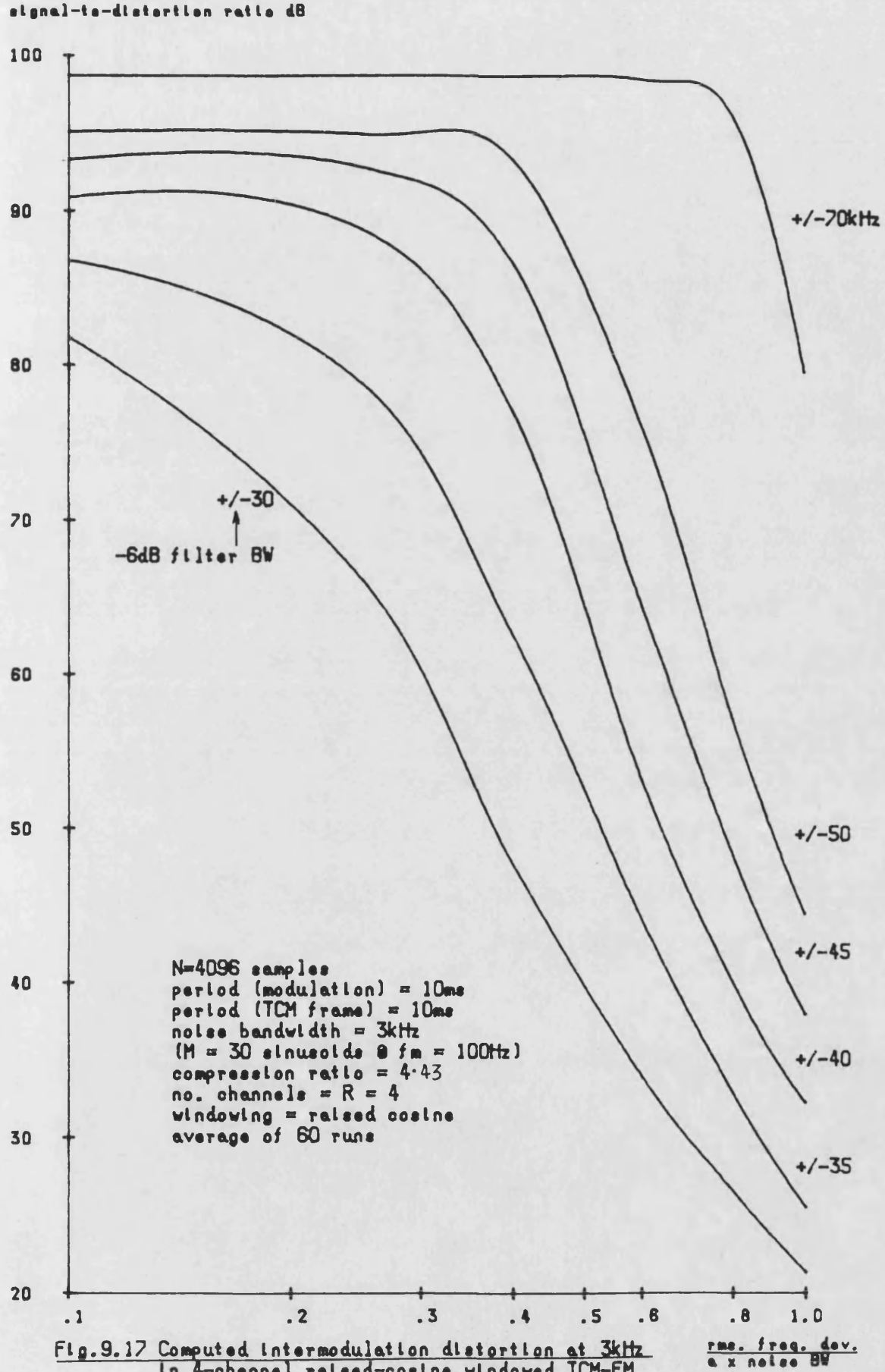

Fig.9.17 Computed intermodulation distortion at 3kHz in 4-channel raised-cosine windowed TCM-FM system with pseudo-rectangular filter.

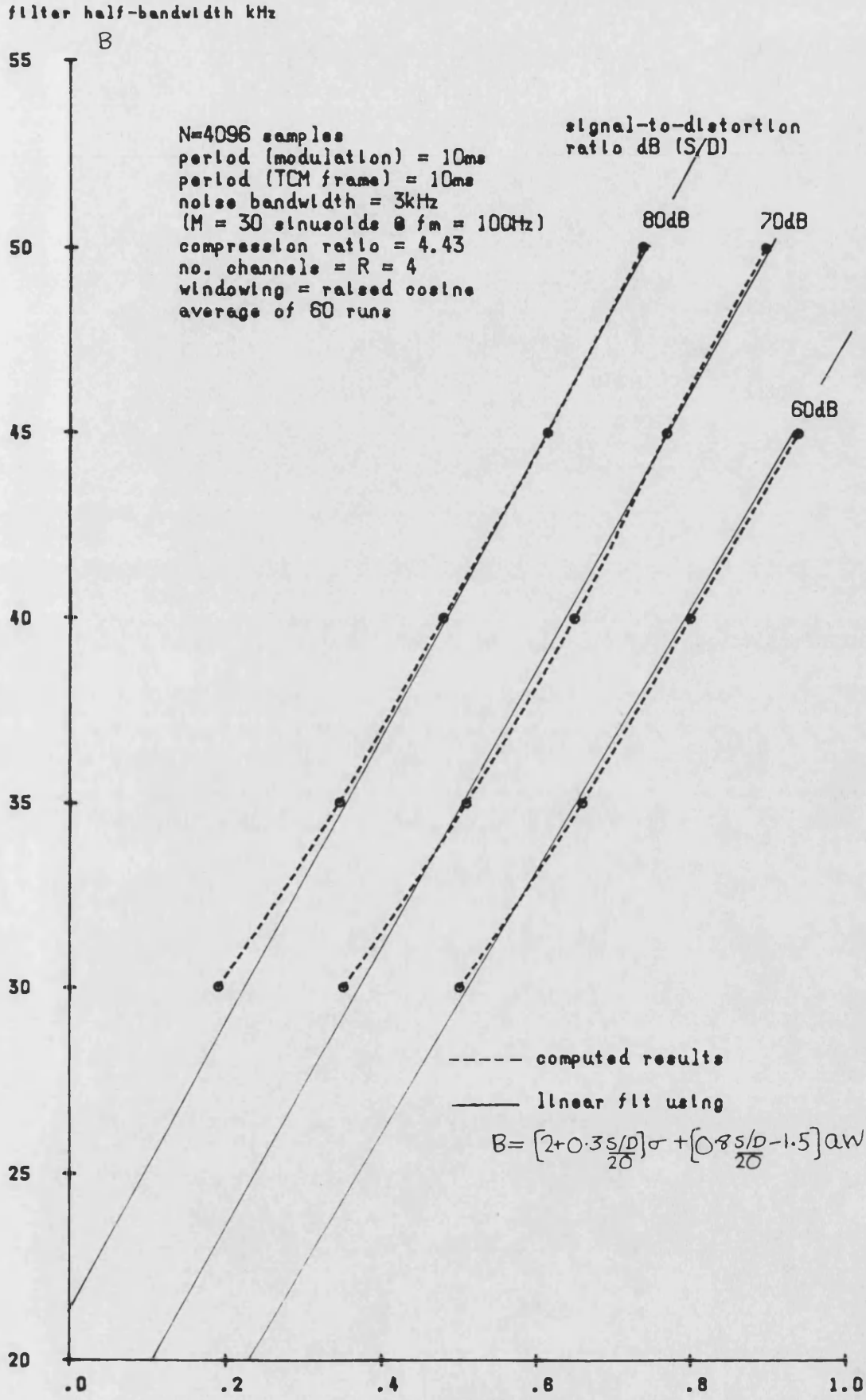

Fig.9.18 Necessary filter bandwidth in 4-channel windowed TCM-FM system for given signal-to- distortion ratio v. normalised freq. dev. Baseband frequency = 1kHz. $\frac{\text{rms. freq. dev.}}{\text{a x noise BW}}$ $\frac{\sigma}{aW}$

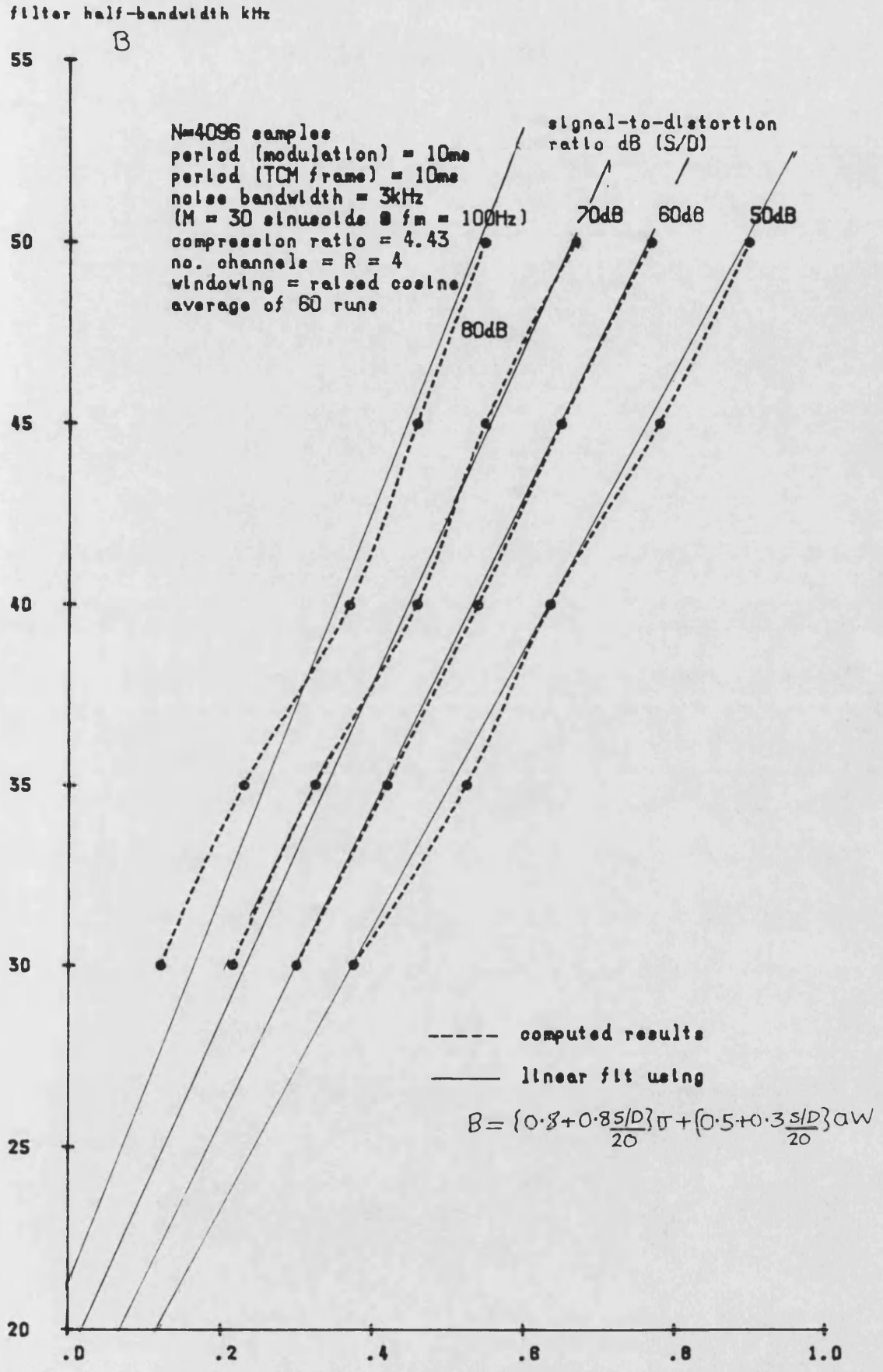

Fig.9.19 Necessary filter bandwidth in 4-channel windowed TCM-FM system for given signal-to- distortion ratio v. normalised freq. dev. Baseband frequency = 3kHz, $\frac{\text{rms. freq. dev.}}{a \times \text{noise BW}}$ $\frac{\sigma}{aW}$

9.6 CONCLUSIONS

A simple time-domain windowing technique operating on the instantaneous frequency waveform of a TCM-FM signal has been shown to produce a substantial increase in spectral roll-off and so lead to improvements in performance in related areas. Weighting intervals equal to about 5% of the TCM segment period have been shown to produce spectra very nearly identical to those for non-multiplexed FM (with appropriate frequency scaling for the number of multiplexed channels). Moreover, these characteristics were maintained over a range of compression ratios, although the improvement is less marked at smaller TCM frame periods.

The weighting intervals were accommodated in the composite TCM-FM signal without loss of information by increasing the compression ratio (over-compression) so as to make the shaped segments redundant. This is a superior technique practically to the system which employs standard compression with equalisation at the receiver. Little variation was observed between the Papoulis, Parzen, Blackman and raised cosine weighting functions considered, with the latter having marginally the best characteristics.

When bandlimiting was investigated, improvements in

signal-to-distortion ratios over simple TCM-FM systems of up to 45dB were observed for larger filter bandwidths. In this respect, the performance is slightly worse than an equivalent non-multiplexed FM system due to the increased bandwidth requirement caused by over-compression. Overall, a system employing about 5% (of segment interval) raised cosine shaping and a frame period of 10ms was found to have a largely identical spectral footprint to a non-multiplexed FM system with an increase of 10-15% in its normalised bandwidth requirement.

9.7 REFERENCES

(1) Geckinli, N.C. and Yavuz, D.:Discrete Fourier transformation and its applications to power spectra estimation', Elsevier, New York, 1983.

CHAPTER TEN

FINAL CONCLUSIONS

Conventional mobile radio systems have been shown to be highly susceptible to intermodulation interference whenever non-linearities occur. As such considerable extra complexity must be included in base station hardware in an attempt to maintain performance at an acceptable level. Alternatively the frequencies on which intermodulation products are likely to fall must be kept unused; a policy which becomes increasingly wasteful of spectrum as the number of channels required in a particular locality rises.

Wideband systems employing significantly fewer carrier frequencies offer obvious benefits in this respect. The use of time-division multiplexing in such a system has received a good deal of attention. However, well-established land-line systems such as PCM are precluded in favour of unproven techniques, eg. sub-band coding, on grounds of spectral efficiency. In addition, complex equalisation is required in the mobile environment to combat the effects of multipath fading. There are still major technical problems unsolved in both of these areas. This thesis is the report of an investigation of the spectral characteristics of an alternative analogue wideband tech-

nique employing time-compression multiplexing on a frequency modulated bearer.

Analysis of angle modulation using classical techniques has been shown to produce little insight into its practical performance unless many over-simplifications are made. When a complex modulating signal such as TCM is considered, the resulting Diophantine expressions have been shown to be particular tedious to solve even with computer aid. Instead extensive use was made of a numerical technique involving the discrete Fourier transform. By using a pseudo-random modulating signal, with averaging over a number of random phase sets using a Monte Carlo procedure, it was possible to obtain results for noise-like signals. Excellent correlation was observed between these results and those from practical measurements and other published works, thus confirming the validity of the techniques.

Extensive comparisons of measurements made on conventional FM systems with those for TCM-FM over a range of system parameters with pseudo-random modulation confirmed that the co-channel rejection of the former was retained. Indeed, a slight improvement of the order of 1-2dB was noted under certain circumstances. Spectral comparisons showed that both systems have a characteristic main lobe which is of almost identical normalised bandwidth. Contours of constant signal-to-distortion ratio for a given

filter bandwidth were plotted for both the non-multiplexed FM system and for TCM-FM. In both cases, it was possible to form a very good linear fit to the data. For TCM-FM, there was little variation in the measured intermodulation distortion with an equivalent filter with either the number of multiplexed channels or the TCM frame period.

An enhanced TCM-FM system was also investigated which employed time-domain windowing of the signal segments to remove the step discontinuities which occur in the otherwise raw TCM signal. Little difference in the performance of Papoulis, Parzen, Blackman and raised cosine windowing functions was found, although the latter did exhibit a marginal improvement. With a windowing interval equal to about 1% of the total segment duration, a significant reduction in the spectral sidelobes from the basic TCM-FM was apparent. When this was increased to approximately 5%, the spectral footprint was virtually identical to that for a non-multiplexed FM system, indicating that the discontinuities had been effectively removed. It was found that the technique of over-compression of the TCM signal to create redundant message segments during the shaping intervals was superior to the system employing normal compression and equalisation at the receiver. The former system, with a frame period of 10ms and 5% raised cosine windowing was shown to require about 10-15% more

(normalised)bandwidth than an equivalent ordinary FM system due to the increase in compression ratio required.

It has been shown that a windowed TCM-FM system is a viable alternative to existing narrowband modulation techniques. It also has the potential to challenge other wideband systems, and has the particular advantage in this respect that all the technology required is well-proven. Major attractive features include the considerable reduction in base station equipment and the complete elimination of antenna combiners, and an overall increase in spectral efficiency since their is no need to employ inefficient intermodulation free frequency groups. Another significant advantage over digital speech systems is that it may be easily re-configured for an effective 12.5kHz per channel spectrum allocation by simply lowering the FM deviation. It remains for the system to be proven in a real environment where it will be necessary to adopt one of the multiplexed channels for frame synchronisation, possibly involving a maximal length Barker code and a correlator at the receiver.

APPENDIX A

THE DISCRETE FOURIER TRANSFORM (DFT) AND THE FAST FOURIER TRANSFORM (FFT)

A.1 THE DISCRETE FOURIER TRANSFORM

The discrete Fourier Transform, DFT, of the N-term complex sequence $(x_0,..x_n,..x_{N-1})$ is another N-term sequence $(X_0,..X_k,..X_{N-1})$ such that

$$X_k = \sum_{n=0}^{N-1} x_n \, e^{-j2\pi nk/N} \qquad (A.1)$$

If the first set of samples represent a complex, single valued function, x(t), over a period of T, then the transformed samples represent the sampled spectrum, X(f), at intervals of 1/T. Now X_k contains both positive and negative frequency samples such that k=1 to N/2+1 are positive, whilst the remainder are negative. Due to the finite interval of observation for x_k, X_n is also periodic such that $X_{(N+n)}=X_n$.

There also exists an inverse discrete Fourier Transform. This may be found [1] by taking the DFT of the conjugate of X_k, forming the conjugate of the result and scaling by 1/N, ie.

$$x_n = \frac{1}{N}\left[\sum_{k=0}^{N-1} X_k^* \, e^{-j2\pi nk/N}\right]^* \qquad (A.2)$$

A subroutine, DFT.for, written in Fortran 77 to evaluate the relatively simple algorithm of the DFT is shown in fig.A.1, which may be used for any value of N.

A.2 THE FAST FOURIER TRANSFORM

Evaluation of each individual X_k in the DFT involves N complex multiplications and N-1 complex additions. Hence the total number of computations for all points is N^2 multiplications and N(N-1) additions. However, by making use of symmetrical patterns of $e^{-jnk/N}$ and x_n products that occur in the evaluation, considerable savings in computational time may be achieved. Algorithms which exploit these symmetries are known as fast Fourier transform (FFT) algorithms. These algorithms are only efficient when N is not a prime number, ie. $N=r_1.r_2.r_3....r_m$ $m>1$, where r is known as the radix of the algorithm. The number of complex calculations is then proportional to $r_1+r_2+..r_m$. When all the r's are equal, the algorithm is known as fixed radix, and of these, the radix-2 is the most efficient which complies N to be a power of two.. In this latter case, the number of complex multiplications is reduced to $(N/2)\log_2 N/2$ and the number of complex additions to $N\log_2 N$. One of the best known examples of this type is the

Cooley-Tukey algorithm [1]. The subroutine, FFT.for, given in fig.A.2 is based on this algorithm. It has been found [2] that this algorithm is more efficient than the DFT when N exceeds 32.

A.3 DETERMINATION OF FM SPECTRA

The DFT and FFT may be readily used to rapidly and accurately calculate FM spectra. Consider the sinusoidally FM modulated carrier

$$e_{FM}(t) = \cos\left[2\pi f_c t + \frac{\Delta f}{f_m}\sin 2\pi f_m t\right] \qquad (A.3)$$

Since the power spectrum is symmetrical about the carrier and the samples from n=1 to N/2+1 represent the positive frequencies in the DFT, then the carrier frequency should be chosen to be $\frac{N/4+1}{T}$. In this case, the period of the composite FM signal, T, is equal to the period of the modulating signal, $1/f_m$, providing N/4+1 is an integer, ie. N=4,8 etc.. When the radix-2 FFT algorithm is used, this condition is always satisfied for $N \geq 4$. The choice of the exact value of N is often on a trail and error basis to ensure that the majority of spectral energy is contained within the N/2T bandwidth to avoid aliasing problems. However, too high a value for N leads to an unnecessary long computation time.

A.4 REFERENCES

(1) Geckinli,N.C., and Yavuz, D.'Discrete fourier transform and its application to power spectra estimation', chapter 2, Elsevier, 1983.

(2) Beauchamp,K.G. and Yuen,C.K.: 'Digital methods for signal analysis', chapter 3.8, George Allen and Unwin, 1979.

```
      subroutine DFT
c     Subroutine to find discrete complex N-term Fourier transform
c     of an N-term complex sequence stored in complex array X.
c     Upon return results are placed in array X.
      complex X,Y(10000),sum
c     Declare common block "sub" for variable N and complex array
c     X (10,000 elements).
      common /sub/X(10000),N
c     Set value of "tpi" to twice "pi".
      tpi=8*atan(1E0)
c     Begin loop for variable "ki"
      do 20 ki=1,N
c     Set complex value "sum" to zero.
      sum=cmplx(0E0,0E0)
c     Begin loop for variable "ni"
      do 10 ni=1,N
c     Form product "nk" reduced modulo N.
      nk=mod((ki-1)*(ni-1),N)
c     Form product X*(cos(arg)-jsin(arg)) where "arg"=nk*tpi/N.
      arg=nk*tpi/N
      sum=sum+cmplx(cos(arg),-sin(arg))*X(ni)
 10   continue
c     Set element "ki" in output array to "sum".
      Y(ki)=sum
 20   continue
c     Transfer results to original array X.
      do 30 i=1,N
      X(i)=Y(i)
 30   continue
      return
      end
```

Fig. A.1. Subroutine DFT.for.

```
      subroutine FFT
c     Single precision subroutine to take DFT of an N-term complex
c     sequence stored in the complex array X(N) efficiently using
c     the Cooley-Tukey radix-2, in-place, decimation-in-time
c     algorithm.
c     N=2**L2N and L2N are positive integers. Upon return result
c     replaces X(N).
      complex X,B,W
c     Declare common block "sub" for complex array X with 10,000
c     elements and variable N.
      common/sub/X(10000),N
c     Set value of 'pi'.
      pi=4*atan(1E0)
c     Set value of log2N.
      L2N=nint(log10(N*1E0)/log10(2E0))
      L=1
c     Loop to perform in-place bit-reversal shuffling of data.
      do 30 K=1,N-1
      if(K.GE.L) go to 10
      B=X(L)
      X(L)=X(K)
      X(K)=B
 10   M=N/2
 20   if(M.GE.L) go to 30
      L=L-M
      M=M/2
      go to 20
 30   L=L+M
      K=1
      do 50 L=1,L2N
      M=K
      BM=M
      K=2*K
      W=(1E0,0E0)
c     Loops to perform DFT calculations.
      do 50 J=1,M
      BJ=J
      do 40 I=J,N,K
      I2=I+M
      B=X(I2)*W
      X(I2)=X(I)-B
 40   X(I)=X(I)+B
      ARG=pi*BJ/BM
 50   W=cmplx(cos(ARG),-sin(ARG))
      return
      end
```

Fig. A.2. Subroutine FFT.for.

APPENDIX B

SPEC.for

```
      program spec
c     subroutine to evaluates FM spectrum for pseudo-random
c     noise modulation using a Monte Carlo procedure.
c     "M" tones in a 3kHz bandwidth are used and the result
c     is averaged over "inum" independent runs. "Beta" is
c     the ratio of rms frequency deviation
c     to the noise modulation bandwidth of 3kHz.
c     specify and dimension variables. Declare common block.
      character *16 filel
      dimension RC(0:200),RS(0:200),C(8200),S(8200),temp(0:100),
     &  spec(8200)
      complex X
      common /cfft/X(17000),N,L2N
c     prompt to terminal and read variables.
      read(5,*)N,L2N,period,beta,M,inum
      pi=4*atan(1E0)
c     open and rewind file "random" containing uniform random
c     phases.
c     set value of certain constants.
      con=2*pi
      incf=3000/M
      dt=period/N
c     calculate initial variables for pseudo-random noise samples
c     using efficient trigonometric series method of Watt
      RC(M+1)=0E0
      RS(M+1)=0E0
      RC(0)=0E0
      RS(0)=0E0
c     set fundamental noise component
      incf=3000/M
c     set sampling interval
      dt=period/N
c     initial arrays C(i) and S(i)
      do 6 i=1,N
      t=-period/2+i*dt
      C(i)=cos(con*amod(incf*t,1E0))
      S(i)=sin(con*amod(incf*t,1E0))
 6    continue
c     open file 'filel' for results
      open(4,file=filel,status='new')
      rewind(4)
c     begin loop for 'inum' independent random phase sets
      do 100 l=1,inum
c     calculate phase of FM carrier with pseudo-random noise
c     modulation consisting of M tones using method of Watt.
```

```
c       loop to calculate M pseudo-random phase angles using function
c       uniran sub program
        do 7 j=1,M
        ran=con*uniran(seed)
        RC(j)=cos(ran)/j
        RS(j)=sin(ran)/j
 7      continue
c       loop to calculate waveform samples over period starting at
c       -period/2
        do 10 i=1,N
        t=-period/2+i*dt
        phasel=0E0
        temp(M)=0E0
        temp(M-1)=RC(M-1)
        do 15 j=M-2,0,-1
        temp(j)=2*temp(j+1)*C(i)-temp(j+2)+RC(j)
 15     continue
        do 16 j=M-2,0,-1
        temp(j)=2*temp(j+1)*C(i)-temp(j+2)+RS(j)
 16     continue
c       normalise signal for correct rms frequency deviation
        phasel=beta*sqrt(2E0*M)*phasel
c       calculate values of FM signal using both in-phase and
c       quadrature carrier components (ie. using complex exponential
c       carrier) with carrier frequency equal to N/(4*period)
        j=mod(i,4)
        if(j.EQ.1) then
        X(i)=cmplx(sin(phasel),cos(phasel))
        elseif(j.EQ.2) then
        X(i)=cmplx(-cos(phasel),sin(phasel))
        elseif(j.EQ.3) then
        X(i)=cmplx(-sin(phasel),-cos(phasel))
        else
        X(i)=cmplx(cos(phasel),-sin(phasel))
        endif
 10     continue
c       call subroutine FFT to find FM spectrum
        call FFT
        total=0E0
c       loop to perform averaging of spectra and calculate
c       total power.
        do 20 i=1,N/2+1
        if(1.EQ.1) then
        spec(i)=real(X(i)*conjg(X(i)))
        else
        spec(i)=(spec(i)/(1-1)+real(X(i)*conjg(X(i))))/1
        if(1.EQ.inum) then
        total=total+spec(i)
        endif
        endif
 20     continue
```

```
 60     continue
c       loop to output N/2+1 averaged spectral components in
c       dB form.
       write(*,*)'Averaged spectral componenta are'
       do 30 i=1,N/2+1
       write(*,*)10*log10*spec(i)
 30    continue
c       loop to calculate 98% and 99% power bandwidths.
       sum=spec(N/4+1)
       do 40 k=1,N/4
       sum=sum+spec(N/4+1+k)+spec(N/4+1-k)
       if(sum.LE.0.98*total) then
       BW1=2*(k+1)/period
       endif
       if(sum.GE.0.99*total) then
       BW2=2*k/period
       goto 70
       endif
 40    continue
c       output bandwidths.
 70    write(4,*)'98%BW= ',BW1,'99%BW= ',BW2,
       end
```

APPENDIX C

RAND.for

```
      function uniran(seed)
c     produces random number in range (0,1) when given
c     seed and returns new seed.
      integer*4 B2E15,B2E16,HI15,HI31,low15,lowprd,modlus,
&     mult1,mult2,ovflow,seed
      data mult1,mult2 /24112,26143/
      data B2E15,B2E16,modlus /32768,65536,
&     2147483647/
      HI15=seed/B2E16
      lowprd=(seed-HI15*B2E16)*mult1
      low15=lowprd/B2E16
      HI31=HI15*mult1+low15
      ovflow=HI31/B2E15
      seed=(((lowprd-low15*B2E16)-modlus)
&     +(HI31-ovflow*B2E15)*B2E16)+ovflow
      if(seed.LT.0)seed=seed+modlus
      HI15=seed/B2E16
      lowprd=(seed-HI15*B2E16)*mult2
      low15=lowprd/B2E16
      HI31=HI15*mult2+low15
      ovflow=HI31/B2E15
      seed=(((lowprd-low15*B2E16)-modlus)
&     +(HI31-ovflow*B2E15)*B2E16)+ovflow
      if(seed.LT.0)seed=seed+modlus
      uniran=(2*(seed/256)+1)/16777216.0
      return
      end
```

APPENDIX D

FILTERING AND DEMODULATION OF FM SIGNALS USING THE DISCRETE FOURIER TRANSFORM

A.1 FILTERING

The effect of filtering upon an FM signal may be readily accounted for by multiplying each complex component in the frequency domain produced by the DFT by the corresponding complex filter coefficient. There is a slight additional complexity in that the negative frequency coefficients of the filter are also required. However, from the properties of the Fourier Transform, the frequency response of a network with a real time response is hermitian, ie. $X(-f)=X(f)^*$. Hence the complete response of any practical filter may be readily obtained using conjugation of the positive frequency components. This process is incorporated into the subroutine FILDEM1.for shown in fig.D.1, where the complex filter coefficients are contained in the array Y(i). Unlike the previous programme, SPECT.for, the full complex representation of the FM signal is used which permits an easier demodulation algorithm to be employed.

A.2 DEMODULATION

After the spectral components have been modified by the filter coefficients, an inverse discrete Fourier transform may be employed to recover the time-domain samples using the algorithm of Appendix A. These samples are of the form

$$X(n) = A_n \cos\left[2\pi f_c t_n + \theta(t_n)\right] + jA_n \sin\left[2\pi f_c t_n + \theta(t_n)\right] \tag{B.1}$$

For a sampled continuous signal, the output of an FM detector, $\dot{\theta}(t)$, may be expressed as

$$\dot{\theta}(t_n + \Delta t/2) = \frac{\theta(t_n + \Delta t) - \theta(t_n)}{\Delta t}$$

$$= \frac{\theta(t_{n+1}) - \theta(t_n)}{T/N} \tag{B.2}$$

ie. the resulting signal samples are obtained at points mid-way between the original signal samples.

Now

$$\text{real}\left[X(n).X(n)^*\right] = A_n A_{n+1} \cos\left[2\pi f_c(t_{n+1}-t_n)+\theta(t_{n+1})-\theta(t_n)\right] \tag{B.2}$$

and

$$A_n.A_{n+1} = \left[\text{real}\left[X(n).X(n)^*\right].\text{real}\left[X(n+1).X(n+1)^*\right]\right]^{1/2} \tag{B.4}$$

Therefore

$$\frac{\text{real}\left[X(n).X(n)^*\right]}{\left[\text{real}\left[X(n).X(n)^*\right] \cdot \text{real}\left[X(n+1).X(n+1)^*\right]\right]^{1/2}}$$

$$= \cos\left[2\pi f_c T/N + \theta(t_{n+1}) - \theta(t_n)\right]$$

$$= \cos\left[\pi/4 + \theta(t_{n+1}) - \theta(t_n)\right]$$

$$= -\sin\left[\theta(t_{n+1}) - \theta(t_n)\right] \qquad \text{(B.5)}$$

since $f_c = N/4T$.

Hence, the inverse sin function may be used to obtain the true demodulated output providing $\theta(t_{n+1}) - \theta(t_n) \leq \pm \pi/2$. For a sinusoidal input of frequency f_m with peak deviation Δf, the maximum value of $\theta(t_{n+1}) - \theta(t_n)$ is

$$\left[\theta(t_{n+1}) - \theta(t_n)\right]_{max} = \frac{2\Delta f}{f_m} \sin\frac{\pi}{N} \leq \pm\frac{\pi}{2} \qquad \text{(B.6)}$$

Hence, for example, with $\Delta f = \pm$ 5kHz and f_m = 100Hz, N must be greater than 4.

```
      program fildeml
c     program to calculate harmonic distortion in FM signal
c     with pseudo-rectangular RF filter and sinusoidal
c     modulation.
      complex X,value
c     declare common block with subroutine FFT.for.
      common /fft/X(17000),N,L2N
c     prompt to terminal and read input variables, no.of points,
c     modulation frequency, period and beta (= $ DELTA f $ /fm ).
      write(5,*)'Enter N,L2N,fm,period,beta
      read(6,*)N,L2N,fm,period,ratio,beta
c     set value of "con" to 2 $ pi $.
      con=8*atan(1E0)
c     calculate max. spectrum width and freq. step.
      span=0.5*N/period
      fstep=1/period
      dt=period/N
      open(4,file='results',status='new')
      rewind(4)
c     loop to form N time domain samples of FM signal.
      do 10 i=1,N
      t=-period/2+i*dt
      phase=beta*cos(con*amod(ratio*fm*t,1E0))
      j=mod(i,4)
      if(j.EQ.1) then
      X(i)=(sin(phase),cos(phase))
      elseif(j.EQ.2) then
      X(i)=(-cos(phase),sin(phase))
      elseif(j.EQ.3) then
      X(i)=(-sin(phase),-cos(phase))
      else
      X(i)=(cos(phase),-sin(phase))
      endif
 10   continue
c     call to FFT.for subroutine.
      call FFT
c     loop to multiply spectral components by filter coefficients
c     in array Y(i), and to conjugate result for IDFT.
      do 20 i=1,N
      X(i)=conjg(X(i)*Y(i))
 20   continue
c     call to FFT.for for IDFT.
      call FFT
c     conjugate results to complete IDFT
      do 25 i=1,N
      X(i)=conjg(X(i))/N
 25   continue
      value=X(1)
c     loop to recover distorted message signal.
      do 40 i=1,N-1
      X(i)=(asin(real(conjg(X(i))*X(i+1))/sqrt(real(X(i)
```

```
@       *conjg(X(i)))*real(X(i+1)*conjg(X(i+1)))),0)
 40     continue
        X(N)=(asin(real(conjg(X(N))*value)/sqrt(real(X(N)
@       *conjg(X(N)))*real(value*conjg(value)))),0)
c       output N time samples to terminal.
        write(*,*)'Recovered time samples are'
        do 45 i=1,N
        write(*,*)sqrt(real(X(i)*conjg(X(i))))
 45     continue
c       call to FFT.for to form demodulated spectrum
        call FFT
c       output N/2+1 spectral components in dB form to file
        write(4,*)'Demodulated signal spectrum components are'
        do 50 i=1,N/2+1
        write(*,*)10*log10(real(X(i)*conjg(X(i))))
 50     continue
        end
```

Fig.D.1. Subroutine FILDEM1.for

APPENDIX E

FILDEM2.for

```
      program fildem2
c     program to calculate intermodulation distortion in FM signal
c     with pseudo-rectangular RF filter using pseudo-random noise
c     modulation, at various baseband (slot) frequencies.
      character *5 filel
c     dimension arrays
      dimension RC(0:200),RS(0:200),C(8200),S(8200),temp(0:100),
     &  islot(10),temp2(0:65),amp(0:64),Y(0:1025)
      integer *4 seed
      complex X,value
c     declare common block 'cfft' (for FFT subroutine)
      common /cfft/X(17000),N,L2N
c     set value of con to '2 pi'
      con=8*atan(1E0)
c     input variables from terminal:
c     N=no.samples of waveform used,
c     period=period of FM signal,
c     beta=ratio rms frequency deviation to noise bandwidth,
c     B=rectangular filter half-bandwidth,
c     M=no. baseband noise components,
c     inum=no. independent runs used for averaging of results,
c     seed=integer seed for pseudo-random phase generator,
c     filel=results file.
      read(5,*)N,period,beta,B,M,inum,seed
      read(5,'(A)')filel
c     set L2N to log2 N
      L2N=nint(log10(real(N))/log10(2E0))
c     initialise array 'islot' with slot numbers
      islot(1)=1
      islot(2)=5
      islot(3)=10
      islot(4)=15
      islot(5)=20
      islot(6)=25
      islot(7)=30
c     find no. FM sidebands in filter BW
      iwidth=nint(aint(2*B*period))
c     calculate filter coefficients, Y(i), using 64-term cosine
c     series with weighting (Anuff and Liou method)
      amp(0)=1E0
      do 2 k=1,32
      amp(k)=8*sin(con*k/4)/(con*k)*((64-k)**3-4*(32-k)**3)
     &  /64E0**3
 2    continue
      do 3 k=33,64
```

```
      amp(k)=8*sin(con*k/4)/(con*k)*(64-k)**3/64E0**3
 3    continue
      temp(65)=0E0
      temp(64)=amp(64)
      do 4 i=0,iwidth
      CS=cos(con*0.25*i/(period*B))
      do 5 k=63,0,-1
      temp2(k)=2*temp2(k+1)*CS-temp2(k+2)+amp(k)
 5    continue
      Y(i)=temp2(0)-temp2(1)*CS-0.5
 4    continue
c     calculate initial variables for pseudo-random noise samples
c     using efficient trigonometric series method of Watt
      RC(M+1)=0E0
      RS(M+1)=0E0
      RC(0)=0E0
      RS(0)=0E0
c     set fundamental noise component
      incf=3000/M
c     set sampling interval
      dt=period/N
c     initial arrays C(i) and S(i)
      do 6 i=1,N
      t=-period/2+i*dt
      C(i)=cos(con*amod(incf*t,1E0))
      S(i)=sin(con*amod(incf*t,1E0))
 6    continue
c     open file 'file1' for results
      open(4,file=file1,status='new')
      rewind(4)
c     begin loop for slot positions
      do 200 nslot=1,7
      SDRT=0E0
      iout=0
c     begin loop for 'inum' independent random phase sets
      do 100 l=1,inum
c     calculate phase of FM carrier with pseudo-random noise
c     modulation consisting of M tones using method of Watt.
c     loop to calculate M pseudo-random phase angles using function
c     uniran sub program
      do 7 j=1,M
      ran=con*uniran(seed)
      RC(j)=cos(ran)/j
      RS(j)=sin(ran)/j
 7    continue
      do 8 j=1,M
      ran=con*uniran(seed)
      RC(M+1+j)=cos(ran)/j
      RS(M+1+j)=sin(ran)/j
 8    continue
c     loop to calculate waveform samples over period starting at
```

```
c       -period/2
        do 10 i=1,N
        t=-period/2+i*dt
        phase1=0E0
        temp(M)=0E0
        temp(M-1)=RC(M-1)
        do 15 j=M-2,0,-1
        temp(j)=2*temp(j+1)*C(i)-temp(j+2)+RC(j)
 15     continue
c       remove component at slot(nslot) from signal
        phase1=temp(0)-temp(1)*C(i)+RC(M)*cos(con*amod(M*incf*t,1E0
&       ))-RC(islot(nslot))*cos(con*amod(islot(nslot)*incf*t,1E0))
        temp(M-1)=RS(M-1)
        do 16 j=M-2,0,-1
        temp(j)=2*temp(j+1)*C(i)-temp(j+2)+RS(j)
 16     continue
        phase1=phase1-temp(1)*S(i)-RS(M)*sin(con*amod(M*incf*t,1E0
&       ))+RS(islot(nslot))*sin(con*amod(islot(nslot)*incf*t,1E0))
c       normalise signal for correct rms frequency deviation
        phase1=beta*sqrt(2E0*M)*phase1
c       calculate values of FM signal using both in-phase and
c       quadrature carrier components (ie. using complex exponential
c       carrier) with carrier frequency equal to N/(4*period)
        j=mod(i,4)
        if(j.EQ.1) then
        X(i)=cmplx(sin(phase1),cos(phase1))
        elseif(j.EQ.2) then
        X(i)=cmplx(-cos(phase1),sin(phase1))
        elseif(j.EQ.3) then
        X(i)=cmplx(-sin(phase1),-cos(phase1))
        else
        X(i)=cmplx(cos(phase1),-sin(phase1))
        endif
 10     continue
c       call subroutine FFT to find FM spectrum
        call FFT
c       loop to modify spectral components with filter coefficients
c       (note: only positive frequencies needed since complex exponential
c       carrier used)
        do 20 i=1,N
        if((i.LE.N/4+1+iwidth).AND.(i.GE.N/4+1-iwidth)) then
        if(i.GE.N/4+1) then
        X(i)=conjg(X(i)*cmplx(Y(i-N/4-1),0E0))
        else
        X(i)=conjg(X(i)*cmplx(Y(N/4+1-i),0E0))
        else
        X(i)=(0E0,0E0)
        endif
 20     continue
c       recover time domain samples after filtering
        call FFT
```

```
      do 25 i=1,N
      X(i)=conjg(X(i))/N
 25   continue
c     loop to frequency demodulate signal, using process of
c     Appendix B
      value=X(1)
      do 30 i=1,N-1
      X(i)=cmplx(asin(real(conjg(X(i))*X(i+1))/sqrt(real(X(i)*conjg
&     (X(i)))*real(X(i+1)*conjg(X(i+1)))),0E0)
 30   continue
      X(N)=cmplx(asin(real(conjg(X(N))*value)/sqrt(real(X(N)*conjg
&     (X(N)))*real(value*conjg(value)))),0E0)
c     calculate spectrum of demodulated signal
      call FFT
      power=0E0
c     loop to find average power in M-1 wanted components
      do 40 i=2,M+1
      write(6,*)i-1,real(X(i)*conjg(X(i)))
      if (i.NE.islot(nslot)+1)then
      power=power+real(X(i)*conjg(X(i)))
      endif
 40   continue
c     calculate average wanted signal power-to-power in 'free' slot
c     ie. signal-to-distortion ratio
      SDR=power/((M-1)*real(X(islot(nslot)+1)*conjg(X(islot(nslot)
&     +1))))
c     average result of above with previous runs
      SDRT=SDRT+1/SDR
c     output results if first run
      if(1.EQ.1) then
      write(4,*)'beta=',beta,'B=',B,'slot= ',islot(nslot),'l= ',l,
&     'average SDR=',-10*log10(SDRT/l)
      iout=iout+1
      endif
c     output result if run is 5,10,15...inum etc.
      if(l.EQ.iout*5) then
      write(4,*)'l= ',l,'average SDR=',-10*log10(SDRT/l)
      iout=iout+1
      endif
 100  continue
 200  continue
      end
```

APPENDIX F

COCHAN.for

```
      program cochan
c     program to calculate intermodulation distortion in FM signal
c     with a single co-channel interferer at various slot
c     frequencies. Both signals modulated with pseudo-random noise.
      character *5 file1
c     dimension arrays
      dimension RC(0:200),RS(0:200),C(8200),S(8200),temp(0:100),
&     islot(10)
      integer *4 seed
      complex X,value
c     declare common block "cfft" (for FFT subroutine)
      common /cfft/X(17000),N,L2N
c     set value of con to " 2 pi "
      con=8*atan(1E0)
c     input variables from terminal:
c     N=no. samples of waveform,
c     period=period of composite FM signal (ie. including
c     interferer),
c     beta1, beta2 =ratio of rms frequency deviation to noise
c     bandwidth for wanted and interfering signals respectively,
c     chan=level of interferer relative to wanted signal,
c     foff= interferer carrier frequency offset,
c     M= no. noise components,
c     inum= no. runs averaged,
c     seed=seed for uniran function,
c     file1=results file.
      read(5,*)N,period,beta1,beta2,chan,foff,M,inum,seed
      read(5,'(A)')file1
c     iset L2N to log2 N
      L2N=nint(log10(real(N))/log10(2E0))
c     initialise array "islot" with slot numbers
      islot(1)=1
      islot(2)=5
      islot(3)=10
      islot(4)=15
      islot(5)=20
      islot(6)=25
      islot(7)=30
c     calculate initial variables for pseudo-random noise samples
      RC(M+1)=0E0
      RS(M+1)=0E0
      RC(0)=0E0
      RS(0)=0E0
c     set fundamental noise component
      incf=3000/M
```

```
c       set sampling interval
        dt=period/N
        SDRT=0E0
c       initialise arrays C(i) and S(i)
        do 2 i=1,N
        t=-period/2+i*dt
        C(i)=cos(con*amod(incf*t,1E0))
        S(i)=sin(con*amod(incf*t,1E0))
 2      continue
c       open "file1" for results
        open(4,file=file1,status='new')
        rewind(4)
c       begin loop for slot positions
        do 200 nslot=1,7
        SDRT=0E0
        iout=0
c       begin loop for "inum" random phase sets
        do 100 l=1,inum
c       calculate carrier phase using efficient trigonometric series
c       method of Watt for both wanted and un-wanted signal.
c       loop to calculate pseudo-random phase angles using uniran
c       sub-program for wanted signal
        do 15 j=1,M
        ran=con*uniran(seed)
        RC(j)=cos(ran)/j
        RS(j)=sin(ran)/j
 15     continue
c       loop to calculate pseudo-random phase angles using uniran
c       sub-program for interfering signal signal
        do 16 j=1,M
        ran=con*uniran(seed)
        RC(M+1+j)=cos(ran)/j
        RS(M+1+j)=sin(ran)/j
 16     continue
c       loop to calculate waveform samples over "period" for both
c       signals
        do 10 i=1,N
        t=-period/2+i*dt
        phase1=0E0
        phase2=0E0
        temp(M)=0E0
        temp(M-1)=RC(M-1)
        do 5 j=M-2,0,-1
        temp(j)=2*temp(j+1)*C(i)-temp(j+2)+RC(j)
 5      continue
c       remove component at slot(nslot) from wanted signal
        phase1=temp(0)-temp(1)*C(i)+RC(M)*cos(con*amod(M*incf*t,1E0
&       ))-RC(islot(nslot))*cos(con*amod(islot(nslot)*incf*t,1E0))
        temp(M-1)=RS(M-1)
        do 6 j=M-2,0,-1
        temp(j)=2*temp(j+1)*C(i)-temp(j+2)+RS(j)
```

```
 6      continue
        phase1=phase1-temp(1)*S(i)-RS(M)*sin(con*amod(M*incf*t,1E0
&       ))+RS(islot(nslot))*sin(con*amod(islot(nslot)*incf*t,1E0))
        temp(M)=0E0
        temp(M-1)=RC(2*M)
        do 7 j=M-2,0,-1
        temp(j)=2*temp(j+1)*C(i)-temp(j+2)+RC(j+M+1)
 7      continue
        phase2=temp(0)-temp(1)*C(i)+RC(2*M+1)*cos(con*amod(M*incf*t
&       ,1E0))
        temp(M-1)=RS(2*M)
        do 8 j=M-2,0,-1
        temp(j)=2*temp(j+1)*C(i)-temp(j+2)+RS(j+M+1)
 8      continue
        phase2=phase2-temp(1)*S(i)-RS(2*M+1)*
&       sin(con*amod(M*incf*t,1E0))
c       normalise signals to obtain correct freq. deviation
        phase1=beta1*sqrt(2E0*M)*phase1
        phase2=beta2*sqrt(2E0*M)*phase2
        co1=chan*cos(con*amod((foff+N/(4*period))*t,1E0)-phase2)
        co2=chan*sin(con*amod((foff+N/(4*period))*t,1E0)-phase2)
c       calculate values of composite FM signal using complex
c       exponential carriers at N/(4*paeriod) and N/(4+period)+foff
c       respectively
        j=mod(i,4)
        if(j.EQ.1) then
        X(i)=cmplx(sin(phase1)+co1,cos(phase1)+co2)
        elseif(j.EQ.2) then
        X(i)=cmplx(-cos(phase1)+co1,sin(phase1)+co2)
        elseif(j.EQ.3) then
        X(i)=cmplx(-sin(phase1)+co1,-cos(phase1)+co2)
        else
        X(i)=cmplx(cos(phase1)+co1,-sin(phase1)+co2)
        endif
 10     continue
c       loop to frequency demodulate signal (Appendix B method)
        value=X(1)
        do 30 i=1,N-1
        X(i)=cmplx(asin(real(conjg(X(i))*X(i+1))/sqrt(real(X(i)
&       *conjg(X(i)))*real(X(i+1)*conjg(X(i+1))))),0E0)
 30     continue
        X(N)=cmplx(asin(real(conjg(X(N))*value)/sqrt(real(X(N)
&       *conjg(X(N)))*real(value*conjg(value)))),0E0)
c       calculate demodulated signal spectrum
        call FFT
        power=0E0
c       loop to find average power in M-1 wanted components
        do 40 i=2,M+1
        if (i.NE.islot(nslot)+1)then
        power=power+real(X(i)*conjg(X(i)))
        endif
```

```
 40     continue
c       calculate effective signal-to-distortion ratio
       SDR=power/((M-1)*real(X(islot(nslot)+1)*conjg(X(islot
&      (nslot)+1))))
       SDRT=SDRT+1/SDR
c       output results if first run
       if(1.EQ.1) then
       write(4,*)'offset=',foff,'amp=',chan,'slot= ',islot
&      (nslot),'l= ',1,'average SDR=',-10*log10(SDRT/1)
       iout=iout+1
       endif
c       output results if run=5,10,15...inum etc.
       if(1.EQ.iout*5) then
       write(4,*)'l= ',1,'average SDR=',-10*log10(SDRT/1)
       iout=iout+1
       endif
 100   continue
 200   continue
```

APPENDIX G

SINTCM.for

```
      program sintcm
c     program to calculate spectrum of TCM-FM signal with one
c     active channel and sinusoidal modulation
      character *6 file1
      dimension spec(8200)
      complex X,value
c     declare common block "cfft" (for FFT subroutine)
      common /cfft/X(17000),N,L2N
c     set value of con to " 2 pi "
      con=8*atan(1E0)
c     input variables from terminal:
c     N=no. samples of waveform,
c     fm=modulating frequency,
c     period=period of TCM-FM signal,
c     beta=ratio of peak frequency deviation to modulating
c     frequency,
c     ratio=TCM compression ratio,
c     span=frequency span for output spectrum (max.=N/(2*period)),
c     file1=results file.
      read(5,*)N,fm,period,beta,ratio,span
      read(5,'(A)')file1
c     set L2N to log2 N
      L2N=nint(log10(real(N))/log10(2E0))
c     open "file1" for results
      open(3,file=file1,status='new')
      dt=period/N
c     set initial phase for FM carrier
      omega=con/2*N/(4*ratio)-beta*cos(con*amod(-fm*period/2,1E0))
c     loop to calculate N/ratio carrier samples (ie. for active
c     channel)
      do 10 i=1,nint(N/ratio)
      t=-period/(2*ratio)+i*dt
      phase=omega+beta*cos(con*amod(ratio*fm*t,1E0))
      j=mod(i,4)
      if(j.EQ.1) then
      X(i)=cmplx(sin(phase),cos(phase))
      elseif(j.EQ.2) then
      X(i)=cmplx(-cos(phase),sin(phase))
      elseif(j.EQ.3) then
      X(i)=cmplx(-sin(phase),-cos(phase))
      else
      X(i)=cmplx(cos(phase),-sin(phase))
      endif
10    continue
      omega=omega+beta*cos(con*amod(fm*period/2,1E0))
```

```
c       loop to calculate remaining samples (ie. no modulation
c       present)
        do 15 i=1+nint(N/ratio),N
        j=mod(i,4)
        if(j.EQ.1) then
        X(i)=cmplx(sin(omega),cos(omega))
        elseif(j.EQ.2) then
        X(i)=cmplx(-cos(omega),sin(omega))
        elseif(j.EQ.3) then
        X(i)=cmplx(-sin(omega),-cos(omega))
        else
        X(i)=cmplx(cos(omega),-sin(omega))
        endif
 15     continue
c       call FFT subroutine to derive FM spectrum
        call FFT
c       find largest component in power spectrum
        peak=0E0
        do 30 i=1,N/2+1
        spec(i)=real(X(i)*conjg(X(i)))
        peak=amax1(peak,spec(i))
 30     continue
c       output scaled results (for plotter) using a 100dB power
c       scale with largest spectral component at 0dB
        write(3,*)nint(span*period)
        do 35 i=1,nint(span*period)+1
        write(3,*)nint(270+2200*(i-1)/(span*period)),',',nint(1450+
&       2.5E2*log10(amax1(spec(i)/peak,1E-5)))
 35     continue
        end
```

APPENDIX H

RANTCM.for

```
      program rantcm
c     program to calculate spectrum of TCM-FM signal with pseudo-
c     random noise modulation and all channels active, and derive
c     98/99% spectral power bandwidths.
      character *5 file1
c     dimension arrays
      dimension RC(0:990),RS(0:990),C(0:8200),S(0:8200),BW1(200)
&     temp(0:100),var(0:100),phase1(17000),spec(8200),CC(0:10),
&     SS(0:10),BW2(200)
      integer *4 seed,h,factor,fact2
      complex X
c     declare common block "cfft"
      common /cfft/X(17000),N,L2N
c     set con to "2 pi "
      con=8*atan(1E0)
c     input variables from terminal:
c     NN=no. samples of complete TCM-FM waveform,
c     frame=TCM frame period,
c     period=period of TCM-FM waveform,
c     beta=ratio of rms frequency deviation to iratio x noise
c     bandwidth,
c     iratio=TCM compression ratio=no. multiplexed channels,
c     M=no. noise components,
c     inum=no. independent runs averaged for final results,
c     seed1=seed for pseudo-random phase generator,
c     span=frequency span for output spectrum (max.=N/(2*period*
c     iratio)),
c     file1=results file.
      read(5,*)NN,frame,period,beta,iratio,M,inum,seed1,span
      read(5,'(A)')file1
c     set factor to ratio of TCM-FM period and TCM frame
      factor=nint(period/frame)
c     set NIR to number of samples per TCM segment
      NIR=NN/(iratio*factor)
c     set NF to iratio x NIR
      NF=NN/factor
c     set fundamental noise frequency
      incf=3000/M
      fact2=nint(period*incf)
c     set sampling interval
      dt=period/NN
c     initialise arrays C(i) and S(i)
      do 1 i=1,NN/iratio
      t=-frame/(2*iratio)+(i-0.5)*dt
      C(i)=cos(con*amod(iratio*incf*t,1E0))
```

```
      S(i)=sin(con*amod(iratio*incf*t,1E0))
 1    continue
      do 2 h=0,factor-1
      t=-frame/(2*iratio)+h*NIR*dt
      CC(h)=cos(con*amod(iratio*incf*t,1E0))
      SS(h)=sin(con*amod(iratio*incf*t,1E0))
 2    continue
c     open "file1" for results
      open(4,file=file1,status='new')
      rewind(4)
      iout=1
      seed=seed1
c     begin loop for "inum" independent phase sets
      do 100 l=1,inum
c     set parameters in common block for FFT
      N=NN
      L2N=log10(real(NN))/log10(2E0)
c     loop to calculate pseudo-random phase angles using
c     function uniran
      do 3 k=0,iratio-1
      RC(k*(M+1))=0E0
      RS(k*(M+1))=0E0
      do 4 j=1,M
      ran=con*uniran(seed)
      RC(k*(M+1)+j)=cos(ran)*iratio*incf*con
      RS(k*(M+1)+j)=sin(ran)*iratio*incf*con
 4    continue
 3    continue
c     loops to calculate complex exponential carrier phase angles
c     segment by segment using efficient trigonometric series method
c     of Watt
      const=0E0
      do 10 h=0,factor-1
      do 12 k=0,iratio-1
      do 14 i=1,NIR
      itemp=h*NIR+i
      ktemp=h*NF+k*NIR+i
      t=-frame/(2*iratio)+dt*(ktemp-0.5)
      temp(M+1)=0E0
      temp(M)=RS((k+1)*M)
      do 5 j=M-1,0,-1
      temp(j)=2*temp(j+1)*C(itemp)-temp(j+2)+RS(k*(M+1)+j)
 5    continue
      phase=temp(0)-temp(1)*C(itemp)
      temp(M)=RC((k+1)*M)
      do 6 j=M-1,0,-1
      temp(j)=2*temp(j+1)*C(itemp)-temp(j+2)+RC(k*(M+1)+j)
 6    continue
      phase=phase+temp(1)*S(itemp)
      if(ktemp.EQ.1) then
      phase1(ktemp)=dt*phase
```

```
      else
      phasel(ktemp)=phasel(ktemp-1)+dt*phase
      endif
 14   continue
 12   continue
 10   continue
      const=phasel(N)
c     loop to normalise phase angles for correct freq. deviation
c     and calculate carrier samples
      do 20 i=1,N
      phasel(i)=-(phasel(i)-i*const/N)*beta*sqrt(2E0*M)
      j=mod(i,4)
      if(j.EQ.1) then
      X(i)=cmplx(sin(phasel(i)),cos(phasel(i)))
      elseif(j.EQ.2) then
      X(i)=cmplx(-cos(phasel(i)),sin(phasel(i)))
      elseif(j.EQ.3) then
      X(i)=cmplx(-sin(phasel(i)),-cos(phasel(i)))
      else
      X(i)=cmplx(cos(phasel(i)),-sin(phasel(i)))
      endif
 20   continue
c     call FFT to obtain FM spectrum
      call FFT
c     loop to calculate total spectral power and value of
c     largest component
      peak=0E0
      total=0E0
c     loop to average spectrum with previous runs
      do 30 i=1,N/2+1
      X(i)=cmplx(real(X(i)*conjg(X(i))),0E0)
      peak=amax1(peak,real(X(i)))
      total=total+real(X(i))
      if(1.EQ.1) then
      spec(i)=real(X(i))
      else
      spec(i)=spec(i)+real(X(i))
      endif
 30   continue
c     loop to calculate 98% spectral power bandwidth and average
c     result with previous runs
      do 35 k=0,N/4
      if(k.EQ.0) then
      sum=real(X(N/4+1))
      else
      sum=sum+real(X(N/4+1+k))+real(X(N/4+1-k))
      endif
      if(sum.GE.0.98*total) then
      if(1.EQ.1) then
      BW1(1)=2*k/period
      else
```

```
      BW1(1)=(BW1(1-1)*(1-1)+2*k/period)/1
      endif
      goto 70
      endif
 35   continue
c     loop to calculate 99% spectral power bandwidth and average
c     result with previous runs
 70   do 40 k=0,N/4
      if(k.EQ.0) then
      sum=real(X(N/4+1))
      else
      sum=sum+real(X(N/4+1+k))+real(X(N/4+1-k))
      endif
      if(sum.GE.0.99*total) then
      if(l.EQ.1) then
      BW2(1)=2*k/period
      else
      BW2(1)=(BW2(1-1)*(1-1)+2*k/period)/1
      endif
      goto 75
      endif
 40   continue
c     output final values for 98/99% power bandwidths
 75   if(l.EQ.inum) then
      write(4,*)'98%BW= ',BW1(1),'99%BW= ',BW2(1),'l=',l,'beta= '
&     ,beta,'M=',M
      peak2=0E0
      do 50 i=1,N/2+1
      spec(i)=spec(i)/inum
      peak2=amax1(peak2,spec(i))
 50   continue
c     output final scaled spectrum results (100dB range with largest
c     component at 0dB)
      do 55 i=1,nint(span*period)
      write(4,*)nint(270+2200*(i-1)/(span*period)),',',nint(1450+
&     1.25E2*log10(amax1(spec(i)/peak2,1E-10)))
 55   continue
      endif
 100  continue
      close(4)
      end
```

APPENDIX I

FILDEM3.for

```
      program fildem
c     program to calculate intermodulation distortion in TCM-FM
c     signal with pseudo-rectangular RF filter using pseudo-
c     random noise modulation, t various baseband (slot)
c     frequencies. All TCM channels active.
      character *5 filel
c     dimension arrays
      dimension RC(0:990),RS(0:990),C(0:8200),S(0:8200),
&     temp(0:100),islot(10),temp2(0:65),amp(0:64),Y(0:4097)
      integer *4 seed,h,factor,fact2
      complex X,value,chan(0:10)
c     declare common block "cfft"
      common /cfft/X(17000),N,L2N
      con=8*atan(1E0)
c     input variables from terminal:
c     NN=no. samples of waveform,
c     frame=TCM frame period,
c     period=period of TCM-FM waveform,
c     beta=ratio of rms frequency deviation to iratio x noise
c     bandwidth,
c     B=rectangular filter half-bandwidth,
c     iratio=TCM compression ratio,
c     M=no. noise components,
c     inum=no. of runs averaged for final results,
c     seed1=seed for pseudo-random phase generator (uniran),
c     filel=results file.
      read(5,*)NN,frame,period,beta,B,iratio,M,inum,seed1
      read(5,'(A)')filel
c     initialise array "islot" with slot numbers
      islot(1)=1
      islot(2)=5
      islot(3)=10
      islot(4)=15
      islot(5)=20
      islot(6)=25
      islot(7)=30
c     set "factor" to ratio of TCM-FM period to TCM frame
      factor=nint(period/frame)
c     set fundamental noise frequency
      incf=3000/M
      fact2=nint(period*incf)
c     set sampling interval
      dt=period/NN
c     find no. sidebands of TCM-FM signal in filter BW
      iwidth=nint(aint(2*B*period))
```

```
c       calculate filter coefficients, Y(i), using 64-term weighted
c       cosine series (from Anuff and Liou)
        amp(0)=1E0
        do 2 k=1,32
        amp(k)=8*sin(con*k/4)/(con*k)*((64-k)**3-4*(32-k)**3)/64E0**3
 2      continue
        do 3 k=33,64
        amp(k)=8*sin(con*k/4)/(con*k)*(64-k)**3/64E0**3
 3      continue
        do 4 i=0,iwidth
        CS=cos(con*0.25*i/(period*B))
        do 5 k=63,0,-1
        temp2(k)=2*temp2(k+1)*CS-temp2(k+2)+amp(k)
 4      continue
        Y(i)=temp2(0)-temp2(1)*CS-0.5
 5      continue
c       initialise arrays C(i) and S(i)
        do 6 i=0,NN/iratio
        t=-frame/(2*ratio)+i*dt
        C(i)=cos(con*amod(iratio*incf*t,1E0))
        S(i)=sin(con*amod(iratio*incf*t,1E0))
 6      continue
c       open "file1" for results output
        open(4,file=file1,status='new')
        rewind(4)
c       begin loop for slot positions
        do 200 nslot=1,7
        iout=1
        seed=seed1
        SDRT=0E0
c       begin loop for "inum" independent random phase sets
        do 100 l=1,inum
c       set N and L2N to NN and log2 NN respectively for FFT
c       subroutine
        N=NN
        L2N=log10(real(NN))/log10(2E0)
c       loop to calculate M pseudo-random phase angles using
c       function "uniran"
        do 7 k=0,iratio-1
        RC(k*(M+1))=0E0
        RS(k*(M+1))=0E0
        do 8 j=1,M
        ran=con*uniran(seed)
        RC(k*(M+1)+j)=cos(ran)/j
        RS(k*(M+1)+j)=sin(ran)/j
 8      continue
 7      continue
        const=0E0
c       calculate carrier phase angles (Watt method), one TCM
c       segment at a time
        do 10 h=0,factor-1
```

```
      do 12 k=0,iratio-1
      do 14 i=1,N/(iratio*factor)
      itemp=h*N/(iratio*factor)+i
      t=-frame/(2*iratio)+itemp*dt
      ktemp=h*N/factor+k*N/(iratio*factor)+i
      temp(M+1)=0E0
      temp(M)=RC((k+1)*M)
      do 15 j=M-1,0,-1
      temp(j)=2*temp(j+1)*C(itemp)-temp(j+2)+RC(k*(M+1)+j)
 15   continue
      phasel=temp(0)-temp(1)*C(itemp)
      temp(M)=RS((k+1)*M)
      do 16 j=M-1,0,-1
      temp(j)=2*temp(j+1)*C(itemp)-temp(j+2)+RS(k*(M+1)+j)
 16   continue
      phasel=phasel-temp(1)*S(itemp)
c     remove component at slot(nslot) from first channel signal
      if(k.EQ.0) then
      phasel=phasel
&     -RC(k*(M+1)+islot(nslot))*cos(con*amod(iratio*islot(nslot)*
&     incf*t,1E0))+RS(k*(M+1)+islot(nslot))*sin(con*amod(iratio*
&     islot(nslot)*incf*t,1E0))
      endif
c     calculate offsets to ensure no step discontinuity in
c     phase waveform at segment boundaries
      if(i.EQ.1) then
      temp(M+1)=0E0
      temp(M)=RC((k+1)*M)
      do 18 j=M-1,0,-1
      temp(j)=2*temp(j+1)*C(itemp-1)-temp(j+2)+RC(k*(M+1)+j)
 18   continue
      offset=temp(0)-temp(1)*C(itemp-1)
      temp(M)=RS((k+1)*M)
      do 19 j=M-1,0,-1
      temp(j)=2*temp(j+1)*C(itemp-1)-temp(j+2)+RS(k*(M+1)+j)
 19   continue
      offset=offset-temp(1)*S(itemp-1)
      const=const-offset
c     modify offsets for channel 1 segments to allow for free slot
      if(k.EQ.0) then
      const=const+RC(k*(M+1)+islot(nslot))*cos(con*amod(iratio*islot
&     (nslot)*incf*(t-dt),1E0))-RS(k*(M+1)+islot(nslot))*sin(con*
&     amod(iratio*islot(nslot)*incf*(t-dt),1E0))
      chan(h)=cmplx(cos(beta*sqrt(2E0*M)*const),-sin(beta*sqrt(2E0*
&     M)*const))
      endif
      endif
c     normalise phase samples for correct freq. dev.
      phase2=beta*sqrt(2E0*M)*(phasel+const)
c     calculate carrier waveform using complex exponential carrier
c     at frequency N/(4*period)
```

```
      j=mod(ktemp,4)
      if(j.EQ.1) then
      X(ktemp)=cmplx(sin(phase2),cos(phase2))
      elseif(j.EQ.2) then
      X(ktemp)=cmplx(-cos(phase2),sin(phase2))
      elseif(j.EQ.3) then
      X(ktemp)=cmplx(-sin(phase2),-cos(phase2))
      else
      X(ktemp)=cmplx(cos(phase2),-sin(phase2))
      endif
      if(i.EQ.N/(iratio*factor)) then
      const=const+phase1
      endif
 14   continue
 12   continue
 10   continue
c     find TCM-FM spectrum
      call FFT
c     modify spectral components by filter coefficients (note:
c     only positive frequencies modified)
      do 29 i=1,N
      if((i.LE.N/4+1+iwidth).AND.(i.GE.N/4+1-iwidth)) then
      if(i.GE.N/4+1) then
      X(i)=conjg(X(i)*cmplx(Y(i-N/4-1),0E0))
      else
      X(i)=conjg(X(i)*cmplx(Y(N/4+1-i),0E0))
      endif
      else
      X(i)=(0E0,0E0)
      endif
 29   continue
c     recover time-domain samples
      call FFT
      do 25 i=1,N
      X(i)=conjg(X(i))/N
 25   continue
c     loops to frequency demodulate TCM-FM signal, using process
c     of AppendixB.
      value=X(1)
      do 30 h=0,factor-1
      do 40 i=1,N/(factor*iratio)-1
      ktemp=h*N/factor+i
      itemp=h*N/(factor*iratio)+i
      X(itemp)=cmplx(asin(real(conjg(X(ktemp))*X(ktemp+1))/sqrt
&     (real(X(ktemp)*conjg(X(ktemp)))*real(X(ktemp+1)*conjg
&     (X(ktemp+1)))))),0E0)
 40   continue
c     algorithm to prevent discontinuities in output across
c     segment boundaries
      if(h.NE.factor-1) then
      ktemp=(h*N/factor+N/(factor*iratio))
```

```
      jtemp=((h+1)*N/factor+1)
      X((h+1)*N/(factor*iratio))=cmplx(asin(real((conjg(X(ktemp
&     ))*chan(h))*(X(jtemp)*conjg(chan(h+1))))
&     /sqrt(real(X(ktemp)*conjg(X(ktemp)))*real(X(jtemp)*
&     conjg(X(jtemp)))),0E0)
      else
      ktemp=((factor-1)*N/factor+N/(iratio*factor))
      X(N/iratio)=cmplx(asin(real((conjg(X(ktemp))*chan(h))*(value*
&     conjg(chan(0))))/sqrt(real(X(ktemp)
&     *conjg(X(ktemp)))*real(value*conjg(value)))),0E0)
      endif
 30   continue
c     redefine parameters for FFT subroutine such that no. samples
c     is now just those for one TCM channel
      N=NN/iratio
      L2N=log10(real(N))/log10(2E0)
c     find demodulated spectrum for channel one
      call FFT
c     calculate effective signal-to-distortion ratio
      power=0E0
      do 90 i=fact2+1,fact2*M+1,fact2
      if (i.NE.fact2*islot(nslot)+1)then
      power=power+real(X(i)*conjg(X(i)))
      endif
 90   continue
c     average above result with those from previous runs
      SDR=power/((M-1)*real(X(fact2*islot(nslot)+1)*conjg(X(fact2*
&     islot(nslot)+1))))
      SDRT=SDRT+1/SDR
c     output results if first run
      if(1.EQ.1) then
      write(4,*)'beta=',beta,'B=',B,'slot= ',islot(nslot),'l= ',l,
&     'average SDR=',-10*log10(SDRT)
      endif
c     output results if run =5,10,....inum etc.
      if(1.EQ.iout*5) then
      write(4,*)'average SDR=',-10*log10(SDRT/1)
      iout=iout+1
      endif
 100  continue
 200  continue
      close(4)
      end
```

APPENDIX E

COCHAN2.for

```
      program cotcm
c     program to calculate intermodulation distortion in TCM-FM
c     signal with a single co-channel interferer. Both signals
c     modulated with pseudo-random noise modulation. Calculation
c     performed at several baseband frequencies.
      character *5 file1
c     dimension arrays
      dimension RC(0:990),RS(0:990),C(0:8200),S(0:8200),
&     temp(0:100),islot(10),RC2(0:990),RS2(0:990)
      integer *4 seed,h,factor,fact2
c     declare common block "cfft"
      complex X,value,chan(0:10)
      common /cfft/X(17000),N,L2N
      con=8*atan(1E0)
c     input variables from terminal:
c     NN=no. samples of waveform,
c     frame=TCM frame period,
c     period=TCM-FM period,
c     beta1, beta2=ratio of rms frequency deviation to iratio x
c     noise bandwidth for wanted and co-channel signals
c     respectively,
c     iratio=TCM compression ratio,
c     foff=interferer carrier frequency offset,
c     xmag=level of interferer relative to wanted signal,
c     M=no. noise samples,
c     inum=no. independent phase sets averaged for final results,
c     seed1=seed for pseudo-random phase generator,
c     file1=results file.
      read(5,*)NN,frame,period,beta1,beta2,iratio,foff,xmag,M,
&     inum,seed1
      read(5,'(A)')file1
c     initialise array "islot" with slot numbers
      islot(1)=1
      islot(2)=5
      islot(3)=10
      islot(4)=15
      islot(5)=20
      islot(6)=25
      islot(7)=30
c     factor is ratio of TCM-FM period to TCM frame duration
      factor=nint(period/frame)
c     set fundamental noise frequency
      incf=3000/M
      fact2=nint(period*incf)
c     set sampling interval
```

```
      dt=period/NN
c     initialise arrays C(i) and S(i)
      do 2 i=0,NN/iratio
      t=-frame/(2*ratio)+i*dt
      C(i)=cos(con*amod(ratio*incf*t,1E0))
      S(i)=sin(con*amod(ratio*incf*t,1E0))
 2    continue
c     open "file1" for results
      open(4,file=file1,status='new')
      rewind(4)
c     begin loop for slot positions
      do 200 nslot=1,7
      iout=1
      seed=seed1
      SDRT=0E0
c     begin loop for "inum" independent random phase sets
      do 100 l=1,inum
c     set N and L2N to NN and log2 NN respectively for FFT
c     subroutine
      N=NN
      L2N=log10(real(NN))/log10(2E0)
c     calculate M pseudo-random phase angles using function
c     "uniran" for both wanted and interfering signals
      do 3 k=0,iratio-1
      RC(k*(M+1))=0E0
      RS(k*(M+1))=0E0
      do 4 j=1,M
      ran=con*uniran(seed)
      RC(k*(M+1)+j)=cos(ran)/j
      RS(k*(M+1)+j)=sin(ran)/j
 4    continue
 3    continue
      do 5 k=0,iratio-1
      RC2(k*(M+1))=0E0
      RS2(k*(M+1))=0E0
      do 6 j=1,M
      ran=con*uniran(seed)
      RC2(k*(M+1)+j)=cos(ran)/j
      RS2(k*(M+1)+j)=sin(ran)/j
 6    continue
 5    continue
      const=0E0
c     calculate carrier phase angles (Watt method), one segment
c     at a time. "phase" is wanted signal, "angle" is interferer
      do 10 h=0,factor-1
      do 12 k=0,iratio-1
      do 14 i=1,N/(iratio*factor)
      itemp=h*N/(iratio*factor)+i
      t=-frame/(2*ratio)+itemp*dt
      ktemp=h*N/factor+k*N/(iratio*factor)+i
      temp(M+1)=0E0
```

```
      temp(M)=RC((k+1)*M)
      do 7 j=M-1,0,-1
      temp(j)=2*temp(j+1)*C(itemp)-temp(j+2)+RC(k*(M+1)+j)
 7    continue
      phase1=temp(0)-temp(1)*C(itemp)
      temp(M)=RS((k+1)*M)
      do 8 j=M-1,0,-1
      temp(j)=2*temp(j+1)*C(itemp)-temp(j+2)+RS(k*(M+1)+j)
 8    continue
      phase1=phase1-temp(1)*S(itemp)
      temp(M)=RC2((k+1)*M)
      do 15 j=M-1,0,-1
      temp(j)=2*temp(j+1)*C(itemp)-temp(j+2)+RC2(k*(M+1)+j)
 15   continue
      angle1=temp(0)-temp(1)*C(itemp)
      temp(M)=RS2((k+1)*M)
      do 16 j=M-1,0,-1
      temp(j)=2*temp(j+1)*C(itemp)-temp(j+2)+RS2(k*(M+1)+j)
 16   continue
      angle1=angle1-temp(1)*S(itemp)
c     remove frequency at islot(nslot) from channel one of
c     wanted signal
      if(k.EQ.0) then
      phase1=phase1
&     -RC(k*(M+1)+islot(nslot))*cos(con*amod(ratio*islot(nslot)*
&     incf*t,1E0))+RS(k*(M+1)+islot(nslot))*sin(con*amod(ratio*
&     islot(nslot)*incf*t,1E0))
      endif
c     calculate offsets to ensure no step discontinuity in phase
c     at segment boundaries (wanted signal)
      if(i.EQ.1) then
      temp(M+1)=0E0
      temp(M)=RC((k+1)*M)
      do 20 j=M-1,0,-1
      temp(j)=2*temp(j+1)*C(itemp-1)-temp(j+2)+RC(k*(M+1)+j)
 20   continue
      offset=temp(0)-temp(1)*C(itemp-1)
      temp(M)=RS((k+1)*M)
      do 22 j=M-1,0,-1
      temp(j)=2*temp(j+1)*C(itemp-1)-temp(j+2)+RS(k*(M+1)+j)
 22   continue
      offset=offset-temp(1)*S(itemp-1)
      const=const-offset
      temp(M)=RC2((k+1)*M)
c     calculate offsets to ensure no step discontinuity in phase
c     at segment boundaries (un-wanted signal)
      do 24 j=M-1,0,-1
      temp(j)=2*temp(j+1)*C(itemp-1)-temp(j+2)+RC2(k*(M+1)+j)
 24   continue
      off2=temp(0)-temp(1)*C(itemp-1)
      temp(M)=RS2((k+1)*M)
```

```
      do 26 j=M-1,0,-1
      temp(j)=2*temp(j+1)*C(itemp-1)-temp(j+2)+RS2(k*(M+1)+j)
 26   continue
      off2=off2-temp(1)*S(itemp-1)
      const2=const2-off2
c     modify offsets for channel one of wanted signal to allow
c     for vacant slot
      if(k.EQ.0) then
      const=const+RC(k*(M+1)+islot(nslot))*cos(con*amod(ratio*
&     islot(nslot)*incf*(t-dt),1E0))-RS(k*(M+1)+islot(nslot))*
&     sin(con*amod(ratio*islot(nslot)*incf*(t-dt),1E0))
      chan(h)=cmplx(cos(beta*sqrt(2E0*M)*const),-sin(beta*sqrt
&     (2E0*M)*const))
      endif
      endif
c     normalise "phase" and "angle" to achieve correct freq. dev
      phase2=beta1*sqrt(2E0*M)*(phase1+const)
      angle2=beta2*sqrt(2E0*M)*(angle1+const2)
      tnew=-frame/(2*ratio)+ktemp*dt
c     calculate complex exponential carrier samples for un-wanted
c     signal (carrier freq. =N/(4*period)+foff)
      col=xmag*cos(con*amod((foff+N/(4*period))*tnew,1E0)-angle2)
      co2=xmag*sin(con*amod((foff+N/(4*period))*tnew,1E0)-angle2)
c     calculate complex exponential carrier samples for wanted
c     signal (carrier freq. =N/(4*period))
      j=mod(ktemp,4)
      if(j.EQ.1) then
      X(ktemp)=cmplx(sin(phase2)+col,cos(phase2)+co2)
      elseif(j.EQ.2) then
      X(ktemp)=cmplx(-cos(phase2)+col,sin(phase2)+co2)
      elseif(j.EQ.3) then
      X(ktemp)=cmplx(-sin(phase2)+col,-cos(phase2)+co2)
      else
      X(ktemp)=cmplx(cos(phase2)+col,-sin(phase2)+co2)
      endif
      if(i.EQ.N/(iratio*factor)) then
      const2=const2+angle1
      const=const+phase1
      endif
 14   continue
 12   continue
 10   continue
c     loops to frequency demodulate TCM-FM signal, using process
c     of Appendix B
      value=X(1)
      do 30 h=0,factor-1
      do 40 i=1,N/(factor*iratio)-1
      ktemp=h*N/factor+i
      itemp=h*N/(factor*iratio)+i
      X(itemp)=cmplx(asin(real(conjg(X(ktemp))*X(ktemp+1))/sqrt
&     (real(X(ktemp)*conjg(X(ktemp)))*real(X(ktemp+1)*conjg
```

```
&       (X(ktemp+1))))),0E0)
 40     continue
c       algorithm to prevent discontinuities in output across segment
c       boundaries
        if(h.NE.factor-1) then
        ktemp=(h*N/factor+N/(factor*iratio))
        jtemp=((h+1)*N/factor+1)
        X((h+1)*N/(factor*iratio))=cmplx(asin(real((conjg(X(ktemp))*
&       chan(h))*(X(jtemp)*conjg(chan(h+1))))/sqrt(real(X(ktemp)*
&       conjg(X(ktemp)))*real(X(jtemp)*conjg(X(jtemp))))),0E0)
        else
        ktemp=((factor-1)*N/factor+N/(iratio*factor))
        X(N/iratio)=cmplx(asin(real((conjg(X(ktemp))*chan(h))*(value*
&       conjg(chan(0))))/sqrt(real(X(ktemp)
&       *conjg(X(ktemp)))*real(value*conjg(value)))),0E0)
        endif
 30     continue
c       redefine parameters for FFT subroutine (samples of a
c       single channel)
        N=NN/iratio
        L2N=log10(real(N))/log10(2E0)
c       get demodulated signal output spectrum
        call FFT
c       calculate effective signal-to-noise ratio
        power=0E0
        do 90 i=fact2+1,fact2*M+1,fact2
        if (i.NE.fact2*islot(nslot)+1)then
        power=power+real(X(i)*conjg(X(i)))
        endif
 90     continue
c       average above result with those from previous runs
        SDR=power/((M-1)*real(X(fact2*islot(nslot)+1)*conjg(X(fact2*
&       islot(nslot)+1))))
        SDRT=SDRT+1/SDR
c       output results if first run
        if(1.EQ.1) then
        write(4,*)'beta=',beta,'amp=',xmag,'offset=',foff,'slot= ',
&       islot(nslot),'l= ',1,'average SDR=',-10*log10(SDRT)
        endif
c       output results if run =5,10,15...inum etc.
        if(1.EQ.iout*5) then
        write(4,*)'l= ',1,'average SDR=',-10*log10(SDRT/1)
        iout=iout+1
        endif
 100    continue
 200    continue
        close(4)
        end
```

APPENDIX K

WTCM1.for

```
      program wtcm
c     program to calculate spectrum of windowed TCM-FM signal
c     with pseudo-random noise modulation and all channels
c     active, and derive 98/99% spectral power bandwidths.
c     windowing is either 3-coefficient, Papoulis or Parzen.
c     both simple and over-compressed TCM-FM systems may be
c     analysed
      character *5 file1,sel1,sel2
c     dimension arrays
      dimension RC(0:990),RS(0:990),C(0:8200),S(0:8200),
&     temp(0:100),var(0:100),phase1(17000),spec(8200),CC(0:10),
&     SS(0:10),BW1(200),BW2(200)
      integer *4 seed,h,factor,fact2,chan
      complex X
c     declare common block "cfft"
      common /cfft/X(17000),N,L2N
      con=8*atan(1E0)
c     input variables from terminal:
c     NN=no. samples of waveform,
c     frame=TCM frame period,
c     period=TCM-FM period,
c     beta=ratio of rms frequency deviation to iratio x
c     noise bandwidth,
c     iss=no. samples in each segment to which windowing is
c     applied,
c     coeff=parameter for 3-coefficient windowing,
c     chan=no. multiplexed channels in TCM-FM system
c     (= compression ratio in simple TCM system),
c     M=no. noise components,
c     inum=no. independent runs averaged for final results,
c     seed1=seed for pseudo-random phase generator,
c     spqn=frequency span for output spectrum,
c     file1=results file,
c     sel1=character variable to select type of windowing
c     (="coef", for 3-coeff., "pap", for Papoulis and
c     "par" for Parzen),
c     sel2=character variable to select type of system
c     ('ord' for simple system and "over" for over-compressed
c     system
      read(5,*)NN,frame,period,beta,iss,coeff,chan,M,inum,seed1
&     ,span
      read(5,'(A)')file1
      read(5,'(A)')sel1
      read(5,'(A)')sel2
      factor=nint(period/frame)
```

```
      NIR=NN/(chan*factor)
      NF=NN/factor
      incf=3000/M
      fact2=nint(period*incf)
      dt=period/N
c     calculate appropriate compression ratio
      if(sel2.EQ.'ord') then
      iratio=chan
      elseif(sel2.EQ.'over') then
      iratio=chan*real(NIR)/(NIR-2*iss)
      endif
c     initialise arrays C(i) and S(i)
      do 3 i=1,NN/chan
      t=-frame/(2*chan)+(i-0.5)*dt
      C(i)=cos(con*amod(iratio*incf*t,1E0))
      S(i)=sin(con*amod(iratio*incf*t,1E0))
 3    continue
      do 4 h=0,factor-1
      t=-frame/(2*chan)+h*NIR*dt
      CC(h)=cos(con*amod(iratio*incf*t,1E0))
      SS(h)=sin(con*amod(iratio*incf*t,1E0))
 4    continue
c     open "file1" for results
      open(4,file=file1,status='new')
      rewind(4)
      iout=1
      seed=seed1
      SDRT=0E0
c     begin loop for "inum" independent runs
      do 100 1=1,inum
c     set parameters in common block for FFT subroutine
      N=NN
      L2N=log10(real(NN))/log10(2E0)
c     calculate pseudo-random phase angles
      do 5 k=0,chan-1
      RC(k*(M+1))=0E0
      RS(k*(M+1))=0E0
      do 6 j=1,M
      ran=con*uniran(seed)
      RC(k*(M+1)+j)=cos(ran)*iratio*incf*con
      RS(k*(M+1)+j)=sin(ran)*iratio*incf*con
 6    continue
 5    continue
c     calculate average value of discontinuity in instantaneous
c     frequency waveform at each segment boundary (for subsequent
c     windowing algorithm)
      do 20 h=0,factor-1
      do 22 k=0,chan-1
      n0=mod(h*chan+k+1,chan*factor)
      n1=mod(h+1,factor)
      if(k.EQ.chan-1) then
```

```
      n2=n1
      else
      n2=h
      endif
      n3=mod(k+1,chan)
      temp(M+1)=0E0
      temp(M)=RS((k+1)*M)
      do 24 j=M-1,0,-1
      temp(j)=2*temp(j+1)*CC(n1)-temp(j+2)+RS(k*(M+1)+j)
 24   continue
      var(n0)=temp(0)-temp(1)*CC(n1)
      temp(M)=RC((k+1)*M)
      do 26 j=M-1,0,-1
      temp(j)=2*temp(j+1)*CC(n1)-temp(j+2)+RC(k*(M+1)+j)
 26   continue
      var(n0)=var(n0)+temp(1)*SS(n1)
      temp(M)=RS((n3+1)*M)
      do 28 j=M-1,0,-1
      temp(j)=2*temp(j+1)*CC(n2)-temp(j+2)+RS(n3*(M+1)+j)
 28   continue
      var(n0)=var(n0)+temp(0)-temp(1)*CC(n2)
      temp(M)=RC((n3+1)*M)
      do 30 j=M-1,0,-1
      temp(j)=2*temp(j+1)*CC(n2)-temp(j+2)+RC(n3*(M+1)+j)
 30   continue
      var(n0)=var(n0)+temp(1)*SS(n2)
      var(n0)=var(n0)/2
 22   continue
 20   continue
      const=0E0
c     calculate carrier instantaneous frequency over period using
c     Watt method, segment by segment
      do 10 h=0,factor-1
      do 12 k=0,chan-1
      do 14 i=1,NIR
      itemp=h*NIR+i
      ktemp=h*NF+k*NIR+i
      t=-frame/(2*chan)+dt*(ktemp-0.5)
      temp(M+1)=0E0
      temp(M)=RS((k+1)*M)
      do 30 j=M-1,0,-1
      temp(j)=2*temp(j+1)*C(itemp)-temp(j+2)+RS(k*(M+1)+j)
 30   continue
      phase=temp(0)-temp(1)*C(itemp)
      temp(M)=RC((k+1)*M)
      do 32 j=M-1,0,-1
      temp(j)=2*temp(j+1)*C(itemp)-temp(j+2)+RC(k*(M+1)+j)
 32   continue
      phase=phase+temp(1)*S(itemp)
c     if iss not zero, then apply windowing selected by "sel1"
c     to iss signal samples at beginning and ends of each segment
```

```
        if(iss.NE.0) then
        if(sell.EQ.'coef') then
c       3-coefficient windowing
        if(i.LE.iss) then
        phase=(phase-var(h*chan+k))*((1-4*coeff)/2E0+0.5*cos(con*
&       (i-0.5-iss)/(2*iss))+2*coeff*cos(con*(i-0.5-iss)/iss))
&       +var(h*chan+k)
        elseif(i.GE.NIR-iss+1) then
        phase=(phase-var(mod(h*chan+k+1,chan*factor)))*((1-4*coeff)
&       /2E0+0.5*cos(con*(i-0.5-(NIR-iss))/(2*iss))+2*coeff*cos(con
&       *(i-0.5-(NIR-iss))/iss))+var(mod(h*chan+k+1,chan*factor))
        endif
        endif
        elseif(sell,EQ.'pap') then
c       Papoulis windowing
        if(i.LE.iss) then
        phase=(phase-var(h*chan+k))*(2/con*sin(con*(iss-i+0.5)
&       /(2*iss))+(1-(iss-i+0.5)/iss)*cos(con*(i-0.5-iss)/(2*iss)))
&       +var(h*chan+k)
        elseif(i.GE.NIR-iss+1) then
        phase=(phase-var(mod(h*chan+k+1,chan*factor)))*(2/con
&       *sin(con*(i-0.5-(NIR-iss))/(2*iss))+(1-(i-0.5-(NIR-iss))/
&       iss)*cos(con*(i-0.5-(NIR-iss))/(2*iss)))+var(mod(h*chan
&       +k+1,chan*factor))
        endif
        elseif(sell.EQ.'par') then
c       Parzen windowing
        if(i.LE.iss) then
        if(i.LE.iss/2) then
        phase=(phase-var(h*chan+k))*(2*(1-(iss-i+0.5)/iss)**3)
&       +var(h*chan+k)
        else
        phase=(phase-var(h*chan+k))*(1-24*(1-(iss-i+0.5)/iss)*
&       ((iss-i+0.5)/(2*iss))**2)+var(h*chan+k)
        endif
        elseif(i.GE.NIR-iss+1) then
        if(i.LT.NIR-iss/2+1) then
        phase=(phase-var(mod(h*chan+k+1,chan*factor)))*(1-24*(1-
&       (i-0.5-(NIR-iss))/iss)*((i-0.5-(NIR-iss))/(2*iss))**2)
&       +var(mod(h*chan+k+1,chan*factor))
        else
        phase=(phase-var(mod(h*chan+k+1,chan*factor)))*(2*(1-
&       (i-0.5-(NIR-iss))/iss)**3)
&       +var(mod(h*chan+k+1,chan*factor))
        endif
        endif
        endif
        endif
        if(ktemp.EQ.1) then
        phasel(ktemp)=dt*phase
        else
        phasel(ktemp)=phasel(ktemp-1)+dt*phase
```

```
      endif
 14   continue
 12   continue
 10   continue
      const=phasel(N)
c     convert frequency samples to phase samples, and calculate
c     complex carrier values (carrier at N/(4*period))
      do 34 i=1,N
c     normalise for correct rms freq. dev.
      phasel(i)=-(phasel(i)-i*const/N)*beta*sqrt(2E0*M)
      j=mod(i,4)
      if(j.EQ.1) then
      X(i)=cmplx(sin(phasel(i)),cos(phasel(i)))
      elseif(j.EQ.2) then
      X(i)=cmplx(-cos(phasel(i)),sin(phasel(i)))
      elseif(j.EQ.3) then
      X(i)=cmplx(-sin(phasel(i)),-cos(phasel(i)))
      else
      X(i)=cmplx(cos(phasel(i)),-sin(phasel(i)))
      endif
 34   continue
c     derive windowed TCM-FM spectrum
      call FFT
c     loop to calculate total spectral power and
c     value of largest component.
c     also average spectrum with previous runs
      peak=0E0
      total=0E0
      do 40 i=1,N/2+1
      X(i)=cmplx(real(X(i)*conjg(X(i))),0E0)
      peak=amax1(peak,real(X(i)))
      total=total+real(X(i))
      if(1.EQ.1) then
      spec(i)=real(X(i))
      else
      spec(i)=spec(i)+real(X(i))
      endif
 40   continue
c     loop to calculate 98% spectral power bandwidth and average
c     result with previous runs
      do 42 k=0,N/4
      if(k.EQ.0) then
      sum=real(X(N/4+1))
      else
      sum=sum+real(X(N/4+1+k))+real(X(N/4+1-k))
      endif
      if(sum.GE.0.98*total) then
      if(1.EQ.1) then
      BW1(1)=2*k/period
      else
      BW1(1)=(BW1(1-1)*(1-1)+2*k/period)/1
```

```
        endif
        goto 70
        endif
 42     continue
c       loop to calculate 99% spectral power bandwidth and average
c       result with previous runs
 70     do 44 k=0,N/4
        if(k.EQ.0) then
        sum=real(X(N/4+1))
        else
        sum=sum+real(X(N/4+1+k))+real(X(N/4+1-k))
        endif
        if(sum.GE.0.99*total) then
        if(1.EQ.1) then
        BW2(1)=2*k/period
        else
        BW2(1)=(BW2(1-1)*(1-1)+2*k/period)/1
        endif
        goto 75
        endif
 44     continue
c       output final values for 98/99% power bandwidths
 75     if(1.EQ.inum) then
        write(4,*)'98%BW= ',BW1(1),'99%BW= ',BW2(1),'1=',1,'beta=
&       ',beta,'M=',M
        peak2=0E0
        do 46 i=1,N/2+1
        spec(i)=spec(i)/inum
        peak2=amax1(peak2,spec(i))
 46     continue
c       output final scaled spectrum results (100dB range, largest
c       component at 0dB)
        do 48 i=1,nint(span*period)
        write(4,*)nint(270+2200*(i-1)/(span*period)),',',nint(1450+
&       1.25E2*log10(amax1(spec(i)/peak2,1E-10)))
 48     continue
        endif
 100    continue
        close(4)
        end
```

APPENDIX L

FILDEM4.for

```
      program filtcm
c     program to calculate intermodulation distortion in
c     windowed TCM-FM signal with pseudo-rectangular RF
c     filter using pseudo-random noise modulation.
c     windowing is 3-coefficient, and both over-compressed
c     and simple TCM systems with post-demodulation equalisation
c     may be analysed
      character *5 filel,sell
c     dimensions arrays
      dimension RC(0:990),RS(0:990),C(0:8200),S(0:8200),
&     temp(0:100),var(0:100),phase1(17000),phase2(17000),islot(10)
&     ,CC(0:10),SS(0:10),temp2(0:65),amp(0:64),Y(0:4097)
      integer *4 seed,h,factor,fact2
      complex X,value
c     declare common block "cfft"
      common /cfft/X(17000),N,L2N
      con=8*atan(1E0)
c     input variables from terminal:
c     NN=no. samples of waveform,
c     frame=TCM frame period,
c     period=TCM-FM period,
c     beta=ratio of rms frequency deviation to iratio x
c     noise bandwidth,
c     iss=no. samples in each segment to which windowing is
c     applied,
c     coeff=parameter for 3-coefficient windowing,
c     chan=no. multiplexed channels in TCM-FM system
c     (= compression ratio in simple TCM system),
c     B=pseudo-rectangular filter half-bandwidth,
c     M=no. noise components,
c     inum=no. independent runs averaged for final results,
c     seed1=seed for pseudo-random phase generator,
c     span=frequency span for output spectrum,
c     filel=results file,
c     sell=character variable to select type of system
c     (='ord' for simple system and "over" for over-compressed
c     system
      read(5,*)NN,frame,period,beta,iss,coeff,chan,B,M,inum,seed1
      read(5,'(A)')filel
      read(5,'(A)')sell
c     initialise array "islot" with slot positions
      islot(1)=1
      islot(2)=5
      islot(3)=10
      islot(4)=15
```

```
      islot(5)=20
      islot(6)=25
      islot(7)=30
      factor=nint(period/frame)
c     set NIR to no. samples in one segment
      NIR=NN/(chan*factor)
      NF=NN/factor
      incf=3000/M
      fact2=nint(period*incf)
      dt=period/N
c     calculate appropriate compression ratio
      if(sel1.EQ.'ord') then
      iratio=chan
      elseif(sel1.EQ.'over')then
      iratio=chan*real(NIR)/(NIR-2*iss)
      endif
c     calculate no. sidebands in TCM-FM spectrum in filter
c     bandwidth
      iwidth=nint(aint(2*B*period))
c     calculate filter coefficients, Y(i), using 64-term
c     weighted cosine series (Anuff and Liou)
      amp()=1E0
      do 2 k=1,32
      amp(k)=8*sin(con*k/4)/(con*k)*((64-k)**3-4*(32-k)**3)/64E0**3
 2    continue
      do 3 k=33,64
      amp(k)=8*sin(con*k/4)/(con*k)*(64-k)**3/64E0**3
 3    continue
      do 4 i=0,iwidth
      CS=cos(con*0.25*i/(period*B))
      do 5 k=63,0,-1
      temp2(k)=2*temp2(k+1)*CS-temp2(k+2)+amp(k)
 5    continue
      Y(i)=temp2(0)-temp2(1)*CS-0.5
 4    continue
c     initialise arrays C(i), S(i), CC(h) and SS(h)
      do 6 i=1,N/chan
      t=-frame/(2*chan)+(i-0.5)*dt
      C(i)=cos(con*amod(iratio*incf*t,1E0))
      S(i)=sin(con*amod(iratio*incf*t,1E0))
 6    continue
      do 7 h=0,factor-1
      t=-frame/(2*chan)+h*NIR*dt
      CC(h)=cos(con*amod(iratio*incf*t,1E0))
      SS(h)=sin(con*amod(iratio*incf*t,1E0))
 7    continue
c     open "file1" for results
      open(4,file=file1,status='new')
      rewind(4)
c     begin loop for slot positions
      do 200 nslot=1,7
```

```
      iout=1
      seed=seed1
      SDRT=0E0
c     begin loop for "inum" independent phase sets
      do 100 1=1,inum
c     set parameters in common block for FFT subroutine
      N=NN
      L2N=log10(real(NN))/log10(2E0)
c     calculate M pseudo-random phases using function "uniran"
      do 8 k=0,chan-1
      RC(k*(M+1))=0E0
      RS(k*(M+1))=0E0
      do 9 j=1,M
      ran=con*uniran(seed)
      RC(k*(M+1)+j)=cos(ran)*iratio*incf*con
      RS(k*(M+1)+j)=sin(ran)*iratio*incf*con
 9    continue
 8    continue
c     calculate average value of discontinuity in instantaneous
c     frequency waveform at each segment boundary (for subsequent
c     windowing algorithm)
      do 20 h=0,factor-1
      do 22 k=0,chan-1
      n0=mod(h*chan+k+1,chan*factor)
      n1=mod(h+1,factor)
      if(k.EQ.chan-1) then
      n2=n1
      else
      n2=h
      endif
      n3=mod(k+1,chan)
      write(6,*)n0,n1,n2,n3
      temp(M+1)=0E0
      temp(M)=RS((k+1)*M)
      do 24 j=M-1,0,-1
      temp(j)=2*temp(j+1)*CC(n1)-temp(j+2)+RS(k*(M+1)+j)
 26   continue
      var(n0)=temp(0)-temp(1)*CC(n1)
      temp(M)=RC((k+1)*M)
      do 28 j=M-1,0,-1
      temp(j)=2*temp(j+1)*CC(n1)-temp(j+2)+RC(k*(M+1)+j)
 28   continue
      var(n0)=var(n0)+temp(1)*SS(n1)
      if(k.EQ.0) then
      var(n0)=var(n0)
&     -RS(islot(nslot))*cos(con*amod(iratio*islot(nslot)*incf*
&     (-frame/(2*chan)+n1*NIR*dt),1E0))
&     -RC(islot(nslot))*sin(con*amod(iratio*islot(nslot)*incf*
&     (-frame/(2*chan)+n1*NIR*dt),1E0))
      endif
      temp(M)=RS((n3+1)*M)
```

```
      do 30 j=M-1,0,-1
      temp(j)=2*temp(j+1)*CC(n2)-temp(j+2)+RS(n3*(M+1)+j)
 30   continue
      var(n0)=var(n0)+temp(0)-temp(1)*CC(n2)
      temp(M)=RC((n3+1)*M)
      do 32 j=M-1,0,-1
      temp(j)=2*temp(j+1)*CC(n2)-temp(j+2)+RC(n3*(M+1)+j)
 32   continue
      var(n0)=var(n0)+temp(1)*SS(n2)
      if(n3.EQ.0) then
      var(n0)=var(n0)-
&     -RS(islot(nslot))*cos(con*amod(iratio*islot(nslot)*incf*
&     (-frame/(2*chan)+n2*NIR*dt),1E0))
&     -RC(islot(nslot))*sin(con*amod(iratio*islot(nslot)*incf*
&     (-frame/(2*chan)+n2*NIR*dt),1E0))
      endif
      var(n0)=var(n0)/2
      write(6,*)'n0=',n0,'var(n0)=',var(n0)
 22   continue
 20   continue
      const=0E0
c     calculate instantaneous carrier frequency over period using
c     Watt method
      do 10 h=0,factor-1
      do 12 k=0,iratio-1
      do 14 i=1,NIR
      itemp=h*NIR+i
      ktemp=h*NF+k*NIR+i
      t=-frame/(2*chan)+dt*(ktemp-0.5)
      temp(M+1)=0E0
      temp(M)=RS((k+1)*M)
      do 40 j=M-1,0,-1
      temp(j)=2*temp(j+1)*C(itemp)-temp(j+2)+RS(k*(M+1)+j)
 40   continue
      phase=temp(0)-temp(1)*C(itemp)
      temp(M)=RC((k+1)*M)
      do 42 j=M-1,0,-1
      temp(j)=2*temp(j+1)*C(itemp)-temp(j+2)+RC(k*(M+1)+j)
 42   continue
      phase=phase+temp(1)*S(itemp)
c     remove component at frequency islot(nslot) from
c     channel one signal
      if(k.EQ.0) then
      phase=phase
&     -RS(islot(nslot))*cos(con*amod(iratio*islot(nslot)*incf
&     *t,1E0))-RC(islot(nslot))*sin(con*amod(iratio*islot(nslot)
&     *incf*t,1E0))
      endif
      phase2(ktemp)=phase
c     if iss not zero, then apply 3-coefficient windowing to
c     iss signal samples at beginning and end of each segment
```

```
        if(iss.NE.0) then
        if(i.LE.iss) then
        phase=(phase-var(h*chan+k))*((1-4*coeff)/2+0.5*cos(con*(i
&       -0.5-iss)/(2*iss))+2*coeff*cos(con*(i-0.5-iss)/iss))
&       +var(h*chan+k)
        elseif(i.GE.NIR-iss+1) then
        phase=(phase-var(mod(h*chan+k+1,chan*factor)))*((1-4*coeff
&       )/2+0.5*cos(con*(i-0.5-(NIR-iss))/(2*iss))+2*coeff*cos(
&       con*(i-o.5-(NIR-iss))/iss))+var(mod(h*chan+k+1,chan*factor))
        endif
        endif
        const=const+phase
        phasel(ktemp)=phase
 14     continue
 12     continue
 10     continue
c       convert frequency samples to phase samples, and calculate
c       complex carrier values (carrier at N/(4*period))
        do 50 i=1,N
        if(i.EQ.1) then
        phasel(1)=(phasel(1)-const/N)*dt
        else
        phasel(i)=(phasel(i)-const/N)*dt+phasel(i-1)
        endif
c       normalise for correct rms freq. dev.
        phase=-phasel(i)*beta*sqrt(2E0*M)
        j=mod(i,4)
        if(j.EQ.1) then
        X(i)=cmplx(sin(phase),cos(phase))
        elseif(j.EQ.2) then
        X(i)=cmplx(-cos(phase),sin(phase))
        elseif(j.EQ.3) then
        X(i)=cmplx(-sin(phase),-cos(phase))
        else
        X(i)=cmplx(cos(phase),-sin(phase))
        endif
 50     continue
c       get TCM-FM spectrum
        call FFT
c       loop to multiply spectral components by filter
c       coefficients
        do 52 i=1,N
        if((i.LE.N/4+1+iwidth).AND.(i.GE.N/4+1-iwidth)) then
        if(i.GE.N/4+1) then
        X(i)=conjg(X(i)*cmplx(Y(i-N/4-1),0E0))
        else
        X(i)=conjg(X(i)*cmplx(Y(N/4+1-i),0E0))
        endif
        else
        X(i)=(0E0,0E0)
        endif
```

```
 52     continue
c       recover time-domain samples
       call FFT
       do 54 i=1,N
       X(i)=conjg(X(i))/N
 54    continue
c       loops to demodulate TCM-FM signal using process of Appendix B
       value=X((factor-1)*NF+NIR)
       do 65 h=factor-1,0,-1
       do 60 i=NIR,2,-1
       ktemp=h*NF+i
       phase2(h*NIR+i)=asin(real(conjg(X(ktemp-1))*X(ktemp))/sqrt(real
&      (X(ktemp)*conjg(X(ktemp)))*real(X(ktemp-1)*conjg(X(ktemp-1)))))
 60    continue
       if(h.NE.0) then
       ktemp=(h-1)*NF+NIR
       jtemp=h*NF+1
       phase2(h*NIR+1)=asin(real((conjg(X(ktemp))*adj(h))*
&      X(jtemp))/sqrt(real(X(jtemp)*conjg(X(jtemp)))*real(X(ktemp)*
&      conjg(X(ktemp)))))
       else
       phase2(1)=asin(real((conjg(value)*adj(0))*X(1))/sqrt(real(value
&      *conjg(value))*real(X(1)*conjg(X(1)))))
       endif
 65    continue
       if(sel1.EQ.'ord') then
c       equalisation of weighted samples
       do 67 i=N,2,-1
       X(i)=cmplx(phase2(i)/(beta*sqrt(2E0*M))-const/N,0E0)
 67    continue
       do 68 h=0,factor-1
       do 69 i=1,NIR
       ktemp=h*NF+i
       if(iss.NE.0) then
       if(i.LE.iss) then
       X(h*NIR+i)=cmplx((real(X(ktemp))-var(h*chan))/
&      (0.5+0.5*cos(con*(i-0.5-iss)/(2*iss)))+var(h*chan),0E0)
       elseif(i.GE.NIR-iss+1) then
       X(h*NIR+i)=cmplx((real(X(ktemp))-var(mod(h*chan+1,chan*
&      factor)))/((1-4*coeff)/2+0.5*cos(con*(i-0.5-(NIR-iss))/
&      (2*iss))+2*coeff*cos(con*(i-0.5-(NIR-iss))/iss))+var(mod
&      (h*chan+1,chan*factor)),0E0)
       else
       X(h*NIR+i)=X(ktemp)
       endif
       else
       X(h*NIR+i)=X(ktemp)
       endif
 69    continue
 68    continue
c       set values of N and L2N for single channel samples
```

```
      N=NN/chan
      L2N=log10(real(N))/log10(2E0)
c     use FFT to calculate output spectrum
      call FFT
      elseif(sel1.EQ.'over')
c     if iss is zero then set N and L2N to appropriate
c     values for samples of one channel (note: N is power of
c     2 enabling FFT to be used)
      if(iss.EQ.0) then
      N=NIR*factor
      L2N=log10(real(N))/log10(2E0)
      do 80 i=1,N
      X(i)=cmplx(phase2(i),0E0)
 80   continue
c     use FFT to calculate output spectrum
      call FFT
      else
c     if iss not zero, then set appropriate values but
c     N is no longer power of 2, therefore inefficient DFT must
c     be used
      N=(NIR-2*iss)*factor
      do 85 h=0,factor-1
      k=0
      do 87 i=1,NIR
      if((i.GT.iss).AND.(i.LT.NIR-iss+1)) then
      k=k+1
      X(h*(NIR-2*iss)+k)=phase2(h*NIR+i)
      endif
 87   continue
 85   continue
c     use DFT to calculate output spectrum
      call DFT
      endif
c     calculate effective signal-to-distortion ratio
      power=0E0
      do 90 i=fact2+1,fact2*M+1,fact2
      if (i.NE.fact2*islot(nslot)+1)then
      power=power+real(X(i)*conjg(X(i)))
      endif
 90   continue
c     average above result with previous runs
      SDR=power/((M-1)*real(X(fact2*islot(nslot)+1)*conjg(
&     X(fact2*islot(nslot)+1))))
      SDRT=SDRT+1/SDR
c     output results if first run
      if(1.EQ.1) then
      write(4,*)'beta=',beta,'B=',B,'slot= ',islot(nslot),'l= ',l,
&     'average SDR=',-10*log10(SDRT)
      endif
c     output results if run is 5,10...inum etc.
      if(l.EQ.iout*5) then
```

```
      write(4,*)'beta=',beta,'B=',B,'slot= ',islot(nslot),'l= ',l,
&     'average SDR=',-10*log10(SDRT/l)
      iout=iout+1
      endif
 100  continue
 200  continue
      close(4)
      end
```